OLEKSIJ FOMIN
PAVLO PROKOPENKO

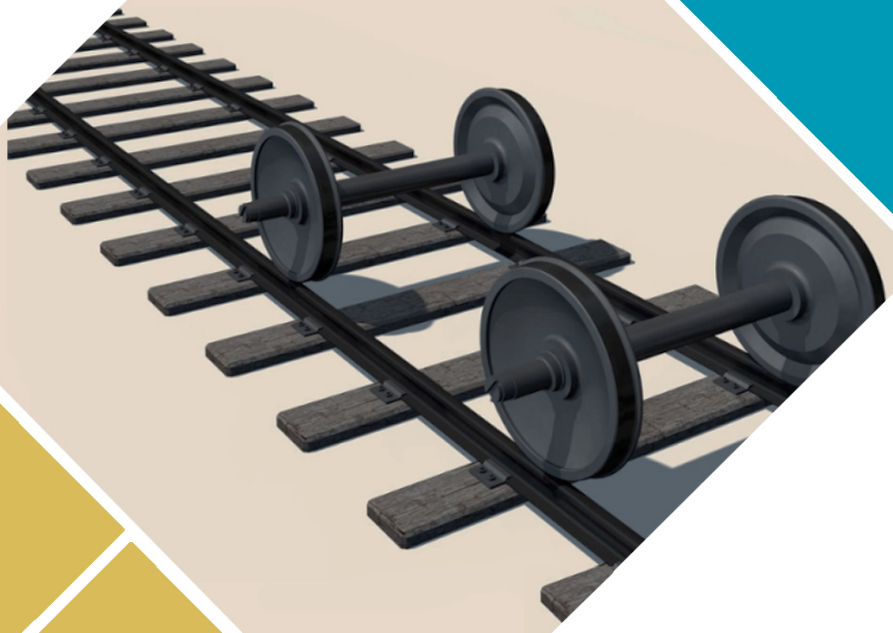

REDUCING THE ACCIDENTAL RATE OF WAGONS BY IMPROVING THE SYSTEM FOR ASSESSING THEIR TECHNICAL CONDITION

MONOGRAPH

2024

Primedia eLaunch

Oleksij FOMIN

Pavlo PROKOPENKO

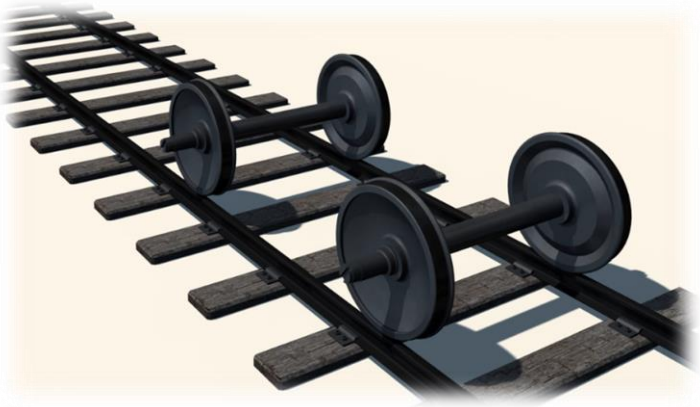

REDUCING THE ACCIDENTAL RATE OF WAGONS BY IMPROVING THE SYSTEM FOR ASSESSING THEIR TECHNICAL CONDITION

Monograph



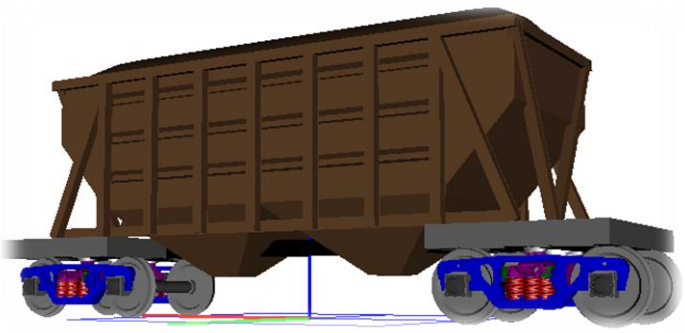

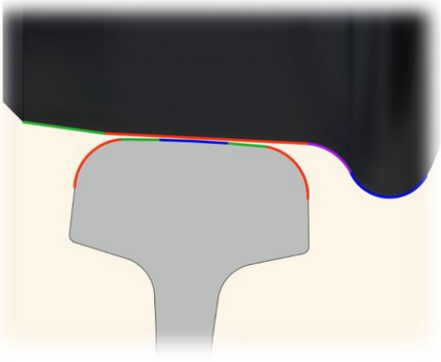

2024

UDC 629.4.02.001.76
F 71

Fomin, O., and Prokopenko, P. *Reducing the accidental rate of wagons by improving the system for assessing their technical condition*. Dallas, USA: Primedia eLaunch LLC, 2024. 362 p.

ISBN 979-8-89217-800-6
DOI 10.36074/rarwisatc-monograph.2024

This monograph is recommended for printing by the Science Council of Volodymyr Dahl East Ukrainian National University (protocol No 06 dd 30.01.2024)

Reviewers:
MASLIYE V Vyacheslav, Doctor of Technical Sciences, Professor, Department of Electric Transport and Heat Engineering, National Technical University «Kharkiv Polytechnic Institute», Ukraine
SAPRONOVA Svitlana, Professor, Doctor of Technical Sciences, Department of cars and carriage facilities, State University of Infrastructure and Technologies, Ukraine
TKACHENKO Viktor, Professor, Doctor of Technical Sciences, Department of Traction Rolling Stock of' Railways, State University of Infrastructure and Technologies, Ukraine
USTENKO Oleksander, Professor, Doctor of Technical Sciences, Dean of the Faculty of Mechanics and Energy , Ukrainian State University of Railway Transport, Ukraine

The monograph will be valuable for researchers, designers, and engineers engaged in activities associated with reducing the accident rate of railway cars through the enhancement of systems assessing their technical condition. Specifically, it addresses issues related to the utilization of laboratory cars during full-scale tests for evaluating motion quality, acceptance, and commissioning of railway rolling stock. However, the current state of measurement equipment development enables the abandonment of such laboratory cars in favor of mobile hardware-software complexes during dynamic testing of rolling stock units in most cases.

The organization of freight train traffic in Ukraine is a critical factor in integrating the country's railway transport into the European system. Currently, a situation has arisen that demands a significant upgrade of the freight wagon fleet with modern wagons to meet the requirements of freight transportation. Another substantial drawback of Ukraine's railway transport is the speed limitation for trains with wagons having reduced tare weight, impacting the speed of rail freight transport. Therefore, there is an immediate need to improve the methodological and software support, along with testing tools, for evaluating the performance and safety indicators of such wagons. Due to their unsatisfactory dynamic behavior, a specific group of freight wagons, such as platform wagons, has a speed limit of 60 km/h, negatively affecting rail freight speed.

Crucial indicators of the railway rolling stock's motion quality include vertical and horizontal dynamics, the wheel flange stability coefficient against derailment, frame forces, and body accelerations. These aspects largely depend on the weight of the rolling stock's tare and the interaction indicators between the crew part and the track. The monograph's objective is to illuminate the results of conceptual solutions aimed at assessing the technical condition and motion quality indicators of wagons under the conditions of operation using modern mobile systems. The book also presents the outcomes of prior theoretical and practical works, including an analysis of railway traffic safety issues and existing systems for determining motion quality indicators. A proposed mobile system for determining the motion quality indicators of wagons in operation and a complex of hardware, software, and mathematical solutions for determining the motion quality indicators of wagons are included. Concepts of freight wagons with improved motion quality characteristics are also discussed.

The book can serve as a textbook for the training of bachelor's, master's, and doctoral students in various specialties related to transport mechanics, including railway transport, transport technologies, mechanical engineering, materials science, and others.

Copyright© 2024 Oleksij Fomin

Copyright © 2024 Pavlo Prokopenko

All rights reserved.

CONTENTS

INTRODUCTION ……..…. 6

SECTION 1

REVIEW AND ANALYSIS OF EMERGENCY SITUATIONS ON THE RAILWAYS AND CAUSES OF THEIR OCCURENCE ……..……... 8

1.1 Study of emergency situations and issues of quality indicators of carriage movement……..... 8

1.2 Analysis of literature sources and approaches for evaluating traffic quality and safety indicators ……..……... 15

1.3 Analysis of existing systems to determine traffic quality and safety indicators……... 28

1.4 Analysis of existing projects to improve the quality and safety indicators of carriage movement ……..… 35

Conclusions on section 1……. 44

SECTION 2

METHODS AND APPROACHES FOR ASSESSING INDICATORS OF QUALITY, TRAFFIC SAFETY AND TECHNICAL CONDITION OF WAGONS ……... 45

2.1 Measurement of deformations of load-bearing structures. General information ……..... 45

2.2 Measurement of forces by local deformations of the bogie frames …….. 50

2.3 Measurement of forces of direct interaction of wheels with rails ……. 51

2.4 Measurement of dynamic indicators of rolling stock ……..…….. 59

Conclusions on section 2…….....… 64

SECTION 3

IMPROVING MEANS AND APPROACHES FOR ASSESSING SAFETY

INDICATORS AND TECHNICAL CONDITION OF FREIGHT WAGONS….. 65

3.1 Mathematical support for determining safety indicators and technical condition of freight wagons ……... 65

3.2 Software for collecting and registering safety indicators and technical condition of wagons ……... 74

3.3 Study of indicators that affect the quality of carriage movement ……. 79

Conclusions on section 3……. 106

SECTION 4

PRACTICAL ASPECTS OF IMPLEMENTATION OF IMPROVED MEANS AND APPROACHES FOR DETERMINING AND ASSESSING INDICATORS OF SAFETY AND TECHNICAL CONDITION OF WAGONS . 107

4.1 A mobile system for determining safety indicators and technical condition in operating conditions ……..……. 107

4.2 Hardware and primary converters of the mobile system ……..… 108

4.3 Software for collecting and recording measurements ……... 117

4.4 Practical studies of quality indicators and movement safety of freight wagons in an empty state ……..…….……. 122

4.5 Restoration of the carrying capacity of the wagon for transporting grain. 162

Conclusions on section 4……...….. 197

SECTION 5

SYSTEM FOR MEASURING THE INTERACTION FORCES OF WHEELS AND RAILS ACCORDING TO THE CHARACTERISTICS OF THE STRESSED AND DEFORMED STATE ……..……. 199

5.1 Determination of the deformation sensitivity zones of the wheel disc to force load …… 199

5.2 Theoretical studies of wheels dynamic loading of passenger wagons at high speeds …….. 209

5.3 Practical study of the direct measurement method of the interaction forces of the wheels with rails …… 224

5.4 Requirements for the system of direct measurement of the interaction forces of the wheel pairs with rails ……..…….. 238

Conclusions on section 5……..……... 245

SECTION 6

MOBILE SYSTEM FOR DETERMINING THE DYNAMIC LOAD OF THE ROLLING PARTS OF THE ROLLING STOCK IN OPERATION ……. 246

6.1 General requirements for software and hardware complex …….. 246

6.2 Measurement information collection subsystem …….. 247

6.3 A system for determining the level of comfortable movement …… 252

6.4 The system for determining the smoothness of movement …….. 259

6.5 System for determining traffic safety indicators ……... 262

6.6 A system for determining the indicators of the interaction of the pantograph and contact network ……. 265

Conclusions on section 6……. 281

GENERAL CONCLUSIONS …….. 283

REFERENCES…….. 286

Addition A. PATENT DEVELOPMENTS FOR IMPROVING WAGON TRAFFIC SAFETY INDICATORS…… 307

INTRODUCTION

The organization of the movement of freight trains in Ukraine is an important factor in the integration of the country's railway transport into the European system. Currently, a situation has arisen that requires a significant renewal of the freight wagon park with modern wagons to meet the requirements of freight transportation. Also, a significant drawback of railway transport of Ukraine is the limitation of the speed of trains, which include freight wagons with a reduced container in an empty state, therefore, at the moment, the issue of improving the methodological and software and instrumental testing means for evaluating the quality and safety indicators of the movement of such wagons is relevant at the moment. Due to their unsatisfactory movement dynamics, a separate group of freight wagons, such as a platform wagon, has a speed limit of 60 km/h, which negatively affects the speed of freight transportation by rail.

Traffic safety is a set of organizational and technical measures aimed at ensuring accident-free operation and maintenance of railway structures, tracks, rolling stock, equipment, mechanisms and devices in constant serviceability.

Important characteristics of the quality of movement of railway rolling stock include indicators of vertical and horizontal dynamics, the coefficient of stability of the wheel from derailment, frame forces and acceleration of the body, which largely depend on the tare mass of the rolling stock and indicators of the interaction of the crew part and the track. Therefore, the definition and assessment of indicators

characterizing driving qualities and traffic safety should be based on in-depth studies of indicators of traffic dynamics.

At present, laboratory wagons are used during field tests related to the evaluation of traffic quality indicators, acceptance and admission to operation of railway rolling stock, but the modern state of development of measuring equipment allows in most cases to abandon the use of such wagons during running tests of units rolling stock in favor of mobile hardware and software complexes.

The above testifies to the relevance of solving issues related to the improvement of methods and means of experimental assessment of the quality and safety indicators of the freight wagons movement with reduced containers, including by improving the methodological and software and instrumental means of testing.

SECTION 1
REVIEW AND ANALYSIS OF EMERGENCY SITUATIONS ON THE RAILWAYS AND CAUSES OF THEIR OCCURENCE

1.1 Study of emergency situations and problems of quality indicators of carriage movement

The declared integration of railway transport of Ukraine into the transport network of the European Union requires an immediate solution to issues related to effective and safe transportation, as well as intermodality and interoperability of transport systems.

The success of work in this area depends significantly on the completion of the processes of harmonization and implementation of current standards, which should encourage the use of the latest approaches to assessing the compliance of vehicles with world-class technical requirements.

Comparing the regulatory requirements regarding dynamic indicators and force action on the track of crew parts of rolling stock on railways with a gauge of 1520 mm, on the one hand, and the relevant European regulatory documents, on the other, it is possible to state a significant difference in the approaches to both calculation cases and experimental procedures evaluation of running properties of rolling stock.

A significant drawback of the Ukrainian railway transport is the speed limit for trains with individual freight wagons in an empty state, equipped with model 18-100 bogies.

Ensuring and maintaining safe transportation on railways is one of the most important requirements for the safe operation of railways. Among the disasters and accidents that occur on the railways, the greatest danger is the derailment of the

rolling stock, because it leads to significant financial losses and serious consequences.

Among the reasons for the derailment are: malfunctions of the running parts of the wagons (breakage of the side frames and suspension beams of the bogies, malfunctions of the roller bearings of the axle box unit), wear of the elements of the friction vibration dampers, unacceptable deviations in the dimensions of the elements of the bogie and the railway track, and features of the wagons design after repairs and modernizations.

In addition, the danger of derailment, especially at high speeds, can be caused by reasons that are not related to malfunctions of the wagon, but are a feature of its design. So, for example, a feature of wagons on bogies 18-100 is a low critical speed from the point of view of stability of movement, upon reaching which non-damping oscillations of wheel pairs appear within the rail track, which leads to the appearance of additional forces of interaction of the wagon on the track.

The main reasons for the derailment of the freight wagons with a reduced tare are related to malfunctions of rolling stock, non-compliance with track maintenance standards, negative dynamics of train movement, as well as their operating conditions. The described malfunctions associated with the destruction of elements of the undercarriage lead to the derailment of wagons. The main reasons for derailment of the freight wagons with a reduced tare are malfunctions of the rolling stock, deviations from the permissible indicators of track maintenance, unsatisfactory indicators of train dynamics and their operating conditions. The described malfunctions are also related to the destruction of elements of the running gear, which directly causes the possibility of wagons derailment. An important factor is the degradative changes in the wagon's tare by more than 10% from the one specified by the factory manufacturer. The described malfunctions, in particular, related to damage to the running gear, directly lead to the wagons derailment. However, some of them do not directly cause the derailment, but are the causes of the development of dynamic processes that cause increased force interaction of the rolling stock. Among

the wagons that have a tendency to derail are cement hopper wagons with the roof removed and empty platform wagons. As a result of the analysis of the causes and circumstances of derailment of empty wagons, it was established that the frequent consequences of derailment are serious damage to the railway track, rolling stock and other elements of the railway infrastructure, a decrease in speed and a violation of the transportation schedule, which in turn entails significant financial losses.

Analysis of information on the operation and derailment of empty wagons.

Statistical data on the derailment of freight wagons in an empty state on the sections of railways of Ukraine show that the most derailments in recent years have occurred with freight wagons with reduced tares: universal platforms model 13-4012 and hopper wagons for cement with a removed cover model 19-758-01. In the period from 2011 to 2023, there were more than 40 cases of train derailments:

- 23.08.2017 on the Kryvyn-Slavuta section of the regional branch (further - the RB) of the South-Western Railway hopper model 19-758-01, speed 67 km/h, 19 out of 21 wagons (in the tail of the train);

- 21.08.2011 on the race Krolevets – Altynivka RB South-Western Railway wagon-platform model13-4012M, speed 67 km/h, 48 out of 53 wagons (in the tail of the train);

- 27.08.2012 on the race Zavorichi – Bobryk RB South-Western Railway wagon-platform model13-4012M, speed 69 km/h, 49 out of 57 wagons (in the tail of the train);

- 25.07.2013 at the race Pysmenka – Ulyanivka RB Southern Railway platform wagon model13-4012, speed 62 km/h, 48 out of 54 wagons (in the tail of the train);

- 26.07.2016 at the race Plysky – Kruty RB South-Western Railway wagon-platform model13-401-17, speed 77 km/h, 47 of 61 wagons (in the tail of the train);

- 08/06/2016 on the race Brivka – Popilnya RB South-Western Railway wagon-platform model13-401-17, speed 68 km/h, 52 of 66 wagons (in the tail of the train);

- 05/23/2017 on the Ryhalske– Vershnytsia RB Southern Railway platform wagon model13-4012, speed 70 km/h, 44 out of 52 wagons (in the tail of the train);

- 29.04.2018 on the race Brivka – Popilnya RB South-Western Railway model platform wagons13-4012, speed 67 km/h, 19, 20 out of 20 wagons (in the tail of the train);

- 05/03/2018 on the race Brivka – Popilnya RB South-Western Railway wagon-platform model13-4012, speed 68 km/h, 6 of 53 wagons (in the head). On the Kozyatyn-Fastiv section, Brivka-Popilnya crossing, 964 km PC4–PC2 (according to the act of May 3, 2018 Art. Fastiv-2 964 km PK7) 05/03/2018 in train #1442 derailment of the fourth wheel pair of the platform wagon model 13-4012, this platform followed the sixth in the train. According to official documents related to this event, it is indicated that train 1442 included a VL80t locomotive (at the head of the train) and 53 platform wagons of model 13-4012. The total weight of the train was 1,114 tons, all wagons were empty. The mode of driving the train before the event is specified as a breakaway with a speed (according to the deputy head of the depot Kozyatyn) equal to 60 km/h. According to other information, the speed of the train at the scene of the incident was 68 km/h and the mode of driving the train was traction according to position 17. The fourth wheel pair of the wagon had signs of damage.

For the period from 2017 to 2023 more than 10 transport incidents were admitted due to the derailment of wagons converted from cement trucks for bulk cargoes (model 19-758-01).

The consequences of these derailments were serious damage to the rolling stock, the railway track and other elements of the railway infrastructure, a decrease in speed and disruption of the train schedule. All cases of departure of wagons must be in an empty state and at a speed of more than 60 km/h.

Also, at present, the task of increasing the speed of passenger rolling stock remains relevant, which requires new approaches to the assessment of train safety indicators and the smoothness of carriages. Stability conditions in the rail track of rolling stock units are determined by the ratio of forces acting in contact between the wheels and the rails. Determining these forces is an extremely difficult task, since the

contact zone is constantly moving along the rolling surfaces of the wheels and rails. In addition, in order to assess the stability of the wheel against rolling onto the rail, it is necessary to constantly calculate the ratio of horizontal and vertical contact forces over a certain period of time, because even isolated cases of exceeding the permissible values of this ratio can cause a violation of traffic safety conditions.

Figures 1.1 - 1.5 show the consequences of freight wagon derailments.



Figure 1.1 – An example of an emergency situation



Figure 1.2 – An example of an emergency situation



Figure 1.3 – An example of an emergency situation



Figure 1.4 – An example of an emergency situation

1.2 Analysis of literary sources and approaches for evaluating traffic quality and safety indicators

In order to assess the quality indicators, the safety of the movement of wagons, locomotives and other types of rail rolling stock, a variety of approaches to the assessment of safety conditions and the solution of the specified problem are noted.

Yes, the problem of ensuring the stability of crews on the track has a long history. Back in 1882, the engineer Pochet derived a formula that determines the ratio between the side pressure of the oscillating crest and its load on the rail, at which it is possible for the wheel to come off the rail. Later Marier [1] noted that this formula became the impetus for the construction of the theory of derailment.

In 1908, M. Nadal [2] proposed a method of determining the ratio of the forces acting on the wheel, which prevents it from sliding on the rail. In this case, the starting position of the wheel is considered to be one in which its rolling surface has risen above the head of the rail, and the wheel contacts the rail only at the point located on the conical part of the ridge. It is assumed that safety from slipping will be ensured if the ratio of the forces applied to the wheel — horizontal transverse Y and vertical Q (under the action of the limit force of dry friction T=μN) is such that the ridge will slide down relative to the rail fig. 1.1), μ is the coefficient of friction.

$N = Q\cos\beta + Y\sin\beta$— normal reaction of the rail at the point of contact.

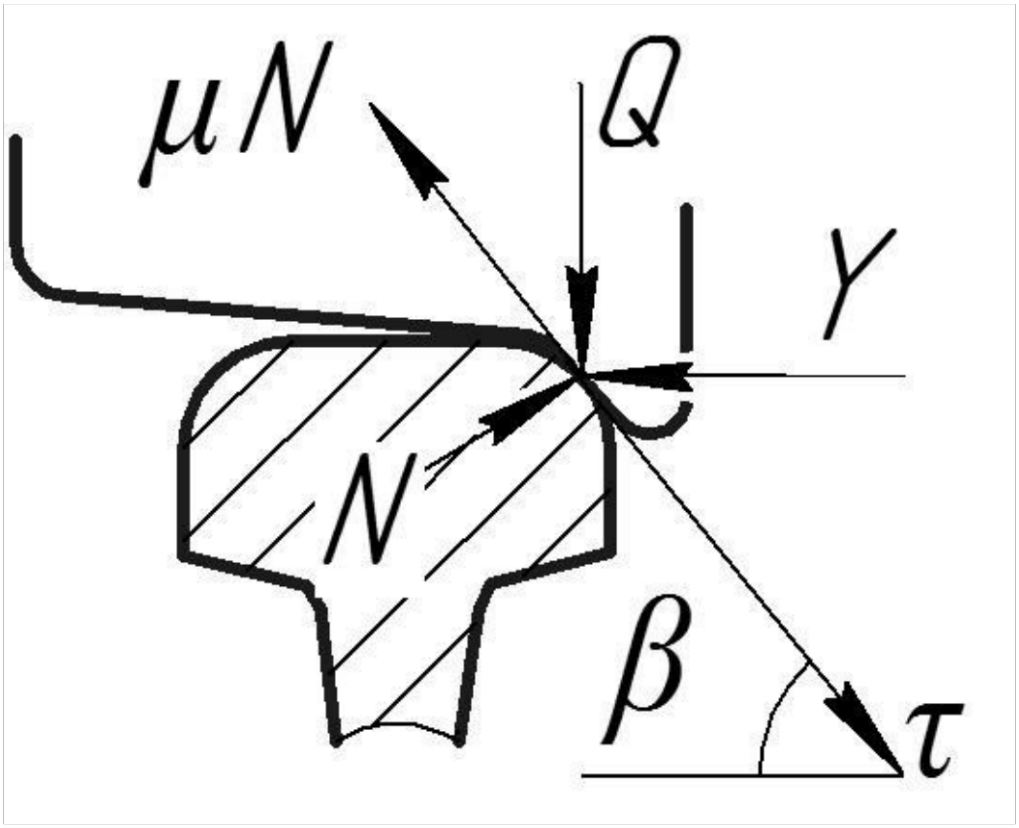

Figure 1.5 – Forces acting at the point of contact when the ridge slides down relative to the head of the rail

In work [2], the author assumes that the forces Y, Q and Q' are applied not at the points of contact of the wheels with the rails, as Marie thought when deriving his formula, but on the edge of the axle neck (force Y) and to the axle necks of the analyzed wheel pair (forces Q and Q'), that is, the author recommends using a scheme that, in his opinion, takes into account the action of all forces and pairs that affect the conditions of wheels coming off the rails (Fig. 1.2).

O.U. Galeev shows with his new formula that the "critical" or maximum permissible value of the ratio of the transverse force to the vertical load, which comes to the neck of the axle of the wheel pair from the side of the running wheel, is a variable value that depends on the ratio of vertical loads that come to the neck of the wheel axle steam

$$\frac{F}{P_1} \leq \frac{P_2}{P_1} \cdot k_1 - k_2, \qquad (1.1)$$

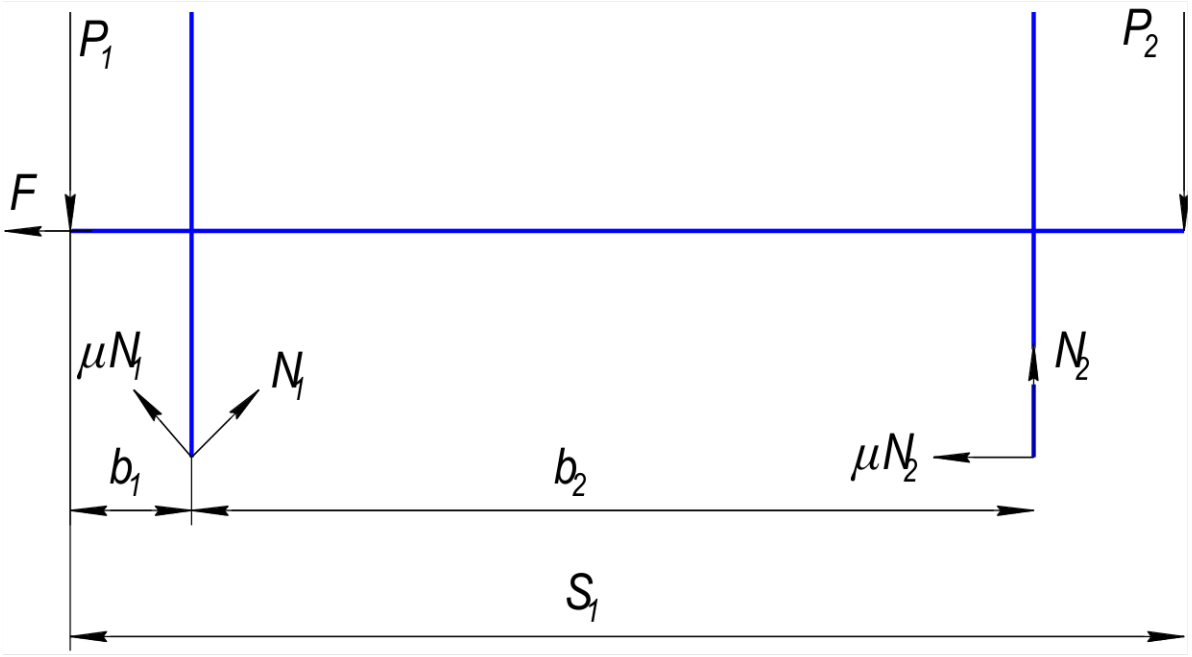

Figure 1.6 – Scheme of forces applied to a pair of wheels (according to work [2])

Formula (1.2) determines the critical value of the ratio of transverse to vertical force for a given vertical load distribution on the axis of one wheel pair.

As noted by K. N. Mishchenko [3] in his work, the question of the interaction of the forces developing between the rail and the wheel running against it is treated differently by different authors. Finally, we have a number of formulas that estimate the possibility of wheel derailment by the ratio of the maximum lateral pressure of the wheel on the rail (directive force) and the vertical pressure of the wheel on the rail.

The further development of the theory of safety from the east, the wheel from the rail was highlighted in such works as [4, 5, 6, 7, 8]. In these works, the state of ultimate equilibrium of the wheel pair was mainly considered.

In the works carried out under the leadership of Professor M. F. Verigo [4, 5, 6, 9], a method of evaluating the stability of the movement against wheel derailment

according to a refined formula that determines the critical value of the ratio of the horizontal frame force and the vertical force at a given distribution is proposed vertical loads on the axis of the same pair of wheels.

The refined condition presented in these works was widely used in experimental works on determining the maximum permissible speeds of movement of new and modernized rolling stock units.

Here we considered the condition that ensures continuous sliding of the rim of the wheel pair on the side surface of the rail head, there is a condition that ensures that the wheel does not slide on the rail.

$$\frac{Y_p}{P_1} \le \frac{P_2}{P_1} \cdot k_1 - k_2 + k_3 \cdot \frac{K}{P_1} \qquad (1.2)$$

$$k_1 = \frac{\mu b_2 - (S_1 - b_2) \cdot \mathrm{tg}(\beta - \varphi)}{(R + r) \cdot [\mathrm{tg}(\beta - \varphi) + \mu] - S_1},$$

$$k_2 = \frac{\mu b_1 + (S_1 + b_1) \cdot \mathrm{tg}(\beta - \varphi)}{(R + r) \cdot [\mathrm{tg}(\beta - \varphi) + \mu] - S_1},$$

$$k_3 = \frac{S_1 \cdot \left\{ \frac{I_2}{K} \cdot \mu - \frac{I_1}{K} \cdot \mathrm{tg}(\beta - \varphi) + [\mu - 2\mathrm{tg}(\beta - \varphi)] \right\}}{(R + r) \cdot [\mathrm{tg}(\beta - \varphi) + \mu] - S_1},$$

where Y_p– frame effort;

P_1, are the forces transmitted to the wheel pair by the spring-loaded parts, applied to the middle of the axle necks.P_2

K– half the weight of the wheel pair;

I_1, I_2– vertical forces of inertia of the wheelset, caused by its movement along the unevenness of the track or the unevenness of the wheelset itself (Fig. 1.7)

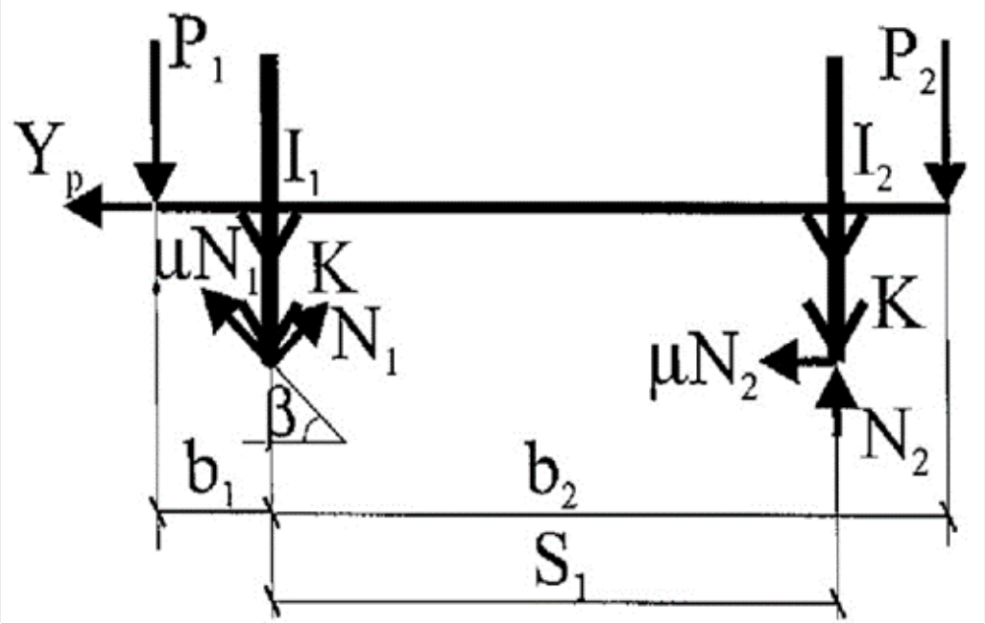

Figure 1.7 – Scheme of forces applied to a pair of wheels (according to work [4])

The authors of the work [5] also proposed one of the possible ways of automating the processing of experimental data when determining the stability margin factor against derailment of a wheel pair. At the same time, it is assumed that the change in time of the coefficient of stability margin is a stationary and random ergodic function. The authors state a sufficient condition for traffic safety from the point of view of the wheel running into the head of the rail. To do this, they consider the trajectory *y(t)* of the wheel during the time *t* when the crest hits the rail. From the comparison of the trajectory of the wheel movement with the maximum permissible value of displacement in the transverse direction, as the adopted horizontal projection forms the conical part of the ridge b_{dop}, a sufficient condition for the safety of movement $y(t) \leq b_{dop}$ at all values of time *t* is obtained.

The work of V. F. Kondratiev [10] is devoted to the problem of the wheel derailment, in which it is proposed to reduce the original system of forces acting on the wheel pair to a simpler, equivalent system. For this, it is sufficient to bring the system of given forces to the center of gravity of the wheel pair and to consider the main vector and the main moment of these forces. Here, the author distinguishes

wheel pairs according to the mode of movement and examines the influence of this factor on the derailment process.

A combined criterion for the purpose of assessing the danger of a rolling stock falling due to the rolling of a wheel on the head of the rail is proposed in works [11, 12]. Here, instead of the coefficient of friction, it is proposed to use the ratio of the transverse component of the creep force to the normal reaction at the contact point. The authors suggest using directly the values of wheel lift above the rail head to assess the danger of derailment, starting from the position at which the ridge contact is first detected at the point where the angle of inclination forms the ridge profile is maximum. However, this approach to safety assessment can be successfully applied with appropriate technical equipment of measuring complexes.

The paper [13] formulates the energy interpretation of the rolling of the wheel on the head of the rail. According to the authors, this is possible when the kinetic energy of the movement attributable to the wheel pair running into the rail exceeds the work of the forces arising in the contact between the surfaces of the ridge and the wheel, which they perform when rising to the height of the ridge. According to the authors, the proposed scheme for assessing the stability margin takes into account the influence of the main factors that cause the occurrence of an emergency state.

In work [14], the authors developed a refined method for determining the danger of derailment, where at each step of integration in the process of computer simulation of the movement of rolling stock, the procedure of comparative evaluation of the values of three coefficients of the stability margin, calculated according to the Marier formula, taking into account the K_{st_Marier} unloading, according to the pressure at the contact points K_{st_d} and the energy ratio K_{st_en}, the minimum value of the stability coefficient is selected, its value is fixed and displayed on the graph as a final value in the form of a combined stability coefficient.

The paper [15] proposes a method for assessing the sufficient condition of stability of a wheel on a rail, taking into account the probabilistic nature of the forces acting in their contact and the angle of contact of the wheel on the rail.

The given estimate is a sufficient, but not a necessary condition for the stability of the wheel on the rail, in the case of which the probability of stability will be ensured in advance.

The author of the paper [16] notes that there are several criteria for evaluating the stability of rolling stock against wheel derailment: by shifting the rail-spanning grid, by sliding the ridge, by overturning the crew, by destroying the rail-spanning grid, and by destroying the wheel track.

Practice shows that the shift of the rail sleeper grids does not occur if the ratio of the frame force acting on the wheel pair of the crew to the vertical load on the wheel is less than 0.4. For practical purposes, the author proposes to create a generalized criterion of stability of rolling stock against the wheel derailment, which will reflect the permissible level of dynamic interaction between the wheel and the rail.

The work [17] discusses some logical inconsistencies in the criteria for wheel rollout evaluations. The authors believe that, with a logical approach, the normalized value of Y/Q should be determined from the actual geometric conditions of the wheels coming off the rails, established as a result of solving the three-dimensional problem of non-linear rolling of the wheel on the rail. For example, it is possible to consider that the limit state is when the contact between the ridge and the rail occurs at the extreme point of the rectilinear section of the profile of the wheel ridge and, setting some margin, proceed to the determination of the corresponding ratio Y/Q.

Extensive research on the problems of traffic safety was carried out by the Research Institute of Railway Transport of the Japanese National Railways during the creation of the rolling stock of the New Tokaido Line. Among numerous tests, special attention was paid to issues of derailment of the wagon and its overturning. The article [18] contains a detailed report on the results obtained during theoretical and experimental research. Here, the ratio of lateral pressure to static load is adopted as a criterion for traffic safety. The maximum allowable value of this ratio depends on the growth process. Thus, when the wheel bounces, the ratio of the indicated forces is proportional to the time of the side pressure, and when the wheel rolls onto the head

of the rail, the ratio of forces equal to 0.8 is taken as the limit. The same criterion found a place in the work [62].

The paper [19] compares the North American, British and European approaches to traffic safety assessment. The authors conclude that the British and European criteria contain limit values for the forces transmitted from the crew to the track. The North American approach does not limit the maximum forces acting on the track, but rather limits the static loads on the track.

In the British approach, there are limitations of vertical and horizontal forces, and the European one - only horizontal transverse ones.

In [20], it is said that a method of indirect determination of the coefficient of stability reserve k_y, against the departure of the wheel from the rails, which uses the correlation dependence of k_y on the transverse accelerations in the pivot (heel) cross-section of the wagon, was proposed. From the experimental data, the authors of the work [20] showed that in the modes of movement of the passenger wagon, which are far from the emergency ones, the determination of the ku coefficient based on the results of the measurement of the horizontal transverse accelerations of the bolt section of the floor of the wagon is associated with great inaccuracy.

The formula for calculating the coefficient of stability reserve against a wheel derailment when processing the results of running dynamic tests of railway rolling stock is derived on the assumption that the inertia force acting on the wheel pair is insignificant compared to the frame force. For a loaded wagon, this is quite reasonable. However, when studying empty wagons, it becomes necessary to take into account the inertia force acting on the wheel pair, since in this case the ratio of the sum of the masses of all wheel pairs to the weight of the wagon increases by 3-4 times (compared to the same ratio for a loaded wagon). Therefore, in work [20], the specified approach to determining the margin of stability was implemented and the value of this value was determined in several experiments. It turned out that the values of the coefficient of stability of the wheel against the derailment of the wheel,

calculated taking into account the forces of inertia, differ by hundredths of a fraction. Therefore, it can be calculated without taking into account the forces of inertia.

1.2.1 Lateral impact of the rolling stock on the track

The requirements regarding the level of forces of interaction between wheels and rails were introduced in order to limit the risks of damage to the upper structure of the track or rapid deterioration of its parameters. These parameters in particular include: track stiffness, level of unevenness, etc. A slight excess of the permissible values of the interaction forces does not mean an imminent threat to the safety of the vehicle. However, such a danger can arise in a short period of time, especially in areas with high train speeds.

In addition to the specified limit on the ratio *Y/Q* under the conditions of stability of the wheels from rolling onto the rail heads, on the railways of European countries, criteria for the lateral impact of the rolling stock on the track are used to assess the safety conditions of the movement of locomotives and wagons. Thus, the magnitude of lateral forces is limited in order to minimize the risk of shear of the rail-sleeper grid. The limit value of the sum of lateral forces ΣY_{max} in kN is determined depending on the axial load P0 according to the expression[13]:

$$\Sigma Y_{\max,\lim} = k_1 (10 + P_0/3), \qquad (1.3)$$

where the coefficient k_1 = 1.0 – for traction rolling stock and passenger wagons and k_1= 0.85 – for freight wagons.

The following restrictions are imposed on the maximum values of horizontal transverse forces H, which act in the primary stage of the spring suspension on the wheel pair[13]:

$$H_{\max,\lim} = k_2 (10 + P_0/3), \qquad (1.4)$$

where the value of the coefficient k_2 is: 0.90 – for traction rolling stock and passenger wagons; 0.75 – for empty freight wagons; 0.85 – for loaded wagons.

From the point of view of the load on the track, the limit values of force action indicators are [13]:

- quasi-static directional force Y_{qst} - $Y_{qst,\lim}$ = 60 kN;

- quasi-static force acting on the wheel, Q_{qst} - Q_{qst} = 145 kN;

- the maximum force acting on the wheel, $Q_{\max}$ - $Q_{\max,\lim}$ = (90+ Q_0) kN.

Table 1.1 shows the values $Q_{\max,\lim}$ independent on the maximum permitted speed for which the crew is designed.

Due to track fatigue conditions, the vertical wheel load Q should not exceed 170 kN. Quasi-static lateral and vertical forces (Y_{qst}, Q_{qst}) acting on the track in curves are limited to the following values: $Y_{qst} \leq 60$ kN; $Q_{qst} \leq 145$ kN.

Table 1.1 – Values of maximum wheel loads

Design speeds	$Q_{\max,\lim}$
$V_{adm} \leq 160$ km/hours	≤ 200 kN
160 km/h $< V_{adm} \leq 200$ km/h	≤ 190 kN
200 km/h $< V_{adm} \leq 250$ km/h	≤ 180 kN
250 km/h $< V_{adm} \leq 300$ km/h	≤ 170 kN
$V_{adm} > 300$ km/h	≤ 160 kN

1.2.2 Calculated safety conditions for the movement of rail vehicles on railways with a gauge of 1520 mm

In contrast to the criteria for the safety of the movement of rail crews, which are used in world practice, the current regulatory documents, according to which full-scale tests of the rolling stock of the 1520 mm track are carried out, provide for the determination of calculated and measured indicators of the safety of the movement

based on the ratio of forces acting on the side of the frame structures of the running parts on wheel pairs, the so-called "frame forces" [19, 20, 21]. That is, the forces Y and Q of the direct interaction of wheels and rails are essentially not determined, on the ratio of which the stability of the wheel pair in the rail track actually depends.

According to the regulatory requirements that apply mainly on railways with a gauge of 1520 mm, the safety conditions for the movement of wagons, locomotives and rolling stock are determined, first of all, by the coefficient of stability of the wheelset against derailment - [k_{cc}19, 20, 21]. In addition, for wagons, there is also a check for stability against overturning under the action of lateral forces when moving in curved sections of the track according to the coefficient of the margin of transverse stability - k_{sp} [19].

1.2.3 Stability of wagons in the rail track

The stability of the wagon wheelset is estimated by the factor of stability reserve of the wheelset against derailment under the condition that the wheel crest rolls onto the head of the rail. In order to predict situations in which there is a threat of wheelsets derailment, their stability in the rail track is checked by the values of the coefficient . The calculation of values is performed for unfavorable combinations of horizontal and vertical forces acting on wheel pairs during movement, according to the formula [$k_{cc}k_{cc}k_{cc}$19]:

$$k_{cc} = \frac{tg\beta - f_{fr}}{1 + f_{fr} \cdot tg\beta} \cdot \frac{P_{vc}}{P_{hc}} \geq [k_{cc}] \qquad (1.5)$$

where β - the angle of inclination to the horizon of the generative cone-shaped surface of the wheel crest; f_{fr}- friction coefficient of sliding surfaces of wheels and rails interacting; P_{vc} - the vertical component of the forces acting from the wheels to

the rails; P_{hc} - the horizontal component of the forces of interaction between the wheel and the rail, which acts simultaneously with the force P_{vc}.

In formula (1.4), the ratio of the vertical and horizontal component forces acting from the wheels to the rails is determined as follows [19]:

$$\frac{P_{vc}}{P_{hc}} = \frac{P_{la}\left[\frac{2(b-a_2)}{l} - k_{vd}^{*}\frac{(2b-a_2)}{l} + k_{vd}^{**}\frac{a_2}{l}\right] + q\frac{b-a_2}{l} + \frac{r}{l}H_p}{f_{fr}\ P_{la}\left[\frac{2(b-a_1)}{l} + k_{vd}^{*}\frac{a_1}{l} - k_{vd}^{**}\frac{(2b-a_1)}{l}\right] + f_{fr}\ q\frac{b-a_1}{l} + \left(1-\frac{r}{l}f_{fr}\right)H_p}, \quad (1.6)$$

where P_{la}- static load on the axle neck;H_{p}– horizontal transverse force acting on the wheel pair from the side of the bogie frame (frame force); q - weight of unsprung parts; $2b$ - the distance between the centers of the necks of the axle of the wheel pair; a_1, a_2 -projections on the axis of the distances from the points of contact with the rails of the running and non-running wheels, respectively, to the middle of the necks; r - the radius of the rolling circle of a medium-worn wheel; l - the average distance between the points of contact of the wheels with the rails; $k_{vd}*\ and\ k_{vd}**$ - coefficients of vertical dynamics for running and non-running wheels.

Maximum allowable values of the coefficient of stability of the wheel pair from derailment $[k_{cc}]$ are taken as equal:

- for passenger wagons $[k_{cc}]$ = 1.6;
- for isothermal wagons $[k_{cc}]$ = 1.4;
- for freight wagons $[k_{cc}]$ = 1.3.

The stability of wagons against overturning is evaluated when they move along curved sections of the track. At the same time, two calculated cases of overturning of wagons are analyzed: outside or inside the curve. In the first case, we consider the movement of a wagon as part of a train with the maximum permissible speed for a curve with a given radius and rise of the outer rail. At the same time, centrifugal and

wind loads directed outside the curve, as well as transverse components of longitudinal quasi-static compressive forces are taken into account. In the second case, we consider the movement of the wagon in the traction mode of the train at low speed. At the same time, wind loads directed inside the curve are taken into account, as well as transverse components of quasi-static tensile forces in the train.

Coefficient k_{ls} is determined by the formula [19]:

$$k_{ls}\frac{P_{st}}{P_{dv}} \geq [k_{ls}] \qquad (1.7)$$

Where P_{st} - vertical static pressure force of the wheel on the rail, taking into account the unloading under the action of the vertical components of the longitudinal forces acting on the wagon through the coupling; P_{dv} - the dynamic vertical force of the pressure of the wheel on the rail, which is caused by the action of transverse forces, taking into account the movements of the centers of mass of the body and bogies.

Permissible values of the coefficient of margin of lateral stability of wagons against overturning $[k_{ls}]$ when checking the possibility of overturning the curve, they are taken as equal:

- for passenger and isothermal wagons $[k_{ls}] = 1.5$;
- for freight wagons $[k_{ls}] = 1.3$.

When checking the possibility of overturning wagons inside the value curve $[k_{ls}]$ are:

- for passenger and isothermal wagons $[k_{ls}] = 1.3$;
- for freight wagons $[k_{ls}] = 1.2$.

1.3 Analysis of existing systems to determine traffic quality and safety indicators

In the arsenal of measuring devices that are currently used in testing rolling stock for admission to operation on railways, there are no regular systems suitable for determining the forces directly in contact with wheels and rails. Instead, rail crew responses in the form of mechanical stresses are measured in structures that are affected by wheel-rail interaction forces.

There are two ways of measuring the interaction forces between wheels and rails:

1 – due to deformations of the elements of the upper structure of the track;

2 – due to deformations of elements of running parts.

The first method is used mainly in tests regarding the effect of rolling stock on the track and consists in equipping a certain section of the rail track with measuring devices. That is, the measurements are carried out on a limited section of the track.Today, stationary devices are quite common, with the help of which the technical condition of the rolling stock is monitored in trains passing through measuring sections of the track.Localization of stationary means of measuring force action on the track is in a certain sense useful from the point of view of detecting defects on the rolling surfaces of the wheels in order to evaluate them and make decisions regarding the removal, if necessary, of wagons from trains for repair.

The current methods of full-scale tests of rolling stock on railways with a gauge of 1520 mm provide for the determination of traffic safety indicators, namely the coefficients of the reserve of stability of wheel pairs against derailment, based on the forces acting on the frame structures of the running parts on the wheel pairs, that is, on the frame forces. Further, the corresponding calculation is carried outan attempt to estimate the ratio of forces acting in the contacts of wheels and rails.

In addition to the fact that the frame forces do not give a direct picture of the force interaction between the wheels and the rails, when conducting running tests of the rolling stock, schemes are used, the reliability of the data obtained with their help is questionable. From this follows the need for scientific substantiation of technical proposals regarding direct measurements of the forces of interaction between wheels and rails to determine the actual margin of stability of wheel pairs from derailment. This will make it possible to increase the level of train traffic safety and increase the effectiveness of forecasted evaluations of dynamic indicators of rolling stock, which will generally improve the conditions for the prevention of traffic events related to derailment of wheelsets.

Modern approaches to the assessment of traffic safety conditions, based on the direct determination of the interaction forces between wheels and rails, have no alternatives when it comes to the introduction of high-speed passenger transport. At the same time, it is advisable to take advantage of the experience gained by the railways of the world in the introduction of high-speed and high-speed traffic. This experience shows that k the fundamental solution to the problem of determining the actual margin of stability of wheel pairs in a rail track is the direct measurement of the interaction forces between wheels and rails.

Experimental studies of traffic safety conditions on EU high-speed rolling stock railways are based on application measuring wheel pairs, that is, wheel pairs equipped with devices for direct measurement of the interaction forces between wheels and rails. According to this method, the forces of interaction between the wheel and the rail are measured with the help of strain gauges installed on the elements of the wheel pair and combined into the corresponding strain gauge bridges.

The use of measuring wheel pairs gives a number of advantages. Such instrumentation provides direct measurement of instantaneous values of contact forces in the wheel-rail system. Direct measurement is opposed to indirect or approximate, which involves determining the forces of interaction of wheels with rails due to deformations of the supporting structures of the running parts.

Among the methods of experimental determination of the wheel-rail interaction forces, the method based on the deformation measurements of the wheel disks is gaining widespread use nowadays. There are a number of different projects within this method. The basic principle is the measurement of stresses in specific places on the wheels.

The Swedish firm Interfleet Technology occupies a leading position in the technology field of so-called instrumented wheel pairs. Currently, on the basis of 50 years of experience, Interfleet Technology has developed projects for measuring wheel pairs IWT (Instrumented Wheelset Technology), among which the IWT3 system is intended for wide use with the ability to measure forces with high-frequency components (Fig. 1.8).



Figure 1.8 – Wheel pair of the system IWT3

The new IWT4 system is fundamentally different from previous projects, using radio telemetry and new software. This system offers a solution using existing wheel pairs without any structural interventions, such as drilling or other machining (Fig. 1.9).

For technologyIWT4measurement of the interaction forces between wheels and rails is carried out using the method of wireless transmission of readings from the strain gauges installed on the wheel pairs to the processing system in the train. Figure 1.8 shows a demonstration display of the IWT4 equipment (Figure 1.9a) and an example of its use on full-scale tests of rolling stock (Figure 1.9b).

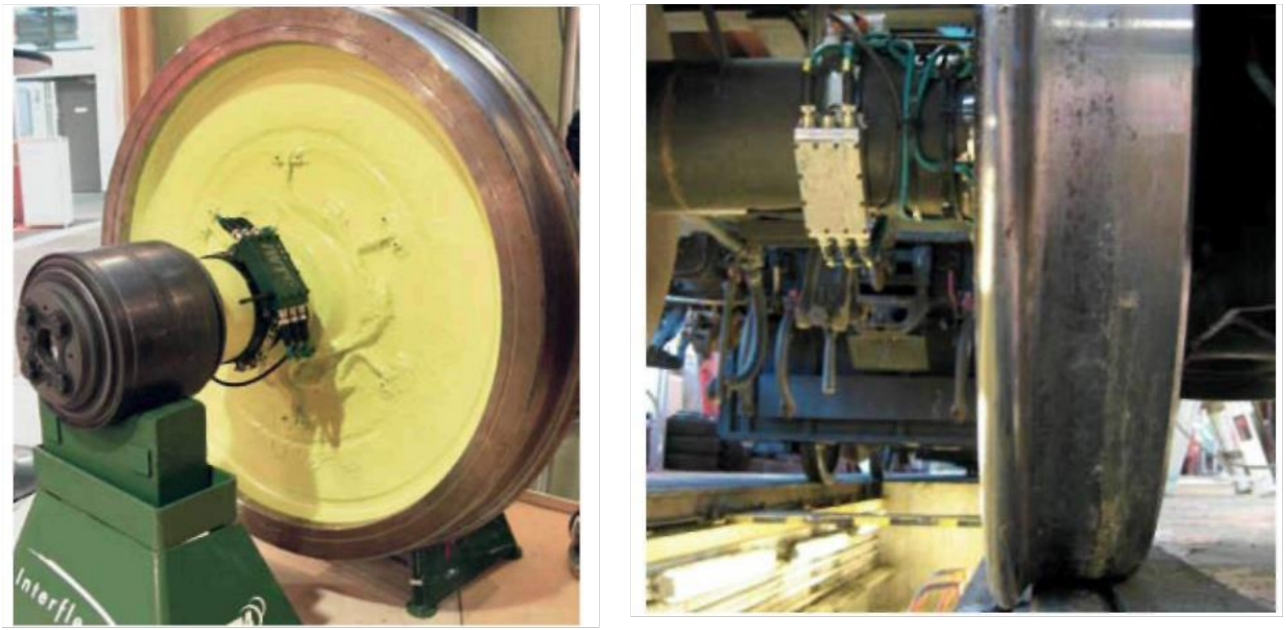

a b

Figure 1.9 - Wheels with equipmentIWT4

In the systemIWT4with signals are digitized on the wheel using a specially designed analog-to-digital converter. This minimizes the length of cables carrying analog signals, thereby reducing the risk of electromagnetic interference degradation of signal quality. The analog-to-digital converter processor, mounted on the wheel pair, provides anti-interference filtering, time requantization and data conversion, after which the digital signals are transmitted using radio telemetry. This, in turn, eliminates the need to use current collectors or other devices. The on-board radio

receiver receives the signals, which are then processed in real time using force-calculating software.

As part of the development process, the system was tested by IWT4 on passenger and cargo crews, using both standard and shortened axles, on driven and non-driven wheel sets, and at speeds in excess of 250 km/h. The system was also tested on interference resistance, temperature test in a climatic chamber, shock and vibration test. The conducted tests confirmed compliance with the requirements of European directives.

KMT Kraus Messtechnik GmbH (Germany) devices are also an advanced system, in particular the MPT-NT model. Based on the fact that the measurements are carried out on an element that rotates, wireless data transmission is used from strain gauges located on the wheel discs to the receiving unit of the equipment. Each sensor module is equipped with a signal converter, anti-spectral filters, an ADC converter and a digital output. Up to 32 modules can be used, which are controlled by a decoder. This structure allows the data acquisition modules to be installed close to the sensors to provide a short distance for the analog sensor lines, which avoids unwanted interference. For interference-insensitive digital outputs, the distance to the encoder module can be up to 5 m. The output of the encoder is presented as a stream of PCM binary signals that can be modulated for the transmission unit.

Different types of high-frequency transmitters allow the system to be used for a wide range of measurements. The system can be used at different distances at different transmission speeds (40, 320, 640, 1280 or 2560 kbit/s). The schematic diagram of the measuring system is presented in Figure 1.10.

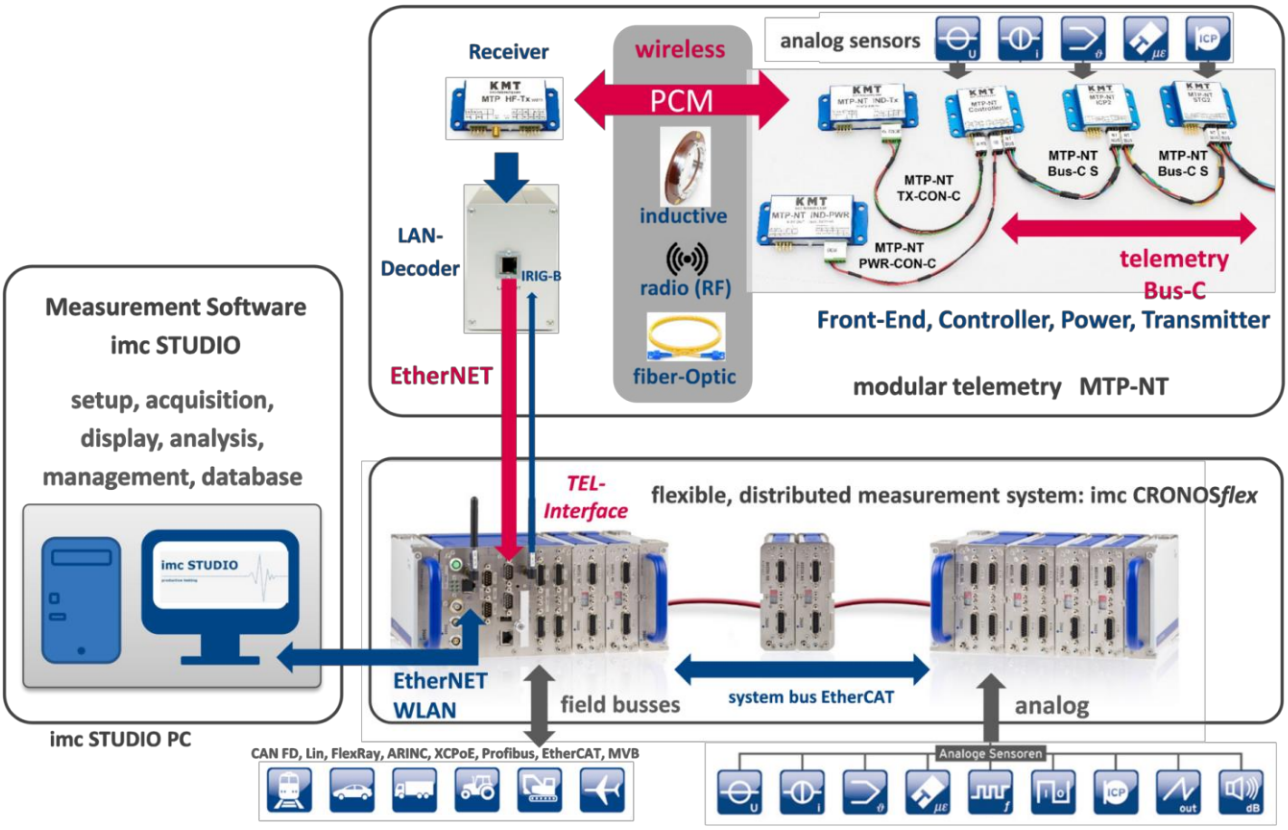

Figure 1.10 – Kraus Messtechnik MPT-NT system

Strain gauges are assembled in such a way that they form a strain gauge half-bridge. Figure 1.11 represents the interaction of the strain gauge half-bridge with the MTP-NT storage equipment module. The MTP-NT equipment allows compensating for asymmetries of the strain gauge bridge. Channels of the MTP-NT equipment are used to measure deformations using strain gauges. In addition, if necessary, acceleration sensors can be connected to the MTP-NT equipment.

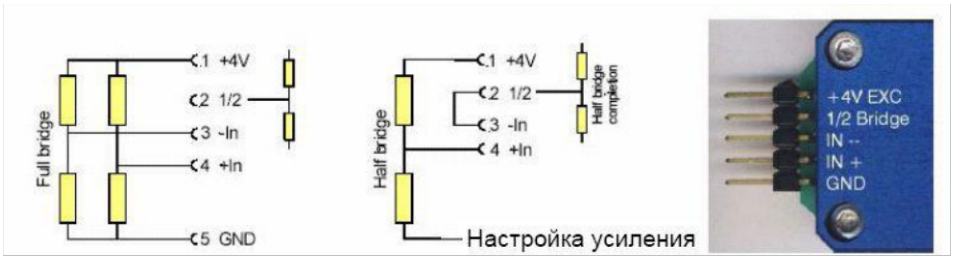

Figure 1.11 – Connecting the strain gauge bridge/half bridge to the storage module

Figure 1.12, 1.13 shows examples of the use of the system in railway transport and the general view of the system.

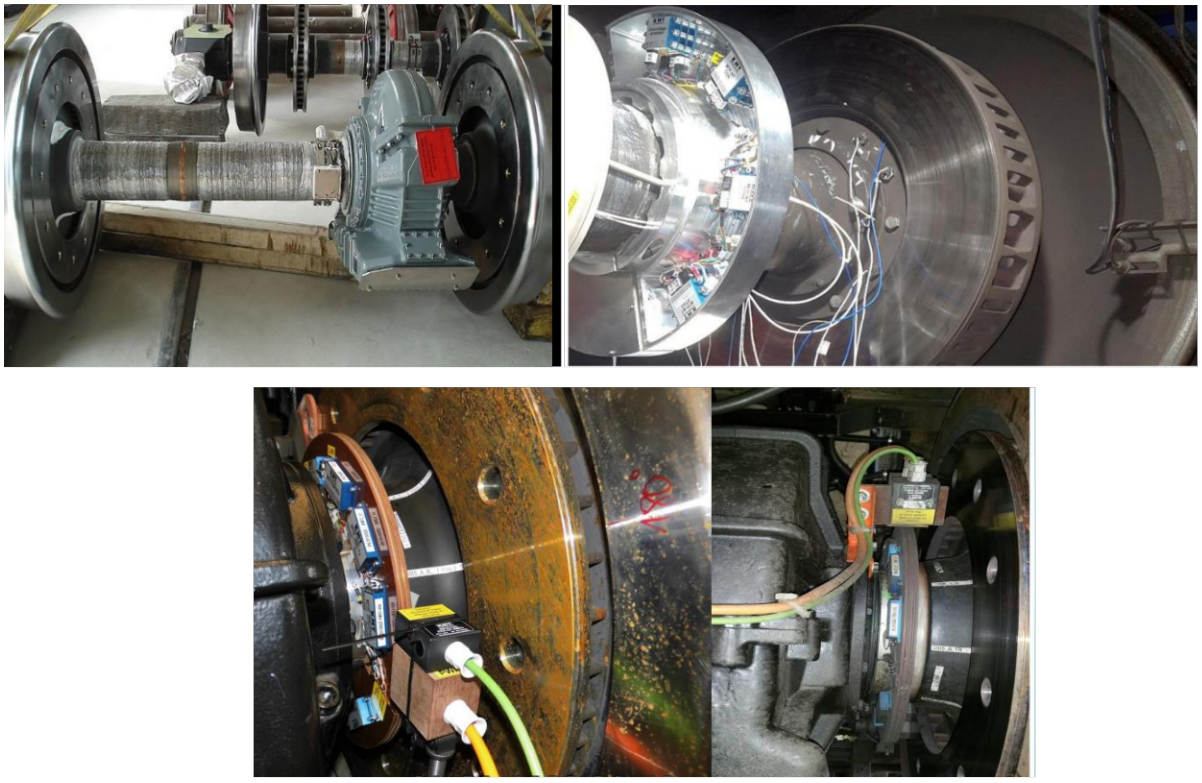

Figure 1.12 – Examples of using the system in railway transport



Figure 1.13 - General view of the measuring system

1.4 Analysis of existing projects to improve the quality and safety indicators of carriage movement

This section presents general information on the types of individual three-element bogies, which are analogues of 18-100 with improved technical and economic indicators, the main differences of which are increased intervals between repairs, improved dynamics indicators, technological features of manufacturing and maintenance. The list of analogues of type 18-100 bogies includes: bogie 18-4112 Dniprovagonmash (Fig. 1.14), 18-9771 "PromtractorVagon" (Fig. 1.15), 18-9810 OJSC "NVC "Vagony", Tikhvin Wagon Building Plant (Fig. 1.16) and 18-9800 VNIKTI (Kolomna) (Fig. 1.17), Barber S-2-R (fig. 1.18), 18-7020 Kryukivskyi VBZ (fig. 1.19) and 18-194-1 OJSC "NPK" Uralvagonzavod (fig. 1.20), bogies model 18-578 and18-9836 JSC NPK Uralvagonzavod (Fig. 1.21 and 1.22, respectively), bogie model 18-4129 "Sofia-Invest" LLC (Fig. 1.23), 18-9750 "Vagony" NVT (Fig. 1.24), bogie 18-7033 type 3 Kryukiv VBZ (Fig. 1.25), bogie 18-7055 type 2 Kryukiv VBZ (Fig. 1.26). Figure 1.27 shows a ZK-1 type bogie. Figure 1.28 shows an examplepromising welded structure of the side frame of the bogie, which is currently undergoing bench resource tests at the E. O. Paton Institute of Electric Welding.

The main project of modernization of type 18-100 bogies in Ukraine is the modernization of C 03.04 with the use of constant contact sliders by A. Staki, improvement of wedges, wheel grooving according to the ITM-73 profile. Analogous are modernization projects C 14.01, M1698. The most profitable is the modernization of new wagons according to the C03.04 project. The discounted payback period is 2.1 years for the C 03.04 project and 2.3 years for the M1698, which is more than twice as effective as for other modernizations. It is advisable to modernize according to the

C 03.04 project during depot repairs, starting with the first depot repair, when the wagonis in service for up to 15 years.

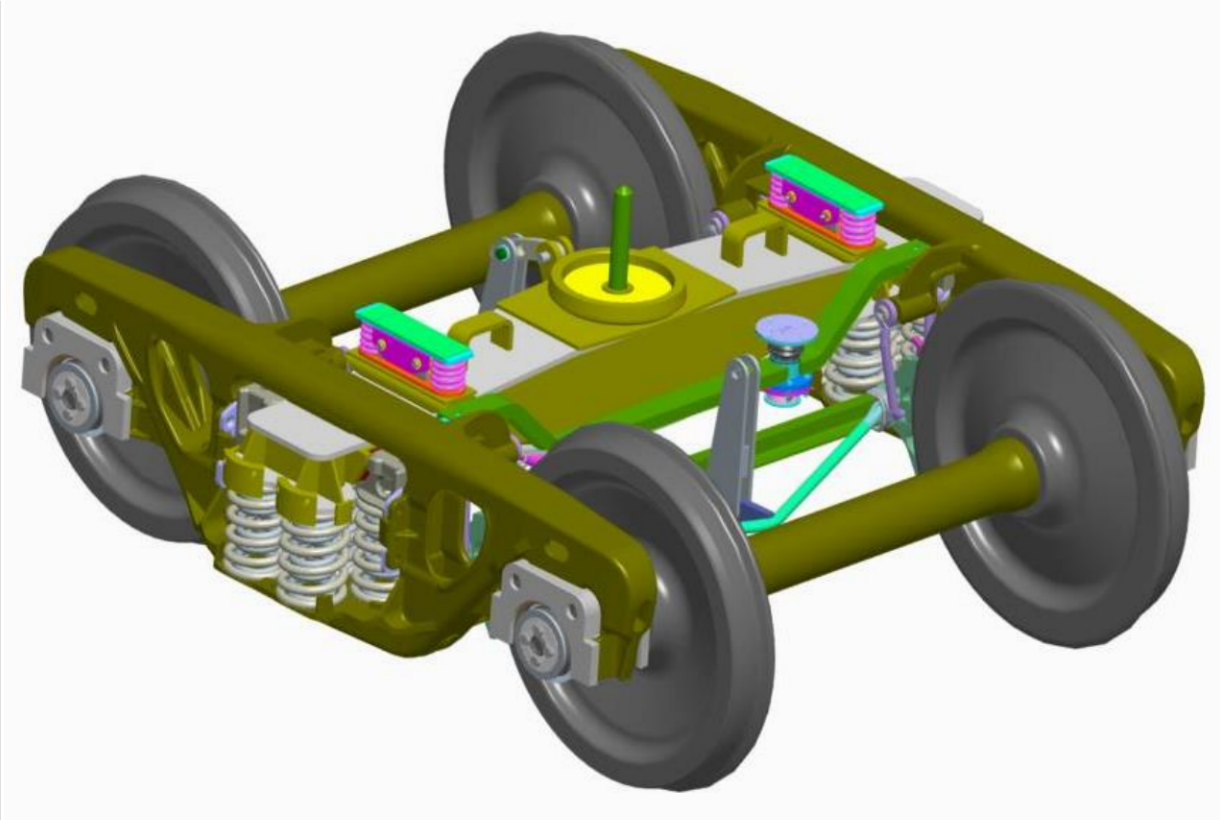

Figure 1.14 –bogie 18-4112 Dniprovagonmash

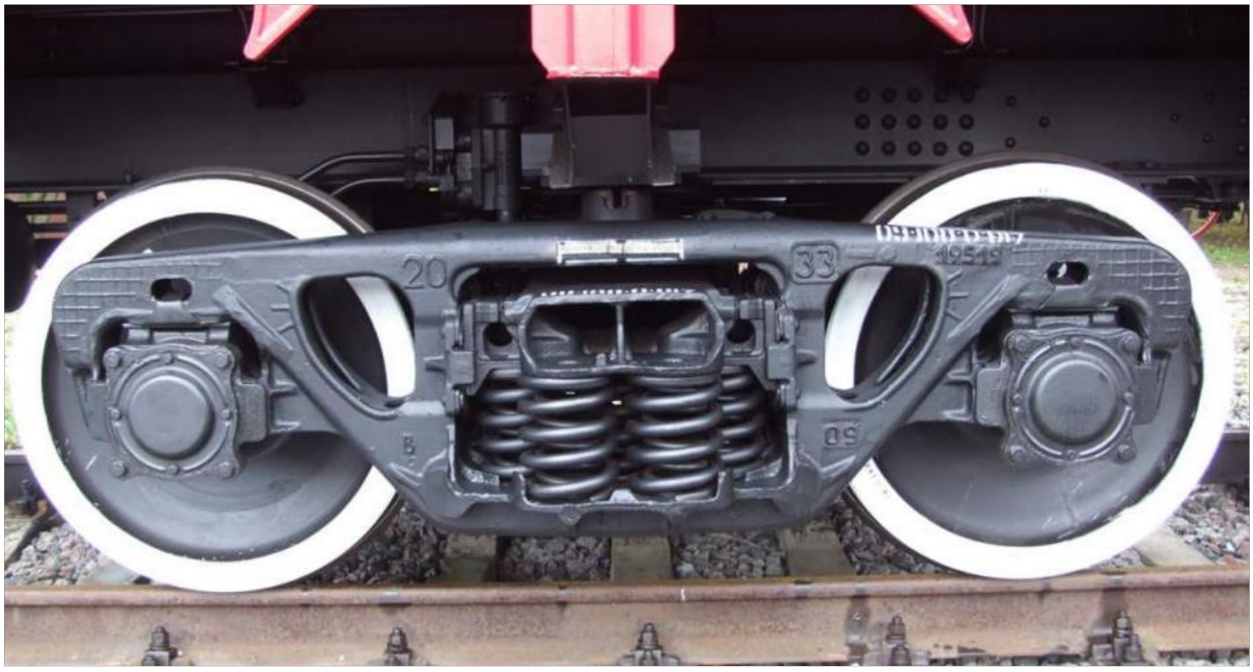

Figure 1.15 - bogie18-9771 "PromtractorVagon"



Figure 1.16 – bogie 18-9810



Figure 1.17 - Bogie 18-9800

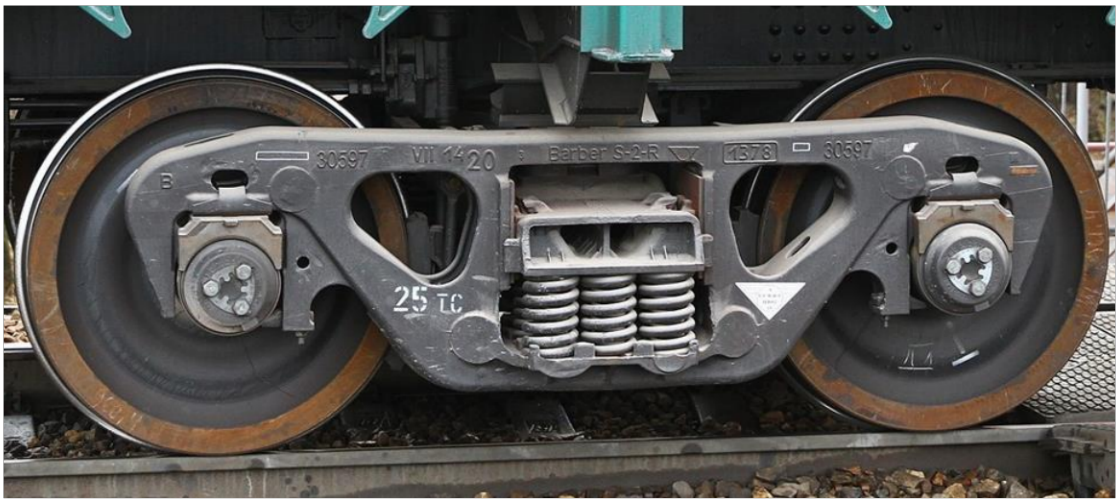

Figure 1.18 - Barber S-2-R bogie

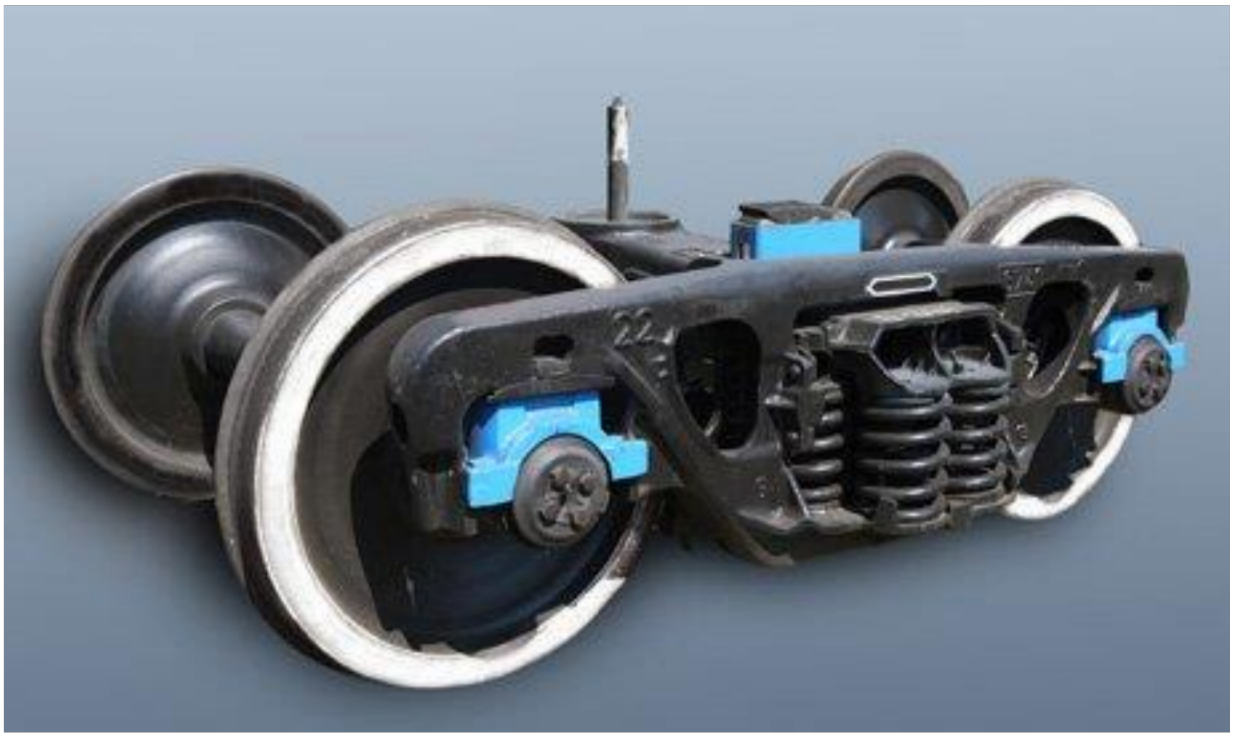

Figure 1.19 - bogie 18-7020

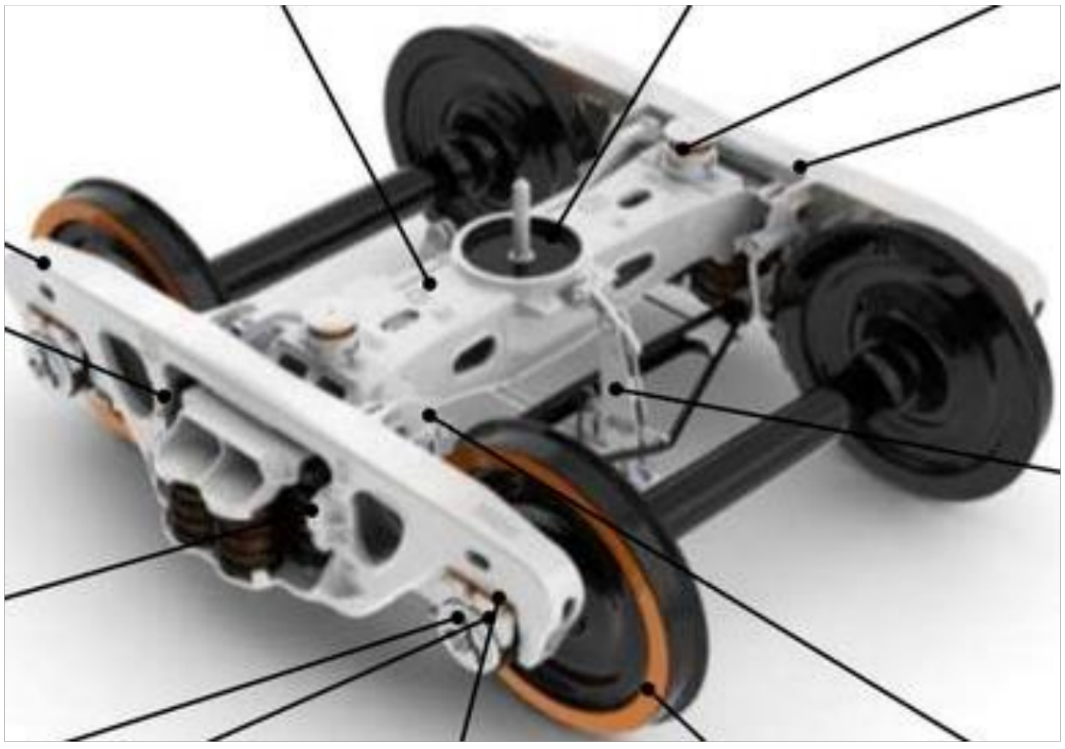

Figure 1.20 - bogie18-194-1

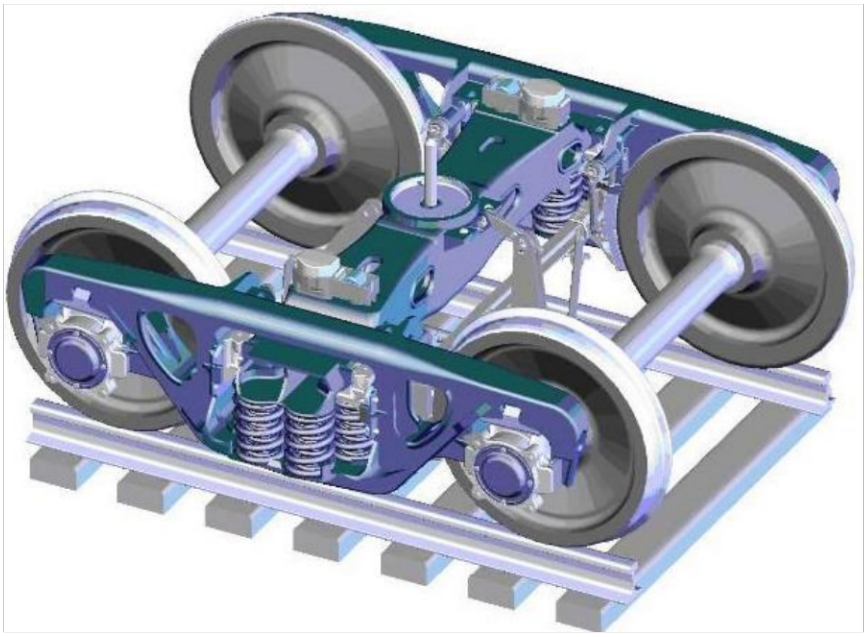

Figure 1.21– bogie 18-578



Figure 1.22 – bogie 18-9836

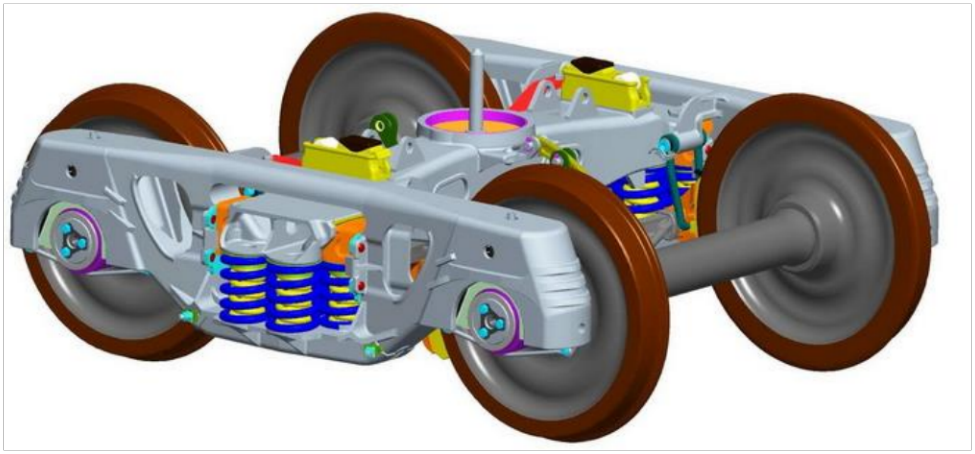

Figure 1.23 – bogie 18-4129



Figure 1.24 – bogie 18-9750



Figure 1.25 – bogie 18-7033 type 3

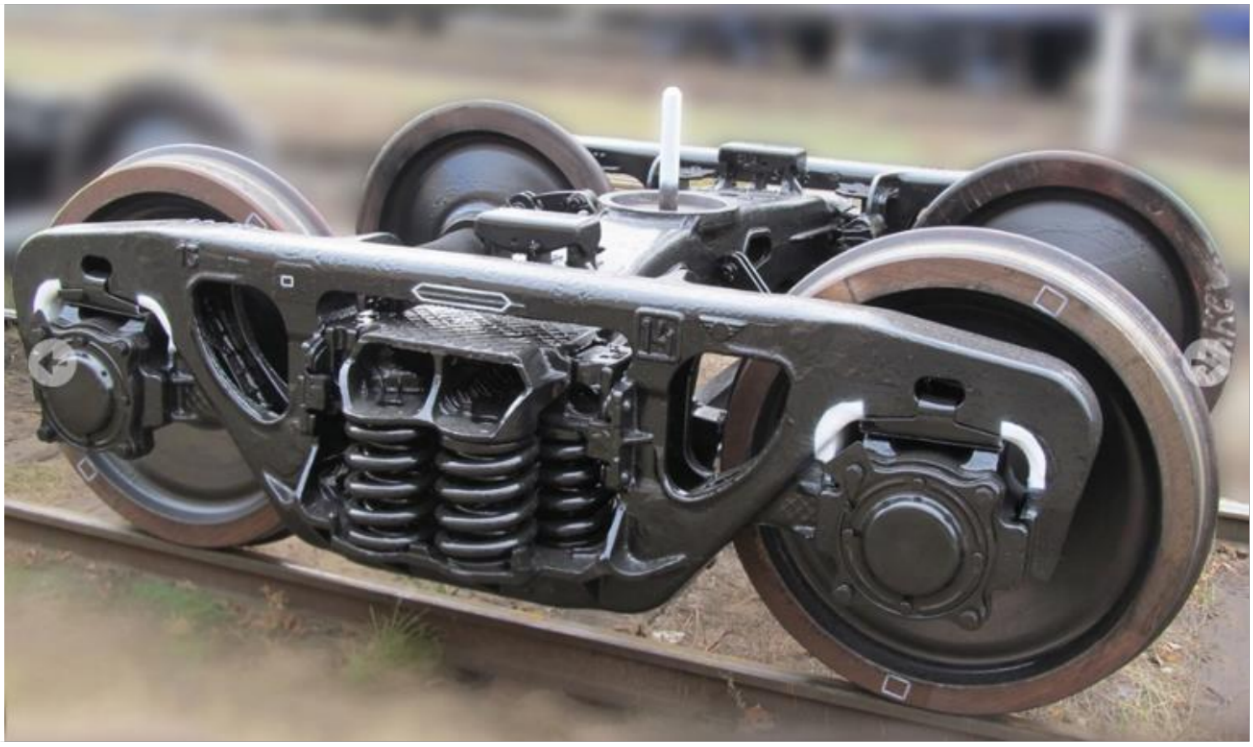

Figure 1.26 - bogie 18-7055 type 2

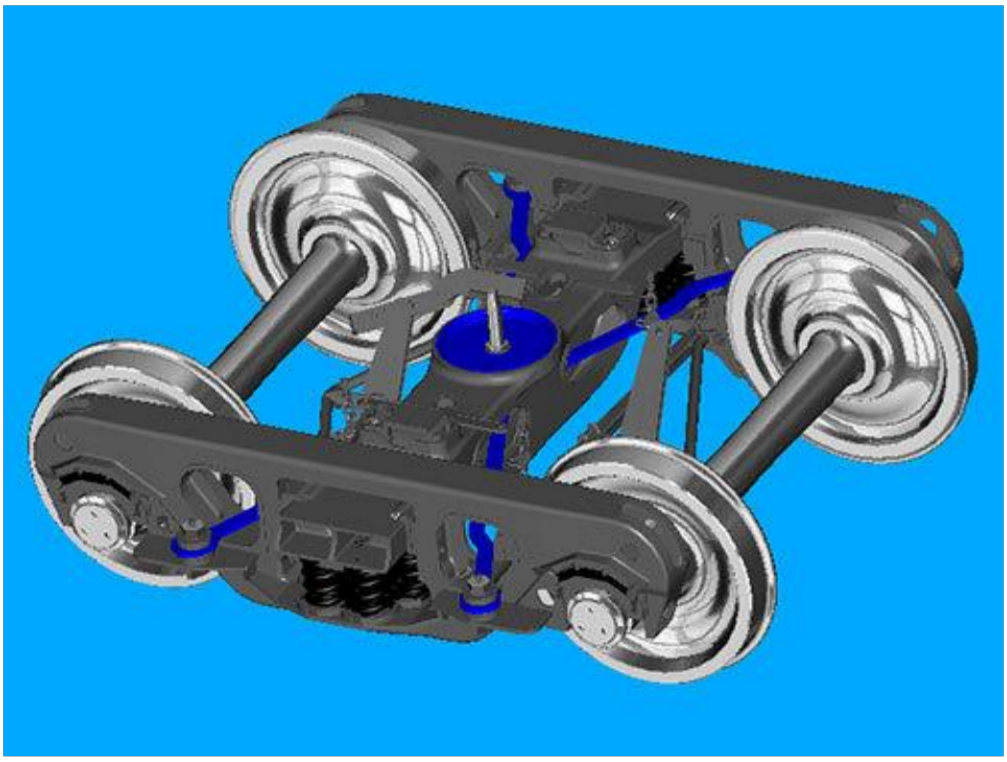

Figure 1.27 - ZK-1 bogie

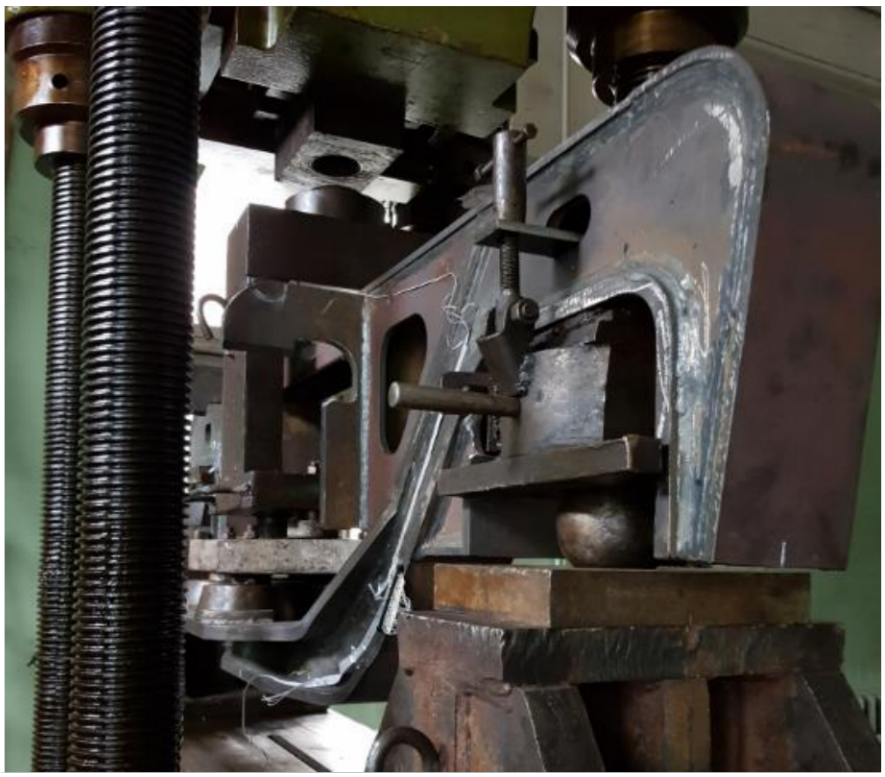

Figure 1.28 – Perspective welded structure of the side frame of the bogie

The basic and more modern than the three-element bogies is the Y25 type bogie (Fig. 1.29), which is the main one in the EU. The frame of the bogie is made of die-welded, closed structure. Single-stage box spring suspension with a friction wedge dampener. The bogie frame is supported by double-row cylindrical springs on the inflows of the box bodies. The box body is held by a jaw and has a limited movement in the vertical plane. The brake lever transmission is made with two-sided pressing of the brake pads on the wheel. Two short ventilated brake pads are attached to each brake shoe. The bogie is equipped with elastic sliders of constant contact. The suspension of the bogie is made spherical. The Y-31 and Y-37 bogies with improved dynamic qualities were created on the basis of the Y-25 bogie.

Currently, the introduction of a bogie based on the Y25 type for 1520 mm track and railways of Ukraine is relevant due to higher speeds, proven efficiency on 1435 mm tracks and a much lower dynamic impact on the rail track.



Figure 1.29– Y25 type bogie

The most recent development among the bogies of (non-motorized) wagons today is the "EfWING" bogie (Fig. 1.30), which uses carbon fiber springs. Conventional bogies use steel side frames and independent springs. Using a carbon fiber spring, efWING combines the functions of these individual components, i.e. the carbon fiber side frame is a load-bearing and elastic-dissipative element at the same time. This approach makes it possible to reduce the weight of the bogie by up to 40%.



Figure 1.30 – "EfWING" brand bogie with elastic-dissipative load-bearing elements

CONCLUSIONS ON SECTION 1

According to the results of the review and analysis of scientific and technical materials on the topic of the study, the problems of the operation of wagons were analyzed, and the problems of experimental evaluation of quality and traffic safety indicators were analyzed.

An analysis of research and existing systems for evaluating indicators of traffic quality and safety was carried out, a review of technical solutions that improve indicators of quality and safety of traffic of freight wagons was carried out.

The need for the development of scientifically based recommendations regarding direct measurements of the forces of interaction between wheels and rails to determine the actual margin of stability of wheel pairs from derailment was noted.

SECTION 2
METHODS AND APPROACHES FOR ASSESSING INDICATORS OF QUALITY, TRAFFIC SAFETY AND TECHNICAL CONDITION OF WAGONS

2.1 Measurement of deformations of load-bearing structures. General information

To measure the mechanical stresses in the surface layers of the elements of the load-bearing structures of the rolling stock, the methods and means of strain measurement are used, that is, strain gauges and recording equipment. The operation of the tensor resistor is based on the tensor effect of the conductor or semiconductor, which is attached to the surface of the supporting element of the structure with a special glue. Thus, deforming together with the metal element when it is loaded, the strain gauge changes its electrical resistance.

Tensor resistors are divided into wire, foil and semiconductor tensors by design. The wire strain gauge, schematically depicted in Figure 2.1, is a wire spiral 1 placed between two layers of thin paper 2. Terminals 3 are soldered to the spiral for connecting the strain gauges to each other in an electrical circuit. Constantan (copper and nickel alloy) or nichrome (nickel and chromium alloy) wire is used for strain gauges. The diameter of such a wire is 0.015...0.025 mm.

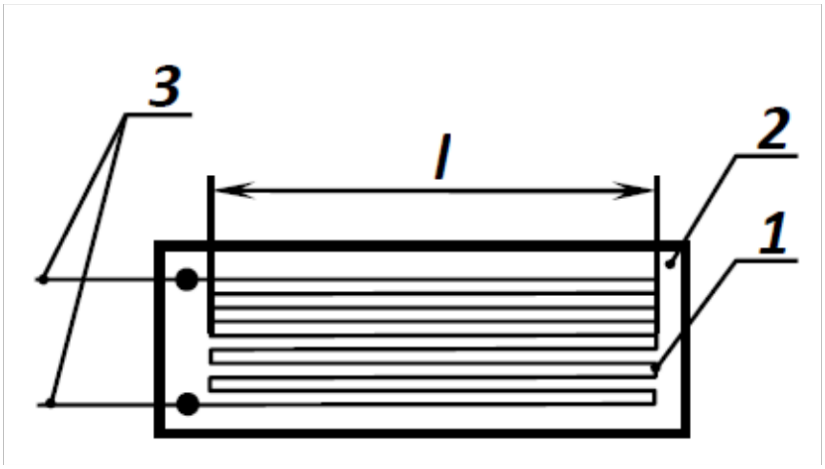

Figure 2.1 - Tensor resistor diagram

Foil strain gauges are made by etching or stamping from Constantan foil fixed on a film or paper base. Semiconductor strain gauges are made of semiconductor materials in the form of thin strips of germanium or silicon with soldered metal leads. Such strain gauges have a sensitivity 1-2 orders of magnitude higher than wire or foil ones.

The main characteristics of strain gauges are nominal resistance R, base l (see Fig. 2.1) and sensitivity ɣ. The sensitivity of the strain gauge is defined as the ratio of the relative change in resistance to its relative elongation:

$$\gamma = \frac{\frac{\Delta R}{R}}{\varepsilon} \tag{2.1}$$

where ΔR– change in the resistance of the tensor when it is deformed; – relative elongation of the conductor.ε

The change in resistance of the strain gauge during deformation is very small, usually of the order of several hundreds of Ohms. One of the most convenient means of measuring such changes is the Wheatstone bridge. It includes four resistors connected to a DC power supply, as shown in Figure 2.2.

If $R_1 = R_2 = R_3 = R_4$, this indicates that the bridge is balanced, and the voltmeter connected to the measuring diagonal of the bridge will show 0 V. The principle of

operation of the bridge circuit is that the electric current flowing through the resistors in the case unbalanced state of the bridge creates a potential difference in the measuring diagonal, and an electric current will flow through the measuring device.

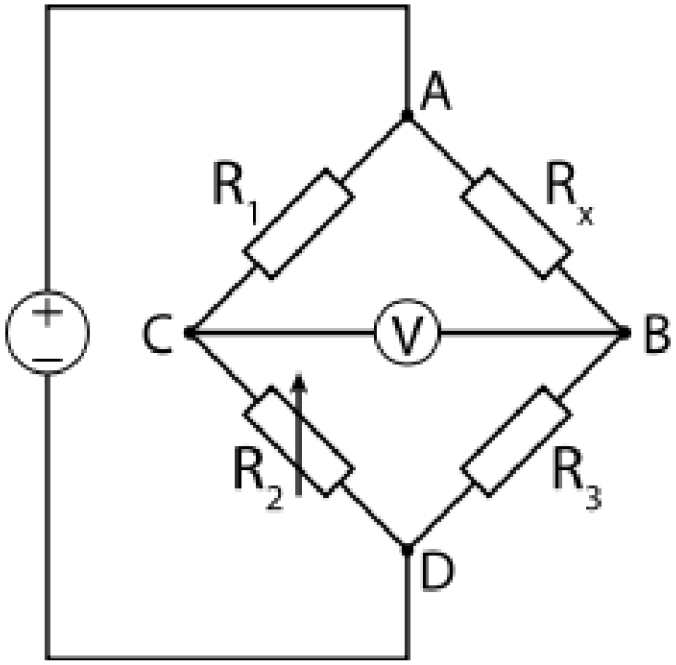

Figure 2.2 – Wheatstone bridge connection diagram with balancing

In order to measure stress, the resistors shown in Figure 2.2 are replaced by one or more strain gauges (which are usually variable resistors whose resistance changes with changes in stress). At the beginning of the test, a balancing potentiometer is used to balance the bridge, setting 0 V on the voltmeter. Applying a test load will change the resistance of the strain gauge and bring the bridge out of balance, producing a voltage proportional to the applied stress.

The bridge can contain one, two or four strain gauges according to the schemes shown in Figure 2.3 such a configuration is known as one fourth, half bridge and full bridge, respectively. Of these three schemes, one fourth of the bridge will have the lowest sensitivity. Failure to do so may result in errors, as strain gauges are sensitive to thermal effects. In order to prevent this, one of the strain gauges adjacent to the active one can be replaced by a so-called compensation one. This strain gauge is

identical to the active one, is in the same ambient conditions, but is not subjected to the load, which is achieved, for example, by installing it on an unstressed part of the object being tested. Both strain gauges are subjected to the same temperature changes, and as a result, the effect of any resulting effect on the balance of the bridge due to thermal effects is canceled out.

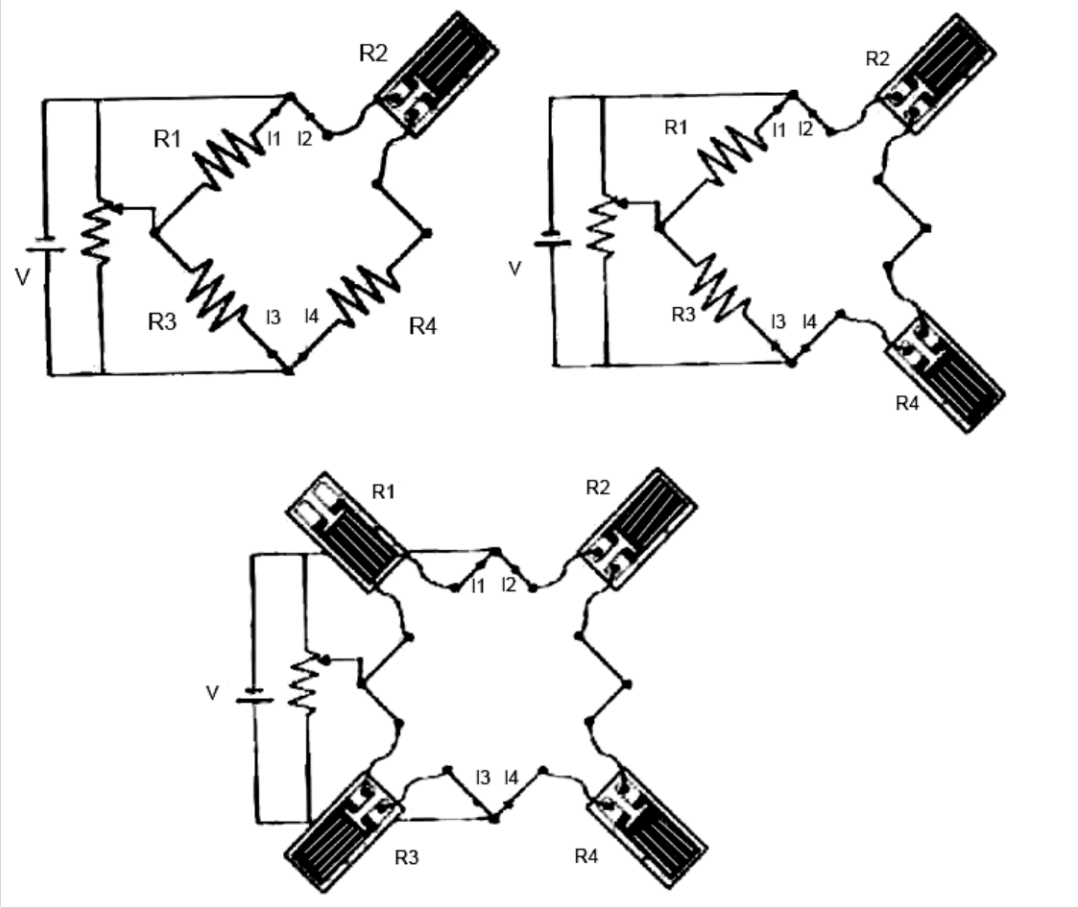

Figure 2.3 – Configurations of bridge schemes

A half bridge will have a higher sensitivity than a quarter bridge because the additional strain gauge will produce a larger unbalanced voltage across the Wheatstone bridge. The presence of two active strain gauges also excludes any thermal effects as described above. Of the three schemes, the full bridge has the highest sensitivity. In addition, it is self-compensating for temperature changes.

It should be noted that changes in the output voltage from bridges for measuring mechanical stresses are usually very small and therefore need to be

amplified as close to the bridge as possible. Cable lines must be fully enclosed and shielded to prevent distortion of test data.

When measuring the deformation of the surface of the wheel disc, a statistical method was adopted to estimate the measurement error with a probability of P=0.95. The deformation ε_i measured by the device under a unit load is determined by the formula:

$$\varepsilon_i = \frac{p \cdot U_{out}}{K \cdot U_{pov}}, \tag{2.1}$$

In which, $U_{out} = \frac{1}{n}\sum_{i=1}^{n} U_{i\,out}$

where $p = 2$– for a half-bridge scheme; U_{pov} – voltage of the measuring system supply, V; U_{out}– the average value of the output voltage, mV; K is the coefficient of tensile sensitivity (1.9 - 2.04).

Average arithmetic value of deformations $\bar{\varepsilon}$ determined by the formula:

$$\varepsilon = \frac{\sum_{i=1}^{n}(\varepsilon_i)}{m}, \tag{2.2}$$

where m is the number of measurement points.

Mean square deviation of measurement results $\tilde{\sigma}(\overset{\circ}{\Delta})$, determined by the formula:

$$\tilde{\sigma}(\overset{\circ}{\Delta}) = \sqrt{\frac{\sum_{i=1}^{n}(\bar{\varepsilon} - \varepsilon_i)^2}{m(\mathrm{m}-1)}}. \tag{2.3}$$

The sum of random and non-excluded systematic errors is determined by the formula:

$$\sigma(\Delta) = \sqrt{\overset{\circ}{\widetilde{\sigma}}(\Delta)^{2} + \widetilde{\sigma}_1(\Delta_s)^2 + \widetilde{\sigma}_2(\Delta_S)^2}, \quad (2.4)$$

where $\widetilde{\sigma}_1(\Delta_s)$ - the non-excluded remainder of the systematic error caused by the error of the measuring system; $\widetilde{\sigma}_2(\Delta_s)$ - the non-excluded remainder of the systematic error due to the error of the strain gauges. Upper $\widetilde{\Delta}_h$ and the lower one $\widetilde{\Delta}_l$ measurement error limits are determined by the formula:

$$\widetilde{\Delta}_h = \widetilde{\Delta}_l = \mathrm{tp}\,\sigma(\Delta), \quad (2.5)$$

where t_p is the Student's coefficient, which depends on the number of measurements and the given probability.

2.2 Measurement of forces by local deformations of the bogie frames

Tensometric bridges are widely used in carrying out static strength and dynamic running tests of rolling stock. For example, the method of determining vertical and horizontal transverse (frame) forces acting on wheel pairs, according to the rules that are currently in force on railways with a gauge of 1520 mm, involves the measurement of deformations of the bogie frames.

Strain gauges are pasted on the outer and inner sides of the side frames and assembled into circuits that have, as a rule, good sensitivity with sufficient compensation for temperature deformations. This method allows you to continuously measure horizontal (frame) and vertical forces when moving along a track section of any length.

Figure 2.4 shows the diagram of the installation of strain gauges on the frame of the 18-100 bogie and their connection into half-bridge circuits for measuring vertical and frame forces.

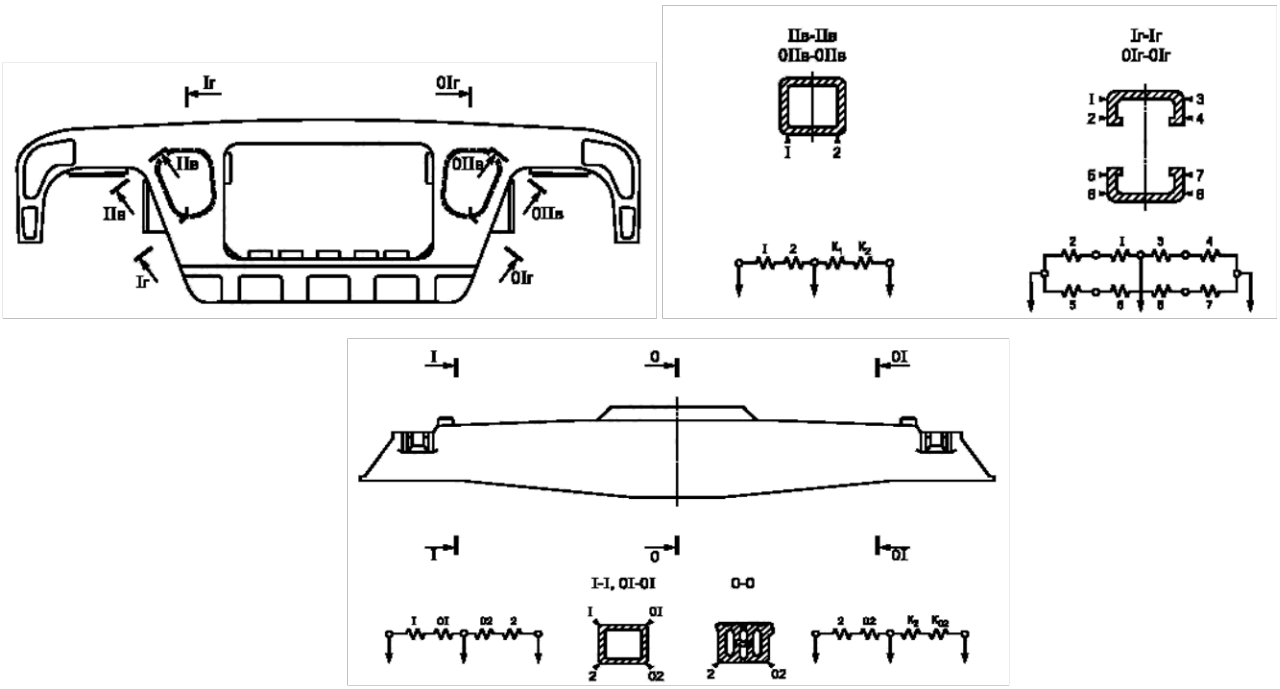

Figure 2.4 – Schematic of strain gauge placement on the bogie frame

The characteristics of the force action measured in this way in the "bogie frame - wheelset" system are calculated using the calculation method to estimate the forces of interaction between the wheels and the rails, the ratio of which determines the so-called reserve coefficient of stability of the wheel from leaving the rail.

2.3 Measurement of forces of direct interaction of wheels with rails

One of the important aspects in the system of direct measurement of the forces of the contact interaction between wheels and rails is the determination of the zones of deformation sensitivity on the wheel disks from the action of vertical and lateral forces. From the determined zones, it is important to localize those in which the deformations were the result of the action of forces in one direction.

To determine these zones, a finite element calculation was performed for three calculation schemes:

a) vertical load of the wheel pair;

b) loading by vertical forces and forces from the action of the tare systems;

in)loading of the wheel pair by vertical and horizontal forces when passing curved sections of the track.

Below are the results of the characteristic calculations for the specified load patterns of the wheel pair.

Vertical load. Based on the task of the research, in order to ensure greater visibility of the results, the maximum value in the legend of the graph was reduced to 10 MPa, since these are the stresses that occur on the wheel disc.

Figure 2.5 shows a picture of the distribution of calculated stresses in the elements of a wheel pair under the action of a vertical load. As can be seen, the greatest stresses occur in the wheel disc at the point of transition of the disc to the hub part of the wheel and amount to 7.78 MPa, as well as in the hub transition between the neck and the hub part - 46 MPa.

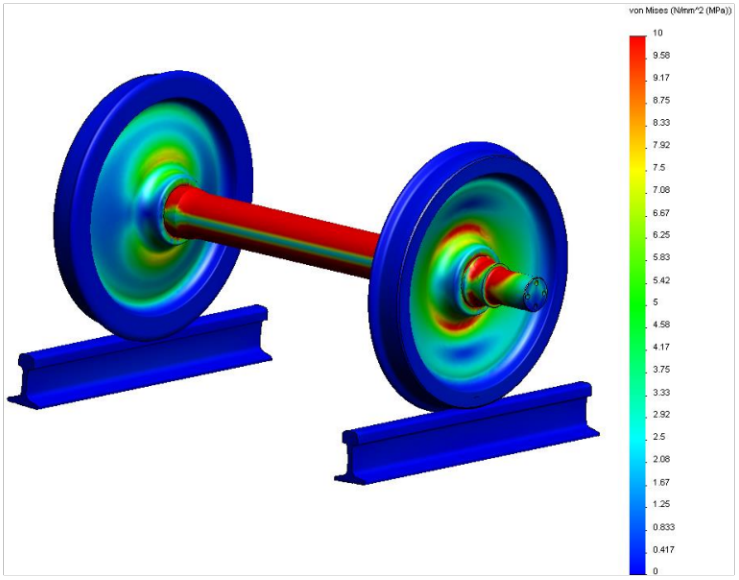

Figure 2.5 – Diagram of equivalent stresses arising in a pair of wheels under vertical load

In the axis of the wheelset, which mainly works for bending, the stresses in the cross sections are unevenly distributed, reaching the largest values in the outer fibers and the smallest in the inner ones, as shown in Figure 2.6.

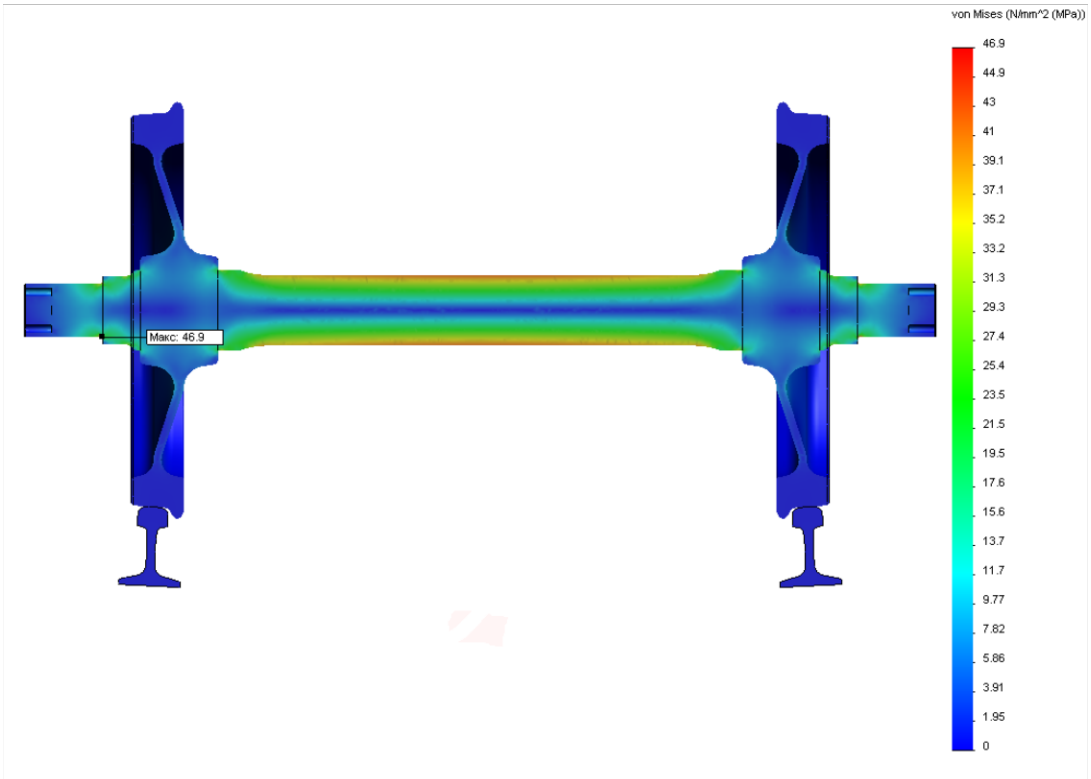

Figure 2.6 –The graph of equivalent stresses arising in a pair of wheels (in cross-section)

Figure 2.7 shows the diagram of normal radial stresses.

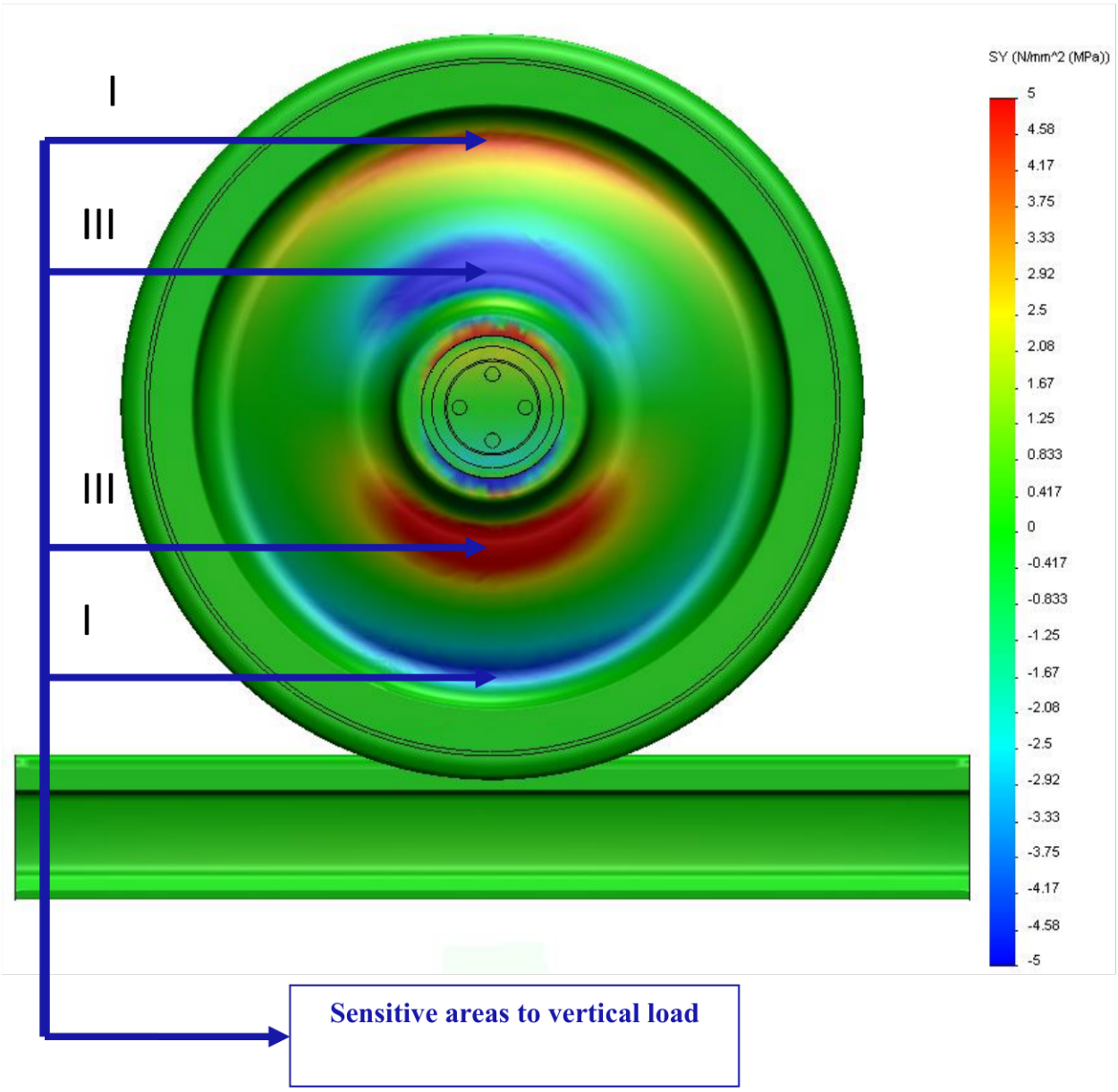

Figure 2.7 – Diagram of normal radial stresses under vertical loading

Figure 2.8 presents a graph of equivalent stresses, from which it can be seen that when simulating the action of the tare device, the greatest stresses occur in the places between the hub part and the disk and amount to 10.49 MPa.

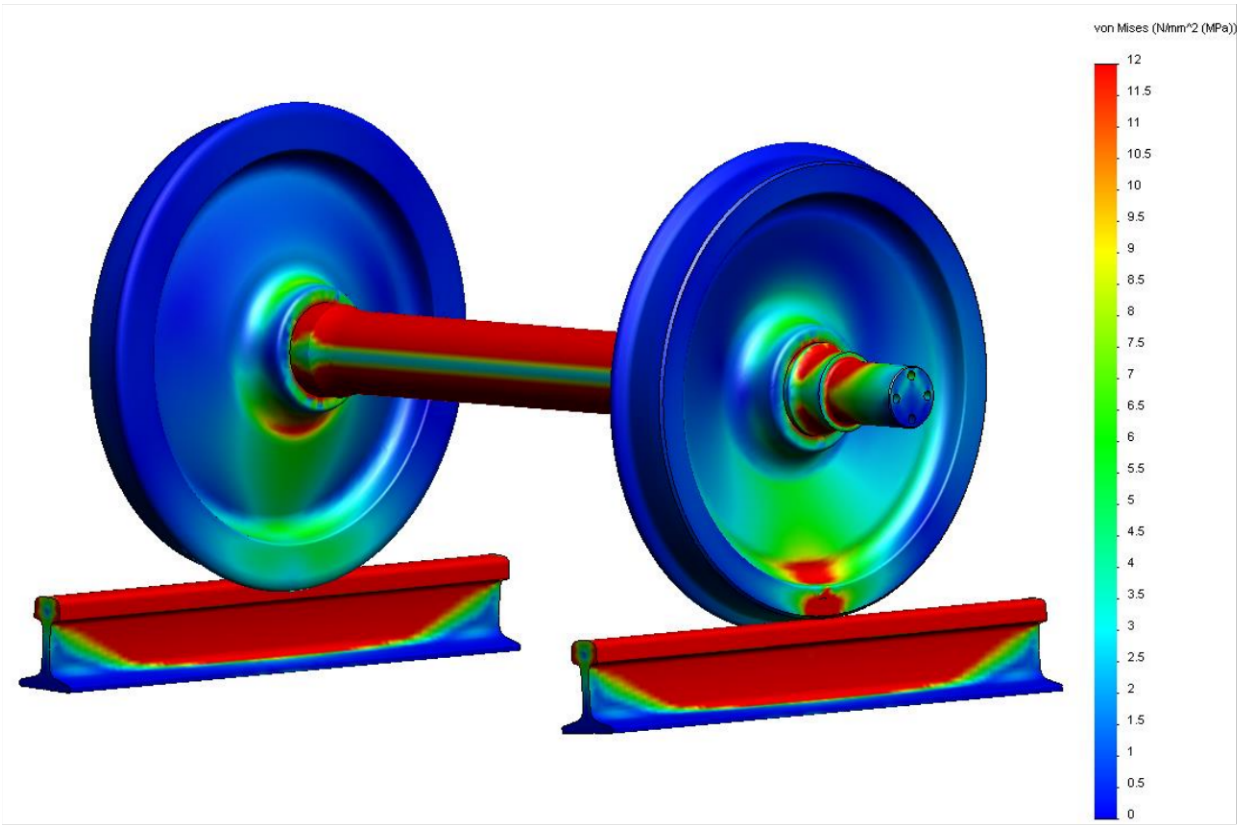

Figure 2.8 – Diagram of equivalent stresses arising in a pair of wheels when loaded with a tare device

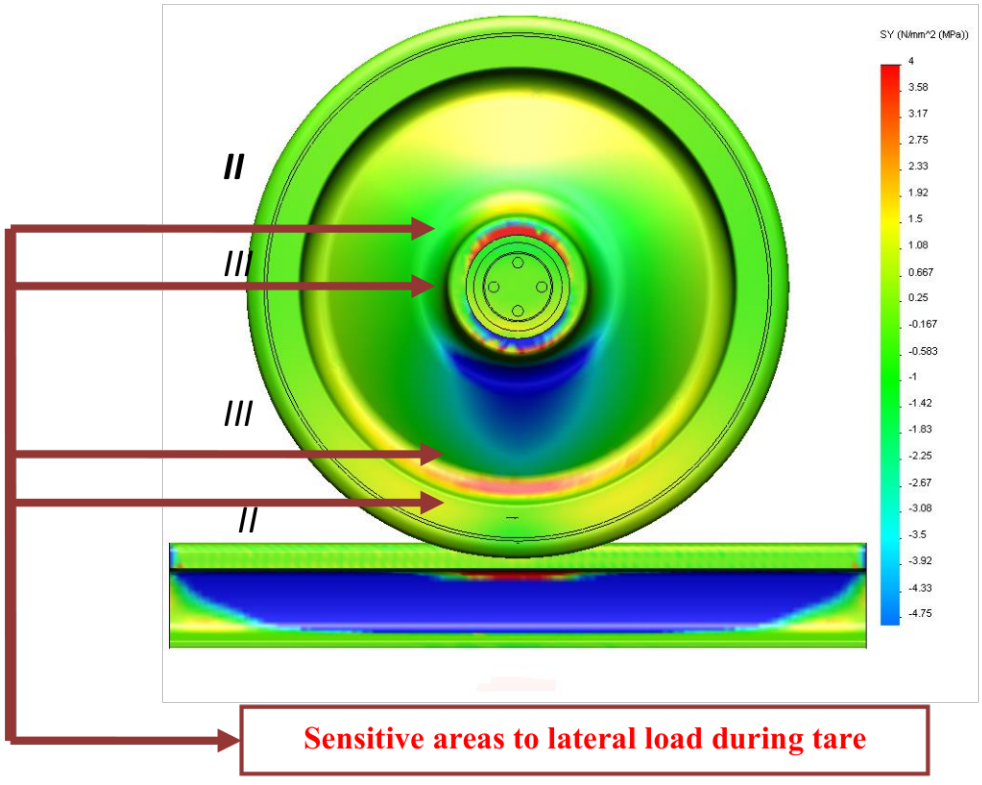

Figure 2.9 – Chart of normal radial stresses during calibration

Figure 2.10 shows a graph of equivalent stresses, from which it can be seen that when simulating the action of a lateral load, the greatest stresses occur in the places between the hub part and the disk and are equal to 12 MPa.

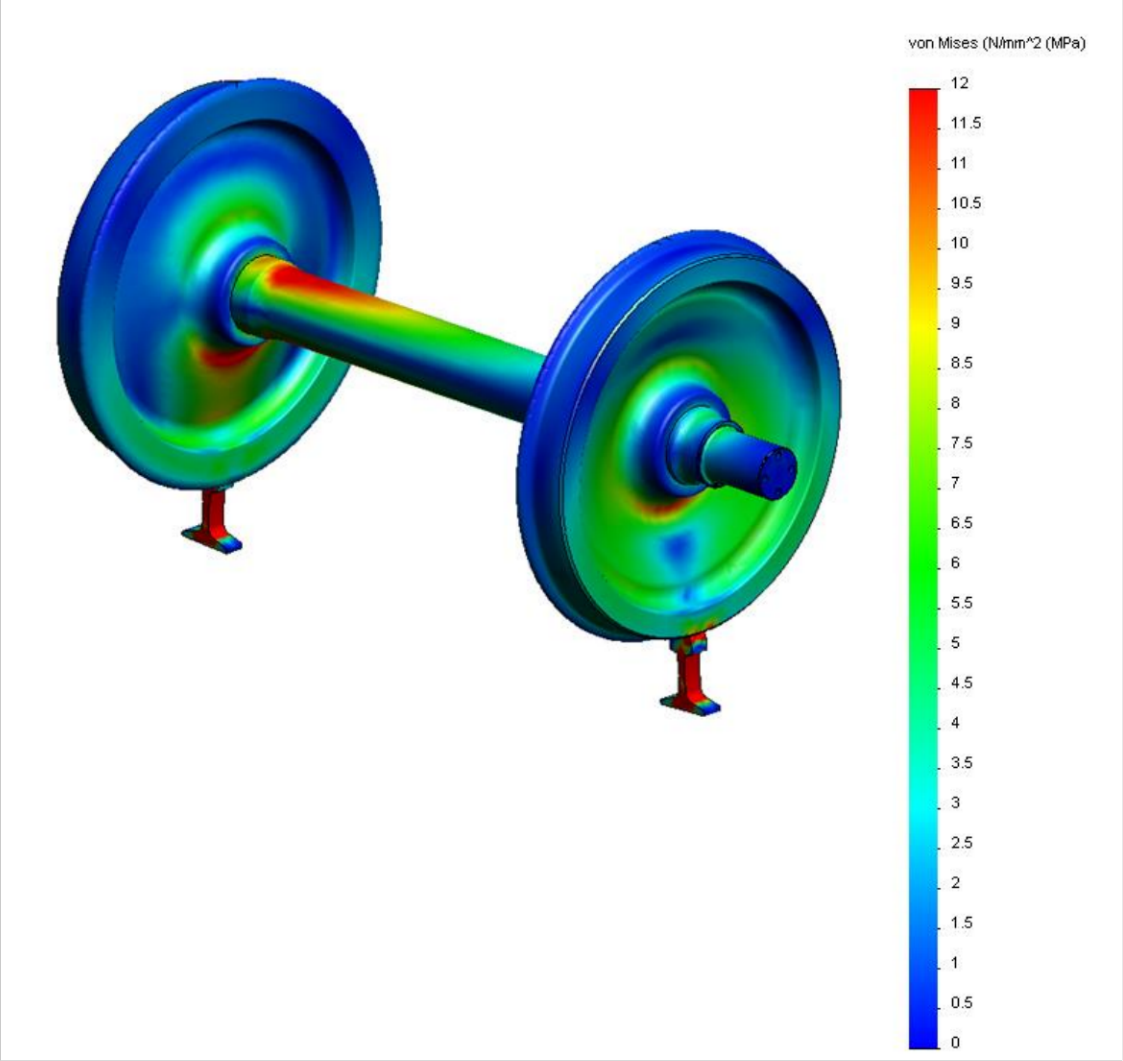

Figure 2.10 –The graph of equivalent stresses arising in a pair of wheels when loaded with vertical and lateral loads

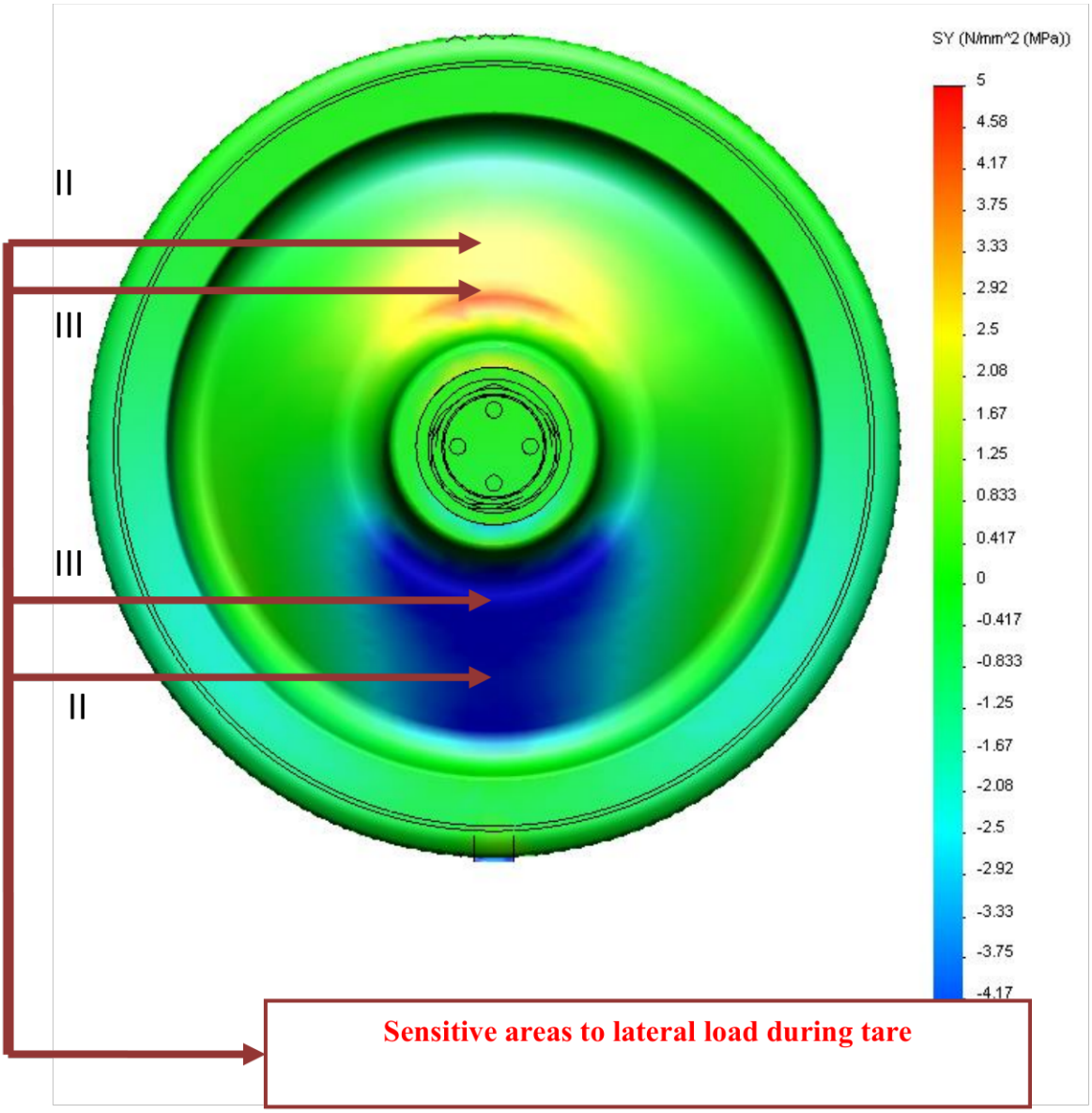

Figure 2.11 –Diagram of normal radial stresses under the action of vertical and lateral forces

Thus, the most sensitive zone is zone III, but it is also the most sensitive to vertical load. Therefore, to measure the lateral load, you should choose zone II, which is practically sensitive only to lateral forces, and to measure the vertical load, choose zone I.

Places of tensor resistors on the disc of a wheel pair and methods of their inclusion in the measuring scheme should be such that, with sufficient sensitivity of

the scheme to the measured force, influence on the scheme of the force of the other direction is excluded.

Thus, for separate registration forces, acting on a pair of wheels, it is necessary to determine the places of the tensor resistors sticker, each of which sensitive only until strength, acting in one direction.

To determine the sensitive zones of action of the vertical and lateral load on the wheel, a diagram of the arrangement of tensor resistors (Figure 2.12) and the coordinates of the location of the tensor resistors on the wheel of the measuring wheelset was developed. The distance between tensorresistors, sensitive only to the horizontal or only to the vertical forces, is about 55 mm.

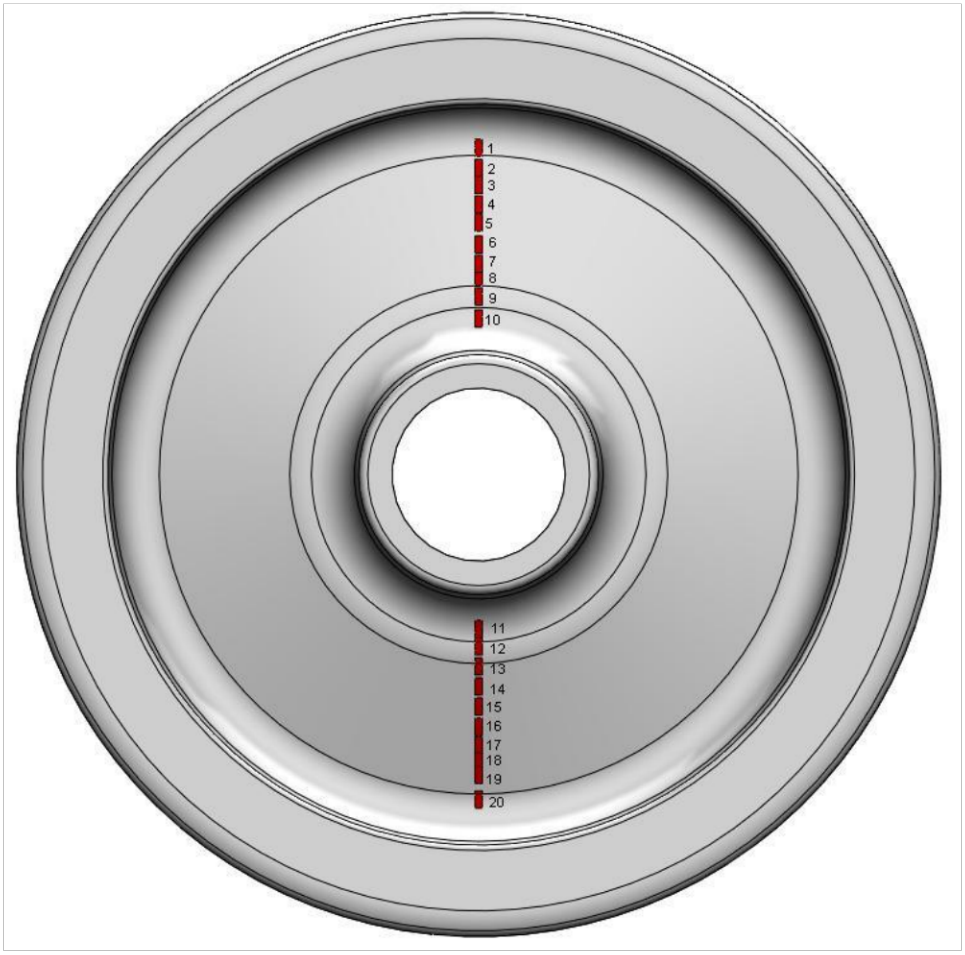

Figure 2.12 - Schematic of placement of tensor resistors on the wheel of the measuring wheelset

2.4 Measurement of dynamic indicators of rolling stock

In order to measure and evaluate the dynamic load of the crew part of the rolling stock, a low-frequency experimental accelerometer of the UM type was developed. In order to use this accelerometer for measuring accelerations on rolling stock, a cubic body was developed. The choice of this design of the accelerometer housing is determined by its ease of use. The created accelerometer is an accelerometer with dimensions of 35x35x31 mm. It consists of a case, a cover, a board with a microcircuit and an electrical connector, as well as fastening elements (magnet, bolts, washers, nuts).

The housing has a cut-out in which the board with the ADXL 278 microcircuit is placed on one side and the electrical connector is installed on the other. The cover and the electrical connector are filled with epoxy glue. The general view of the accelerometer is shown in Figure 2.13.

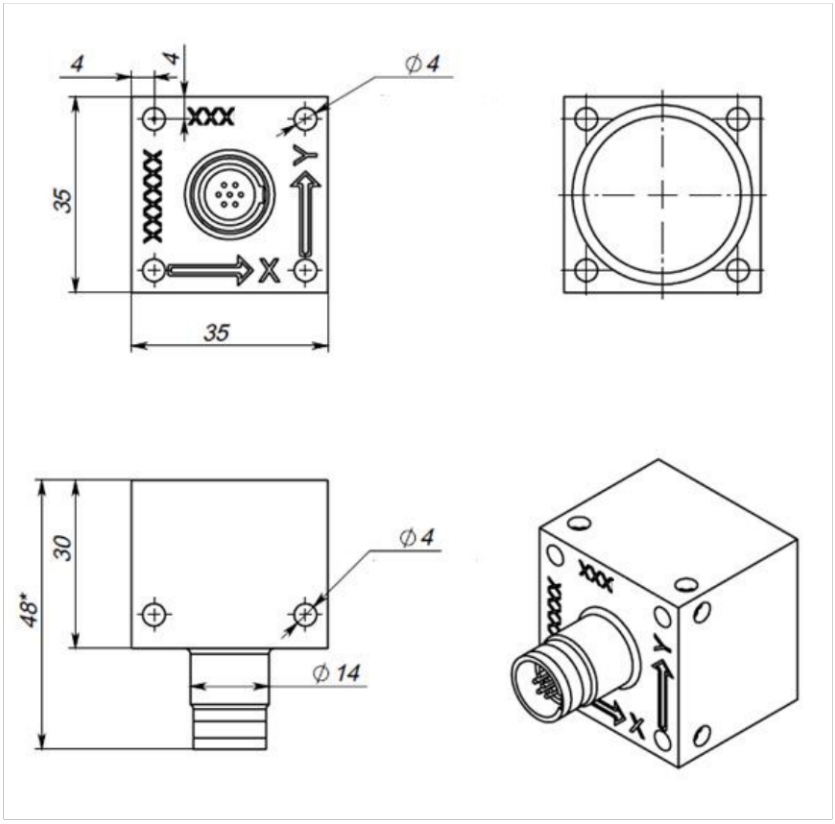

Figure 2.13 – Low-frequency experimental accelerometer type UM

The board includes an Analog Devices ADXL 278 microcircuit. The soldering scheme is shown in Figure 2.14.

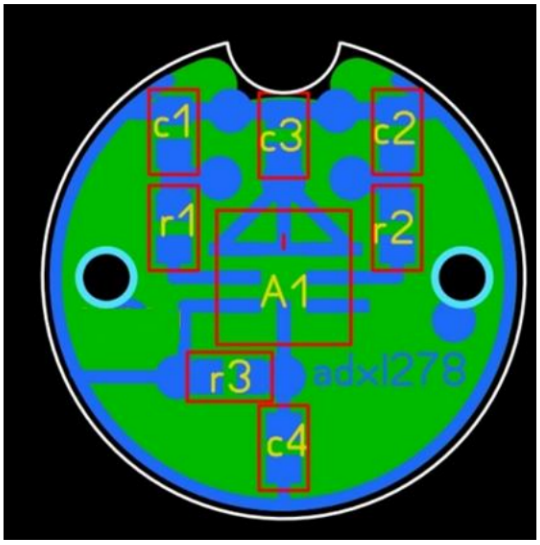

Figure 2.14 – Board with the ADXL 278 chip

The production of the board together with the microcircuit was fully performed according to the technical requirements of the manufacturer of the microcircuit ADXL 278 (temperature and soldering profile), which are specified in the passport. The schematic diagram of the accelerometer is shown in Figure 2.15.

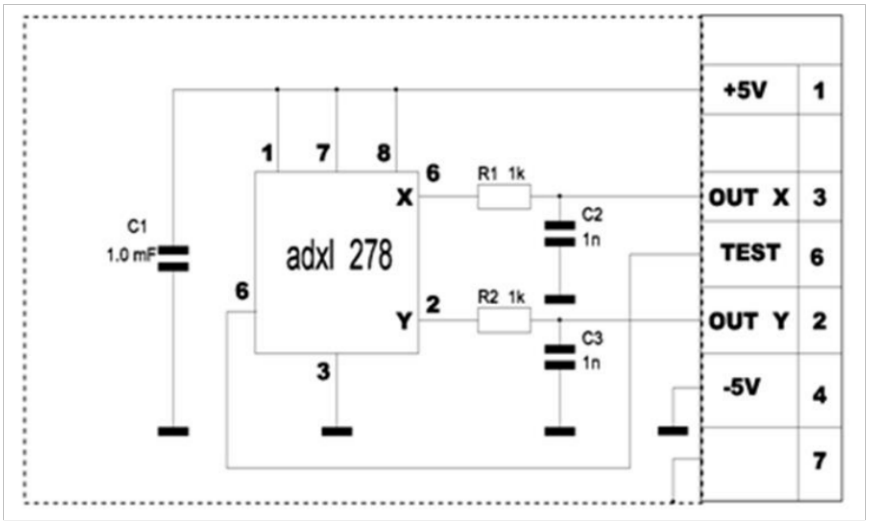

Figure 2.15 – Schematic diagram of the accelerometer

The test batch of accelerometers has undergone testing and metrological certification as a means of measurement.

Table 2.1 shows the general technical requirements for accelerometers, which must be used when running dynamic strength tests to determine the dynamic load of running parts under the conditions of rolling stock operation.

Table 2.1 – General technical requirements for accelerometers

№	Accelerometer installation area		Recommended range, m/s2	Operating frequency range (microcircuit sensitivity), Hz	Additional requirements
1	Box knot		+/- 500	0...100 (0...250)	a) general transmission of frequencies in the range of 0.4 Hz ±0.5 dB; b) non-linearity and hysteresis: – ≤ 0.3% measuring range; c) sensitivity of intersecting axes: ≤ 0.05 (m/s)2 ; d) temperature effect: - for ≤ 3% of the measuring range; - for sensitivities ≤ 5.10% – 4.0/0C.
2	bogie	with single-stage spring suspension	+/- 100	0...100 (0...250)	
		with two or more degrees of suspension	+/- 50	0...40 (0...100)	
3	Body		+/- 15	0...20 (0...50)	

The measured accelerations can be used as indicators of the quality of the track geometry and to detect local geometric deviations affecting the dynamic behavior of the rolling stock. These measurements should be used in conjunction with basic parameter measurements.

Measurement of accelerations should be carried out in specified places on the body and bogies, depending on the need for a specific assessment. Thus, the vertical accelerations of the boxes are measured to detect defects on the rail surfaces and isolated geometric irregularities. Transverse accelerations of the bogie are used to detect irregularities with short waves. According to the lateral and vertical accelerations of the body, track defects are detected, which affect the dynamic indicators of comfort.

The sampling frequency should be at least 2.5 times higher than the cutoff frequency applied to the signal. Measurements of the accelerations of the bogies and the body must be performed in the working speed range for the line within the tolerance of + / -10%.

In order to measure displacements and evaluate dynamic qualities, cable displacement sensors are used (Fig. 2.16). Cable sensors measure linear displacement using a steel cable. At the same time, the cable drum is connected to a sensitive element that converts the movement of the cable into an output linear signal. The measurement is performed with high accuracy and dynamics. Mounting grooves on four sides of the sensor ensure ease and reliability of installation.



Figure 2.16 – Cable-type movement sensors

Based on the comparative characteristics of the static deflections of the four types of bogies Y-32, GP-200, KVZ TsNII, 68-7007, displacement sensors with the following measurement ranges were determined to be optimal: 300 mm – for measuring displacements in the primary suspension stage, 625 mm – in the secondary suspension stage.

CONCLUSIONS ON SECTION 2

The section offers three methods and approaches for evaluating quality indicators, traffic safety, and the technical condition of wagons.

The method of measuring the mechanical stresses in the surface layers of the elements of the load-bearing structures of the rolling stock by the tensometry method allows to assess the indicators of the technical condition and safety of the movement of the railway rolling stock in its defined dangerous zones. For example, this method allows you to determine the vertical and horizontal transverse (frame) forces acting on wheel pairs, according to the rules that are currently in force on railways with a gauge of 1520 mm.

The method of measuring contact forces: due to the deformation of the discs of the wheels of the wheel pairs. The proposed method of measuring contact forces makes it possible to directly measure contact forces, thereby evaluating the real traffic safety indicators for this experimental rolling stock, in contrast to the existing method: measurement by deformations of bogie frames, which gives only an indirect assessment and does not apply to the conditions of passenger train traffic above 140 km/h.

SECTION 3
IMPROVING MEANS AND APPROACHES FOR ASSESSING SAFETY INDICATORS AND TECHNICAL CONDITION OF FREIGHT WAGONS

3.1 Mathematical support for determining safety indicators and technical condition of freight wagons

Software evaluation of the obtained experimental data of movement quality indicators developed in the LabView software shell.

The LabView software system implements the process of in-depth processing of the results of running dynamic tests to identify connections between the oscillating processes of load-bearing structures, estimate the frequencies at which the interaction between them occurs and the levels of interaction.

The above-mentioned processing of the test results consists in performing a correlation and spectral analysis of the processes investigated for various elements of the load-bearing structures. The values measured during the tests are compiled into a multidimensional time series $X(t)=\left[\frac{X_1(t)}{X_p(t)}\right]$, in which each row is a one-dimensional row of one measuring channel.$X_p(t) = \left[x_{p1} \dots x_{pn} \dots x_{pN}\right]$

Figure 3.1a and 3.1b shows the block diagram of the developed software for evaluating the received experimental data of traffic quality indicators and consists of 5 main blocks.

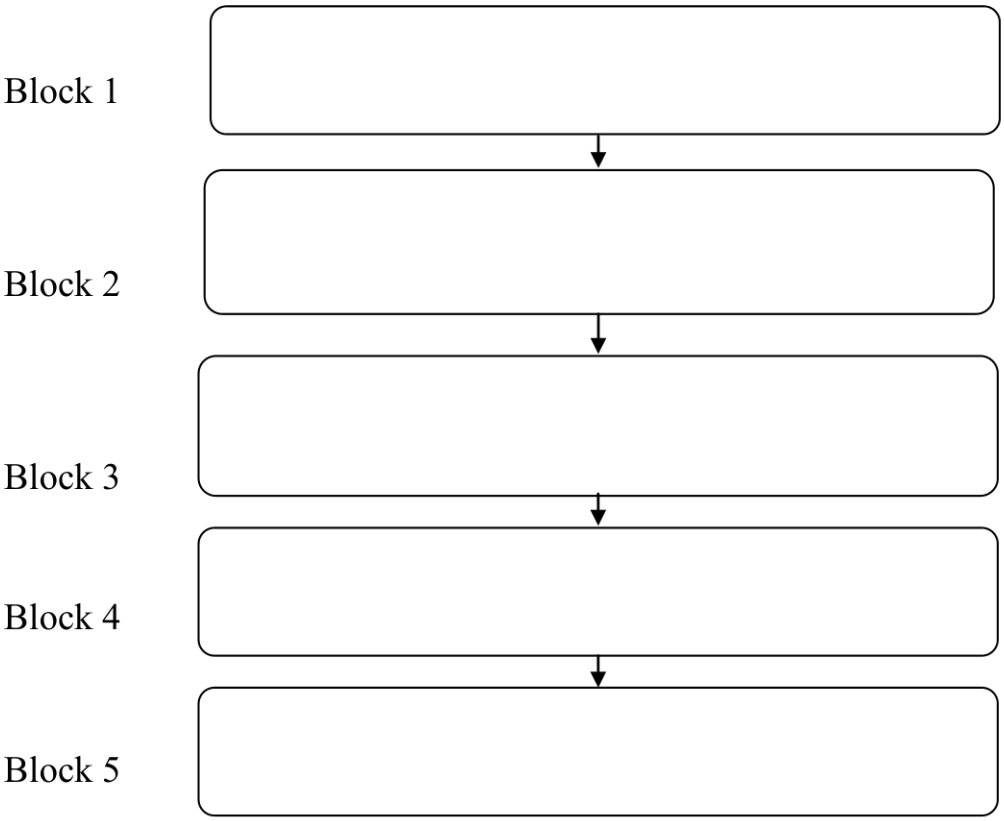

a)

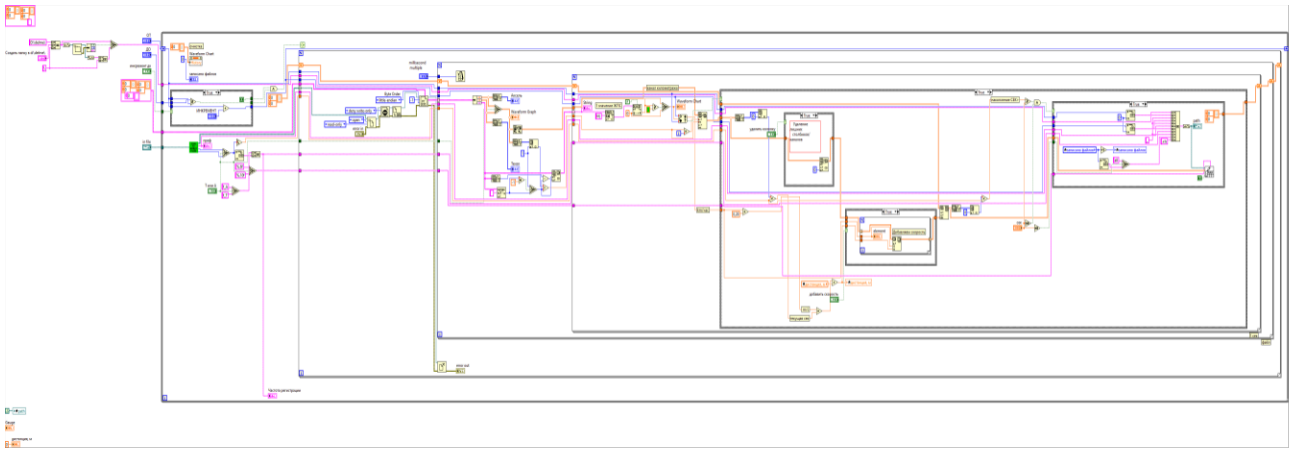

b)

Figure 3.1 is a diagram of the software for evaluating the obtained experimental data

In block 1, the input parameters for processing the results are set and the place of creation of the resulting file is indicated (Fig. 3.2).

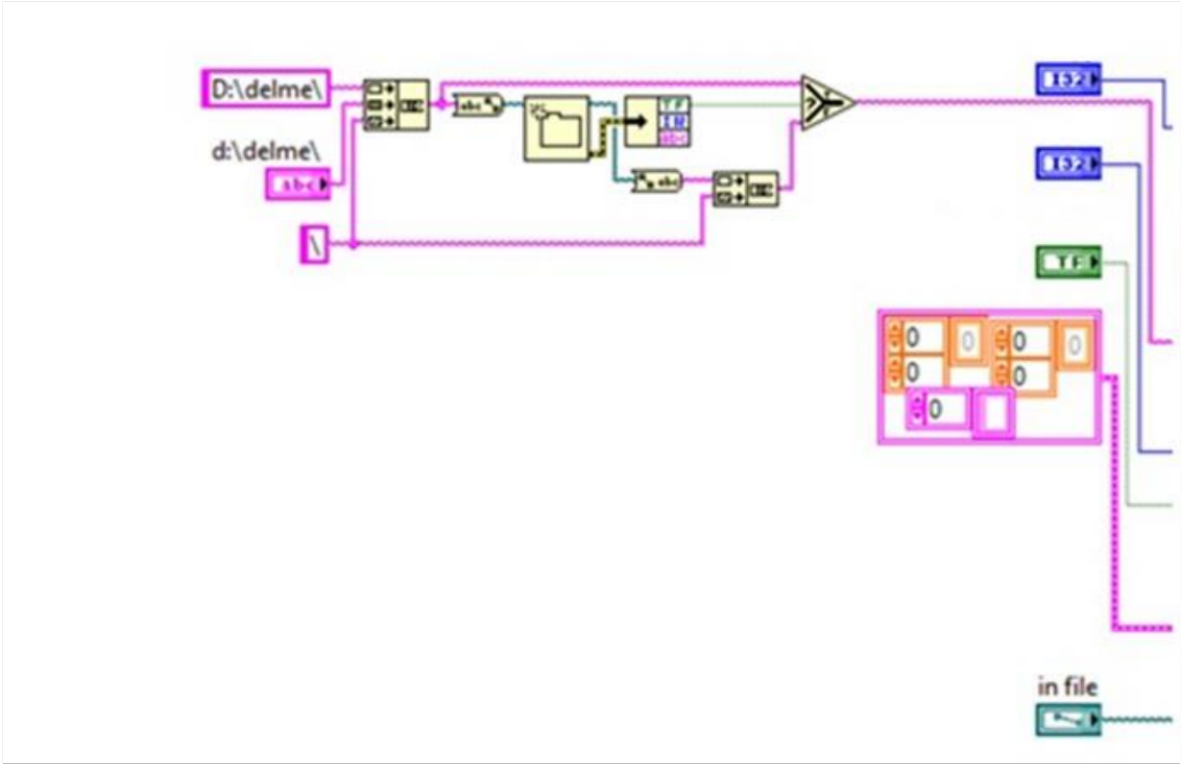

Figure 3.2 – Scheme of block 1

In block 2, primary binary data is read from primary files. Data conversion from binary to text and numbers (Fig. 3.3)

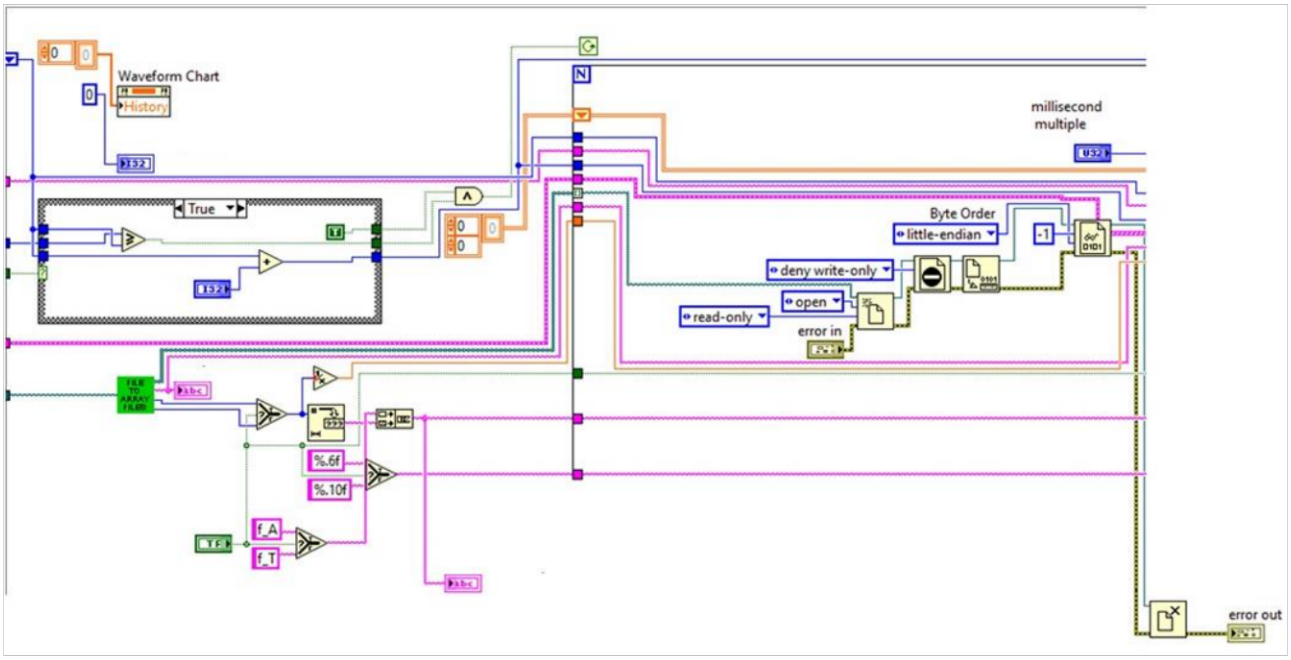

Figure 3.3 – Scheme of block 2

In block 3, the array of data used in further work is defined (so many values of strain gauges, accelerometers, GPS are obtained). The number of received GPS values is determined in relation to the number of values obtained from tensors and accelerometers, an array of values is formed that come to one GPS value (Fig. 3.4).

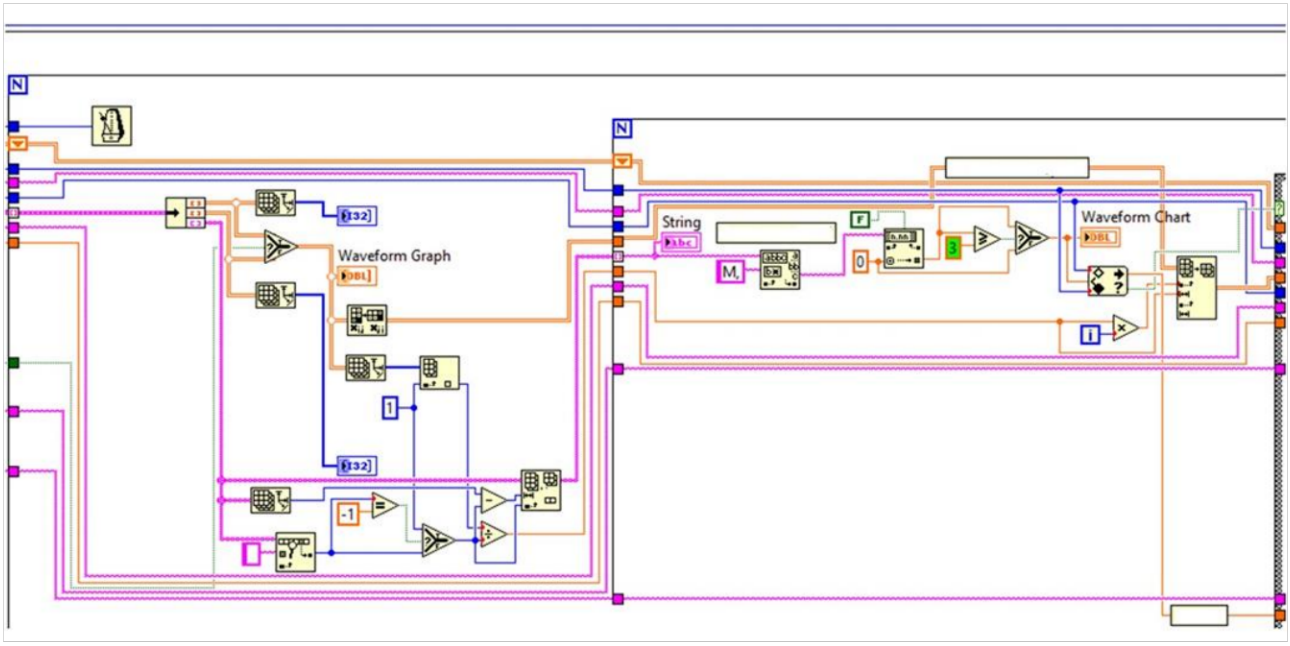

Figure 3.4 – Scheme of block 3

In block 4, the array of data is filled that meets the previous requirements for processing in block 1: speed ranges, the number of values per range, etc. (Fig. 3.5).

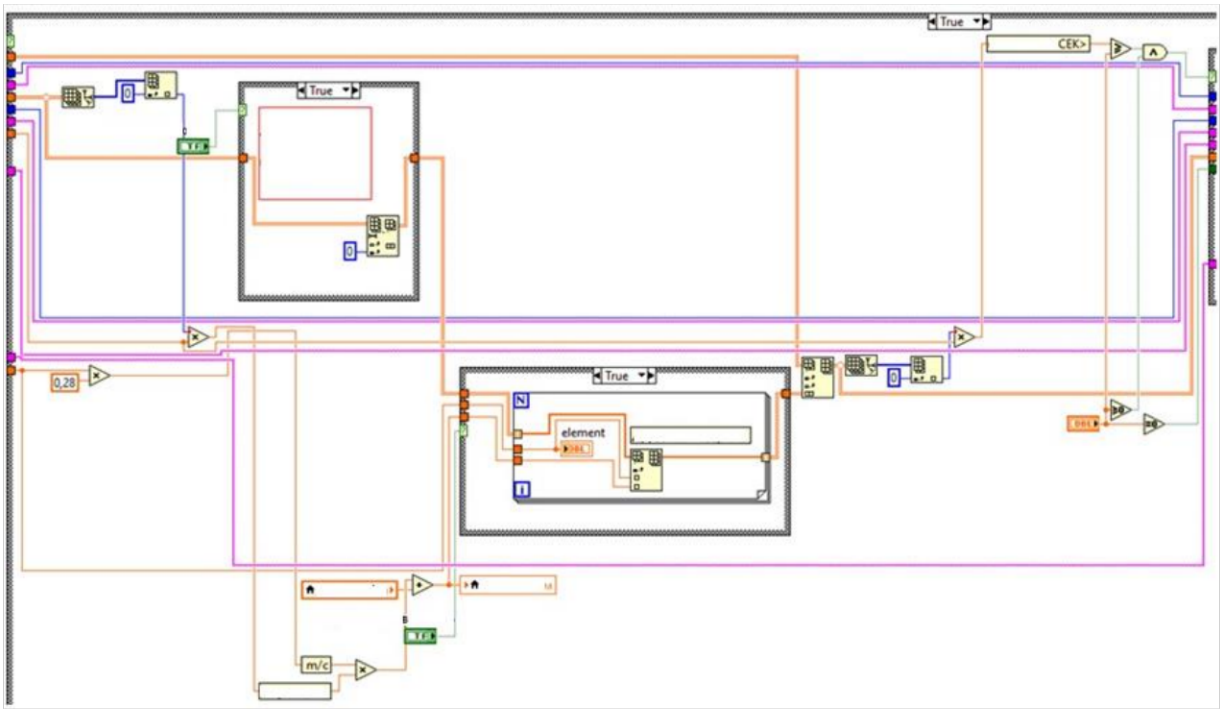

Figure 3.5 – Scheme of block 4

In block 5 (Fig. 3.6), the resulting file based on the accumulated array of data in block 4 is written in text form and represents an oscillogram (Fig. 3.7).

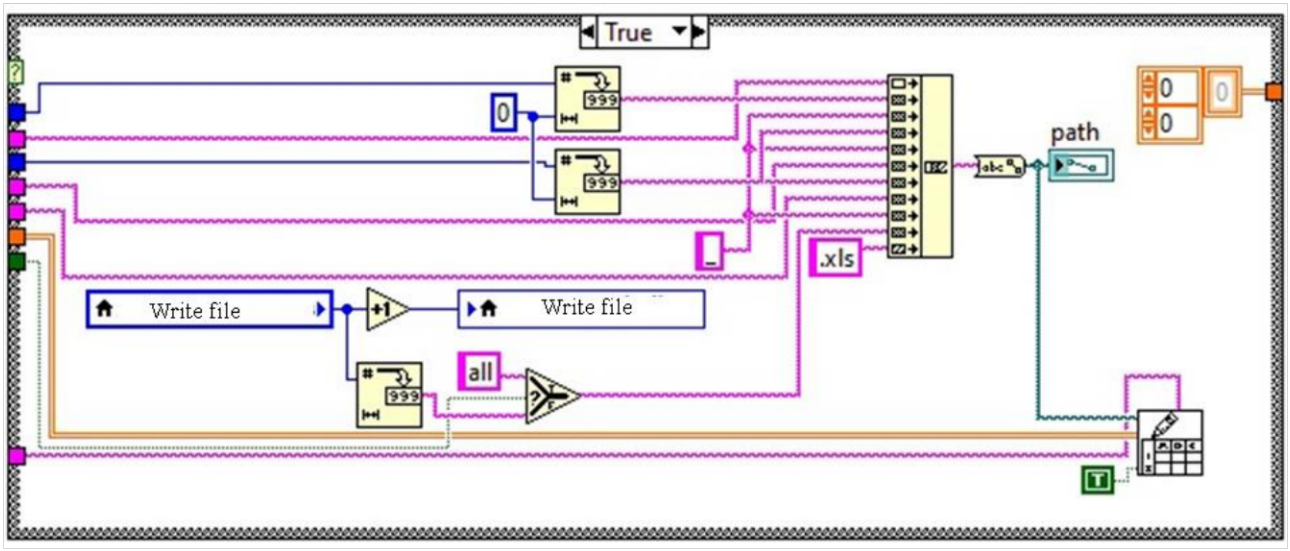

Figure 3.6 – Scheme of block 5

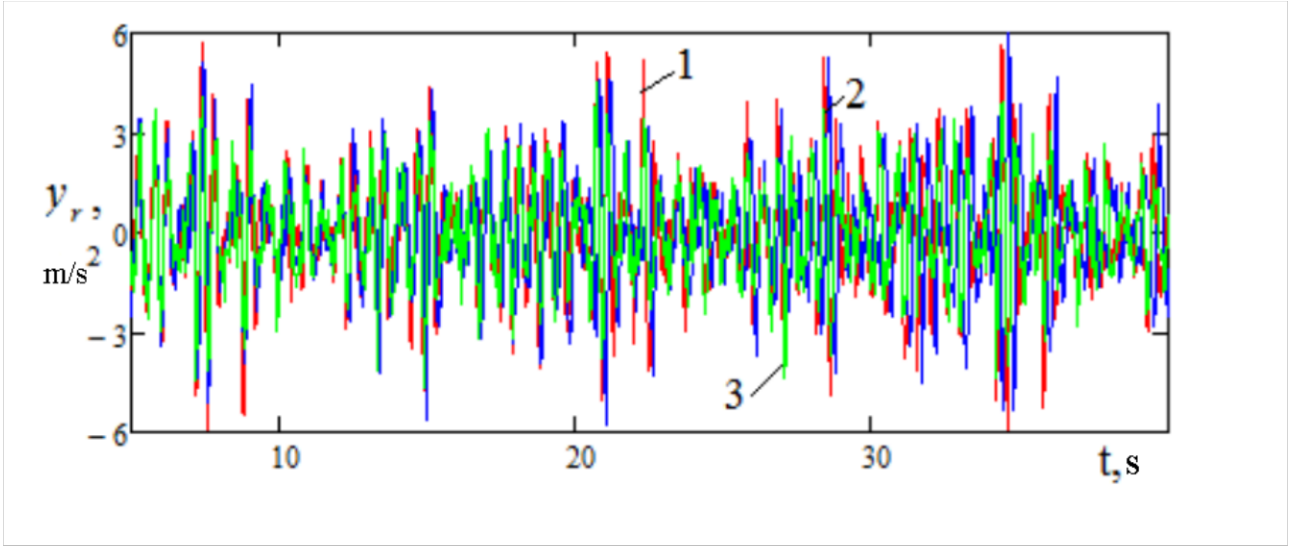

Figure 3.7 – An example of an oscillogram of the resulting file from t he measurement of accelerations

Next, the resulting file must be filtered with a linear digital filter.

A specialized software module in the LABVIEW software shell is used to evaluate the smoothness index of rolling stock.

The software module is a finished application, the input data of which are the digitized oscillograms received from the acceleration sensors and registered by the software hardware recorder based on the programmable controller after initial processing.

The result is the smoothness index value W for the input registration.

The input data for the application is presented in the form of a two-dimensional array (i, j), where the column is the number of the measuring channel, and the line is represented by the function F(t).

The general appearance of the LabView block diagram is shown in Figure 3.8.

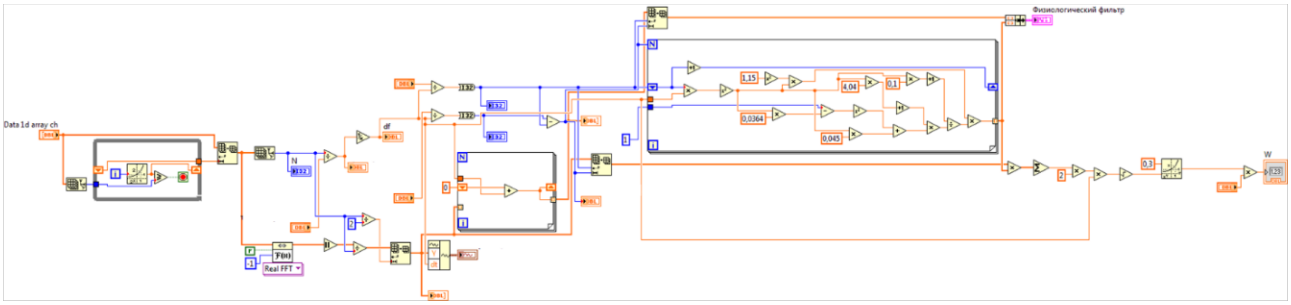

Figure 3.8 – Block diagram of the developed filter

The algorithm of the application is as follows:

The size of the input block for calculations is determined. The size of the input block is determined by a base-2 number.

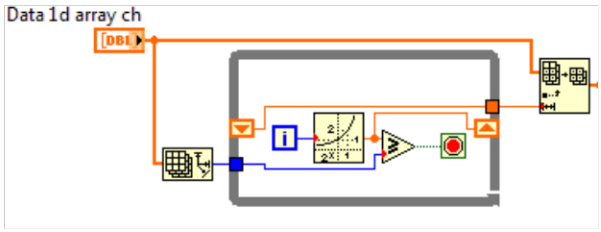

Using a built-in LABVIEW function, a Fourier transform is performed to construct the power spectrum.

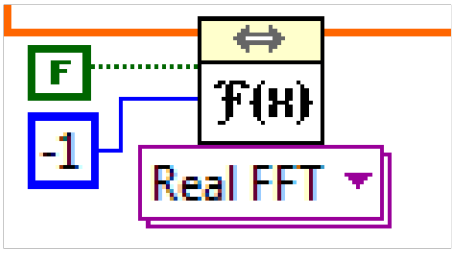

On the basis of the Fourier transformation, frequency arrays and a data array are built in the given frequency range from 0.5 Hz to 20 Hz.

The values of the normalized amplitude-frequency characteristic of the correction filter $q_н(f)$ are calculated according to the formula:

$$q_н(f) = 1.15f\sqrt{\frac{(1+0{,}1f^2)}{(1+4{,}04f^2)((1+0{,}0364f^2)^2+0.045f)}} \qquad 3.1$$

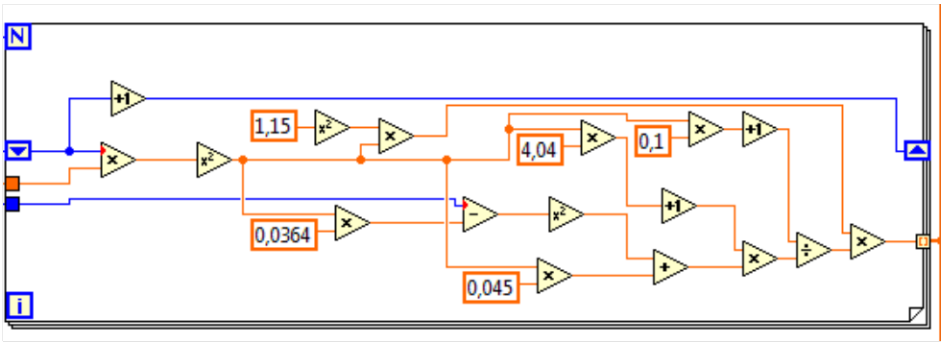

The final smoothness indicator W for the input array is calculated by the formula:

$$W = \alpha \cdot \widetilde{a_k^{0.3}}$$

where α=4.346 for vertical oscillations;

α=4.676 for horizontal (transverse) oscillations;

$\tilde{a}_k^{0.3}$- mean square value of vibration acceleration at the output of the correcting filter, m/s^2

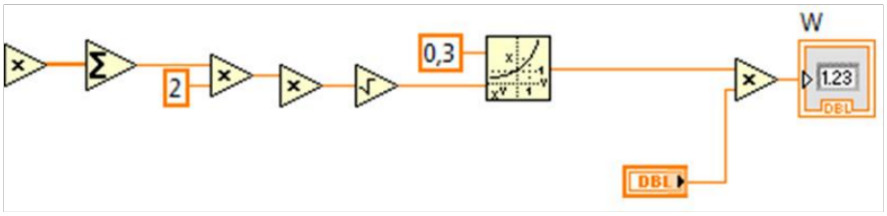

The Butterworth digital filter function of the LABVIEW software shell (Fig. 3.9) is used to assess safety indicators and quality of rolling stock movement.

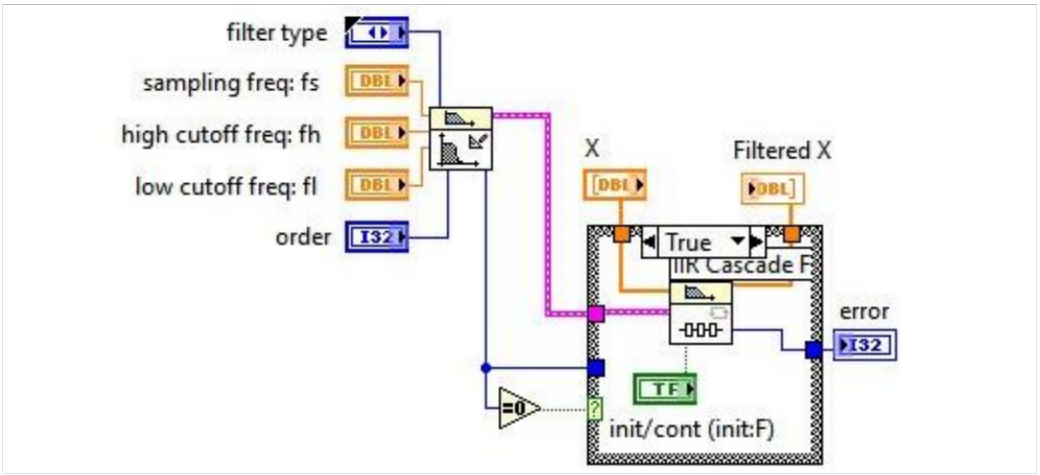

Figure 3.9 – Block diagram of the Butterworth filter

The transfer function of the Butterworth filter is given below:

$$K(\omega)=\frac{1}{\sqrt{1+(\frac{\omega}{\omega_0})^{2n}}}, \quad (3.2)$$

where ω_0- cutoff frequency (it is 1 rad/s), n is the order of the filter.

The transmission coefficient at 0 is often 1, at the cutoff frequency, regardless of the order of the filter, it is $1/\sqrt{2}$= 3dB. At which approaches to ω ∞Frequency response approaches zero. The amplitude-frequency characteristic of the Butterworth filter is maximally flat at $\omega=0$ and $\omega=\infty$. In general, the amplitude-frequency characteristicdecreases from 1 to 0 when the frequency changes from 0 to ∞ (Fig. 3.10).

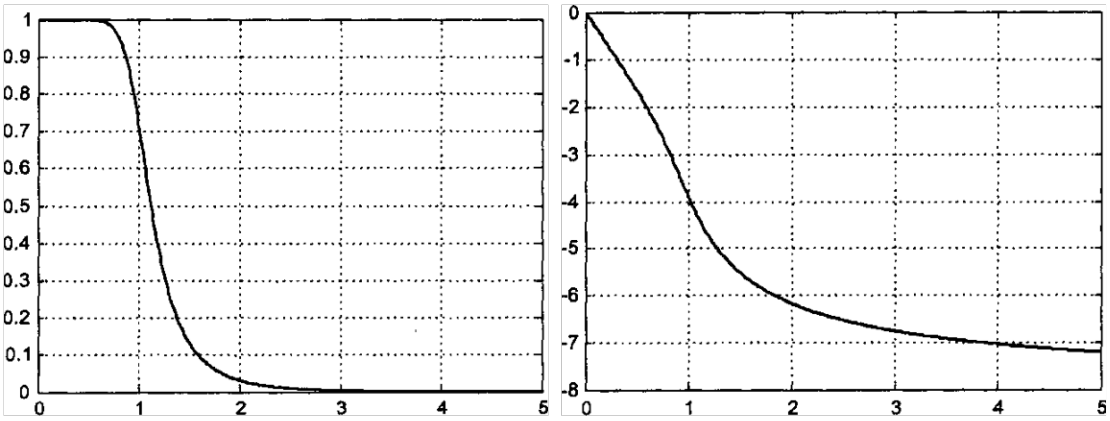

AFC FFC

Figure 3.10 - Characteristics of the Butterworth filter

Figure 3.11 shows the results of signal filtering, before filtering (Figure 3.11 a) and after (Figure 3.12 b) passing the filter.

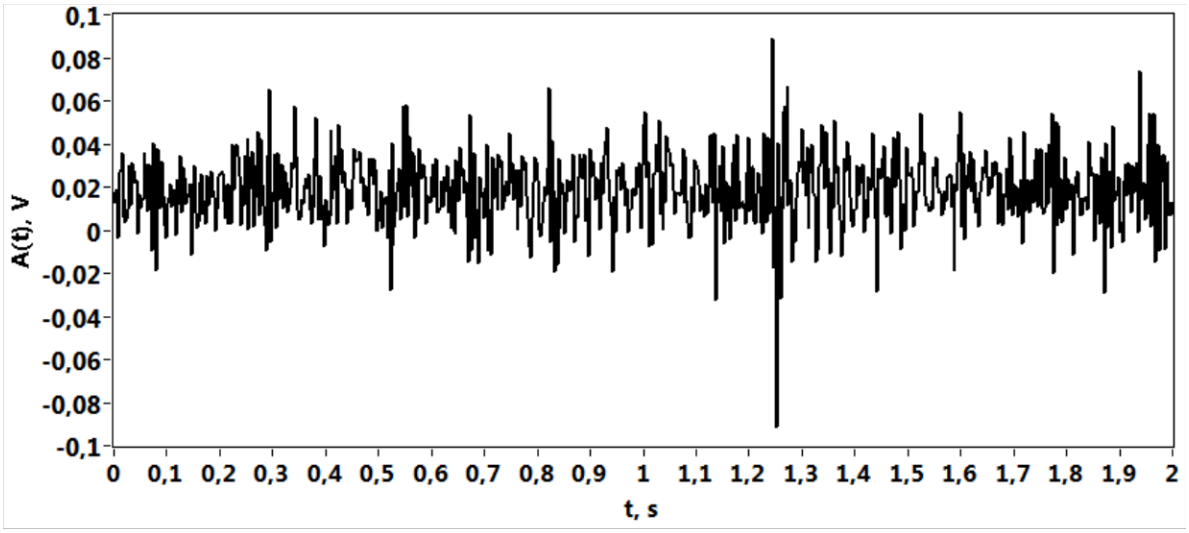

a)

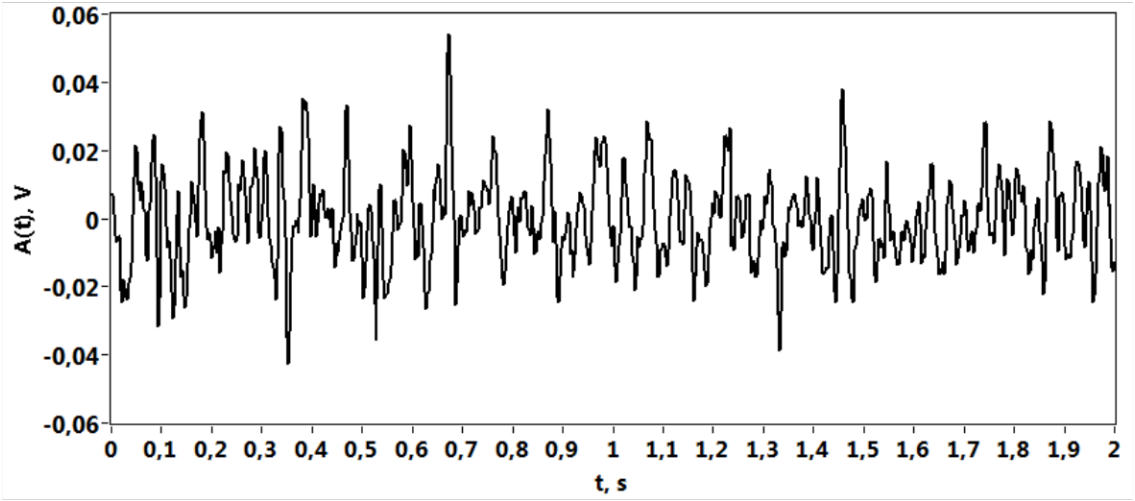

b)

Figure 3.12 – An example of filter operation

3.2 Software for collecting and registering safety indicators and technical condition of wagons

The software of the data collection and registration system performs registration, storage and visualization of changes in information channels (accelerometers, strain gauges). GPS module readings are used to analyze the influence of speed of movement on changes in research parameters.

The developed acquisition subsystem provides the operation of the CompactRIO controller with a chassis of 8 modules with a built-in programmable logic integrated circuit (PLC) and two universal 9205 ADC modules with a maximum sampling frequency of 250 kHz and five 9237 strain gauge modules with a maximum frequency of 50 kHz per channel, module - GPS signal receiver.

Thanks to the built-in FPGA, CompactRIO has the ability to implement measurement data processing algorithms at the hardware level with a deterministic execution time of 25 ns without transferring the load to the central processor of the controller. A typical CompactRIO setup includes a controller with a PharLab or VxWorks real-time operating system, a chassis, and I/O modules. The chassis carries the FPGA core, is directly connected to universal or specialized input-output modules that have built-in means of matching and processing information signals. There are different chassis models that have different numbers of module slots and differ in the characteristics of the FPGA chips.

Due to its autonomy, hardware and mass-dimensional characteristics, as well as the ability to work in adverse conditions, CompactRIO can be used to solve a wide range of tasks related to the collection of measurement information and process management.

Most of the software for CompactRIO is developed according to a scheme that assumes its conditional separation into three levels: a virtual device HOST VI on a PC with a Windows operating system, an RT VI on a controller with a real-time OS, and an FPGA VI on a FPGA that does not have its own OS, since the logic of the program was implemented directly at the hardware level. Each of the presented levels has its own specific functionality and implements individual functions of the system as a whole [61].

Typical tasks performed using the HOST VI on a Windows computer are:

- data storage on the computer and access to databases; - integration with external information systems; - organization of the interface.

Typical tasks performed in RT VI on a real-time controller:

- data processing; - management; - saving data in the built-in memory of the controller and on external media. Typical tasks performed in FPGA VI on the FPGA: - input-output operations; - hardware clocking and control of the process of interaction with the equipment; - low-level processing of measurement signals.

An FPGA is a chip whose functionality is defined by programming or "configuration", which is the more common term when working with this class of integrated circuits. The LabView FPGA Module package is an addition to the LabView software environment, which allows you to specify the logic operations of the FPGA in the form of a regular virtual device instead of programming it using a specialized VHDL language. This package allows you to create programs with synchronous and asynchronous parallel loops that are executed at the hardware level and provides time-deterministic data collection and analysis.

The LabVIEW FPGA Module software package completely takes over the multi-step process of converting a virtual device into binary FPGA code. At the first stage, the virtual instrument is converted into text code in VHDL language, which is then compiled by the standard Xilinx ISE industrial compiler into binary form. During the compilation process, the code is optimized according to the speed of execution and the number of logic gates involved.

The result of compilation is a binary file, which completely defines the configuration of the FPGA. When the program starts, the binary file is loaded on the chassis, that is, the FPGA configuration process takes place. The binary file can be written to the built-in flash memory and automatically loaded when the system is turned on. The configuration is not saved when the power is turned off, so the binary must be downloaded again after powering up again. With the appropriate configuration, it can be loaded automatically from the flash memory of the FPGA device or by the program using the controller.

FPGA VI virtual instruments can run completely independently of other system components and remain functional even when the controller fails. Moreover, a buffer can be organized on the FPGA, which prevents data loss in a similar situation.

FPGA is primarily intended for timing, synchronization, control, data collection and pre-digital processing of information signals, control of each input-output module.

A virtual device for a CompactRIO controller usually includes two or more loops: a loop with critical priority, in which the control and data processing algorithms are implemented, and a loop with normal priority, which is responsible for saving data, a remote web interface, and communication over an Ethernet network or RS-232 bus.

To raise the data received from the modules to the level of the real-time controller, the CompactRIO platform provides three ways: through the elements of the front panel, using the mechanism known in LabView as local variables (Local Variables), and through the DMA FIFO buffer. The first two approaches are relatively simple from the point of view of implementation, but suboptimal from the point of view of efficiency. At the same time, the DMA FIFO method allows you to receive data received at high sampling rates from a large number of modules without delay. One of the advantages of DMA mode is that data transfer occurs independently of the central processor.

FPGA devices that support DMA FIFO buffers have direct access to memory, unlike other methods that require the mandatory participation of the processor. Direct memory access is implemented by capturing the PCI bus (bus mastering) by the FPGA device, in which it gets access to bus management, and therefore, access to memory, bypassing the processor.

The DMA FIFO buffer consists of two parts: one part is in the memory of the FPGA, the other part is in the memory of the controller. The FPGA can be written to or read from the buffer element by element using the FIFO Read and FIFO Write methods, and the controller can be written to or read from samples of elements. Communication between the two parts of the buffer is carried out using a software-hardware DMA controller. Thus, from a software perspective, look like a single FIFO buffer.

The FPGA VI virtual device, placed on the FPGA, implements the functionality of initialization, clocking, polling of data collection modules and subsequent loading of the received readings into the DMA FIFO buffer. To ensure a deterministic sequence of command execution, the structure of the programming language in LabView "Flat Sequence Structure" is used, in which the elements of polling modules and writing to the buffer are located.

The DMA FIFO buffer is polled cyclically at a time interval set by a timer at the real-time controller level, after which the readings obtained as integers according to the dynamic range and bit rate of the acquisition module are normalized by the values of accelerations and deformations. The received data is sent to a virtual device, which ensures their processing and storage on an external drive connected via a USB bus.

CompactRIO controllers have a built-in USB 2.0 controller, but not all storage devices support this standard, which can lead to significant recording delays, which, in turn, lead to overflow of the DMA FIFO buffer and incorrect operation of the system as a whole. In the presented system, there is no virtual control device placed on a personal computer, and the LabView Remote Panel mechanism is used instead. This function implements the so-called Client-Server model, where the server is the controller, and the client is any computer with LabView installed. By default, CompactRIO is licensed for one external connection, but the number can be expanded. To activate the Remote Panel on the controller, it is necessary to activate the Web server in the project settings and select those virtual devices to which remote access must be allowed. This function allows you to significantly reduce the time required for the development of HOST VI, but it can create a load on the data transmission network [79].

In addition to the collection modules, for time synchronization and acquisition of current speed and coordinates, a GPS receiver is also connected to the controller, which is installed on the chassis in the same way as standard modules. Because the receiver is manufactured by a third-party company, the LabView Real Time Module

does not have a standard means of acquiring GPS data, so it uses a set of closed virtual devices installed separately to interact with it. In addition, to ensure the correct functioning of the module as part of the project, the SubVIs supplied with the module should also be added to the FPGA VI. If the initialization is successful, the GPS data is presented as a cluster or directly in a text format that can be used to debug the software or perform other tasks.

3.3 Study of indicators that affect the quality of carriage movement

To study the dynamics of a freight wagon, hopper wagons for the transportation of bulk cargoes that do not require protection from atmospheric effects converted from cement wagon and mineral wagon were selected, a dynamic model was developed in the licensed software complex "UM 6.0", adjustments were made taking into account the design features of converted hopper wagons on bogiess models 18-100 (body, wagon base, centers of mass) with the possibility of varying the condition of the track, the technical condition of the wagons, and the weight of the container.

The model of the wagon was built using the solid body system (SST) approach, according to which the studied mechanical system is represented by a set of solid bodies connected by hinges and power elements. The wagon model includes 19 rigid bodies: body, 2 beams, 4 side frames, 8 wedges, 4 wheel pairs. For each rigid body, 6 degrees of freedom are provided, thus the mechanical system has 114 degrees of freedom.

When developing a computer model of the dynamics of a freight wagon, the approach of subsystems was applied. The use of the subsystems approach in modeling provides an opportunity to form subsystems of the same type once and use them in the model the required number of times.

The lower level consists of subsystems of two types: four subsystems of the wheel pair "KP_*N*", N = 1.4, and eight subsystems of wedges "Klyn_*K*", K = 1.8. Subsystem "Bogie_*M*", where M = 1.2 is the number of the bogie, formed by two included subsystems "KP_*N*", N = 1.2 - for the first bogie and N = 3.4 - for the second bogie; four included subsystems "Klyn_*K*", K = 1.4 - for the first bogie, and K = 5.8 - for the second bogie; as well as solid bodies: over-spring beam "Balka_*M*" and two side frames "Frame_*N*" (N= 1.2 – for the first bogie and N = 3.4 – for the second).General model of wagon contains one body "Body" and two included subsystems "Bogie_1" and "Bogie_2".

The developed dynamic model, firstly, includes friction wedge dampers as separate bodies, each of which is in contact interaction with the side frame and super-spring beam, secondly, it contains a spatial description of the contact interaction of the side frames with the wheel pairs in the axle assemblies, according to the third, ensures the contact interaction of the wagon body with the super-spring beams in the hinge units and sliders.

A pair of wheels. Permanent characteristics of the "KP_N" wheelset subsystem (designation of the subsystem in the model), to which the mass and central moments of inertia are assigned, are given in table 3.1.

Table 3.1 – Wheel set parameters

Parameter	Identifier	Value
Weight, kg	*mkp*	1450
Moment of inertia about the longitudinal axis, kg·m^2	*ikp*	875
Moment of inertia about the transverse axis, kg·m^2	*iky*	200
Moment of inertia about the vertical axis, kg·m^2	*ikp*	875

According to the design features of the running parts of the wagon, which are shown in the structural diagram of the model, each bogie contains two pairs of

wheels. Wheel pair subsystems "KP_N" are placed in the bogie subsystem in the longitudinal direction at distances ±xwheel (N = 1,2) and ±xwheel (N = 3,4), where xwheel is the half base of the bogie. Figure 3.13 presents a 3D model (visualization) of a wheel pair of the dynamics model.

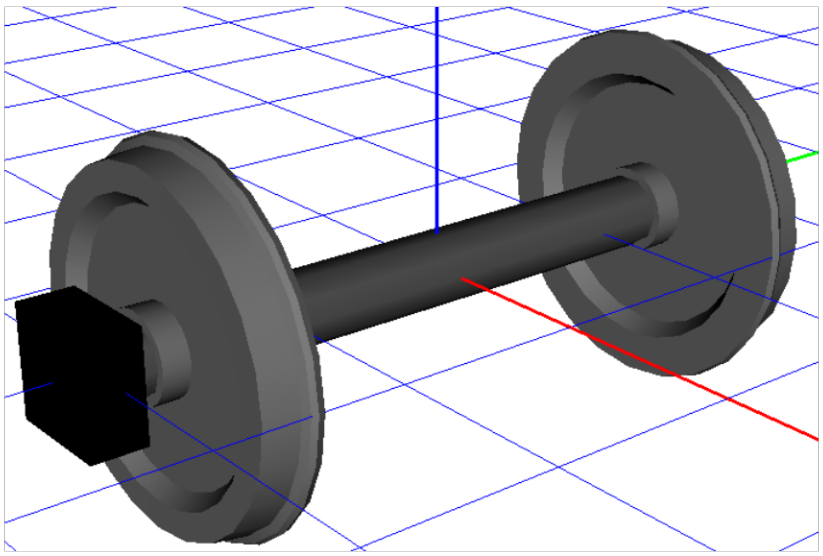

Figure 3.13 – 3D model of a wheel pair

Table 3.2 – Inertial and geometric parameters of the wedge

Parameter	Identifier	Value
Weight of the wedge, kg	*mklin*	21.6
The moment of inertia of the wedge about the longitudinal axis, kg·m2	*iklinx*	0.0810245
The moment of inertia of the wedge relative to the transverse axis, kg·m2	*ikliny*	0.103346
The moment of inertia of the wedge relative to the vertical axis, kg·m2	*iklinz*	0.1028
Coordinate of the center of mass of the wedge in the longitudinal direction, m	*xcklin*	-0.07612
The coordinate of the center of mass of the wedge in the vertical direction, m	*zcklin*	0.04842

According to the design features of the running parts of the wagon, each bogie contains four wedges. The coordinates of the placement of subsystems "Klyn_K", K = 1.4 for the first bogie, and K = 5.8 for the second bogie, in relation to the coordinate systems of the bogies, are determined based on the parameters, as shown in table 3.3.

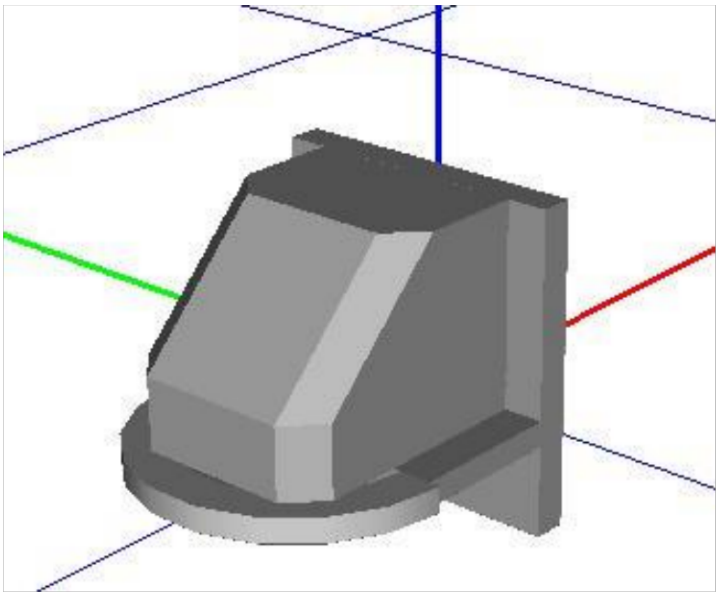

Figure 3.14 – Klin subsystem

Table 3.3 - Coordinates of the placement of subsystems "Klyn_K"

Subsystem	x	y	Z
Wedge_1	xklin	b2	hkl – fst_klin + r
Wedge_2	xklin	-b2	hkl – fst_klin + r
Wedge_3	- xklin	b2	hkl – fst_klin + r
Wedge_4	- xklin	-b2	hkl – fst_klin + r
Wedge_5	xklin	b2	hkl – fst_klin + r
Wedge_6	xklin	-b2	hkl – fst_klin + r
Wedge_7	- xklin	b2	hkl – fst_klin + r
Wedge_8	- xklin	-b2	hkl – fst_klin + r

The following notations are used in this table:

xklin– the distance in the longitudinal direction from the bogie axis to the support point on the wedge, xklin = 0.335 m;

*b*2 – the distance in the transverse direction from the bogie axis to the support point on the wedge; b2 = 1.018 m;

hkl– the distance in the vertical direction from the wheel axis to the support point on the wedge with an undeformed spring, hkl = 0.089 m;

fst_klin– static deformation of the sub-wedge spring, calculated automatically;

*r*is the radius of the rolling circle.

To model the contact interaction of each wedge with the super-spring beam and the side frame, four force elements of the point-plane type are introduced:

– *"InclPlane"*– contact of the wedge with the upper spring beam, inclined contact with the angle alpha;

– *"Frontal"*– contact with the side frame, the points lie in a vertical plane;

– *"LeftPlane"* -leftlateral contact of the wedge with the upper spring beam, the points lie in the vertical plane;

– *"RightPlane"*– the right side contact of the wedge with the super-spring beam, the points lie in the vertical plane.

Each of these contact elements has four contact points on the body of the wedge, the second body in contact is specified as the outer one. These force elements are close contact type without autonormal detection. The coordinates of the contact points and normal vectors of these force elements are defined as shown in tables 3.4-3.6. The general parameters of the "Klyn_K" subsystem and contact power elements are given in table 3.8.

Table 3.4 - Coordinates of the contact points of the "InclPlane" element

Parameter	Identifier	Value
Contact point 1, m	*–x_cont_low* *–w_wedge·0.5+dy_wedge* *z_cont_low*	-0.1504 - 0.069 0.0316
Contact point 2, m	*–x_cont_high* *–w_wedge·0.5+dy_wedge* *z_cont_high*	-0.07615 -0.069 0.10585
Contact point 3, m	*–x_cont_high* *–w_wedge·0.5–dy_wedge* *z_cont_high*	-0.07615 0.069 0.10585
Contact point 4, m	*–x_cont_ low* *–w_wedge·0.5–dy_wedge* *z_cont_low*	-0.1504 0.069 0.0316
Point of contact on external body, m	*–x_cont_low* *–w_wedge·0.5+dy_wedge* *z_cont_low*	-0.1504 -0.069 0.0316
Normal to the surface of the external body		0.7071 0 -0.7071

Table 3.5 – Coordinates of the contact points of the "Frontal" element

Parameter	Identifier	Value
Contact point 1, m	*0* *–wfrontal·0.5* *- dzfrontal*	0 -0.089 -0.015
Contact point 2, m	*0* *wfrontal·0.5* *- dzfrontal*	0 0.089 -0.015
Contact point 3, m	*-hincl* *wfrontal·0.5* *hfrontal–dzfrontal*	-0.00331613 0.089 0.155
Contact point 4, m	*-hincl* *–wfrontal·0.5* *hfrontal–dzfrontal*	-0.00331613 -0.089 0.155
Point of contact on the external body, m	*0* *–wfrontal·0.5* *- dzfrontal*	0 -0.089 -0.015
Normal to the surface of the external body		-0.9998 0 -0.0195

Table 3.6 - Coordinates of the contact points of the "leftplane" element

Parameter	Identifier	Value
Contact point 1, m	*–x_cont_high* *–w_wedge·0.5* *z_cont_high–dy_wedge*	-0.761513 -0.089 0.0858462
Contact point 2, m	*–x_cont_low+dy_wedge* *–w_wedge·0.5* *z_cont_low*	-0.1304 -0.089 0.0316
Contact point 3, m	*–x_cont_low+dy_wedge+dxadditional* *–w_wedge·0.5* *z_cont_low*	-0.1004 -0.089 0.0316
Contact point 4, m	*–x_cont_high* *–w_wedge·0.5* *z_cont_high-dy_wedge–dxadditional*	-0.761513 -0.089 0.0558462
Point of contact on the external body, m	*–x_cont_high* *–w_wedge·0.5* *z_cont_high-dy_wedge*	-0.761513 -0.089 0.0858462
Normal to the surface of the external body		0 1 0

Table 3.7 - Coordinates of the contact points of the "rightplane" element

Parameter	Identifier	Value
Contact point 1, m	*–x_cont_high* *w_wedge·0.5* *z_cont_high–dy_wedge*	-0.761513 0.089 0.0858462
Contact point 2, m	*–x_cont_high* *w_wedge·0.5* *z_cont_high–dy_wedge–dxadditional*	-0.761513 0.089 0.0558462
Contact point 3, m	*–x_cont_low+dy_wedge* *w_wedge·0.5* *z_cont_low*	-0.1304 0.089 0.0316
Contact point 4, m	*–x_cont_low+dy_wedge+dxadditional* *w_wedge·0.5* *z_cont_low*	-0.1004 0.089 0.0316
Point of contact on the external body, m	*–x_cont_high* *w_wedge·0.5* *z_cont_high–dy_wedge*	-0.761513 0.089 0.0858462
Normal to the surface of the external body		0 -1 0

Table 3.8 – General parameters of the "Klyn_K" subsystem

Parameter	Identifier	Value
Contact stiffness at one point, N/m	*cklin*	7·107
Contact dissipation at one point, N·s/m	*dklin*	8·104
Angle of inclination of the friction bar on the side frame, in degrees	*beta_klin*	1°
Angle of inclination of the wedge to the super-spring beam, in degrees	*alpha*	45°
Angle of inclination of the wedge to the super-spring beam, in radians	*ralph*	0.78539816
The width of the wedge	*w_wedge*	0.178
Narrowing of the inclined contact plane, m	*dy_wedge*	0.02
Coordinate of the point of intersection of the inclined plane with the XY plane, m	*l_incl*	0.182
Displacement of the beginning of the inclined plane, m	*dx_cont_incl*	0.0316
The height of the inclined plane, m	*h_incl_cont*	0.0883883
Reduction of the length of the inclined surface due to rounding, m	*dl_incl_cont_high*	0.02
The length of the inclined contact plane = l_incl_cont_full-dl_incl_cont_high	*l_incl_cont*	0.10499993
x coordinate of the beginning of the inclined surface (= l_incl-dx_cont_incl)	*x_cont_low*	0.1504
x coordinate of the top of the inclined surface (= x_cont_low-l_incl_cont*cos(ralpha))	*x_cont_high*	0.076153836
z coordinate of the beginning of the inclined surface (= dx_cont_incl)	*z_cont_low*	0.0316
z coordinate of the top of the inclined surface =z_cont_low+l_incl_cont*sin(ralpha)	*z_cont_high*	0.10584616
Width of the frontal contact surface, m	*wfrontal*	0.178
Height of the frontal contact surface, m	*hfrontal*	0.17
Displacement in the x direction of the upper points of the frontal contact surface, m	hincl = 0.190· beta_klin·pi/180	0.003316125
Downward displacement of the frontal contact surface, m	*dzfrontal*	0.015
Displacement of a pair of points on the side contacts	*dxadditional*	0.03

Side frame. The inertial parameters of the solid body "Frame_N", which represent the side frames of the bogies, are given in table 3.9. Table 3.9 also provides the coordinates of the center of mass of the side frame in the bogie subsystem.

Table 3.9 – Inertial and geometric parameters of the body "Frame_N"

Parameter	Identifier	Value
Weight, kg	*msr*	526.3
Moment of inertia about the longitudinal axis, kg·m^2	*isrx*	13.96
Moment of inertia about the transverse axis, kg·m^2	*isry*	175.8
Moment of inertia about the vertical axis, kg·m^2	*isrz*	161.8
The coordinate of the center of mass of the side frame in the transverse direction in the bogies coordinate system, m	± *b2*	1,018
The coordinate of the center of mass of the side frame in the vertical direction relative to the wheel axis, m	*Mr*	0.05

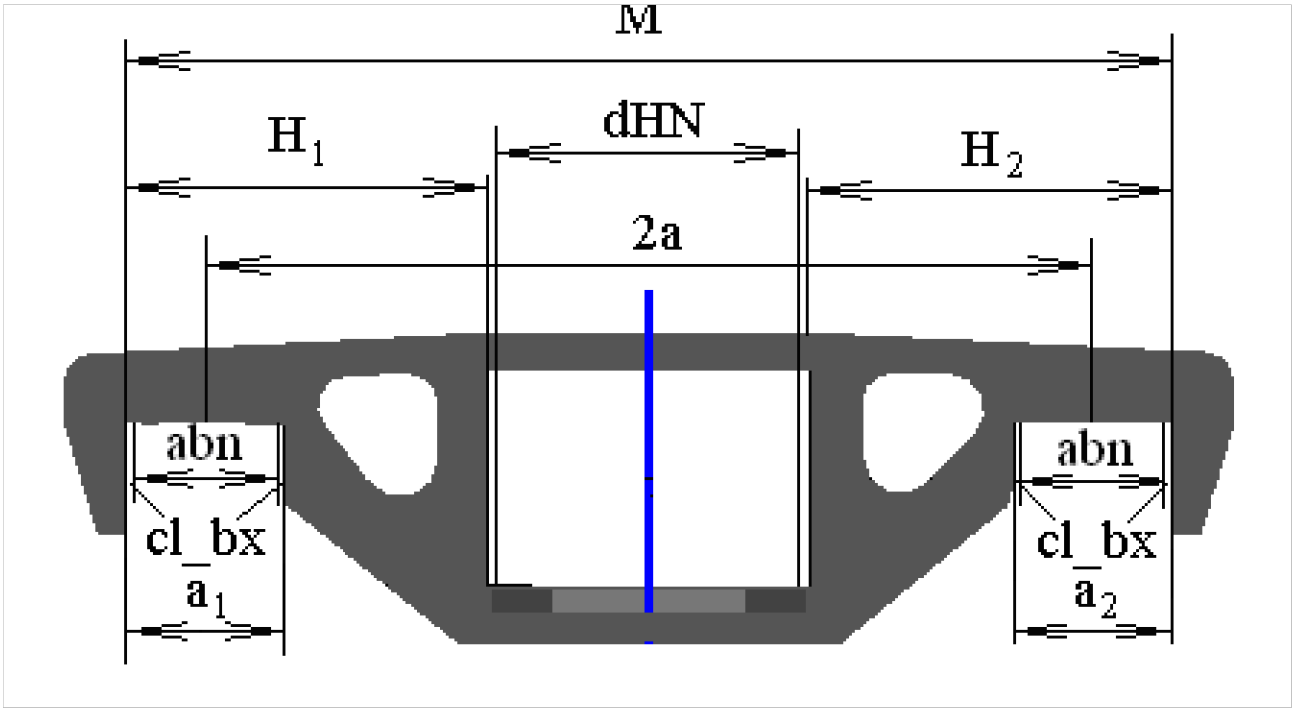

Figure 3.15 – 3D model of the side frame with the parameters of the gaps in the axle box slots in the longitudinal direction

The axlebox units of the bogies are modeled as an elastic-dissipative interaction of the side frames directly with the axes of the wheel pairs, while the characteristics of rigidity, dissipation, and movement restrictions are set individually in each of the three directions.

Suspension beam. Inertial and geometric parameters of the solid body "Balka_M", which represents the over-spring beam of the M bogie are given in table 3.10.

Table 3.10 – Inertial and geometric parameters of the body "Balka_M"

Parameter	Identifier	Value
Weight, kg	*mnb*	596.2
Moment of inertia about the longitudinal axis, kg·m^2	*imnbx*	323
Moment of inertia about the transverse axis, kg·m^2	*imnby*	7,055
Moment of inertia about the vertical axis, kg·m^2	*imnbz*	166.3
The coordinate of the center of mass of the beam in the vertical direction in the undeformed state of the springs relative to the wheel axis, m	*hnb*	0.226

The central spring suspension of the freight wagon is represented by generalized linear force elements. The task of both linear and bilinear springs is provided. The spring type is switched using the bilinear_key identifier, in case of bilinear_key = 0 – linear springs are modeled, in case of bilinear_key = 1 – bilinear ones. The static forces specified by the identifiers pst_balka and pst_klin are calculated automatically for the given values of overestimation or underestimation of the wedges.

Table 3.11 – Rigidities of external springs of bilinear suspension

Spring	CX	CY	CZ	CaZ
PruzhinaP PruzhinaL	cyexternal *5	cyexternal *5	czexternal *5	caz
Spring PKL1 Spring PKL2 Spring LKL1 Spring LKL2	Cyexterna l	Cyexterna l	czexternal	-

Values of stiffnesses outside the selection Cyexternal=6.43e5 N/m, Czexternal=3.035e5 N/m,

Table 3.12 – Stiffnesses of internal springs of bilinear suspension

Spring	CX	CY	CZ	CaZ
PruzhinaP PruzhinaL	cyinternal *5	cyinternal *5	internal *5	caz
Spring PKL1 Spring PKL2 Spring LKL1 Spring LKL2	Cyinterna l	Cyinterna l	czinternal	-

Stiffness values outside the selection Cyinternal=0 N/m, Czinternal=2.366e5 N/m.

Body. The parameters set for modeling the body are as follows: the height of the center of mass of the wagon *hc*, the mass of the wagon body *mcuz*, the central moments of inertia of the body relative to the horizontal longitudinal, horizontal transverse and vertical axes, respectively, *cuzx*, *icuzy, icuzz*, as well as the half-base of the wagon *xbogie* and half the length of the wagon by the coupling axes of auto couplings x_as.

Table 3.13 – Wagon body parameters

Parameter	Identifier	Value
Movement speed, m/s	v0	16,667
Body weight, kg	mcuz	22,000
Weight of the body with cargo, kg	mcuz1	84,400
The central moment of inertia of the body relative to the longitudinal axis, kg·m^2	icuzx	89,000
The central moment of inertia of the body relative to the transverse axis, kg·m^2	icuzy	1,118,000
The central moment of inertia of the body relative to the vertical axis, kg·m^2	icuzz	1,130,000
The distance in the vertical direction from the center of mass of the body with cargo to the plane of support on the heels, m	hcuz	1,396
Wagon-base, m	xbogie	4,325
Static load from the wheel to the rail, N		230 535 (53955)

The interaction between the body and the super-spring beams in the Pyatnik knots is represented in the model by means of 10 contact force elements: eight "Pyatnik_MN" elements, M=1.2, N=1.4, represent the contact interaction in the horizontal plane and two "Vert_Pyatnik_M" elements - in the vertical direction, that is, describe the interaction that transmits the vertical load.

Table 3.14 – Parameters of "Pyatnik_MN" contact elements in the horizontal plane

Contact name	Coordinates of points on overspring beam	Coordinates points on the plane of the side frame	Normal to the plane of the frame
Friday_11	*(contrad+cl_pp_long1; 0; hnp)*	*(xbogie+contrad -wearpx1; 0; –hcuz)*	(1; 0; 0)
Friday_12	*(-contrad–cl_pp_long1; 0; hnp)*	*(xbogie–contrad -wearpx1; 0; –hcuz)*	(–1; 0; 0)
Friday_13	*(0; -contrad–cl_pp_lat1; hnp)*	*(xbogie; –contrad +wearpy1; –hcuz)*	(0; –1; 0)
Friday_14	*(0; contrad+cl_pp_lat1; hnp)*	*(xbogie; contrad –wearpy1; –hcuz)*	(0; 1; 0)
Friday_21	*(contrad+cl_pp_long1; 0; hnp)*	*(–xbogie+contrad -wearpx2; 0; –hcuz)*	(1; 0; 0)
Friday_22	*(-contrad–cl_pp_long2; 0; hnp)*	*(–xbogie–contrad +wearpx2; 0;–hcuz)*	(–1; 0; 0)
Friday_23	*(0; -contrad–cl_pp_lat2; hnp)*	*(–xbogie; –contrad +wearpy2; –hcuz)*	(0; –1; 0)
Friday_24	*(0; contrad+cl_pp_lat2; hnp)*	*(–xbogie; contrad –wearpy2; –hcuz)*	(0; 1; 0)

Table 3.15 – Parameters of "Pyatnik_MN" contact elements in the vertical direction

Contact name	Coordinates of points on overspring beam	Coordinates points on the plane of the side frame	Normal to the plane of the frame
Vert_ Friday _1	*(–contrad_e; 0; hnp-wearpz1)* *(contrad_e; 0; hnp-wearpz1)* *(0; contrad_e; hnp-wearpz1)* *(0; –contrad_e;hnp-wearpz1)* *(contrad_e·0.707; contrad_e·0.707; hnp-wearpz1)* *(contrad_e·0.707;–contrad_e·0.707; hnp-wearpz1)* *(–contrad_e·0.707; contrad_e·0.707; hnp-wearpz1)* *(–contrad_e·0.707;–contrad_e·0.707; hnp-wearpz1)*	*xbogie* *0* *-hcuz*	0 0 -1
Vert_ Friday _2	*(–contrad_e; 0; hnp-wearpz1)* *(contrad_e; 0; hnp-wearpz1)* *(0; contrad_e; hnp-wearpz1)* *(0; –contrad_e;hnp-wearpz1)* *(contrad_e·0.707; contrad_e·0.707; hnp-wearpz1)* *(contrad_e·0.707;–contrad_e·0.707; hnp-wearpz1)* *(–contrad_e·0.707; contrad_e·0.707; hnp-wearpz1)* *(–contrad_e·0.707;–contrad_e·0.707; hnp-wearpz1)*	*–xbogie* *0* *-hcuz*	0 0 -1

Table 3.16 – Parameters of "Pyatnik_N" contact elements

Contact name	Coordinates of points on the upper spring beam	Coordinates of surface points on the body	Normal to the surface on the body
Slider_1	*(0.05; 0.762; hnsk–gapSk1–wearSk1)* *(0; 0.762; hnsk–gapSk1–wearSk1)* *(-0.05; 0.762; hnsk–gapSk1–wearSk1)*	*xbogie* *0.762* *-hcuz+0.096*	0 0 -1
Slider_2	*(0.05; –0.762; hnsk–gapSk2–wearSk2)* *(0; –0.762; hnsk–gapSk2–wearSk2)* *(-0.05 –0.762; hnsk–gapSk2–wearSk2)*	*xbogie* *- 0.762* *-hcuz+0.096*	0 0 -1
Slider_3	*(0.05; 0.762; hnsk–gapSk3–wearSk3)* *(0; 0.762; hnsk–gapSk3–wearSk3)* *(-0.05; 0.762; hnsk–gapSk3–wearSk3)*	*xbogie* *0.762* *-hcuz+0.096*	0 0 -1
Slider_4	*(0.05; –0.762; hnsk–gapSk4–wearSk4)* *(0; –0.762; hnsk–gapSk4–wearSk4)* *(-0.05; –0.762; hnsk–gapSk4–wearSk4)*	*xbogie* *- 0.762* *-hcuz+0.096*	0 0 -1

Table 3.17 - General parameters of "Pyatnik" contact elements

Parameter	Identifier	Value
Contact stiffness at one point, N/m	*cstiff_bz*	108
Contact dissipation at one point, N·s/m	*cdiss_bz*	3·104
z coordinate of city center beams above the axis of the number of pairs in an undeformed state	*hnb*	0.226
Coef. friction in the bushings. node x,y	*ftr_by*	0.17
Coef. friction in the bushings. node z	*ftr_bz*	0.17
Static deformation of the bushing	f0buksa	

The description of the bearing of the body on the super-spring beam through the sliders is represented by four contact force elements of the Point-Plane "Slider_N" type, N = 1.4. Three contact points are introduced for each slider on the superspring beam, as shown in Figure 3.16. The parameters of these contact elements are listed in Table 3.18.

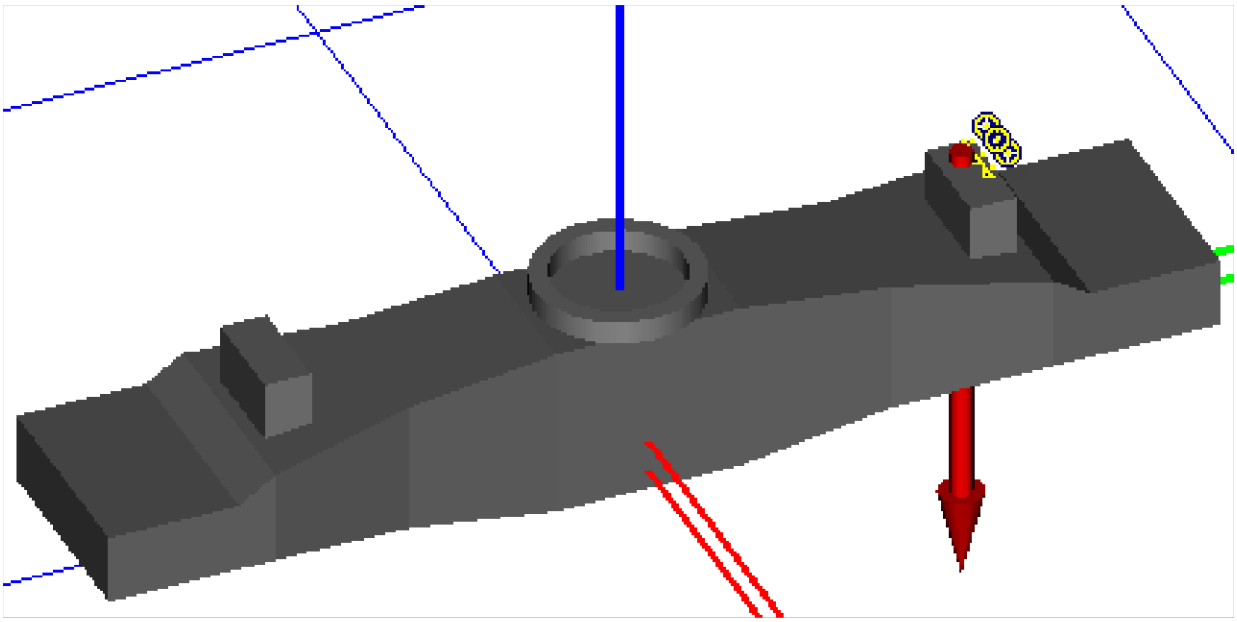

Figure 3.16 – Contact points on the superspring beam and the normal to the contact plane on the body of the "Slider_N" element

Table 3.18 – Parameters of "Slider_N" contact elements

Contact name	Coordinates of points on the upper spring beam	Coordinates of surface points on the body	Normal to the surface on the body
Slider_1	*(0.05; 0.762; hnsk–gapSk1–wearSk1)* *(0; 0.762; hnsk–gapSk1–wearSk1)* *(-0.05; 0.762; hnsk–gapSk1–wearSk1)*	*xbogie* *0.762* *-hcuz+0.096*	0 0 -1
Slider_2	*(0.05; –0.762; hnsk–gapSk2–wearSk2)* *(0; –0.762; hnsk–gapSk2–wearSk2)* *(-0.05 –0.762; hnsk–gapSk2–wearSk2)*	*xbogie* *- 0.762* *-hcuz+0.096*	0 0 -1
Slider_3	*(0.05; 0.762; hnsk–gapSk3–wearSk3)* *(0; 0.762; hnsk–gapSk3–wearSk3)* *(-0.05; 0.762; hnsk–gapSk3–wearSk3)*	*xbogie* *0.762* *-hcuz+0.096*	0 0 -1
Slider_4	*(0.05; –0.762; hnsk–gapSk4–wearSk4)* *(0; –0.762; hnsk–gapSk4–wearSk4)* *(-0.05; –0.762; hnsk–gapSk4–wearSk4)*	*xbogie* *- 0.762* *-hcuz+0.096*	0 0 -1

In this table, the *hnsk* parameter indicates the distance in the vertical direction between the center of mass of the upper spring beam and the bottom of the slider on the body, *hnsk* = 0.2434 m. The gaps in the sliders are set using the identifiers *gapSk_N, N* = 1.4, in addition, using the identifiers *wearSk_N* wear of sliders. The general parameters of these contact power elements, in particular the stiffness and dissipation factor, are given in Table 3.19.

Wheel profile. The profile of each wheel can be determined separately using the appropriate program tool in the special coordinate system shown in Figure 3.17.

Table 3.19 - General parameters of "Slider_N" contact elements

Parameter	Identifier	Value
Contact stiffness at one point, N/m	*cstiff_sk*	108
Contact dissipation at one point, N·s/m	*cdiss_sk*	1·105
Coefficient of friction	*ftr_sk*	0.17

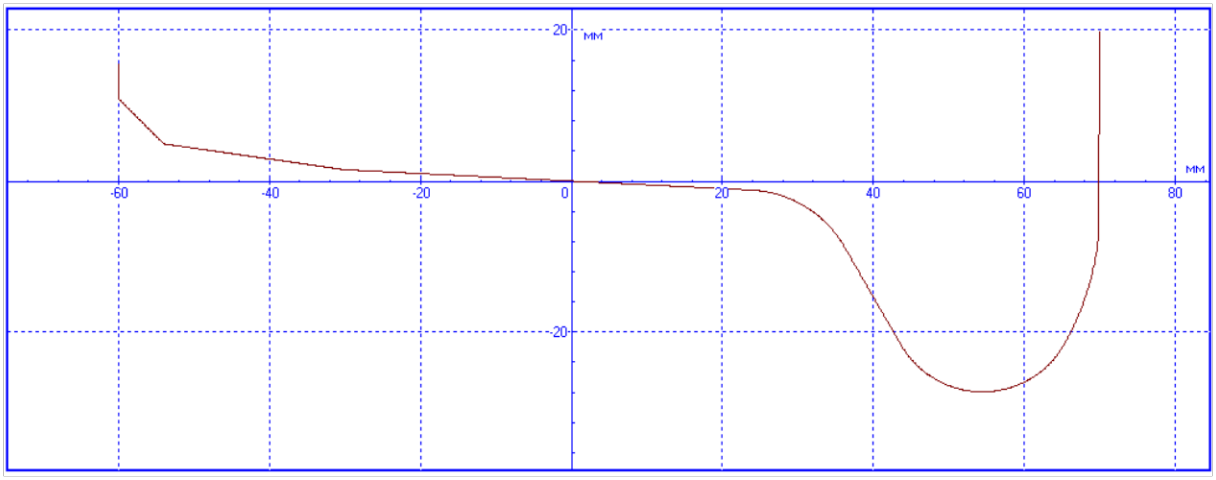

Figure 3.17 - Wheel profile coordinate system

General view of the basic computer model of the dynamics of a hopper wagon in Figure 3.18, in Figure 3.19, experimental hopper bodies of converted wagons are shown in a simplified form.

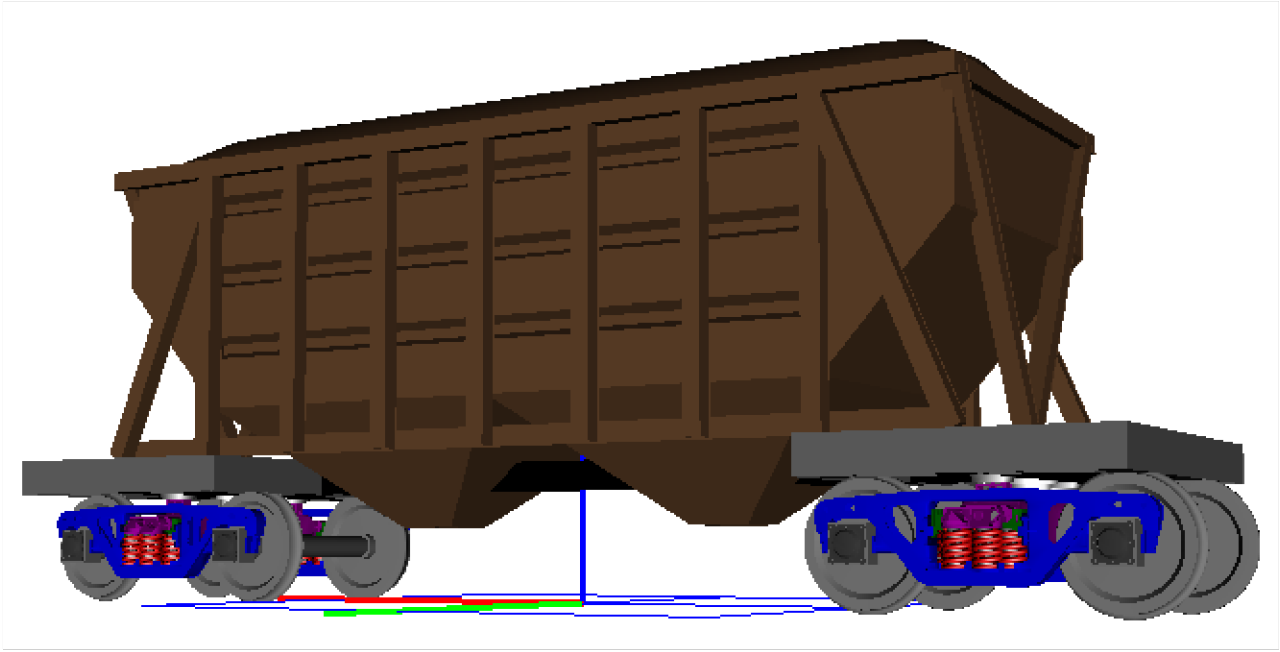

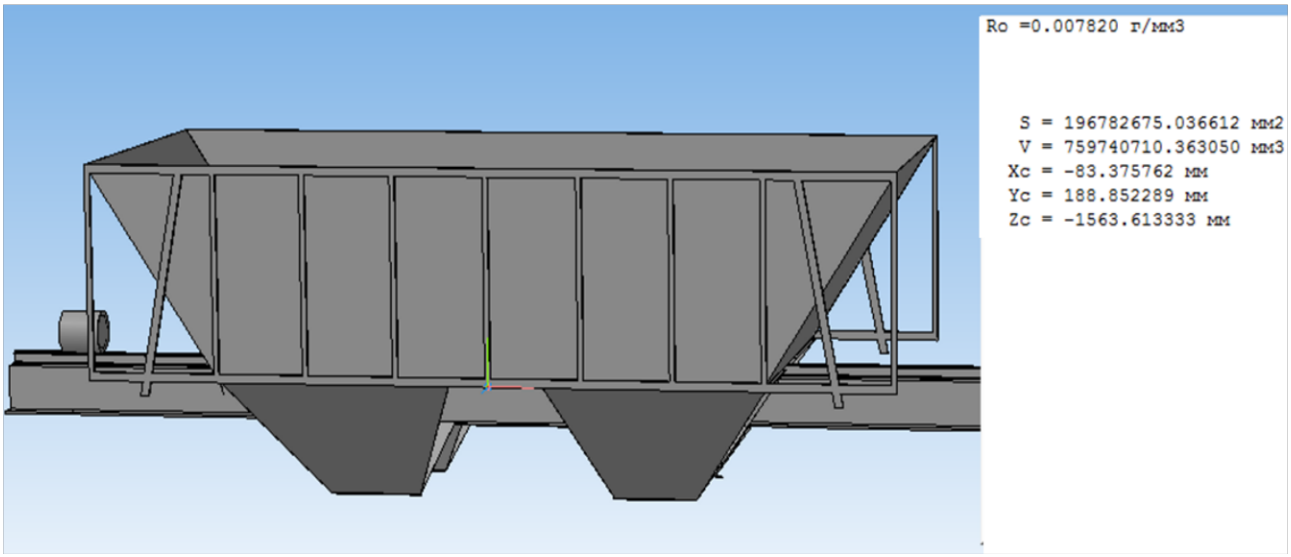

Figure 3.18 – General view of the computer model of wagon dynamics

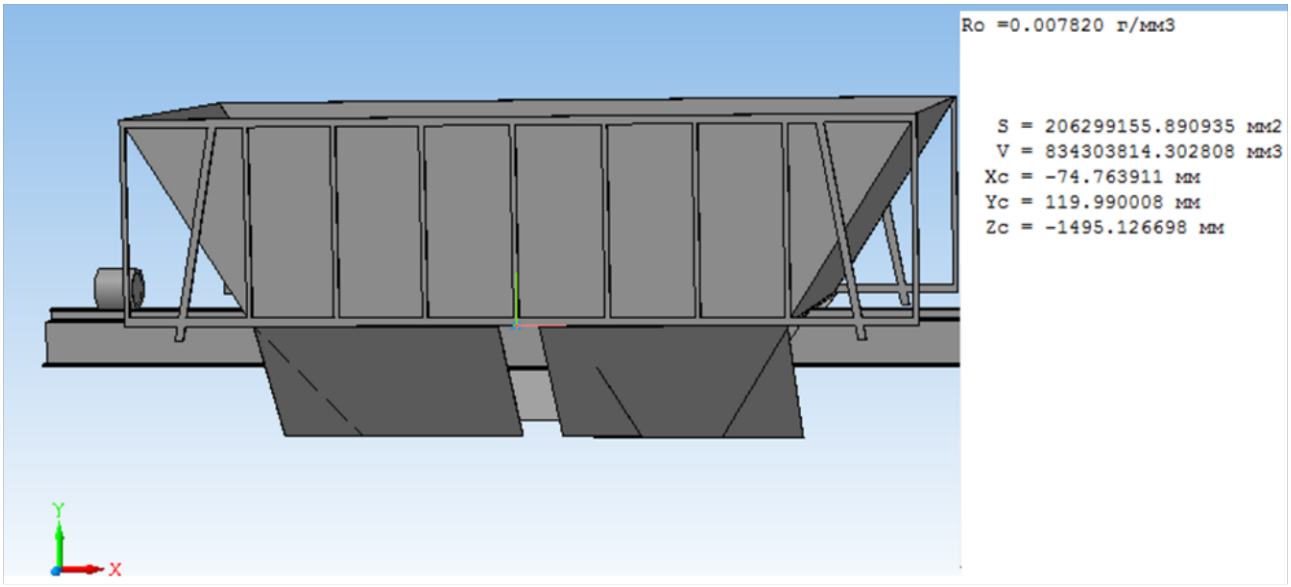

Figure 3.19 – General view of the computer model of wagon dynamics

3.3.1 Verification of the computer model

As the first stage of checking (verification) of the model, the calculation of a simple model of vertical oscillations of the wagon with one degree of freedom was carried out. The results of simulation (numerical integration) of the computer (mathematical) model compared to the results of the analytical solution of the differential equation of oscillations:

$$m \cdot \ddot{z} + \beta \cdot \dot{z} + G \cdot z = 0$$

where m is the mass, β is the vibration damping coefficient, and G is the elasticity.

As the second stage of checking the computer model of the dynamics of the wagon, the data of measurements of the accelerations of the elements of the wagon during running dynamic tests performed in the empty and loaded state were used. Accelerometers were installed on the axles of the first bogie, the side frame and the

upper spring beam. Theiler coefficient of discrepancy was used to assess the adequacy of the mathematical model ε:

$$\varepsilon = \frac{\sqrt{\sum_{i=1}^{n}(x_i^e - x_i^M)^2}}{\sqrt{\sum_{i=1}^{n}(x_i^e)^2} + \sqrt{\sum_{i=1}^{n}(x_i^M)^2}}, \quad (3.3)$$

where x_i^M and x_i^e – predicted and experimental values; n– the number of values to be checked.

According to the standard deviations of the accelerations of the elements of the wagon, determined from the measurement data, and those obtained from the computer dynamics model, Theil's coefficients of discrepancy were calculated. The obtained values do not exceed 0.11, which indicates acceptable differences between calculated and experimental data.

According to the results of the spectral analysis of acceleration realizations, registered during running dynamic and strength tests and obtained by modeling, the main frequencies of the running parts were determined. The overall relative average deviation of calculated and measured frequencies is 7.47%. Therefore, the experimentally obtained frequencies are quite close to the calculated ones. The general calculation scheme of the wagon for the study of traffic dynamics is presented in Figure 3.20.

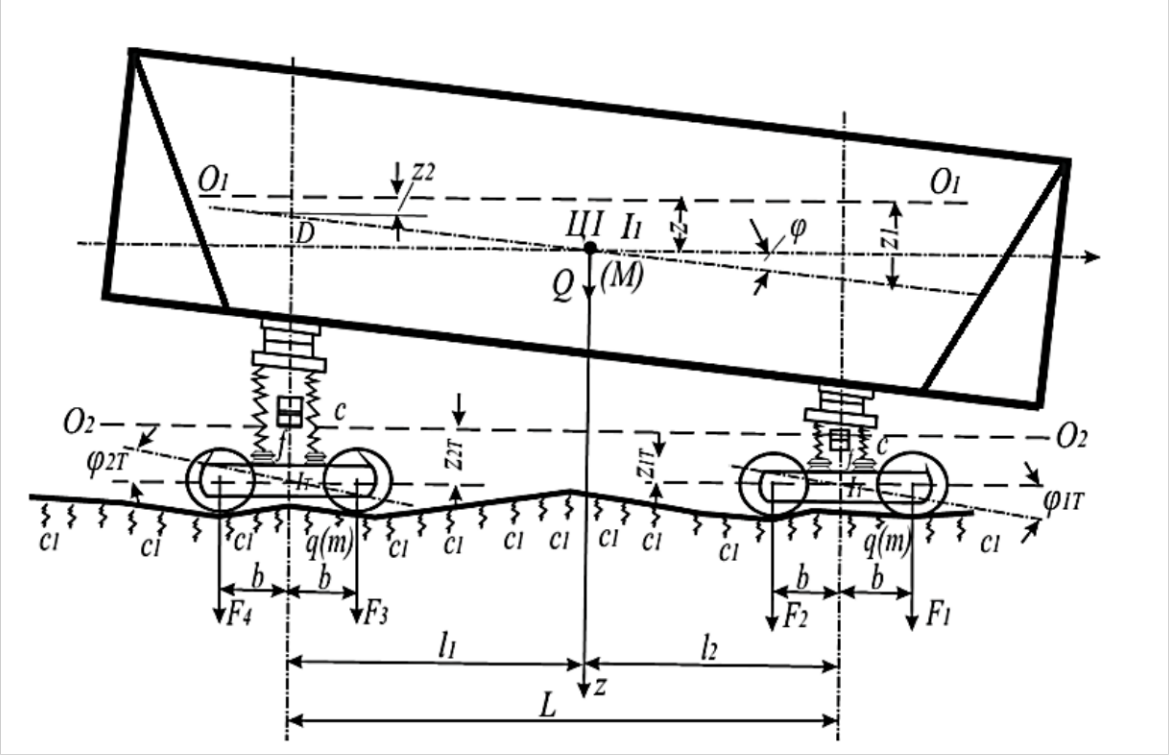

Figure 3.20 –The general calculation scheme of the wagon for study of movement dynamics

3.3.2 Results of modeling dynamics with variation of various indicators

Study of the dynamic qualities of the wagon. According to the result of the simulation of the experimental hopper wagon, which corresponds to the general parameters of wagons converted from cement carriers and mineral carriers depending on the condition of the track, the technical condition of the wagons and the weight of the container, the following results were obtained.

Modeling of the experimental wagon in a technically sound condition of the wagon and track. The averaged path profile was used for modeling and tested in previous studies. The general results of modeling are given in Table 3.20.

Table 3.20 – General simulation results with the wagon and track in a technically sound condition

Speed range	Coefficient of vertical dynamics of the weight of the bogie, Kd	Coefficient of vertical dynamics of the unreinforced bogie frame, Kdn	Stock factor stability of the wheel from derailment on straight and curved sections of the track
40-50 km/h	0.30–0.40	0.39–0.49	1.50–2.00
50-60 km/h	0.31–0.41	0.40-0.52	1.46–1.70
60-70 km/h	0.33–0.45	0.50–0.56	1.42–1.75
70-80 km/h	0.38–0.51	0.51–0.60	1.38–1.42
80-90 km/h	0.39–0.50	0.52–0.60	1.38–1.41

The wagon, when simulating movement in a technically sound condition of the wagon and track, has a sufficient level of dynamics indicators to ensure safe operation.

Modeling of an experimental wagon in a technically sound condition of the track with a reduction in the tare weight. An averaged path profile, developed and tested in previous studies, was used for modeling. The general simulation results are given in Tables 3.21, 3.22 with two steps of reducing the tare weight: up to 18.5 t and up to 17.0 t for the model wagon 11-715-01; up to 20 t and up to 19 t for the model wagon 19-923-01.

Table 3.21 – General simulation results with technically sound condition of the track and reduced tare weight of the model wagon 11-715-01

Speed range	Coefficient of vertical dynamics of the weight of the bogie, Kd		Coefficient of vertical dynamics of the unreinforced bogie frame, Kdn		Stock factor stability of the wheel from derailment on straight and curved sections of the track	
	The weight of the container is 18.5 tons	The weight of the container is 17.0 tons	Tare weight - 18.5 t	The weight of the container is 17.0 tons	The weight of the container is 18.5 tons	The weight of the container is 17.0 tons
40-50 km/h	0.29–0.40	0.26–0.35	0.39–0.48	0.38–0.52	1.49–2.00	1.42–2.00
50-60 km/h	0.31–0.40	0.30–0.39	0.40-0.51	0.39–0.54	1.45–1.65	1.42–1.62
60-70 km/h	0.32–0.46	0.29–0.45	0.49–0.55	0.48–0.56	1.42–1.73	1.39–1.58
70-80 km/h	0.37–0.50	0.35–0.50	0.50–0.59	0.51–0.61	1.37–1.44	1.34–1.42
80-90 km/h	0.38–0.51	0.35–0.52	0.50–0.60	0.53–0.55	1.35–1.42	1.32–1.39

Table 3.22 – General simulation results with technically sound condition of the track and reduced tare weight of the model wagon 19-923-01

Speed range	Coefficient of vertical dynamics of the weight of the bogie, Kd		Coefficient of vertical dynamics of the unreinforced bogie frame, Kdn		Stock factor stability of the wheel from derailment on straight and curved sections of the track	
	The weight of the container is 20.0 tons	The weight of the container is 19.0 tons	The weight of the container is 20.0 tons	The weight of the container is 19.0 tons	The weight of the container is 20.0 tons	The weight of the container is 19.0 tons
40-50 km/h	0.29–0.39	0.29–0.38	0.40–0.48	0.39–0.51	1.55–1.90	1.53–1.88
50-60 km/h	0.31–0.39	0.31–0.38	0.41-0.52	0.39–0.53	1.50–1.68	1.48–1.64
60-70 km/h	0.32–0.45	0.31–0.44	0.48–0.56	0.48–0.56	1.43–1.70	1.40–1.60
70-80 km/h	0.38–0.49	0.38–0.50	0.51–0.60	0.52–0.62	1.39–1.50	1.39–1.46
80-90 km/h	0.39–0.52	0.39–0.51	0.51–0.60	0.52–0.61	1.39–1.49	1.38–1.44

Wagons, when simulating traffic in a technically sound condition of the track and with reduced mass of the bodies, have a sufficient level of dynamics indicators to ensure safe operation. There is a tendency to decrease the coefficient of stability of the wheel from derailment, but the value is at an acceptable level.

Modeling of an experimental wagon in a technically sound condition in the presence of track deviations. The averaged track profile, developed taking into account the recommendations and tested in previous studies, with additional track unevenness coefficients (track unevenness coefficient) of 1.5 and 2.0, which is a generally accepted practice, was used for modeling. From the experience of modeling the dynamics of wagons, it was established that the coef. unequal track in the range of 1.0...1.5 corresponds to the actual technical condition of the track of JSC "Ukrzaliznytsia", the value of 1.5 approximately corresponds to the maximum permissible level of deviations, the value of the coef. unequal ruts at the level of 2.0 corresponds to exceeding the permissible values of deviations.

The general results of modeling are given in table 3.23.

Table 3.23 – General results of modeling the wagon in a technically sound condition in the presence of track deviations

Speed range	Coefficient of vertical dynamics of the weight of the bogie, Kd		Coefficient of vertical dynamics of the unreinforced bogie frame, Kdn		Stock factor stability of the wheel from derailment on straight and curved sections of the track	
	Coef. unequal tracks - 1.5	Coef. unequal tracks - 2.0	Coef. unequal tracks - 1.5	Coef. unequal tracks - 2.0	Coef. unequal tracks - 1.5	Coef. unequal tracks - 2.0
40-50 km/h	0.38–0.48	0.40–0.49	0.44–0.50	0.48–0.56	1.51–1.81	1.50–1.81
50-60 km/h	0.39–0.52	0.41–0.48	0.45-0.58	0.49-0.66	1.44–1.55	1.43–1.56
60-70 km/h	0.40–0.52	0.45–0.59	0.51–0.65	0.53–0.71	1.38–1.42	1.32–1.40
70-80 km/h	0.41–0.51	0.51–0.68	0.55–0.71	0.57–0.75	1.32–1.37	1.29–1.37
80-90 km/h	0.41–0.53	0.55–0.71	0.59–0.74	0.60–0.80	1.32–1.37	1.28–1.36

The wagon, when simulating movement in a technically sound condition in the presence of track deviations, has a tendency to decrease the levels of dynamics indicators. With a significant increase in track unevenness, a reduction in the coefficient of stability of the wheel from derailment to an unacceptable level is possible. The speed at which the decrease in the level of stability margin begins is 70±5 km/h.

Modeling of the experimental wagon with deviations in the technical condition.

The averaged track profile developed and tested in previous studies, a bogie with deviation of the technical condition in the form of maximum wear and a bogie with deviation of the technical condition in the form of maximum wear increased by 15% were used for modeling. The general results of modeling are given in Table 3.24.

Table 3.24 – General results of modeling the wagon with deviations in the technical condition

Speed range	Coefficient of vertical dynamics of the weight of the bogie, Kd		Coefficient of vertical dynamics of the unreinforced bogie frame, Kdn		Stock factor stability of the wheel from derailment on straight and curved sections of the track	
	Maximum wear	Maximum wear +15%	Maximum wear	Maximum wear +15%	Maximum wear	Maximum wear +15%
40-50 km/h	0.30–0.41	0.32–0.42	0.40–0.49	0.42–0.49	1.50–1.91	1.50–1.91
50-60 km/h	0.31–0.41	0.33–0.44	0.41-0.52	0.43-0.55	1.45–1.57	1.43–1.53
60-70 km/h	0.33–0.45	0.37–0.39	0.51–0.56	0.53–0.58	1.37–1.48	1.28–1.37
70-80 km/h	0.38–0.50	0.38–0.50	0.53–0.61	0.56–0.62	1.31–1.40	1.28–1.39
80-90 km/h	0.39–0.50	0.39–0.50	0.54–0.62	0.56–0.66	1.33–1.37	1.29–1.40

Simulation results

The wagon, when simulating the movement with deviations in the technical condition, has a tendency to decrease the levels of the dynamics indicators. When the deviations (wear) of the bogie elements increase, a decrease in the coefficient of stability of the wheel from derailment to an unacceptable level is observed.

According to the results of computer modeling of the dynamics of experimental wagons, the following was established:

When simulating the movement of experimental wagons, provided that the wagons and the track are in a technically sound condition, the experimental wagons have a level of dynamics indicators that ensures safe operation.

When simulating the movement of experimental wagons, provided that the track is in a technically sound condition, but with reduced tare masses of the bodies, the wagons have a level of dynamic indicators that ensures safe operation.

When the mass decreases, there is a tendency to decrease the coefficient of stability of the wheel from derailment, but its values do not go beyond the permissible limits.

Pry simulation of the movement of experimental wagons, provided that they are in a technically sound condition, but there are deviations in track maintenance, the wagons have a tendency to deteriorate the dynamics indicators. With a significant increase in track unevenness, a reduction in the coefficient of stability of the wheel from derailment to an unacceptable level is possible. The speed at which the level of stability margin begins to decrease is 70±5 km/h.

When simulating the movement of experimental wagons with deviations in the technical condition, the wagons have a tendency to deteriorate the dynamics indicators. When the deviations (wear) of the elements of the bogie increase, the coefficient of stability of the wheel from derailment may decrease to an unacceptable level.

Summarizing the results of running dynamic tests and computer modeling of the dynamics of the movement of hopper wagons in an empty state, the following was established:

According to the results of computer simulation, it was established that:

– if the wagons and track are in good technical condition, the dynamics indicators are within the permissible values.

– with deviations in the technical condition of the wagons and track, the dynamics of the wagons deteriorates to an unacceptable level.

– the speed at which the level of stability margin decreases below the minimum permissible in the presence of deviations - 70±5 km/h.

– the simultaneous presence of deviations in the maintenance of the track and in the technical condition of the wagon reduces the speed at which the margin of stability reaches a value less than the minimum permissible.

CONCLUSIONS ON SECTION 3

A methodology for in-depth processing of the results of rolling stock running tests is proposed. The essence is to perform a spectral analysis of dynamic processes for various elements of the load-bearing structures of the freight wagon, with the aim of identifying the relationships between the oscillatory processes of the load-bearing structures and the frequencies at which the interaction between them occurs. A software algorithm for in-depth assessment of experimental indicators of the quality of the movement of freight wagons with reduced tare has been developed.

Taking into account the main causes and hypotheses regarding the derailment of freight wagons, the results of computer modeling can be concluded that the main reasons of the wagons derailment are malfunctions of the carriage chassis, wear of the elements of the friction dampers and the body support unit on the bolsters, unacceptable deviations in the dimensions of the bogies, non-compliance with the requirements for the rail track maintenance. Also, an important reason is the negative reduction of the wagon's tare by more than 10% from the one set by the manufacturer.

SECTION 4
PRACTICAL ASPECTS OF IMPLEMENTING IMPROVED MEANS AND APPROACHES FOR DETERMINING AND ASSESSING INDICATORS OF SAFETY AND TECHNICAL CONDITION OF WAGONS

4.1 A mobile system for determining safety indicators and technical condition in operating conditions

The operation of rolling stock and complex technical hardware and software systems is usually subject to failures. The reasons for such failures may be non-compliance with manufacturing technology, difficult conditions of use, non-compliance with the requirements for the operation of such systems and rolling stock, aging and wear of components. Therefore, a relevant and important task is the introduction of periodic testing and diagnostics of rolling stock on the Ukrainian railways during their life cycle.

Currently, the development of measuring equipment and systems makes it possible to implement advanced instrumental approaches to assess the quality and safety indicators of train traffic and take measures to prevent emergency situations. The successful experience of implementing diagnostic systems for locomotives and passenger wagons justifies the feasibility of further improving methods and means of experimental assessment of dynamic qualities and indicators of quality and traffic safety during the entire period of operation of rolling stock.

4.1.1 General requirements for a mobile system to determine indicators of quality and traffic safety.

A mobile system for determining the quality and safety indicators of rolling stock in operation should include:

- primary sensors;
- GPS receiver;
- signal transmission cables;
- systems for collecting and recording measurement characteristics;
- transferring data about the location and status of the system to the server;
- determination and assessment of quality and traffic safety indicators in express processing mode.

Primary sensors – strain gauges and accelerometers. The cables are designed for connecting sensors with recording devices, the voltage of which is ±10 V. Shielded 6-wire cables, resistant to external factors with operating temperatures from -40 to +80°C.

The mobile system must ensure autonomous dynamic testing of rolling stock to determine the stability factor of the wheel from the derailment, vertical and lateral forces and acceleration of sprung and unsprung parts of rolling stock, as the basis for assessing the quality of planned types of repairs and determining indicators of quality and traffic safety in operating conditions

When conducting dynamic running tests, the following indicators are recorded: vertical and horizontal accelerations of bogie frames and the wagon body, dynamic stresses in the frames of the body and bogies under various driving modes.

4.2 Hardware and primary converters of the mobile system

A mobile system for dynamic running tests and assessment of quality and traffic safety indicators based on National Instruments CompactRIO solves a wide range of tasks aimed at monitoring the technical condition of rolling stock during testing and in normal operation.

Strain gauges are connected to the NI 9237 strain gauge module (Fig. 4.1), and accelerometers are connected to the NI 9205 ADC module (Fig. 4.2), they scale instantaneous input voltage values and analog-to-digital conversion to digital code.



Figure 4.1 – NI 9237 module



Figure 4.2 – NI 9205 module

Digital signals are transmitted via the internal bus from the NI 9237 and NI 9205 modules to the NI 9012 controller (Fig. 4.3), from the output of which they enter the computer via the Ethernet interface bus, where measurement information is processed, displayed and stored.



Figure 4.3 – NI 9012 controller

The software performs the functions of controlling the recording process, initial setup of the mode for recording signals from measuring channels, operating modes of the automatic recorder, mathematical functions for processing, presenting and storing measurement information. Consists of the following blocks:

– software for firmware programmable logic

– integrated circuit (FPGA), located in the NI 9104 chassis (Fig. 4.4);

– application software of the NI 9012 controller;

– client part of the application software of the host computer recorder.



Figure 4.4 – NI 9104 chassis

The hardware and software recorder software is developed in the LabView FPGA software shell.

Application software is designed to read measurement data from user-selected channels at the hardware level with a given sampling frequency, select the type of connection for the outputs of measuring primary converters, and set voltage measurement limits.

The NI 9012 controller application software consists of two parts. The first part reads data from the NI 9237 and NI 9205 ADC modules, processes the data and writes to the controller's non-volatile memory. The second part transmits data via the Transmission Control Protocol (TCP) to an external computer.

Computer software, using a user interface, performs general control functions and displays current measurements on the monitor screen.

The mobile system can operate in two functional modes: assessment of quality indicators, traffic safety and strength indicators in real time (Fig. 4.5) and measurement of acceleration and deformation values offline on rolling stock with subsequent processing (Fig. 4.6). When processing the obtained values, data obtained using a GPS receiver is used to assess the impact of changes in movement speed on the monitored parameters.

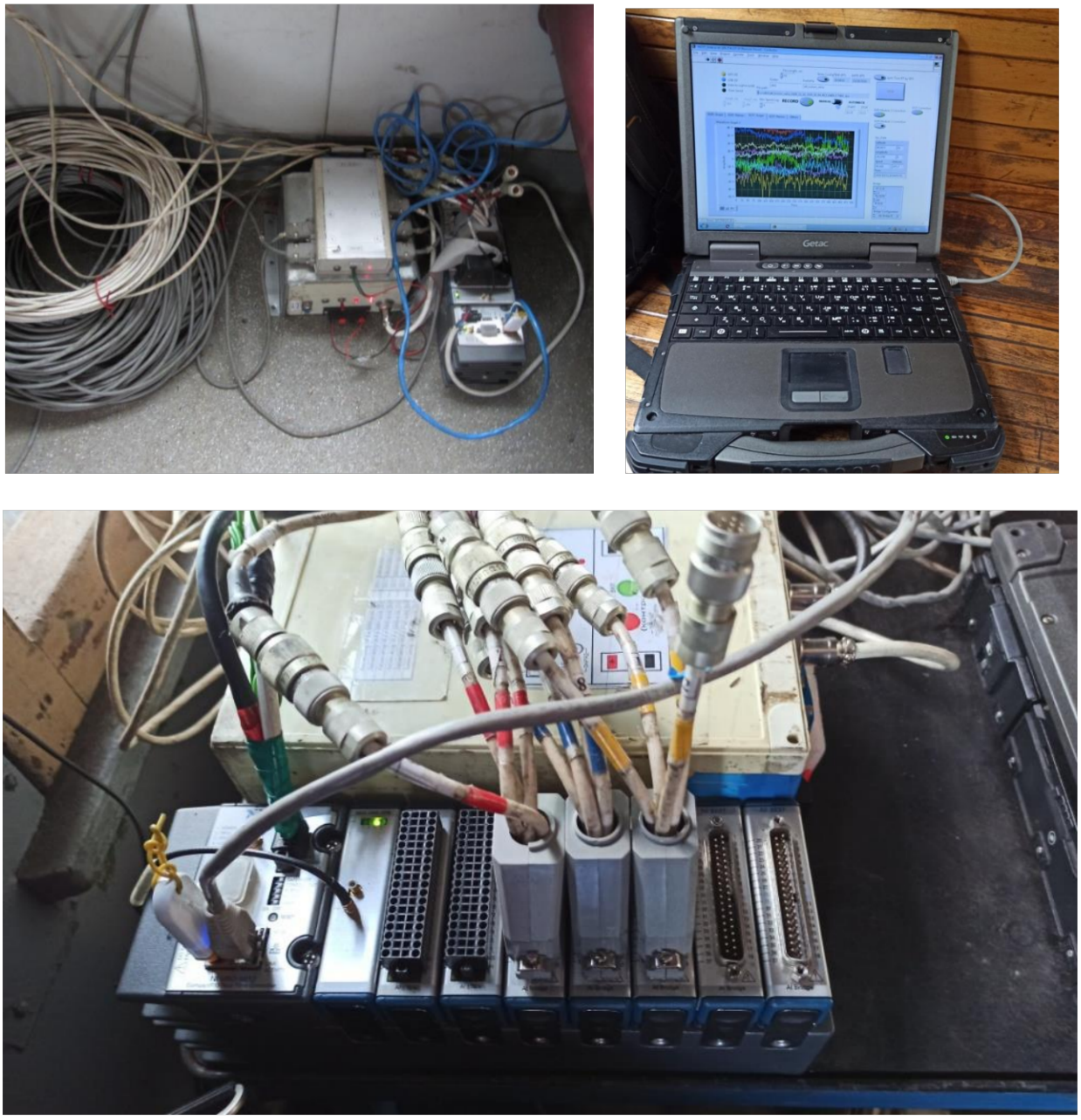

Figure 4.5 – Mobile system in real time



Figure 4.6 – Mobile system in offline mode

The general block diagram of the mobile diagnostic system is shown in Figure 4.7.

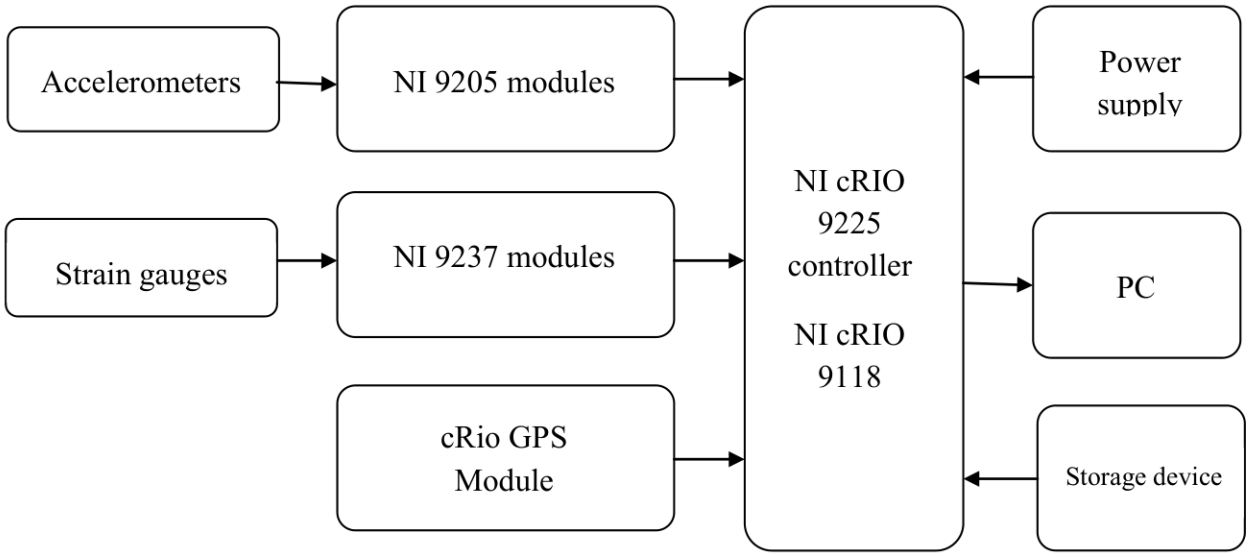

Figure 4.7 – Block diagram of the mobile system

To measure and evaluate the dynamic characteristics of rolling stock, low-frequency accelerometers of the UM type are used. It consists of a shockproof and impenetrable case, a board with an ADXL 278 chip, a detachable UZNTs 05-7/12VP11 and fastening elements. The general view of the accelerometer is shown in Figure 4.8.

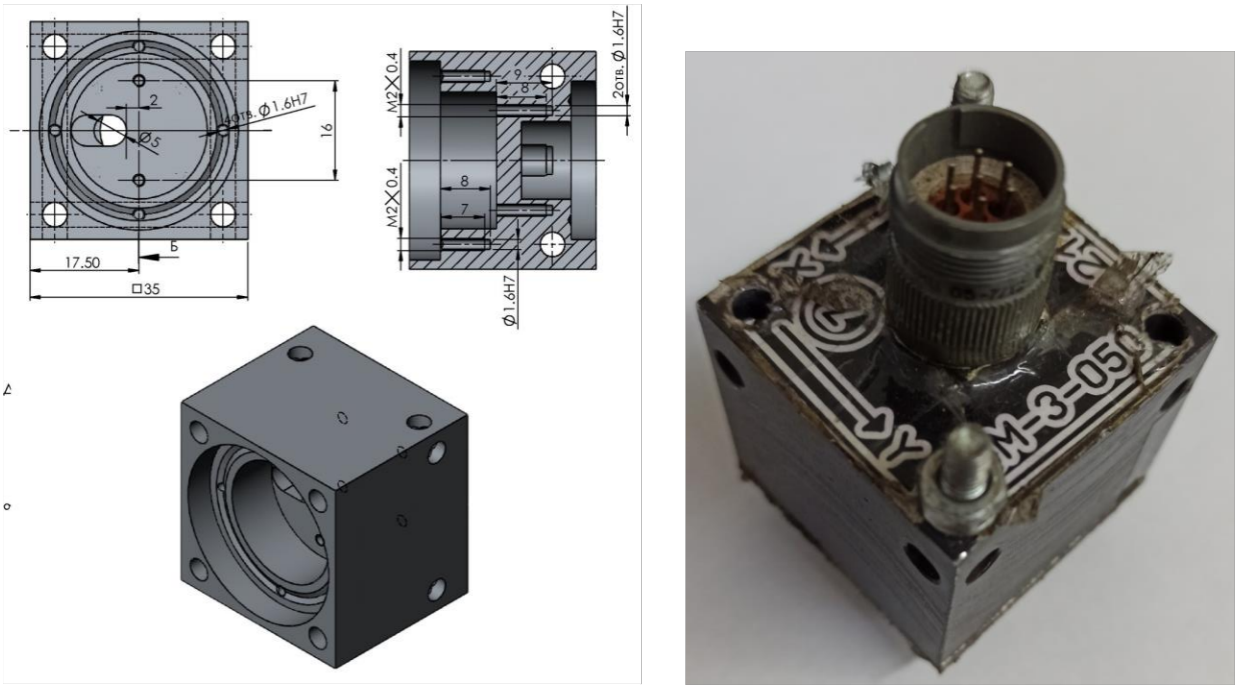

Figure 4.8 – UM type accelerometer

The accelerometer diagram is shown in Figure 4.9.

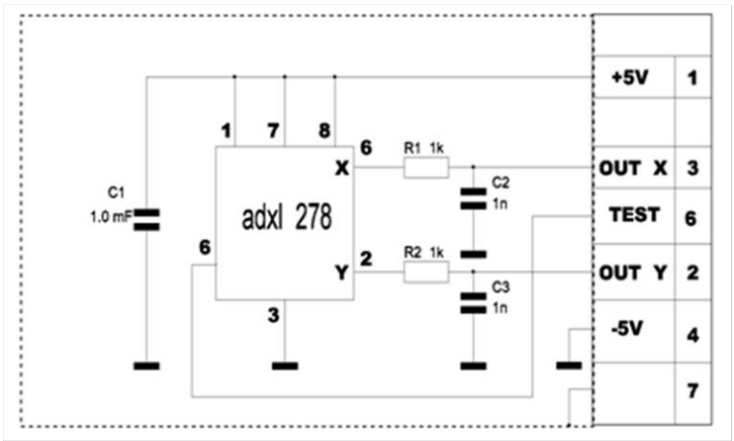

Figure 4.9 – Accelerometer diagram

General technical requirements for accelerometers used in a mobile diagnostic system.

Table 4.1 – Technical requirements for accelerometers

No.	Accommodation area	Range, m/s^2	Frequency range, Hz	Uncertainty
1	Axle box unit	±500	0.5-100	From 0.5 to 5 Hz U=2.5% From 5.1 to 19 Hz U=1.5% From 20 to 100 Hz U=1%
2	Bogie frame	±350	0.5-100	From 0.5 to 5 Hz U=2.5% From 5.1 to 19 Hz U=1.5% From 20 to 100 Hz U=1%
3	Body	±100	0.5-100	From 0.5 to 5 Hz U=2.5% From 5.1 to 19 Hz U=1.5% From 20 to 100 Hz U=1%

The obtained vibration accelerations can be used to assess track quality indicators to detect point geometric deviations that affect the dynamics of rolling stock movement. The measurement data must be used with data obtained from GPS and basic measurement parameters.

Vibration acceleration must be measured in certain places of the body and bogie; places are chosen depending on what indicator needs to be assessed. Vertical accelerations at the axle boxes are measured to assess the surface irregularities of the track. The trolley's lateral accelerations are measured to evaluate short-wave path

deflections. Measuring the lateral and vertical accelerations of the body makes it possible to evaluate the dynamic indicators of the quality of movement of rolling stock. The speed at which body and bogie acceleration measurements are taken must be within the established operating range.

The measured accelerations can be used as indicators of the quality of track geometry and to detect local geometric deviations affecting the dynamic behavior of rolling stock. These measurements should be used in combination with basic parameter measurements.

Acceleration measurements should be made at specific locations on the body and bogies, depending on the need for a specific assessment. Thus, vertical accelerations of axle boxes are measured to identify rail surface defects and isolated geometric irregularities. The lateral accelerations of the trolley serve to detect irregularities with short waves. Transverse and vertical accelerations of the body reveal track defects that affect the dynamic characteristics of comfort.

The sampling frequency must be at least 2.5 times the cutoff frequency applied to the signal. Measurement of bogie and body accelerations should be carried out in the operating speed range for the line within a tolerance of +/-10%.

In order to measure movements and evaluate dynamic qualities, cable displacement sensors are used (Fig. 4.10). Rope sensors measure linear movement using a steel cable. In this case, the cable drum is connected to a sensitive element, which converts the movement of the cable into a linear output signal. The measurement is carried out with high accuracy and dynamics. Mounting grooves on four sides of the sensor ensure easy and secure installation.



Figure 4.10 – Cable-type displacement sensors

Based on the comparative characteristics of the static deflections of bogies of four types Y-32, GP-200, KVN TsNII, 68-7007, displacement sensors with the following measurement ranges were determined to be optimal: 300 mm for measuring displacements in the primary suspension stage, 625 mm for the secondary stage.

4.3 Software for collecting and recording measurements

The measurement information collection subsystem collects, stores and visualizes changes in information signals from displacement sensors, vibration accelerations and mechanical deformations. In addition, GPS receiver data is used to analyze the influence of movement speed on changes in controlled parameters, obtain precise time signals and determine current coordinates. Generalized withstructuremeasurement information subsystems are shown in Figure 4.11.

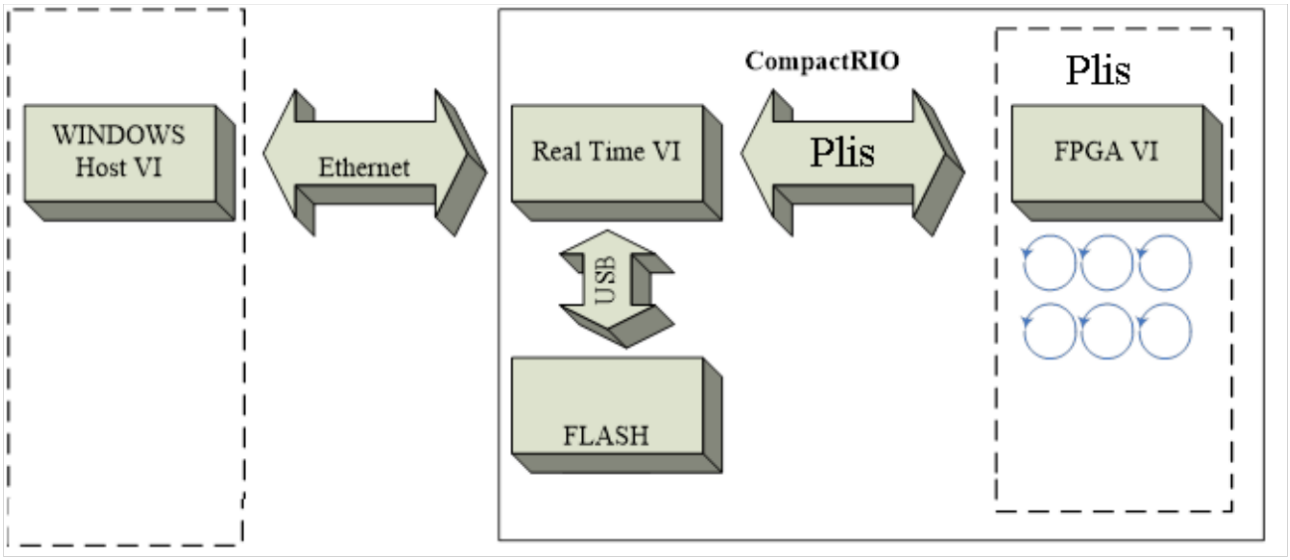

Figure 4.11–Software structure

The developed acquisition subsystem provides operation of a CompactRIO controller with an 8-module chassis with a built-in programmable logic integrated circuit (FPGA) and two universal 9205 ADC modules with a maximum sampling frequency of 250 kHz and five 923 strain gauge modules - a GPS signal receiver.

Thanks to the built-in FPGA, CompactRIO has the ability to implement measurement data processing algorithms at the hardware level with a deterministic execution time of 25 ns without transferring the load to the controller's central processor. A typical CompactRIO device includes a controller running a PharLab or VxWorks real-time operating system, a chassis, and I/O modules. The chassis carries an FPGA core that is directly connected to universal or specialized input/output modules that have built-in means for matching and processing information signals. There are different chassis models that have different numbers of slots for modules and differ in the characteristics of FPGA chips.

Thanks to its autonomy, hardware and weight-size characteristics, as well as the ability to operate in adverse conditions, CompactRIO can be used to solve a wide range of problems in collecting measurement information and controlling processes.

Most software for CompactRIO is developed according to a scheme that provides for its conditional division into three levels: the HOST VI virtual instrument

on a control PC running Windows OS, RT VI on a controller with a real-time OS, and FPGA VI on an FPGA that does not have its own OS, since the logic The program's operation was implemented directly at the hardware level. Each of the presented levels has its own specific functionality and implements individual functions of the system as a whole.

Common tasks performed using HOST VI on a Windows computer:

- saving data on a computer and accessing databases; - integration with external information systems; - interface organization.

Typical tasks performed in RT VI on a real-time controller:

- data processing; - management; - saving data in the built-in memory of the controller and on external media. Typical tasks performed in FPGA VI on FPGA:

- input-output operations;

- hardware clocking and control of the process of interaction with equipment; - low-level processing of measuring signals.

An FPGA is a chip whose functionality is determined by programming or "configuration", which is the more common term when working with this class of integrated circuits. The LabView FPGA Module package is an addition to the LabView software environment that allows you to specify the logical operation of the FPGA as a regular virtual device instead of programming using a specialized VHDL language. This package allows you to create programs with synchronous and asynchronous parallel loops running in hardware, and provides time-deterministic data collection and analysis.

The LabVIEW FPGA Module software package completely takes care of the multi-step process of converting a virtual device into FPGA binary code. At the first stage, the virtual device is converted into text code in the VHDL language, after which it is compiled into binary form by the standard industrial compiler Xilinx ISE. During the compilation process, the code is optimized for execution speed and the number of logic gates involved.

The result of compilation is a binary file (bitstream file) that completely defines the FPGA configuration. When the program starts, the binary file is loaded onto the chassis, that is, the FPGA configuration process occurs. The binary file can be written to the built-in flash memory and automatically loaded when the system is turned on. The configuration is not saved when the power is turned off, so the binary file must be downloaded again when power is turned on again. With appropriate configuration settings, it can be loaded automatically from the flash memory of the FPGA device or by a program using the controller.

FPGA VI virtual instruments can be produced completely, independently of other system components, and remain operational even if the controller fails. Moreover, a buffer can be organized on the FPGA to prevent data loss in such a situation.

The FPGA is designed primarily for clocking, synchronization, control, data acquisition and preliminary digital processing of information signals, control of each input/output module.

A virtual device for a CompactRIO controller typically includes two or more loops: a critical priority loop, which implements control and data processing algorithms, and a normal priority loop, which is responsible for data safety, a remote web interface, and communication over an Ethernet network or RS bus. 232.

The CompactRIO platform provides three paths to elevate data from modules to the real-time controller level: through front panel elements, through a mechanism known in LabView as Local Variables, and through a DMA FIFO buffer. The first two approaches are relatively simple in terms of implementation, but suboptimal in terms of efficiency. At the same time, the DMA FIFO method allows you to receive data obtained at high sampling rates from a large number of modules without delay. One of the advantages of DMA mode is that data transfer occurs regardless of the central processor.

FPGA devices that support DMA FIFO buffers have direct memory access, unlike other methods that require the CPU. Direct memory access is implemented by

capturing the PCI bus (bus mastering) by the FPGA device, in which it gains access to bus control, and therefore access to memory, bypassing the processor.

The DMA FIFO buffer consists of two sections: one part is located in the FPGA memory, the other in the controller memory. The FPGA can write or read from the buffer element by element using the FIFO Read and FIFO Write methods, and the controller can write or read samples of elements. The two parts of the buffer are connected using a hardware-software DMA controller. Thus, from a software point of view, they look like a single FIFO buffer.

The FPGA VI virtual device, located on the FPGA, implements the functionality of initialization, clocking, polling of data acquisition modules and subsequent loading of the received samples into the DMA FIFO buffer. To ensure a deterministic sequence of command execution, the programming language structure in LabView Flat Sequence Structure is used, which contains elements for polling modules and writing to a buffer.

The DMA FIFO buffer is cyclically polled at intervals set by a timer at the real-time controller level, after which the samples obtained in the form of integers according to the dynamic range and bit capacity of the acquisition module are normalized by the values of acceleration and deformation. The received data is fed to a virtual device, which processes and stores it on an external drive connected via a USB bus.

CompactRIO controllers have a built-in USB 2.0 controller, but not all drives support this standard, which can lead to significant write delays, which, in turn, lead to DMA FIFO buffer overflow and incorrect operation of the system as a whole. The presented system does not have a virtual control device located on a personal computer, but instead uses the LabView Remote Panel mechanism. This function implements the so-called Client-Server model, where the controller is the server, and the client is any computer with LabView installed. By default, CompactRIO is

licensed for one external connection, but the number can be expanded. To activate the Remote Panel on the controller, you need to activate the Web server in the project settings and select the virtual devices to which you want to allow remote access. This feature can significantly reduce the time required to develop HOST VI, but can create a load on the data network [79].

In addition to the acquisition modules, to synchronize time and acquire current speed and coordinates, a GPS receiver is also connected to the controller, installed on the chassis in the same way as standard modules. Because the receiver is manufactured by a third party, the LabView Real Time Module does not have a standard means of acquiring GPS data, so it uses a set of separately installed virtual devices to communicate with it. In addition, to ensure correct functioning of the module as part of the project, the SubVIs supplied with the module should also be added to the FPGA VI. If initialization is successful, the GPS data is presented as a cluster or directly in text format, which can be used to configure software or perform other tasks.

4.4 Practical studies of quality indicators and movement safety of freight wagons in an empty state

The objects of research were a universal platform wagon model 13-4012 (Fig. 4.12), tank wagon model 15-1443 (Fig. 4.13) and cement hopper wagon with roof removed model 19-758-01 (Fig. 4.14) in an empty state.



Figure 4.12 – Flat wagon model 13-4012



Figure 4.13 – Tank wagonmodel 15-1443



Figure 4.14 – Hopper wagon model 19-758-01

The weight of the flat wagon model 13-4012 is 20.4 tons, the weight of the tank wagon model 15-1443 is 22.15 tons, the weight of the hopper wagon for cement with the roof removed model 19-758-01 is 18.15 tons.

Dynamic running tests were carried out on the Darnitsa-Nizhyn section of the South-Western Railway as part of an experimental coupling and train set. The experimental coupling was formed from a flat wagon model 13-4012, a tank wagon model 15-1443, a cement hopper wagon with the roof removed model 19-758-01, a locomotive, and a laboratory wagon.

Tests on the train were carried out in 3 options: option 1 – locomotive – 6 empty gondola wagon – experimental coupling – 30 loaded gondola wagon; option 2 locomotive – 15 loaded gondola wagon – experimental coupling – 6 empty gondola wagon – 15 loaded gondola wagon; option 3 – locomotive – 30 loaded gondola wagon – experimental coupling – 6 empty gondola wagon.

The section of the track on which the tests were carried out, in terms of the composition of straight and curved sections, met the requirements for the track for conducting dynamic running tests.



Figure 4.15 – Experienced coupling



Figure 4.16 – Experienced coupling



Figure 4.17 – Experienced coupling on a train

The registration of processes was carried out using strain gauges installed on the structural elements of the bogie.



Figure 4.18 – Side frame of the wagon, channel 1



Figure 4.19 – Side frame channel 2

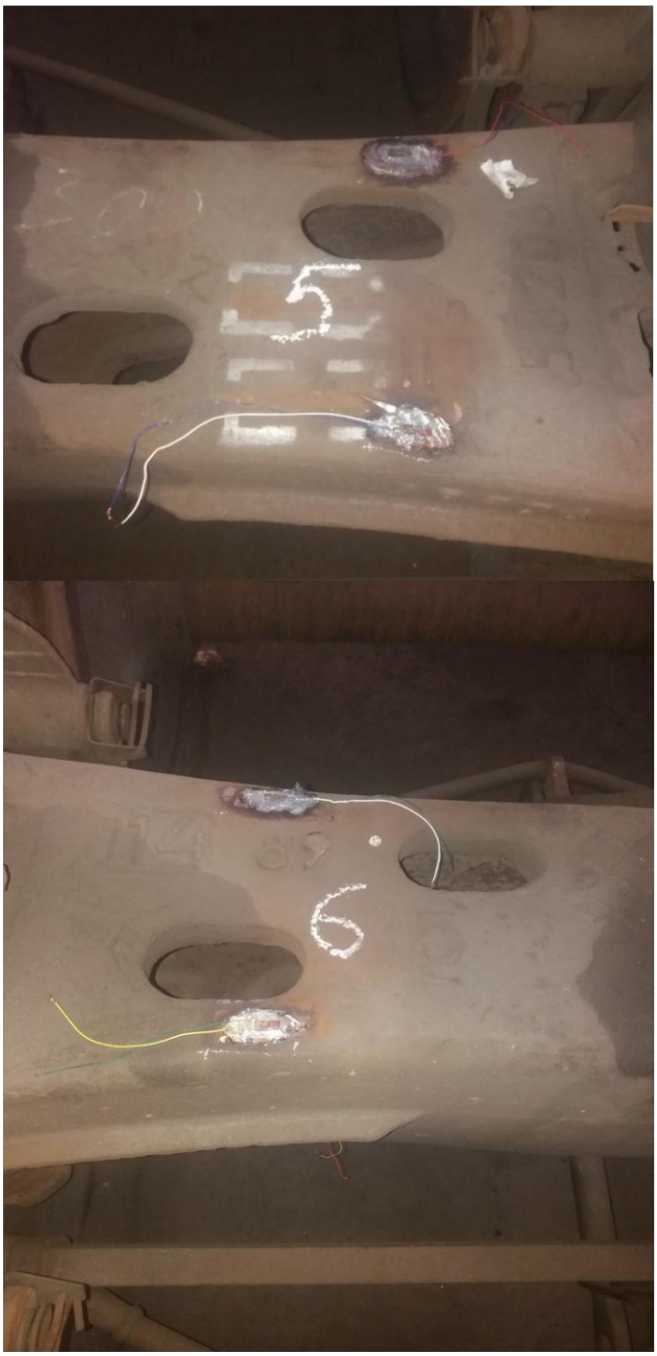

Figure 4.20 – Wagon bolster, channel 5, 6



Figure 4.21 – R55 wagon channel 9, 10

All other ducts on the Model 15-1443 tank wagon and the Model 19-758-01 roofless cement hopper wagon were installed similarly.



Figure 4.22 – Deflection meter on a flat wagon model 13-4012

Proginometers on the tank wagon model 15-1443 No. 74084252 and on the hopper wagon for cement with the roof removed model 19-758-01 No. 96914908 were installed similarly.

To determine the longitudinal forces acting on the test wagon, an automatic coupler-dynamometer was used (Figure 4.23), equipped with strain gauges and a pre-calibrated static load on the stand with a force of up to 3.5 MN.



Figure 4.23 – Automatic coupler-dynamometer

After installing the measuring equipment on the experimental wagon, the bogies were calibrated against vertical and horizontal forces (Figure 4.24).



Figure 4.24 – Bogie packaging

To record the readings of strain gauges and vibration transducers, a software and hardware complex is used, consisting of a cRIO NI 9012 controller with strain gauge

ADC modules NI 9237, ADC modules NI 9205 and specialized software developed in the LabVIEW software package.

Data processing under static loads was carried out using automated complexes for processing experimental data. The magnitude of stresses during static tests was determined by the difference in readings of measuring equipment before and after lifting the platform frame:

$$\sigma_{ver} = (\Delta - \Delta_0) \cdot K \quad (4.1)$$

where: - readings of measuring equipment in the loaded state of the test object:Δ

- readings of measuring equipment in the empty state of the test object:Δ_0

K – calibration coefficient of measuring equipment, determined by formula (4.2):

$$K = \frac{R_d}{R_h A_h} \quad (4.2)$$

where: – resistance of the strain gauge, Ohm; R_d

- resistance of the calibration shunt, Ohm; R_h

- amplitude (deviation) of the process measured during calibration, V. A_h

The results of running dynamic tests were determined from the data (measurements, calculations, control, visual inspection) recorded during the measurements.

The stability of the wheel from the east of the wheel from the rail was determined for the most dangerous cases of a combination of a large lateral force of interaction between the oncoming wheel and the rack and a small vertical load on this wheel. With the simultaneous action of such a combination of extreme forces for some time, it is possible for the oncoming wheel flange to roll onto the rail head and the subsequent easting of the wagon from the rail.

Processing data from running dynamic tests of wagon s involves

decoding, identification and systematization of parameters of recorded dynamic processes. During processing, wagon running quality indicators are taken into account - up to 20 Hz. The quantization frequency when processing experimental data on a computer must be at least 100 Hz.

Research data is grouped by speed ranges (10-20 km/h), characteristic features of track sections (straight, curve, arrows, etc.).

To assess driving performance based on the values of the measured dynamic indicators of the wagon, using ratios taking into account the calibration data, the probable maximum values of the coefficients of vertical dynamics of the spring $К_{ds}$and non-sprung masses $К_{dn}$ of the wagon, lateral (frame) forces, and the value of the safety factor against derailment are determined.$К_{st}$

The maximum values of the coefficients of vertical dynamics and frame forces are determined with a confidence probability of 0.97 (based on the amplitude value) and 0.97 (based on the instantaneous values), and the minimum values of the safety factors against derailment with a confidence probability of no more than 0.0001. For the amount of lateral (frame) forceH_p the sum of frame forces acting at the same time on the frame from each axlebox of one wheel pair is taken.

The calculation of the safety factor of the wagon against derailment when the wheel flange crawls onto the rail under the influence of dynamic forces arising during movement, the coefficients of the vertical dynamics of the sprung and unsprung masses of the wagon are given below. The coefficient of vertical dynamics in general is determined from the following expression:$К_d$

$$К_d = \frac{\sigma_{ds}}{\sigma_{sl}}, \qquad (4.3)$$

σ_{ds} – where is the dynamic stress from the vertical load in the cross section of this element;

σ_{sl} – static load from vertical load in the same section.

The coefficients of vertical dynamics were determined for the sprung ($К_{ds}$) and unsprung ($К_{dn}$) masses of the bogie.

Horizontal dynamics coefficient (frame force in fractions of axial load) - determined by the formula:$К_h$

$$К_h = \frac{H_{lf}}{P_a}$$

where: H_{lf} – horizontal lateral frame force;

P_a– vertical static load from the axle on the rails.

The stability factor of the wheel from the east from the rail $К_{st}$ is determined by calculation using the integral coefficient calculated for the range of operating speeds with a probability of 0.001, according to formula (3.4; 3.5):

The wheel resistance against derailment was assessed using the formula (4.4; 4.5),

$$К_{st} = \varepsilon \frac{P_v}{P_h} \geq [К_{st}], \quad (4.4)$$

$$\varepsilon = \frac{tg\beta - \mu}{1 + \mu tg\beta}, \quad (4.5)$$

where is the angle of inclination of the generatrix of the wheel flange to the horizontal axis;β

β=60°;

μ– friction coefficient, =0.25;μ

P_v- vertical component of the reaction force of the oncoming wheel on the rail head;

P_h- the horizontal component of the reaction force of the oncoming wheel on the simultaneously acting rail head; $P_в$

$[K_{st}]$– permissible value of the stability safety factor.

When using trolleys model 18-100, formula (4.6) looks like:

$$K_{st} = \frac{tg\beta - \mu}{1 + \mu tg\beta} \cdot \frac{Q_{wf}(1{,}03 - 1{,}17K_d^{on} + K_d^{nn}) + 0{,}515q_{gf} + 0{,}305H_{lf}}{Q_{wf}(0{,}242 + 0{,}042K_d^{on} - 0{,}285K_d^{nn}) + 0{,}121q_{qf} + 0{,}92H_{lf}}, \quad (4.6)$$

where is the gravity force of the bolster parts of the wagon acting on the journal of the wheelset axle, kN, determined by the formula:Q_{wf}

$$Q_{wf} = \frac{Q - nq_{gf}}{2n_0}, \quad (4.7)$$

Q_{wf}- wagon weight force, kN,

q_{gf}- gravity force of untrimmed parts per wheel pair, kN;

n_0- number of wagon axles;

K_d^{on}- coefficient of vertical dynamics on the oncoming wheel;

K_d^{nn}- coefficient of vertical dynamics on the non-running wheel;

H_{lf}- horizontal lateral frame force.

The value of H_{lf} is taken to be positive when it is directed in the direction of the wheel running, and K_d^{on}, K_d^{nn} - when the wheels are unloaded.

Results of running dynamic tests. The forces on automatic couplers-dynamometers during running-dynamic tests at different locations on the train are shown in Figures 4.25 - 4.27, and indicators of the quality of movement of wagon given in Tables 4.2 - 4.15.

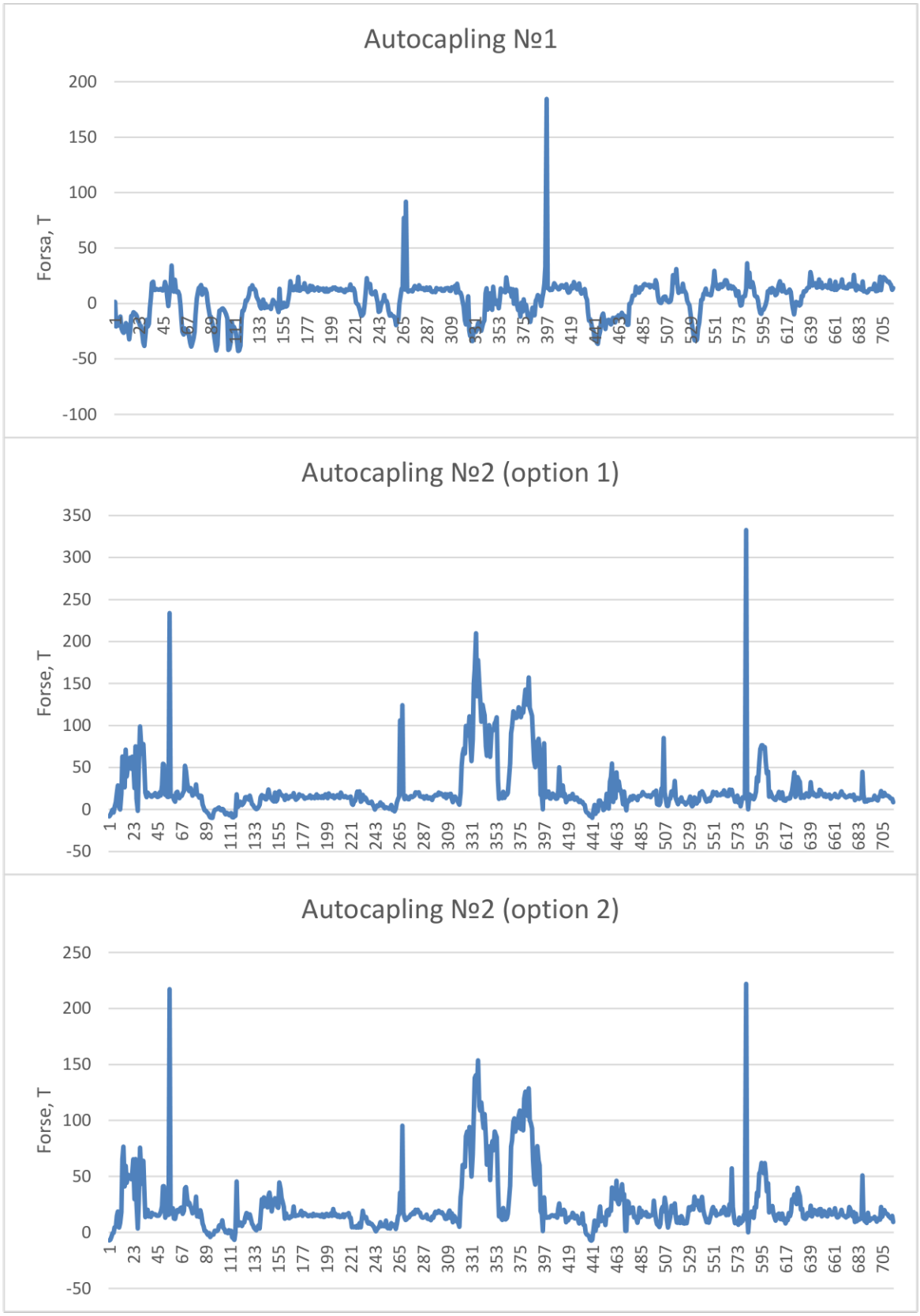

Figure 4.25 – Head of the train

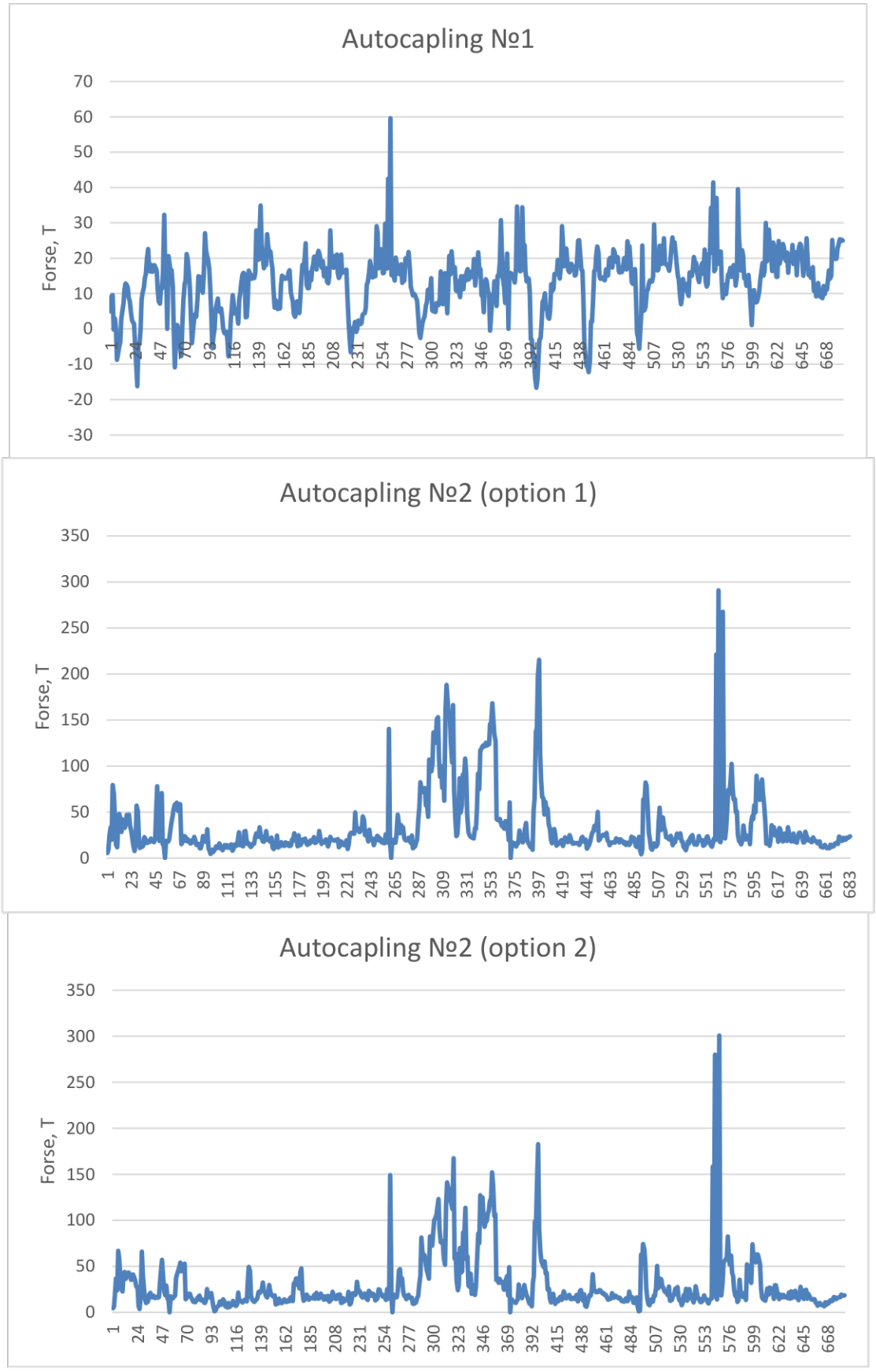

Figure 4.26 – Middle of the train

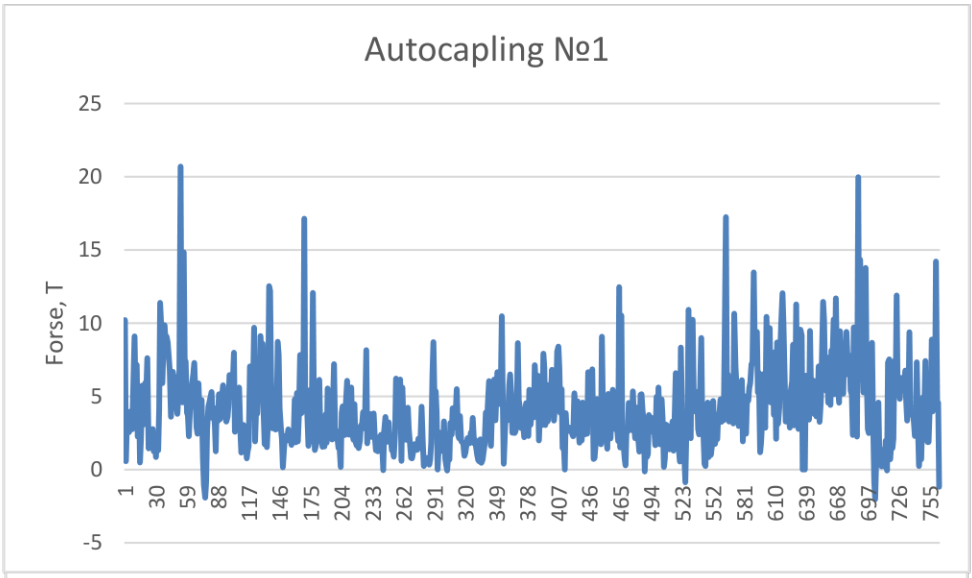

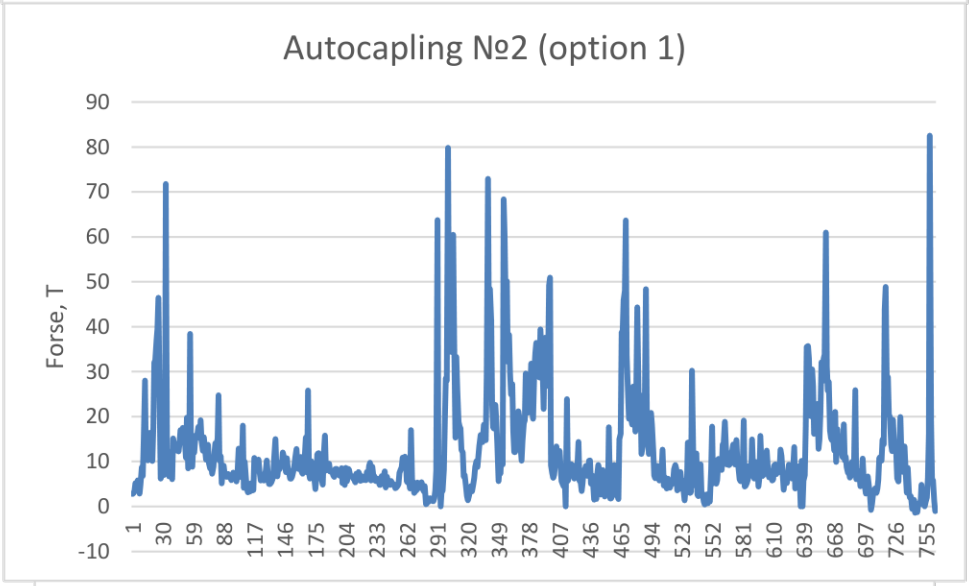

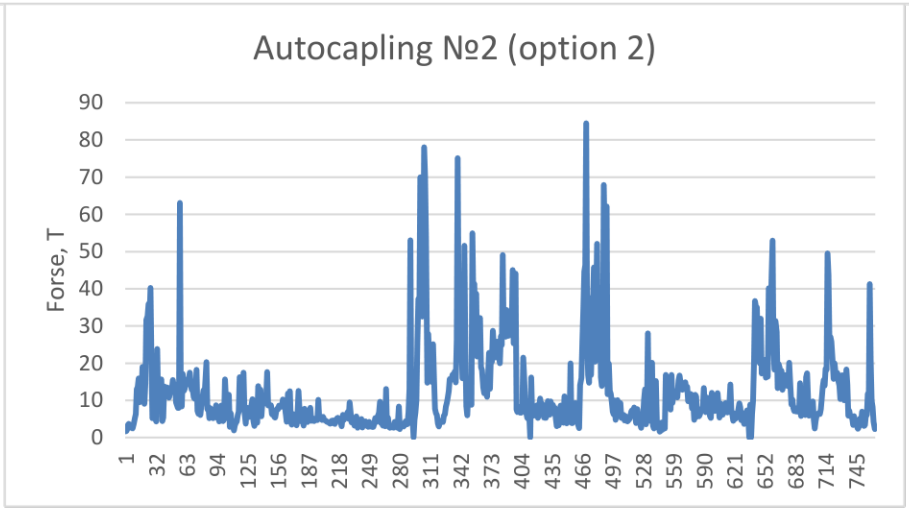

Figure 4.27 – End of the trai

Table 4.2 – Results of running dynamic tests of the universal flat wagon model 13-4012 in empty mode (research coupling)

Controlled characteristics (wagon elements, section, point)	Regulatory documentation containing the value, requirement for the parameter	Indicator value											
		Permissible value	Actual value (by speed intervals)										
			At speed, km/h										
			40±5	Uncertainty	50±5	Uncertainty	60±5	Uncertainty	70±5	Uncertainty	80	Uncertainty	Note
Coefficient vertical dynamics of the sprung mass of the bogie, K_d, no more	DSTU 7598 DSTU GOST 33211-2017	0.75 0.75	0.34	0.01	0,35	0.01	0.39	0.01	0.42	0.01	0.48	0.01	
Coefficient of vertical dynamics of the unsprung bogie frame, K_{dn}, no more	DSTU 7598 DSTU GOST 33211-2017	0.90 0.90	0.45	0.01	0.48	0.01	0.56	0.01	0.52	0.01	0.63	0.01	
Frame forces H_p, t	-	-	1,4	0.02	1.5	0.02	1.5	0.02	1,8	0.02	1,8	0.02	
Coefficient Horizontal dynamics (frame force in fractions of P_0 (Hp/P_0), from the wheel pair to the bogie frame), no more	DSTU 7598 DSTU GOST 33211-2017	0.40 0.40	0.28	0.01	0.33	0.01	0.32	0.01	0.35	0.01	0.36	0.01	
Coefficient safety margin of the wheel from the derailment on straight and curved sections of the track, not less	DSTU 7598 DSTU GOST 33211-2017	1,3 1,3	1.46	0.025	1,41	0.025	1.31	0.025	**1.29**	0.025	**1.24**	0.025	

Continued table 4.2

Controlled characteristics (wagon elements, section, point)	Regulatory documentation containing the value; requirement for the parameter	Indicator value											
		Actual value (by speed intervals)											
		At speed, km/h											
		Permissible value	40±5	Uncertainty	50±5	Uncertainty	60±5	Uncertainty	70±5	Uncertainty	80	Uncertainty	Note
Body acceleration vertical Z_{sq}, in fractions of g, no more	DSTU 7598 DSTU GOST 33211-2017	0.75 0.75	0.29	2.5%	0.40	2.5%	0.49	2.5%	0.56	2.5%	0.71	2.5%	
Body acceleration horizontal Y_{kg}, in fractions of g, no more	DSTU 7598 DSTU GOST 33211-2017	0.55 0.55	0.26	2.5%	0.3	2.5%	0.41	2.5%	0.47	2.5%	0.5	2.5%	

Table 4.5 – Results of dynamic running tests of the tank wagon model 15-1443 in empty mode (research coupling)

Controlled characteristics (wagon elements, section, point)	Regulatory documentation containing the value, requirement for the parameter	Indicator value										
		Permissible value	Actual value (by speed intervals)									
			At speed, km/h									
			40±5	Uncertainty	50±5	Uncertainty	60±5	Uncertainty	70±5	Uncertainty	80	Uncertainty	N
Coefficient vertical dynamics of the sprung mass of the bogie, K_d, no more	DSTU 7598 DSTU GOST 33211-2017	0.75 0.75	0.3	0.01	0.32	0.01	0.4	0.01	0.41	0.01	0.45	0.01	
Coefficient of vertical dynamics of the unsprung bogie frame, K_{dn}, no more	DSTU 7598 DSTU GOST 33211-2017	0.90 0.90	0.41	0.01	0.45	0.01	0.49	0.01	0.5	0.01	0.6	0.01	
Frame forces H_p, t	-	-	1.6	0.02	1.7	0.02	1.6	0.02	1.8	0.02	1.9	0.02	
Coefficient Horizontal dynamics (frame force in fractions of P_0 (Hp/P_0), from the wheel pair	DSTU 7598 DSTU GOST 33211-2017	0.40 0.40	0.21	0.01	0.23	0.01	0.3	0.01	0.31	0.01	0.33	0.01	
Coefficient safety margin of the wheel from the derailment on straight and curved sections of the track, not less	DSTU 7598 DSTU GOST 33211-2017	1,3 1,3	1.5	0.025	1,47	0.025	1.38	0.02	1.35	0.025	1.33	0.025	

Continued table 4.5

Controlled characteristics (wagon elements, section, point)	Regulatory documentation containing the value, requirement for the parameter	Indicator value											
		Actual value (by speed intervals)											
		At speed, km/h											
		Permissible value	40±5	Uncertainty	50±5	Uncertainty	60±5	Uncertainty	70±5	Uncertainty	80	Uncertainty	Note
Body acceleration vertical Z_{sq}, in fractions of g, no more	DSTU 7598 DSTU GOST 33211-2017	0.75 0.75	0.26	2.5%	0.38	2.5%	0.42	2.5%	0.5	2.5%	0.53	2.5%	
Body acceleration horizontal Y_{kg}, in fractions of g, no more	DSTU 7598 DSTU GOST 33211-2017	0.55 0.55	0.23	2.5%	0.28	2.5%	0.32	2.5%	0.39	2.5%	0.42	2.5%	

Table 4.6 – Results of running dynamic tests of the hopper wagon model 19-758-01 in empty mode (research coupling)

Controlled characteristics (wagon elements, section, point)	Regulatory documentation containing the value; requirement for the parameter	Indicator value										
		Permissible value	Actual value (by speed intervals)									
			At speed, km/h									
			40±5	Uncertainty	50±5	Uncertainty	60±5	Uncertainty	70±5	Uncertainty	80	Uncertainty	Note
Coefficient vertical dynamics of the sprung mass of the bogie, K_d, no more	DSTU 7598 DSTU GOST 33211-2017	0.75 0.75	0.32	0.01	0.34	0.01	0.41	0.01	0.43	0.01	0.47	0.01	
Coefficient of vertical dynamics of the unsprung bogie frame, K_{dn}, no more	DSTU 7598 DSTU GOST 33211-2017	0.90 0.90	0.43	0.01	0.47	0.01	0.5	0.01	0.52	0.01	0.62	0.01	
Frame forces H_p, t	-	-	1.6	0.02	1.5	0.02	1.7	0.02	1.8	0.02	1.9	0.02	
Coefficient Horizontal dynamics (frame force in fractions of P_0 (Hp/P_0), from the wheel pair to the bogie frame), no more	DSTU 7598 DSTU GOST 33211-2017	0.40 0.40	0.30	0.01	0.28	0.01	0.32	0.01	0.34	0.01	0.36	0.01	
Coefficient safety margin of the wheel from the derailment on straight and curved sections of the track, not less	DSTU 7598 DSTU GOST 33211-2017	1,3 1,3	1.48	0.025	1,45	0.025	1.38	0.02	1.32	0.025	1.3	0.025	

Continued table 4.6

Controlled characteristics (wagon elements, section, point)	Regulatory documentation containing the value; requirement for the parameter	Indicator value											
		Actual value (by speed intervals)											
		At speed, km/h											
		Permissible value	40±5	Uncertainty	50±5	Uncertainty	60±5	Uncertainty	70±5	Uncertainty	80	Uncertainty	Note
Body acceleration vertical Z_{sq}, in fractions of g, no more	DSTU 7598 DSTU GOST 33211-2017	0.75 0.75	0.28	2.5%	0.4	2.5%	0.44	2.5%	0.52	2.5%	0.55	2.5%	
Body acceleration horizontal Y_{kg}, in fractions of g, no more	DSTU 7598 DSTU GOST 33211-2017	0.55 0.55	0.25	2.5%	0.26	2.5%	0.34	2.5%	0.41	2.5%	0.44	2.5%	

Table 4.7 – Results of running dynamic tests of the universal platform wagon model 13-4012 in empty mode (research coupling at the head of the train)

Controlled characteristics (wagon elements, section, point)	Regulatory documentation containing the value; requirement for the parameter	Indicator value											
		Permissible value	Actual value (by speed intervals)										
			At speed, km/h										
			40±5	Uncertainty	50±5	Uncertainty	60±5	Uncertainty	70±5	Uncertainty	80	Uncertainty	Note
Coefficient vertical dynamics of the sprung mass of the bogie, K_d, no more	DSTU 7598 DSTU GOST 33211-2017	0.75 0.75	0.39	0.01	0,49	0.01	0.5	0.01	0.6	0.01	0.71	0.01	
Coefficient of vertical dynamics of the unsprung bogie frame, K_{dn}, no more	DSTU 7598 DSTU GOST 33211-2017	0.90 0.90	0.58	0.01	0.62	0.01	0.7	0.01	0.73	0.01	0.81	0.01	
Frame forces H_p, t	-	-	1,6	0.02	1.7	0.02	1.8	0.02	1.9	0.02	1.9	0.02	
Coefficient Horizontal dynamics (frame force in fractions of P_0 (Hp/P_0), from the wheel pair to the bogie frame), no more	DSTU 7598 DSTU GOST 33211-2017	0.40 0.40	0.3	0.01	0.33	0.01	0.34	0.01	0.37	0.01	0.39	0.01	
Coefficient safety margin of the wheel from the derailment on straight and curved sections of the track, not less	DSTU 7598 DSTU GOST 33211-2017	1,3 1,3	1.38	0.025	1,36	0.025	1.31	0.025	**1.16**	0.025	**1.12**	0.025	

Continued table 4.7

Controlled characteristics (wagon elements, section, point)	Regulatory documentation containing the value; requirement for the parameter	Indicator value											
		Actual value (by speed intervals)											
		At speed, km/h											
		Permissible value	40±5	Uncertainty	50±5	Uncertainty	60±5	Uncertainty	70±5	Uncertainty	80	Uncertainty	Note
Body acceleration vertical Z_{sq}, in fractions of g, no more	DSTU 7598 DSTU GOST 33211-2017	0.75 0.75	0.31	2.5%	0.45	2.5%	0.55	2.5%	0.69	2.5%	0.72	2.5%	
Body acceleration horizontal Y_{kg}, in fractions of g, no more	DSTU 7598 DSTU GOST 33211-2017	0.55 0.55	0.36	2.5%	0.4	2.5%	0.43	2.5%	0.49	2.5%	0.51	2.5%	

Table 4.8 – Results of dynamic running tests of the tank wagon model 15-1443 in empty mode (research coupling at the head of the train)

Controlled characteristics (wagon elements, section, point)	Regulatory documentation containing the value; requirement for the parameter	Indicator value										
		Permissible value	Actual value (by speed intervals)									
			At speed, km/h									
			40±5	Uncertainty	50±5	Uncertainty	60±5	Uncertainty	70±5	Uncertainty	80	Uncertainty	Note
Coefficient vertical dynamics of the sprung mass of the bogie, K_d, no more	DSTU 7598 DSTU GOST 33211-2017	0.75 0.75	0.36	0.01	0.47	0.01	0.48	0.01	0.53	0.01	0.61	0.01	
Coefficient of vertical dynamics of the unsprung bogie frame, K_{dn}, no more	DSTU 7598, DSTU GOST 33211-2017	0.90 0.90	0.53	0.01	0.61	0.01	0.63	0.01	0.66	0.01	0.71	0.01	
Frame forces H_p, t	-	-	1.7	0.02	1.8	0.02	1.8	0.02	2.1	0.02	2.1	0.02	
Coefficient Horizontal dynamics (frame force in fractions of P_0 (Hp/P_0), from the wheel pair to the bogie frame), no more	DSTU 7598 DSTU GOST 33211-2017	0.40 0.40	0.29	0.01	0.3	0.01	0.31	0.01	0.36	0.01	0.36	0.01	
Coefficient safety margin of the wheel from the derailment on straight and curved sections of the track, not less	DSTU 7598 DSTU GOST 33211-2017	1,3 1,3	1.43	0.025	1,4	0.025	1.34	0.025	1.32	0.025	1.3	0.025	

Continued table 4.8

Controlled characteristics (wagon elements, section, point)	Regulatory documentation containing the value; requirement for the parameter	Indicator value											
		Actual value (by speed intervals)											
		At speed, km/h											
		Permissible value	40±5	Uncertainty	50±5	Uncertainty	60±5	Uncertainty	70±5	Uncertainty	80	Uncertainty	Note
Body acceleration vertical Z_{sq}, in fractions of g, no more	DSTU 7598 DSTU GOST 33211-2017	0.75 0.75	0.36	2.5%	0.48	2.5%	0.51	2.5%	0.6	2.5%	0.68	2.5%	
Body acceleration horizontal Y_{kg}, in fractions of g, no more	DSTU 7598 DSTU GOST 33211-2017	0.55 0.55	0.26	2.5%	0.31	2.5%	0.38	2.5%	0.4	2.5%	0.52	2.5%	

Table 4.9 – Results of dynamic running tests of the hopper wagon model 19-758-01 in empty mode (research coupling at the head of the train)

Controlled characteristics (wagon elements, section, point)	Regulatory documentation containing the value; requirement for the parameter	Indicator value											
		Permissible value	Actual value (by speed intervals)										
			At speed, km/h										
			40±5	Uncertainty	50±5	Uncertainty	60±5	Uncertainty	70±5	Uncertainty	80	Uncertainty	Note
Coefficient vertical dynamics of the sprung mass of the bogie, K_d, no more	DSTU 7598 DSTU GOST 33211-2017	0.75 0.75	0.36	0.01	0.48	0.01	0.49	0.01	0.54	0.01	0.63	0.01	
Coefficient of vertical dynamics of the unsprung bogie frame, K_{dn}, no more	DSTU 7598, DSTU GOST 33211-2017	0.90 0.90	0.54	0.01	0.62	0.01	0.65	0.01	0.69	0.01	0.72	0.01	
Frame forces H_p, t	-	-	1.7	0.02	1.8	0.02	1.8	0.02	2.1	0.02	2.1	0.02	
Coefficient Horizontal dynamics (frame force in fractions of P_0 (Hp/P_0), from the wheel pair to the bogie frame), no more	DSTU 7598 DSTU GOST 33211-2017	0.40 0.40	0.3	0.01	0.31	0.01	0.32	0.01	0.37	0.01	0.37	0.01	
Coefficient safety margin of the wheel from the derailment on straight and curved sections of the track, not less	DSTU 7598 DSTU GOST 33211-2017	1,3 1,3	1.42	0.025	1,39	0.025	1.35	0.025	1.33	0.025	1.31	0.025	

Continued table 4.9

Controlled characteristics (wagon elements, section, point)	Regulatory documentation containing the value; requirement for the parameter	Indicator value											
		Actual value (by speed intervals)											
		At speed, km/h											
		Permissible value	40±5	Uncertainty	50±5	Uncertainty	60±5	Uncertainty	70±5	Uncertainty	80	Uncertainty	Note
Body acceleration vertical Z_{sq}, in fractions of g, no more	DSTU 7598 DSTU GOST 33211-2017	0.75 0.75	0.38	2.5%	0.49	2.5%	0.52	2.5%	0.61	2.5%	0.69	2.5%	
Body acceleration horizontal Y_{kg}, in fractions of g, no more	DSTU 7598 DSTU GOST 33211-2017	0.55 0.55	0.27	2.5%	0.32	2.5%	0.39	2.5%	0.41	2.5%	0.47	2.5%	

Table 4.10 – Results of running dynamic tests of the universal platform wagon model 13-4012 in empty mode (research coupling inside the train)

Controlled characteristics (wagon elements, section, point)	Regulatory documentation containing the value; requirement for the parameter	Indicator value											
		Permissible value	Actual value (by speed intervals)										
			At speed, km/h										
			40±5	Uncertainty	50±5	Uncertainty	60±5	Uncertainty	70±5	Uncertainty	80	Uncertainty	Note
Coefficient vertical dynamics of the sprung mass of the bogie, K_d, no more	DSTU 7598 DSTU GOST 33211-2017	0.75 0.75	0.38	0.01	0,47	0.01	0.48	0.01	0.58	0.01	0.69	0.01	
Coefficient of vertical dynamics of the unsprung bogie frame, K_{dn}, no more	DSTU 7598 DSTU GOST 33211-2017	0.90 0.90	0.57	0.01	0.6	0.01	0.69	0.01	0.71	0.01	0.79	0.01	
Frame forces H_p, t	-	-	1,5	0.02	1.6	0.02	1.6	0.02	1.8	0.02	1.8	0.02	
Coefficient Horizontal dynamics (frame force in fractions of P_0 (Hp/P_0), from the wheel pair to the bogie frame), no more	DSTU 7598 DSTU GOST 33211-2017	0.40 0.40	0.28	0.01	0.31	0.01	0.32	0.01	0.35	0.01	0.36	0.01	
Coefficient safety margin of the wheel from the derailment on straight and curved sections of the track, not less	DSTU 7598 DSTU GOST 33211-2017	1,3 1,3	1.4	0.025	1,33	0.025	1.32	0.025	**1.18**	0.025	**1.14**	0.025	

Continued table 4.10

Controlled characteristics (wagon elements, section, point)	Regulatory documentation containing the value; requirement for the parameter	Indicator value											
		Actual value (by speed intervals)											
		At speed, km/h											
		Permissible value	40±5	Uncertainty	50±5	Uncertainty	60±5	Uncertainty	70±5	Uncertainty	80	Uncertainty	Note
Body acceleration vertical Z_{sq}, in fractions of g, no more	DSTU 7598 DSTU GOST 33211-2017	0.75 0.75	0.3	2.5%	0.43	2.5%	0.52	2.5%	0.68	2.5%	0.7	2.5%	
Body acceleration horizontal Y_{kg}, in fractions of g, no more	DSTU 7598 DSTU GOST 33211-2017	0.55 0.55	0.33	2.5%	0.36	2.5%	0.4	2.5%	0.46	2.5%	0.49	2.5%	

Table 4.11 – Results of dynamic running tests of the tank wagon model 15-1443 in empty mode (research coupling inside the train)

Controlled characteristics (wagon elements, section, point)	Regulatory documentation containing the value; requirement for the parameter	Indicator value											
		Permissible value	Actual value (by speed intervals)										
			At speed, km/h										
			40±5	Uncertainty	50±5	Uncertainty	60±5	Uncertainty	70±5	Uncertainty	80	Uncertainty	Note
Coefficient vertical dynamics of the sprung mass of the bogie, K_d, no more	DSTU 7598 DSTU GOST 33211-2017	0.75 0.75	0.34	0.01	0,45	0.01	0.46	0.01	0.51	0.01	0.6	0.01	
Coefficient of vertical dynamics of the unsprung bogie frame, K_{dn}, no more	DSTU 7598 DSTU GOST 33211-2017	0.90 0.90	0.51	0.01	0.6	0.01	0.62	0.01	0.64	0.01	0.7	0.01	
Frame forces H_p, t	-	-	1,5	0.02	1.6	0.02	1.6	0.02	1.8	0.02	1.8	0.02	
Coefficient Horizontal dynamics (frame force in fractions of P_0 (Hp/P_0), from the wheel pair to the bogie frame), no more	DSTU 7598 DSTU GOST 33211-2017	0.40 0.40	0.28	0.01	0.29	0.01	0.3	0.01	0.34	0.01	0.35	0.01	
Coefficient safety margin of the wheel from the derailment on straight and curved sections of the track, not less	DSTU 7598 DSTU GOST 33211-2017	1,3 1,3	1.45	0.025	1,42	0.025	1.34	0.025	1.33	0.025	1.31	0.025	

Continued table 4.11

Controlled characteristics (wagon elements, section, point)	Regulatory documentation containing the value; requirement for the parameter	Indicator value											
		Actual value (by speed intervals)											
		At speed, km/h											
		Permissible value	40±5	Uncertainty	50±5	Uncertainty	60±5	Uncertainty	70±5	Uncertainty	80	Uncertainty	Note
Body acceleration vertical Z_{sq}, in fractions of g, no more	DSTU 7598 DSTU GOST 33211-2017	0.75 0.75	0.34	2.5%	0.46	2.5%	0.49	2.5%	0.58	2.5%	0.66	2.5%	
Body acceleration horizontal Y_{kg}, in fractions of g, no more	DSTU 7598 DSTU GOST 33211-2017	0.55 0.55	0.26	2.5%	0.31	2.5%	0.36	2.5%	0.4	2.5%	0.43	2.5%	

Table 4.12 – Results of running dynamic tests of the hopper wagon model 19-758-01 in empty mode (research coupling in the middle of the train)

Controlled characteristics (wagon elements, section, point)	Regulatory documentation containing the value; requirement for the parameter	Indicator value											
		Permissible value	Actual value (by speed intervals)										
			At speed, km/h										
			40±5	Uncertainty	50±5	Uncertainty	60±5	Uncertainty	70±5	Uncertainty	80	Uncertainty	Note
Coefficient vertical dynamics of the sprung mass of the bogie, K_d, no more	DSTU 7598 DSTU GOST 33211-2017	0.75 0.75	0.34	0.01	0,45	0.01	0.47	0.01	0.51	0.01	0.61	0.01	
Coefficient of vertical dynamics of the unsprung bogie frame, K_{dn}, no more	DSTU 7598 DSTU GOST 33211-2017	0.90 0.90	0.52	0.01	0.6	0.01	0.63	0.01	0.67	0.01	0.7	0.01	
Frame forces H_p, t	-	-	1,5	0.02	1.6	0.02	1.6	0.02	1.8	0.02	1.8	0.02	
Coefficient Horizontal dynamics (frame force in fractions of P_0 (Hp/P_0), from the wheel pair to the bogie frame), no more	DSTU 7598 DSTU GOST 33211-2017	0.40 0.40	0.29	0.01	0.3	0.01	0.31	0.01	0.35	0.01	0.35	0.01	
Coefficient safety margin of the wheel from the derailment on straight and curved sections of the track, not less	DSTU 7598 DSTU GOST 33211-2017	1,3 1,3	1.42	0.025	1,4	0.025	1.37	0.025	1.35	0.025	1.33	0.025	

Continued table 4.12

Controlled characteristics (wagon elements, section, point)	Regulatory documentation containing the value; requirement for the parameter	Indicator value											
		Actual value (by speed intervals)											
		At speed, km/h											
		Permissible value	40±5	Uncertainty	50±5	Uncertainty	60±5	Uncertainty	70±5	Uncertainty	80	Uncertainty	Note
Body acceleration vertical Z_{sq}, in fractions of g, no more	DSTU 7598 DSTU GOST 33211-2017	0.75 0.75	0.36	2.5%	0.47	2.5%	0.5	2.5%	0.59	2.5%	0.66	2.5%	
Body acceleration horizontal Y_{kg}, in fractions of g, no more	DSTU 7598 DSTU GOST 33211-2017	0.55 0.55	0.25	2.5%	0.31	2.5%	0.37	2.5%	0.39	2.5%	0.45	2.5%	

Table 4.13 – Results of dynamic running tests of the universal platform wagon model 13-4012 in empty mode (research coupling at the tail of the train)

Controlled characteristics (wagon elements, section, point)	Regulatory documentation containing the value; requirement for the parameter	Indicator value											
		Permissible value	Actual value (by speed intervals)										
			At speed, km/h										
			40±5	Uncertainty	50±5	Uncertainty	60±5	Uncertainty	70±5	Uncertainty	80	Uncertainty	Note
Coefficient vertical dynamics of the sprung mass of the bogie, K_d, no more	DSTU 7598 DSTU GOST 33211-2017	0.75 0.75	0.35	0.01	0.36	0.01	0.4	0.01	0.43	0.01	0.5	0.01	
Coefficient of vertical dynamics of the unsprung bogie frame, K_{dn}, no more	DSTU 7598 DSTU GOST 33211-2017	0.90 0.90	0.46	0.01	0.49	0.01	0.53	0.01	0.57	0.01	0.64	0.01	
Frame forces H_p, t	-	-	1.5	0.02	1.6	0.02	1.7	0.02	1.8	0.02	1.8	0.02	
Coefficient Horizontal dynamics (frame force in fractions of P_0 (Hp/P_0), from the wheel pair to the bogie frame), no more	DSTU 7598 DSTU GOST 33211-2017	0.40 0.40	0.29	0.01	0.34	0.01	0.32	0.01	0.36	0.01	0.37	0.01	
Coefficient safety margin of the wheel from the derailment on straight and curved sections of the track, not less	DSTU 7598 DSTU GOST 33211-2017	1,3 1,3	1.45	0.025	1,4	0.025	1.3	0.025	**1.28**	0.025	**1.23**	0.025	

Continued table 4.13

Controlled characteristics (wagon elements, section, point)	Regulatory documentation containing the value; requirement for the parameter	Indicator value											
		Actual value (by speed intervals)											
		At speed, km/h											
		Permissible value	40±5	Uncertainty	50±5	Uncertainty	60±5	Uncertainty	70±5	Uncertainty	80	Uncertainty	Note
Body acceleration vertical Z_{sq}, in fractions of g, no more	DSTU 7598 DSTU GOST 33211-2017	0.75 0.75	0.3	2.5%	0.41	2.5%	0.5	2.5%	0.57	2.5%	0.72	2.5%	
Body acceleration horizontal Y_{kg}, in fractions of g, no more	DSTU 7598 DSTU GOST 33211-2017	0.55 0.55	0.27	2.5%	0.31	2.5%	0.42	2.5%	0.48	2.5%	0.51	2.5%	

Table 4.14 – Results of dynamic running tests of tank wagon model 15-1443 No. in empty mode (research coupling at the tail of the train)

Controlled characteristics (wagon elements, section, point)	Regulatory documentation containing the value; requirement for the parameter	Indicator value										
		Permissible value	Actual value (by speed intervals)									
			At speed, km/h									
			40 ±5	Uncertainty	50 ±5	Uncertainty	60 ±5	Uncertainty	70 ±5	Uncertainty	80	Uncertainty	Note
Coefficient vertical dynamics of the sprung mass of the bogie, K_d, no more	DSTU 7598 DSTU GOST 33211-2017	0.75 0.75	0.32	0.01	0.33	0.01	0.41	0.01	0.42	0.01	0.47	0.01	
Coefficient of vertical dynamics of the unsprung bogie frame, K_{dn}, no more	DSTU 7598 DSTU GOST 33211-2017	0.90 0.90	0.42	0.01	0.47	0.01	0.49	0.01	0.51	0.01	0.62	0.01	
Frame forces H_p, t	-	-	1.5	0.02	1.6	0.02	1.7	0.02	1.8	0.02	1.8	0.02	
Coefficient Horizontal dynamics (frame force in fractions of P_0 (Hp/P_0), from the wheel pair to the bogie frame), no more	DSTU 7598 DSTU GOST 33211-2017	0.40 0.40	0.22	0.01	0.24	0.01	0.31	0.01	0.32	0.01	0.34	0.01	
Coefficient safety margin of the wheel from the derailment on straight and curved sections of the track, not less	DSTU 7598 DSTU GOST 33211-2017	1,3 1,3	1.48	0.025	1,46	0.025	1.37	0.025	1.34	0.025	1.33	0.025	

Continued table 4.14

Controlled characteristics (wagon elements, section, point)	Regulatory documentation containing the value; requirement for the parameter	Indicator value											
		Actual value (by speed intervals)											
		At speed, km/h											
		Permissible value	40±5	Uncertainty	50±5	Uncertainty	60±5	Uncertainty	70±5	Uncertainty	80	Uncertainty	Note
Body acceleration vertical Z_{sq}, in fractions of g, no more	DSTU 7598 DSTU GOST 33211-2017	0.75 0.75	0.27	2.5%	0.39	2.5%	0.43	2.5%	0.51	2.5%	0.53	2.5%	
Body acceleration horizontal Y_{kg}, in fractions of g, no more	DSTU 7598 DSTU GOST 33211-2017	0.55 0.55	0.24	2.5%	0.29	2.5%	0.33	2.5%	0.39	2.5%	0.42	2.5%	

Table 4.15 – Results of dynamic running tests of the hopper wagon model 19-758-01 in empty mode (research coupling at the tail of the train)

Controlled characteristics (wagon elements, section, point)	Regulatory documentation containing the value; requirement for the parameter	Indicator value											
		Permissible value	Actual value (by speed intervals)										
			At speed, km/h										
			40±5	Uncertainty	50±5	Uncertainty	60±5	Uncertainty	70±5	Uncertainty	80	Uncertainty	Note
Coefficient vertical dynamics of the sprung mass of the bogie, K_d, no more	DSTU 7598 DSTU GOST 33211-2017	0.75 0.75	0.33	0.01	0.36	0.01	0.42	0.01	0.43	0.01	0.48	0.01	
Coefficient of vertical dynamics of the unsprung bogie frame, K_{dn}, no more	DSTU 7598 DSTU GOST 33211-2017	0.90 0.90	0.44	0.01	0.49	0.01	0.51	0.01	0.54	0.01	0.64	0.01	
Frame forces H_p, t	-	-	1.5	0.02	1.6	0.02	1.7	0.02	1.8	0.02	1.8	0.02	
Coefficient Horizontal dynamics (frame force in fractions of P_0 (Hp/P_0), from the wheel pair to the bogie frame), no more	DSTU 7598 DSTU GOST 33211-2017	0.40 0.40	0.28	0.01	0.30	0.01	0.32	0.01	0.34	0.01	0.34	0.01	
Coefficient safety margin of the wheel from the derailment on straight and curved sections of the track, not less	DSTU 7598 DSTU GOST 33211-2017	1,3 1,3	1.47	0.025	1,40	0.025	1.36	0.025	1.33	0.025	1.3	0.025	

Continued table 4.15

Controlled characteristics (wagon elements, section, point)	Regulatory documentation containing the value; requirement for the parameter	Indicator value											
		Actual value (by speed intervals)											
		At speed, km/h											
		Permissible value	40±5	Uncertainty	50±5	Uncertainty	60±5	Uncertainty	70±5	Uncertainty	80	Uncertainty	Note
Body acceleration vertical Z_{sq}, in fractions of g, no more	DSTU 7598 DSTU GOST 33211-2017	0.75 0.75	0.29	2.5%	0.41	2.5%	0.45	2.5%	0.53	2.5%	0.55	2.5%	
Body acceleration horizontal Y_{kg}, in fractions of g, no more	DSTU 7598 DSTU GOST 33211-2017	0.55 0.55	0.26	2.5%	0.27	2.5%	0.34	2.5%	0.42	2.5%	0.45	2.5%	

4.5 Restoration of the carrying capacity of the wagon for transporting grain

In recent years, there has been a significant aging of the grain carrier fleet. The average age of grain carriers in Ukraine is 27.4 years, which is 2.8 years (12%) more than the average European railway with a 1520 mm gauge. It should also be noted that 69% of Ukrainian grain carriers have been in operation for more than 27 years, with a standard service life of 30 years. To resolve the issue of the possibility of further operation of hopper wagon s for transporting grain with expired service life, their technical diagnostics are carried out found that the inspected wagon s of model 19-752, in the amount of more than 113 wagons, have cracks in the area of the connection of the rear stop of the automatic coupling device with the frame of the wagon body out of a total of 1,453 wagon s inspected since 2016.

To resolve the issue of the appearance of cracks in the area of connection of the rear stop of the automatic coupling device, modernization was carried out by welding a reinforcing plate in the damaged area. Carrying out these control and standard life tests will allow us to practically confirm the feasibility of this modernization and extend the service life of the grain wagon by 7 years.

The purpose of conducting control tests of modernized grain wagon s is to establish the effectiveness of the modernization performed and to determine the residual life after the modernization has been completed.

The purpose of the wedge drop test is to determine the stresses in the supporting structure elements of the body frame and bogie bolster.

The purpose of a typical contact strength test is to determine and evaluate dynamic stresses and deformations in the load-bearing structures of the wagon when standard impact forces are applied through the automatic coupling device.

The purpose of testing for life is to determine the appearance and development of damage and residual deformations in the load-bearing structures of the wagon under repeated exposure to longitudinal loads through the automatic coupling device, as well as calculation of service life, which can be determined based on test results.

4.5.1 Analysis of the frequency of unscheduled repairs of grain wagons

To analyze the frequency of unscheduled repairs of grain carriers, data on unscheduled repairs performed for the period from 01/01/2016 were analyzed. until 04/30/2023 So, according to the certificate for this period, unscheduled repairs (OOO-1 and OOO-2) of grain carriers of the Ukrzaliznytsia JSC fleet were carried out on 20,597 wagon s, of which OOO-1 was 8,768 wagon s, OOO-2 - 11,829 wagons. As of 05/01/2023, according to the certificate, the fleet of grain carriers of Ukrzaliznytsia JSC is 11,649 wagons, with an average wear rate of 98.43%. Thus, the average number of unscheduled repairs per 1 wagon of the total grain carrier fleet is 1.77. The years of construction of the grain carriers of this fleet are in the range of 1976 – 1993. (Figure 4.28).

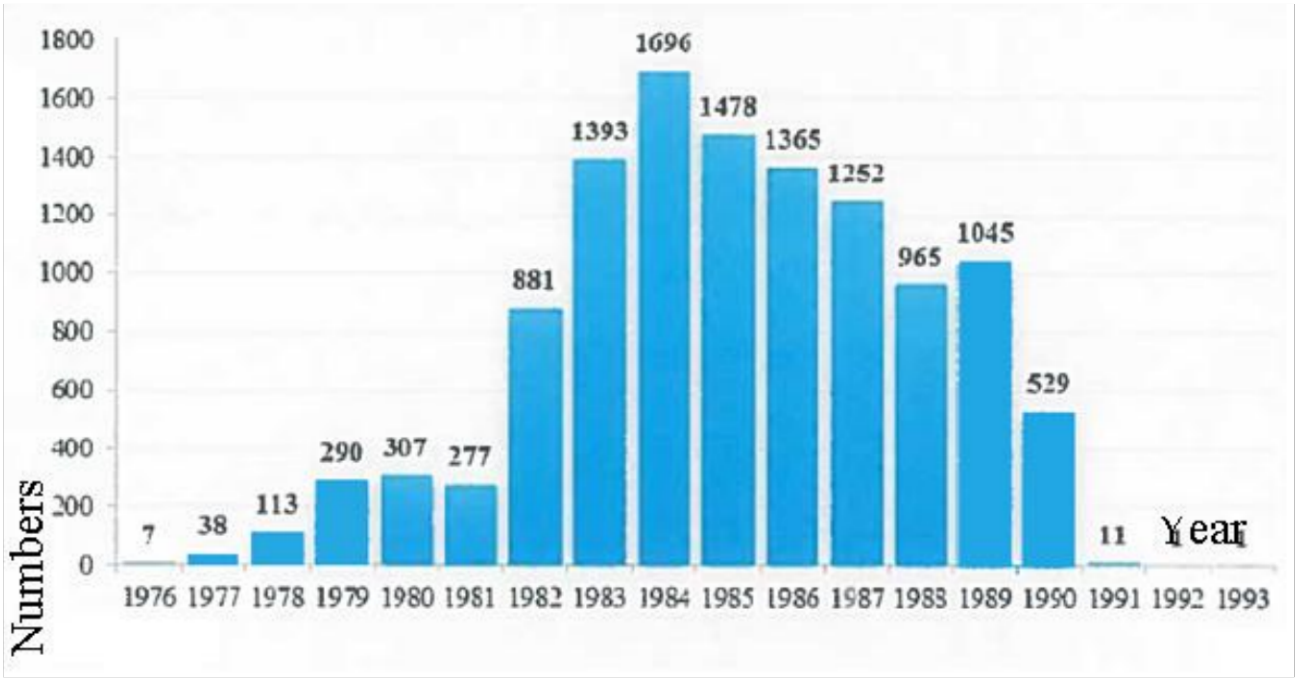

Figure 4.28 – Distribution of the number of grain carriers by year of construction

The standard service life of grain carriers is 30 years, and given that the wear and tear of the grain carrier fleet reaches 98%, grain carriers with expired service life are subject to a technical condition survey to extend their service life and subsequent operation on the railways of Ukraine. During the technical condition surveys carried out for the period from 01/01/2016 to 04/30/2023, grain carriers (total number of about 200 units) were discovered, for which cases of typical cracks in load-bearing structures were recorded.

4.5.2 Investigation of places where the body frame is damaged

At the wagon repair enterprise, a study was carried out of the locations of damage to the body frame of grain wagons model 19-752 using the magnetic particle non-destructive testing method.

Non-destructive testing specialists carried out visual and magnetic particle inspection of the back stop and the place of its riveted connection with the center beam (Figure 4.29).



Figure 4.29 - Magnetic particle testing of the backgauge

Based on the results of the control, the following was revealed:

- cracks in the center beams of two wagons, which were examined in the area of the riveted connection with the rear stop (Figure 4.30);

- weakening of rivets in places where cracks occur (Figure 4.31);

- cracks in the welded joints of the bottom sheet of the pivot beam with the center beam in the two wagons under study (Figure 4.31);

a crack in the rear stop of one of the wagon on the draft gear side (Figure 4.32).

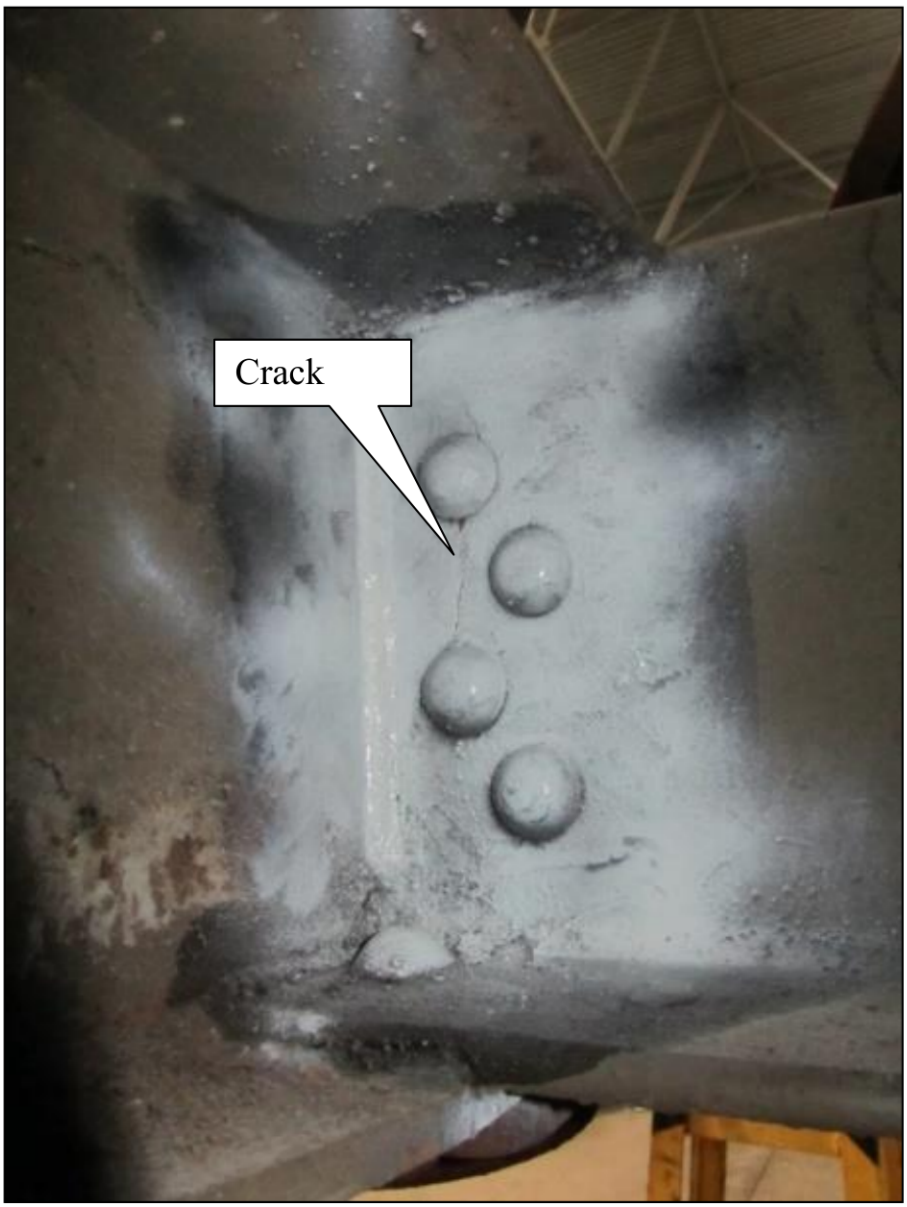

Figure 4.30 – Crack in the center beams of grain wagons



Figure 4.31 Crack in the welded joints of the bottom sheet of the pivot beam

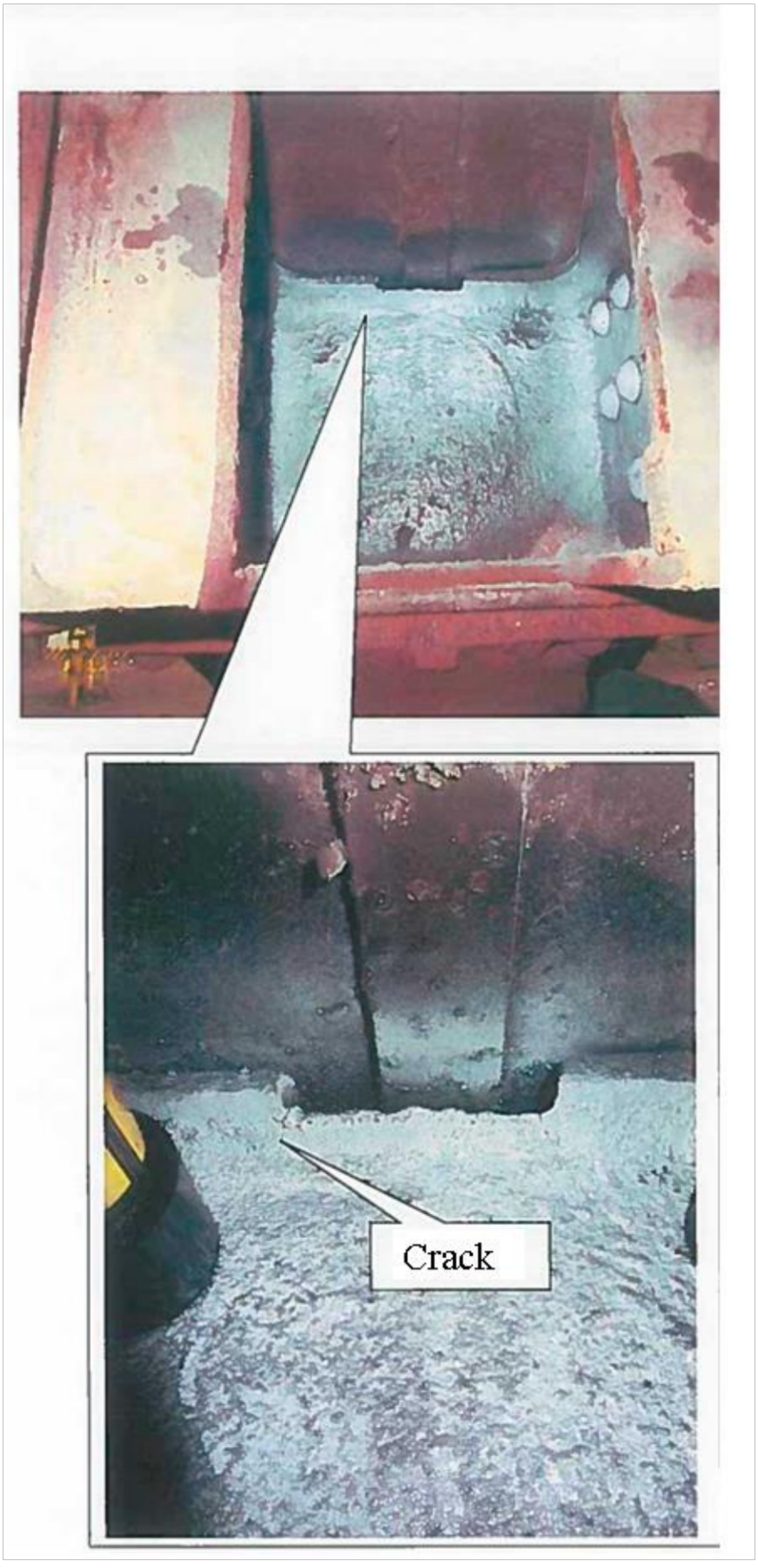

Figure 4.32 – Crack in the back stop

4.5.3 Study of the stress-strain state of grain truck bodies of model 19-752

To assess the stress-strain state (strength calculation according to DSTU 7598: 2014) of the load-bearing structures of the grain wagon model 19-752 using the finite element method, the corresponding 3D models were built in the Solid Works computer package.

The bodies of model 19-752 grain wagon are all-metal load-bearing structures and are made of a set of longitudinal and transverse stiffeners covered with thin corrugated sheets.

The 3D model of the grain wagon body of model 19-752 was built in accordance with the design documentation of the manufacturing plant and consists of 554 parts (Figure 4.33).

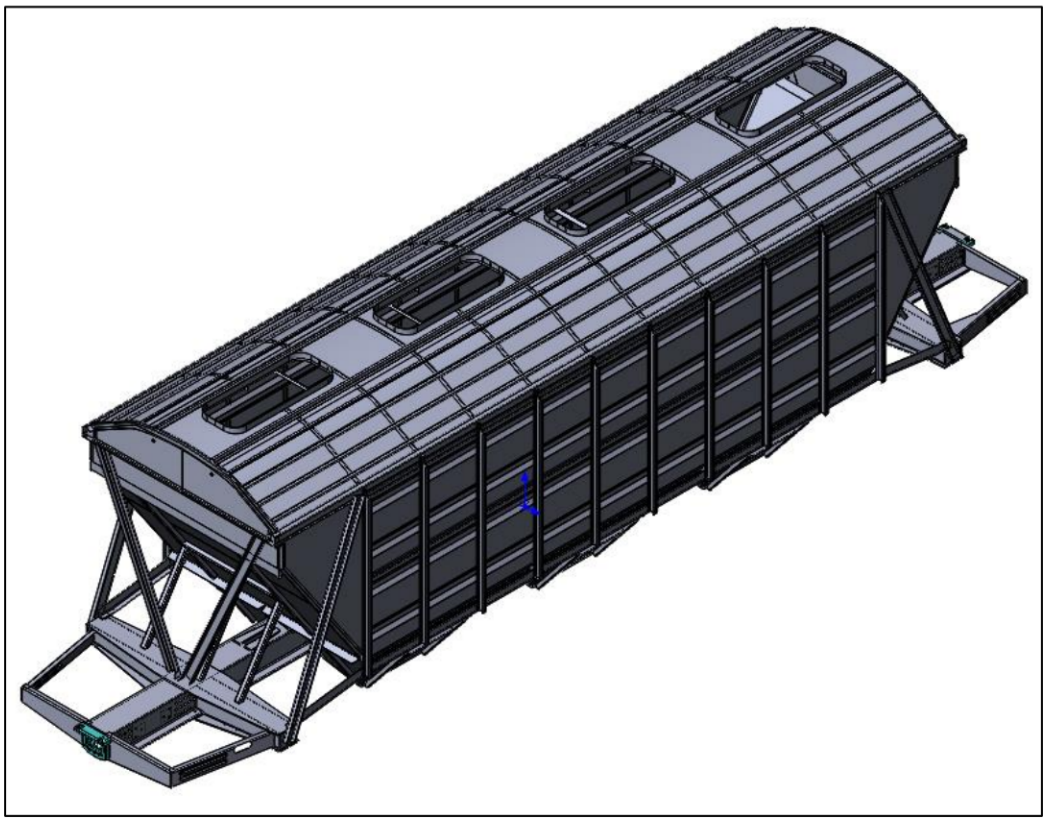

Figure 4.33 – 3D model of the wagon body

To carry out strength calculations, a combined finite element model of the grain wagon body with different sizes of end elements and different types of

elements - 6 mm and 24 mm (Figure 4.34) has been developed. This choice of element sizes was made based on the geometric features of the structure.

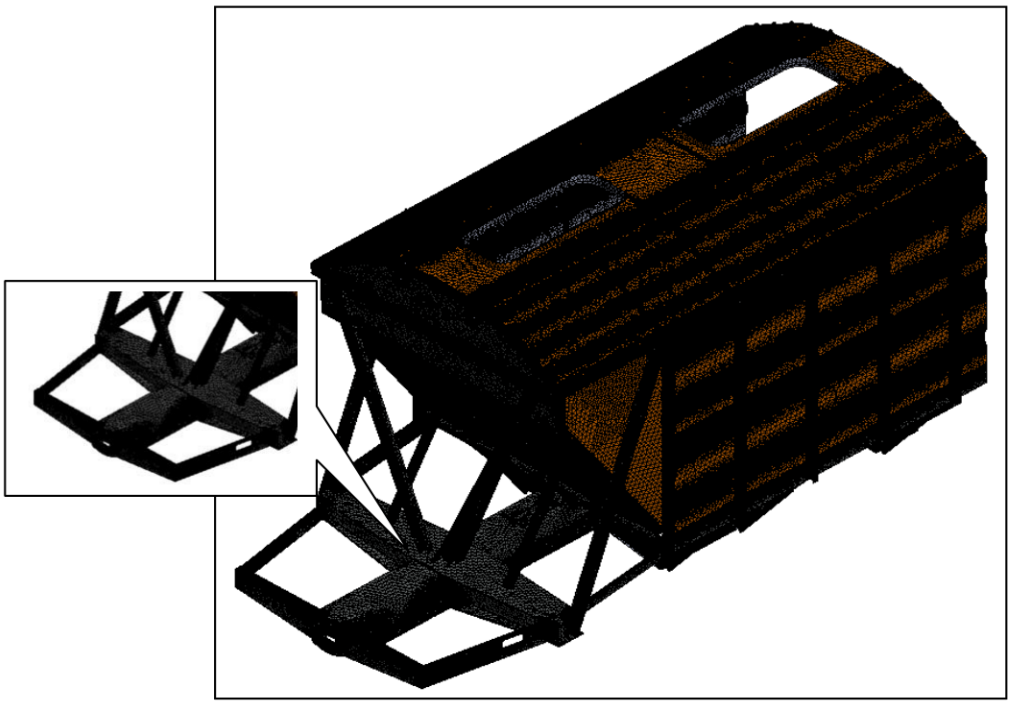

Figure 4.34 – Finite element model of the wagon body (6mm and 24mm mesh)

The loading scheme for the grain wagon body 19-752 was developed in accordance with DSTU 7598:2014. Calculations were performed for the most unfavorable possible combination of simultaneously acting normative forces in accordance with the established design modes I and III.

Mode I – conditional security mode. Operating conditions according to the first calculation mode for freight wagons correspond to settling and shifting of heavy rolling stock, collision of wagons during maneuvers, including when dismantling from hills, emergency braking on trains at low speeds or collision of wagons in emergency situations, and also emergency jerk (push).

Mode III – operational mode. Under operating conditions III, the design mode corresponds to cases of movement of a wagon with a full load as part of a train along straight and curved sections of track and turnouts of the corresponding design and condition at an acceptable speed, up to the design speed, during periodic service

control braking, periodic moderate jerks and shocks from the normal operation of the mechanisms and components of the wagon.

The calculated forces are given in table 4.16.

Table 4.16 – Static and kinematic boundary conditions

Design forces	Design modes	
	Body	
	AND (jerk, stretch-impact, compression)	III (tension-compression)
Vertical forces (division 5.2 DSTU 7598:2014)		
Gross gravity (82.4t)	808344 N	808344 N
Dynamic forces at design speed **(k_{dv}=0.352)**	-	285345 N
Vertical component of the longitudinal force of body inertia (50%)	256000 N	-
Lateral forces (division 5.3 DSTU 7598:2014)		
Centrifugal force	-	67689 N
Transverse component of longitudinal quasi-static force	(-) 200000 N (+) 26400 N	-
Longitudinal forces (division 5.4 DSTU 7598:2014)		
Hit	-3.5 MN	-
Jerk	+2.5 MN	-
Compression	-2.5 MN	-1.0 MN
Stretching	+2.0 MN	+1.0 MN
Self-balanced loads (division 5.5 DSTU 7598:2014)		
Expansion forces (ɣ=0.75)	2763.1 Pa	6375.6 Pa
Thrust forces for end wall	(-) 531760 N (+) 425400 N	212700 N
Limit conditions		
Total rigidity of the spring suspension of the wagon	Longitudinal stiffness 7584000 N/m Horizontal stiffness 7704000 N/m	Longitudinal stiffness 7584000 N/m Horizontal stiffness 7704000 N/m

4.5.4 Results of standard calculations of the wagon body

When determining the material properties necessary for strength calculations, certain assumptions were applied. Firstly, the material from which a particular part is made is considered homogeneous. In addition, the actual characteristics of the real material from which any structure is made have some deviations from the characteristics given in reference books.

Wagon bodies are made of 09G2S steel. The permissible stresses adopted in accordance with DSTU 7598:2014 when calculating the strength of load-bearing frame elements are given in Table 4.17.

Table 4.17 - Permissible stresses

Material	Mode I			Mode III		
	$[\sigma]$ MPa	$[\tau_{зр}]$ MPa	$[\sigma_{зм}]$ MPa	$[\sigma]$ MPa	$[\tau_{зр}]$ MPa	$[\sigma_{зм}]$ MPa
Vertebral and pivot beams of the body frame						
Rolled steel, 09G2S	$0.9\sigma_t$	$0.55\sigma_t$	$1.2\sigma_t$	195	120	290
Body elements, with the exception of the center and pivot beams						
Rolled steel, 09G2S	$0.95\sigma_t$	$0.6\sigma_t$	$1.3\sigma_t$	205	125	305

In the impact and compression modes, the rivet connection works as a single-shear lap connection (Fig. 2.7).

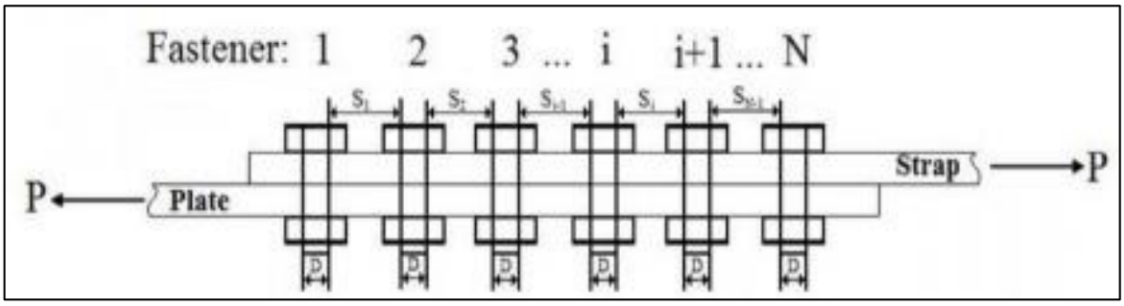

Figure 4.35 – Single-cut lap joint

In this case, the center beam will be in compression, and the opening of a crack in a solid body can only be of the “shear” type (type II). With plane displacement, a

crack is formed by moving the edges of the crack in a plane and perpendicular to its frontal line (Fig. 4.36).

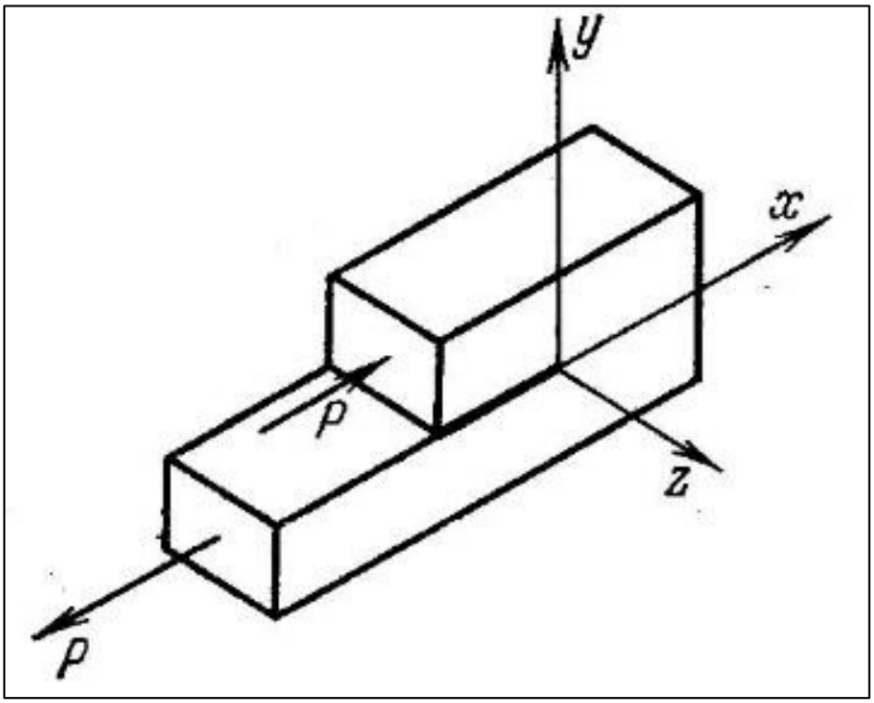

Figure 4.36 – Type II “shear” crack

For such a crack to form during compression on the center beam, large shearing forces must act, which can only arise from vertical loads.

In the jerk and tension modes, the rivet connection operates as a single-shear connection with a lining (Fig. 4.37).

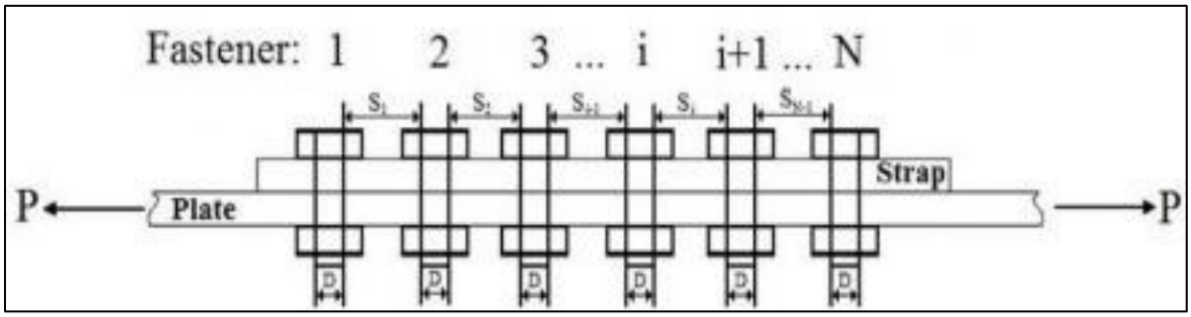

Figure 4.37 – Single-cut connection with cover plate

In this case, the center beam will be in tension, and the opening of a crack in a solid body can only be of the "rupture" type (type I). Under normal stresses, a crack occurs when the edges of the crack move perpendicular to the plane of the crack (Fig. 4.38).

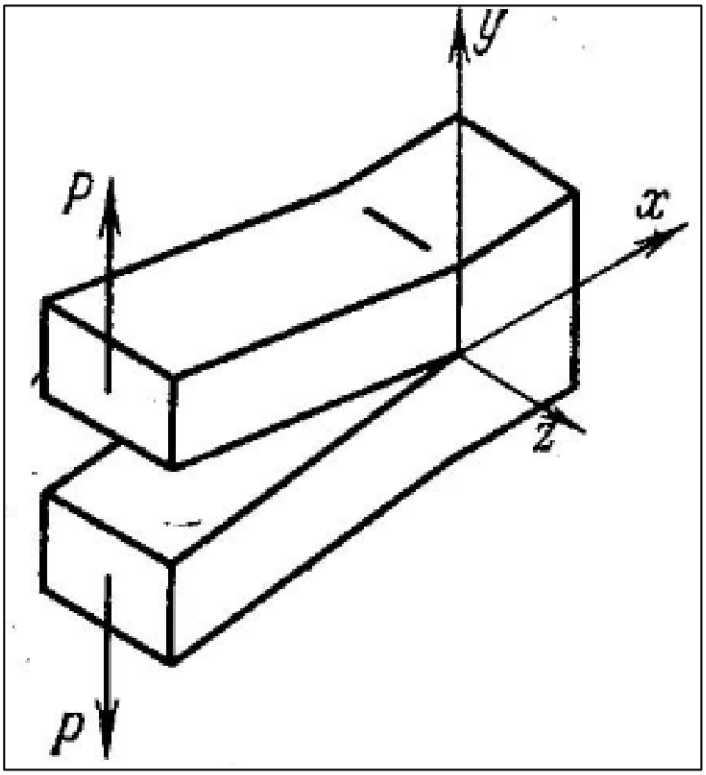

Figure 4.38 – Type I "rupture" crack

In order for such a crack to form during tension on the center beam, large transverse forces must act.

Solid calculations of the grain wagon body were made on the basis of the constructed calculation diagrams. Figures 4.39-4.41 show the results of calculating a rivet joint for standard impact and compression modes.

The sum of forces must be equal to the applied load in mode I (impact) = 3.5 MN divided in half.

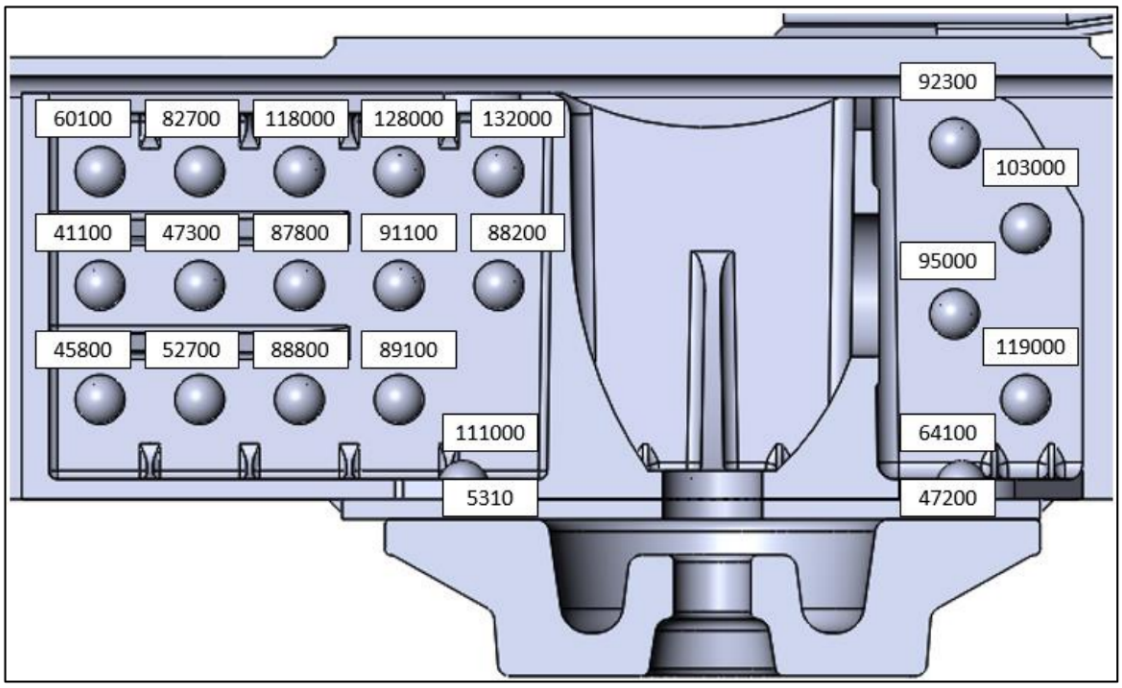

Figure 4.39 – Forces acting in a single-shear lap rivet connection in mode I (impact)

The sum of forces must be equal to the applied load in mode I (compression) = 2.5 MN divided in half.

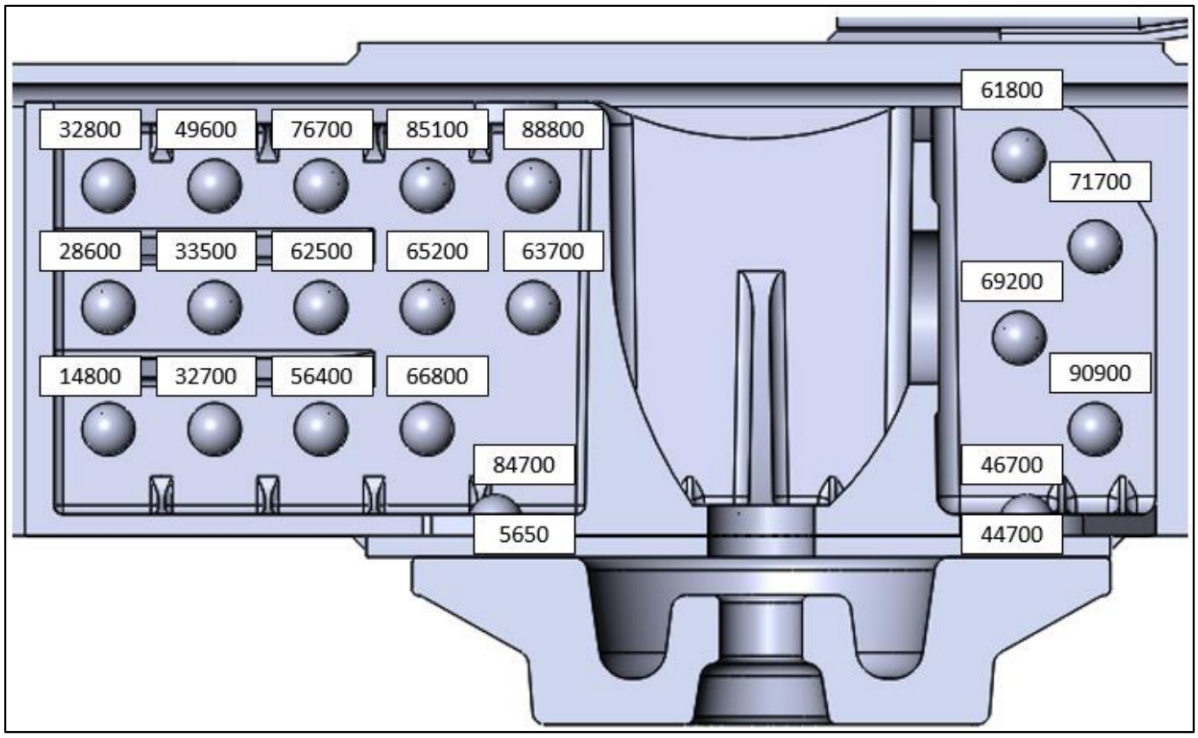

Figure 4.40 – Forces acting in a single-shear lap rivet connection in mode I (compression)

The sum of forces must be equal to the applied load in mode III (compression) = 1.0 MN divided in half.

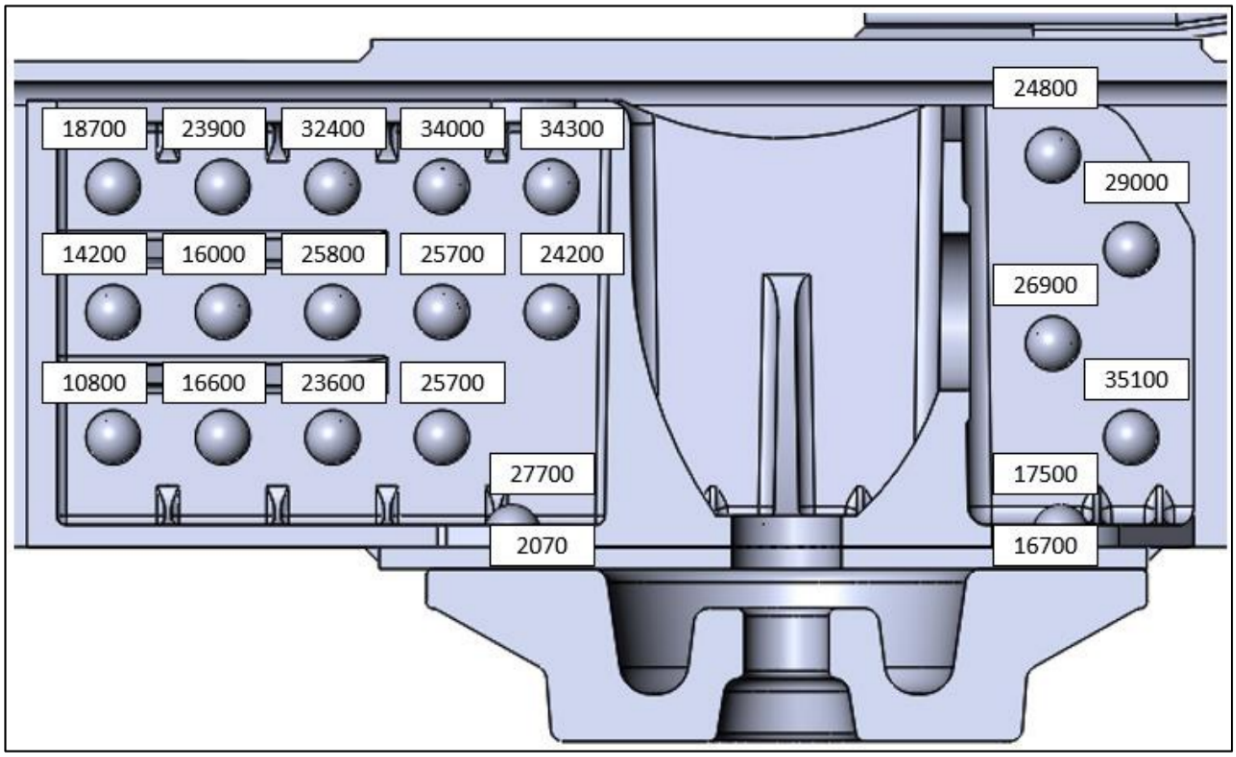

Figure 4.41 – Forces acting in a single-shear lap rivet connection in mode III (compression)

Let us consider the distribution of normal and contacting stresses on the center beam under the rivets from longitudinal compression forces. The possible stress accumulation is assessed by comparing the obtained stresses with the endurance limit for contacting stresses during a pulsating cycle τ_0=70 MPa.

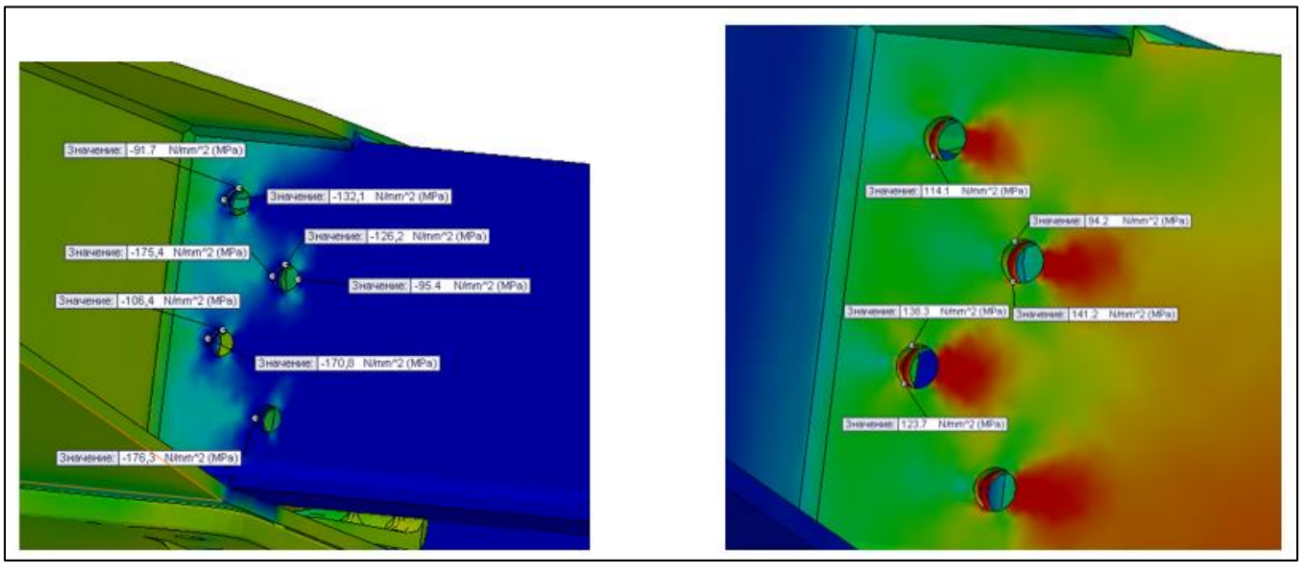

Figure 4.42 – Stress distribution on the center beam under the rivets due to longitudinal forces. Mode I (2.5 MN compression)

Based on the calculation results presented in 2.13, it can be concluded that fatigue damage can accumulate in the center beam at a load of 2.5 MN and above. In this case, the crack will propagate at an angle of about 45°.

Let us separately consider the influence of vertical forces on the total shear stresses. Let's compare calculations based on gravity forces for a gross volume of 70 tons with calculations based on gravity forces gross 70t with a dynamics coefficient of 0.352 and based on gravity forces, gross 75t (overload) with a dynamic coefficient of 0.352.

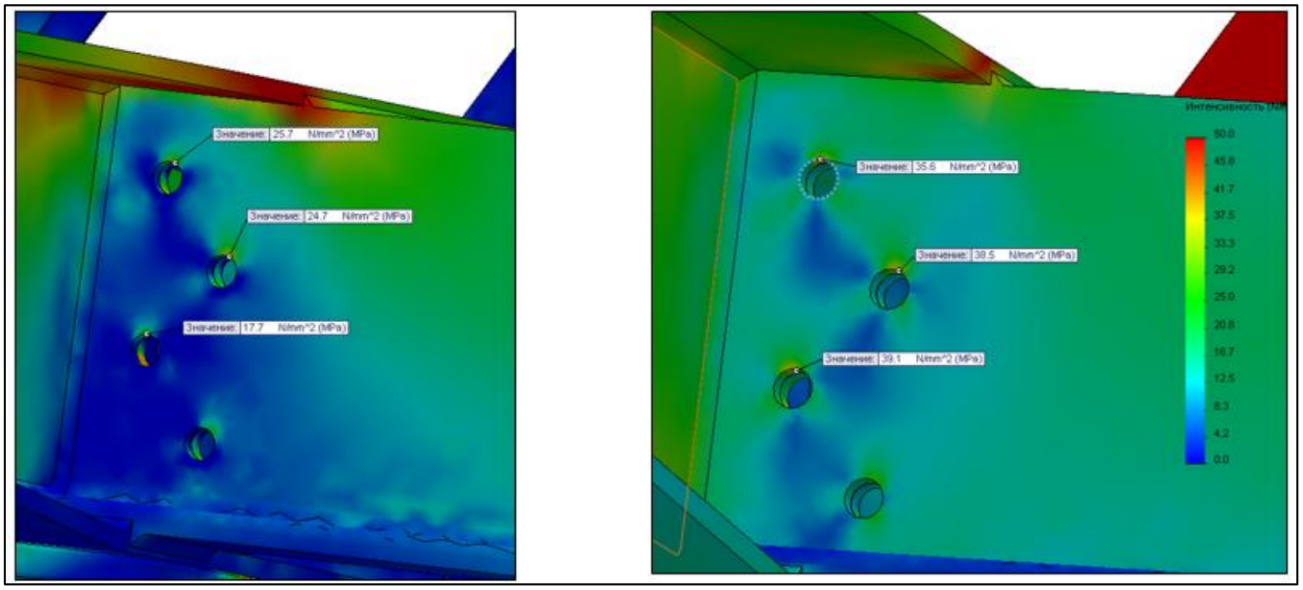

Figure 4.43 – Stress distribution on the center beam under rivets due to gravity (70t)

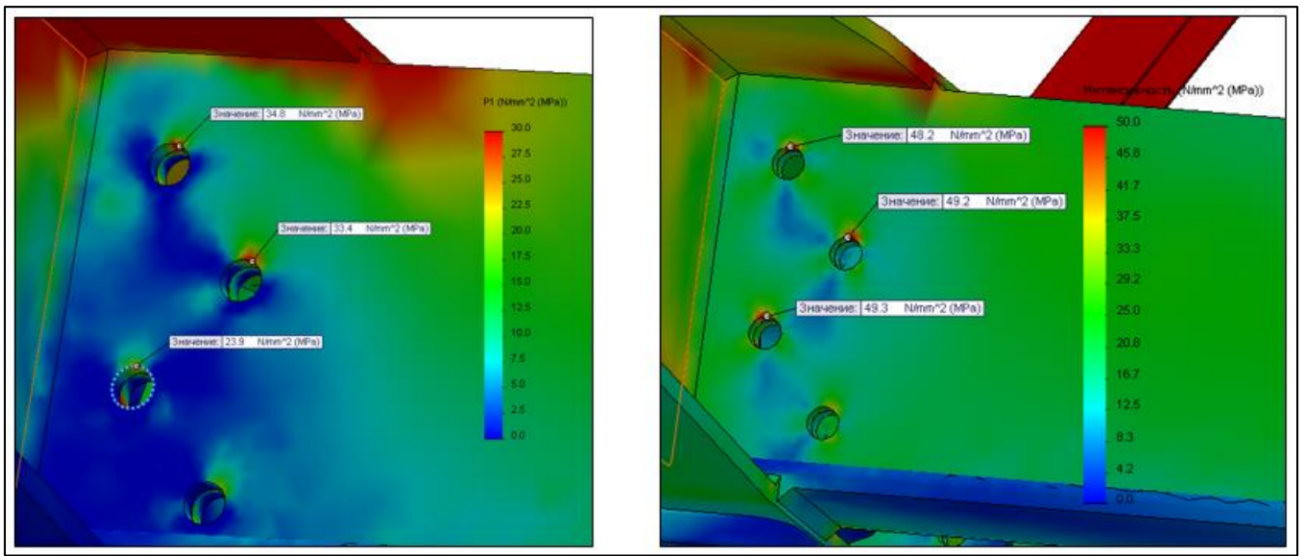

Figure 4.44 – Stress distribution on the center beam under rivets from gravity forces with a dynamics coefficient of 0.352 (70t)

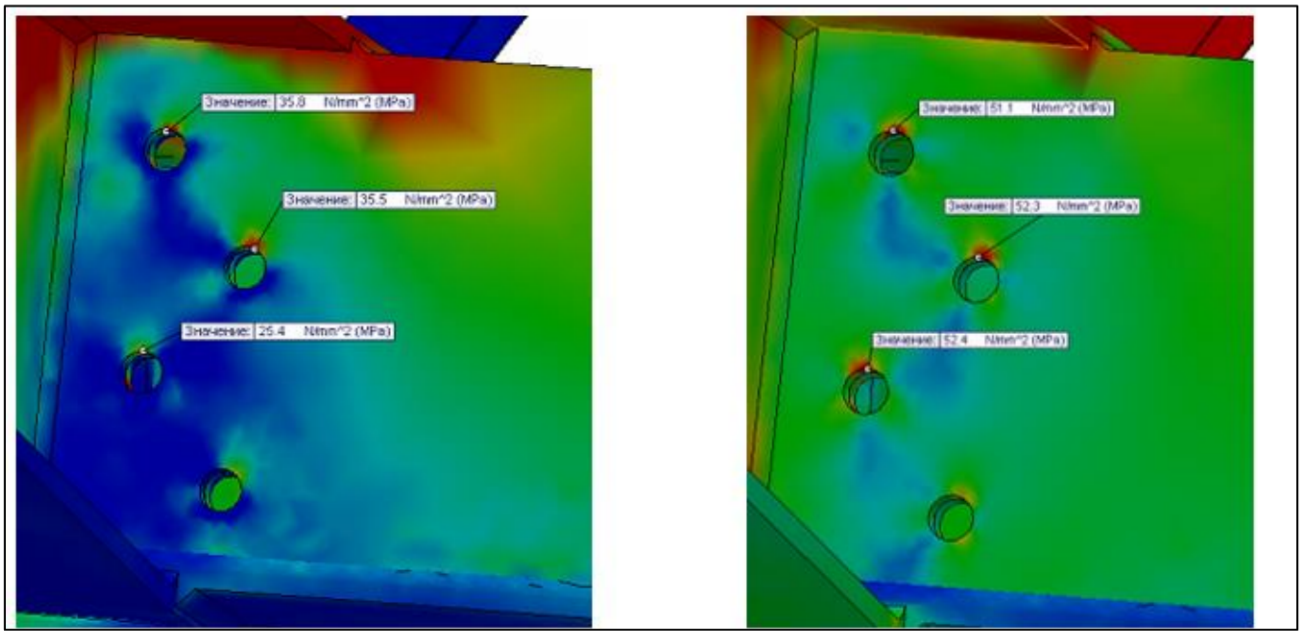

Figure 4.45 – Stress distribution on the center beam under rivets from gravity forces with a dynamic coefficient of 0.352 (75t)

Thus, the impact, mode I and mode III compression modes are not the causes of fatigue cracks in the riveted joint area. The stress from vertical forces is not the main stress in the riveted joint area, and an overload of 5 tons gives a stress change of 2 MPa.

Let's consider the snatch, stretching modes I and mode III. Figures 4.46-4.48 show the results of calculating a rivet joint for standard impact and compression modes.

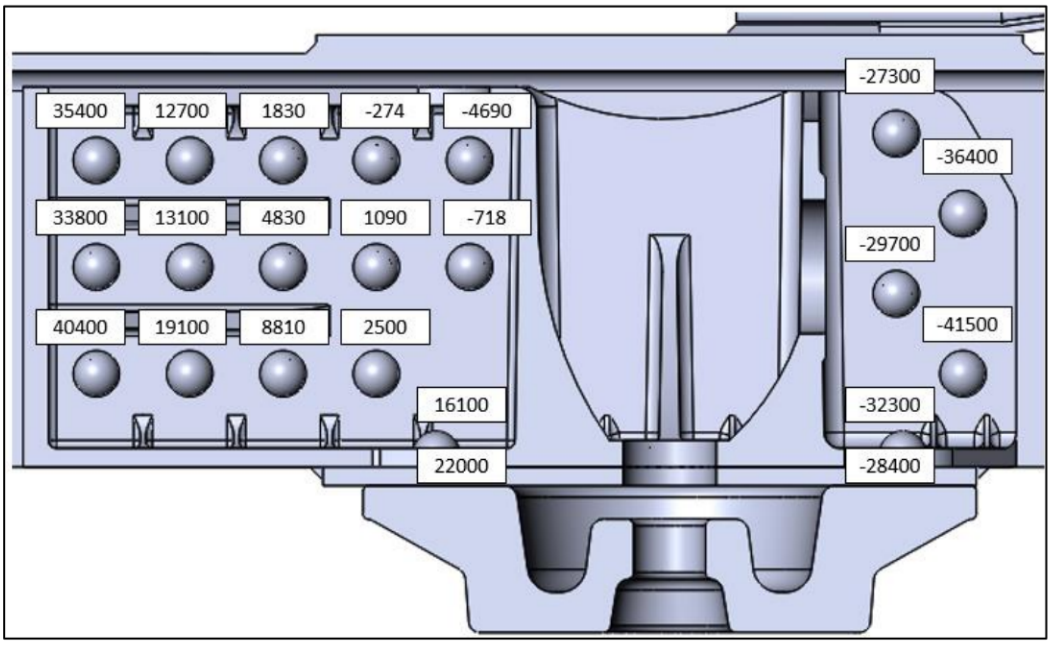

Figure 4.46 – Forces acting in a single-shear lap rivet connection in mode I (jerk)

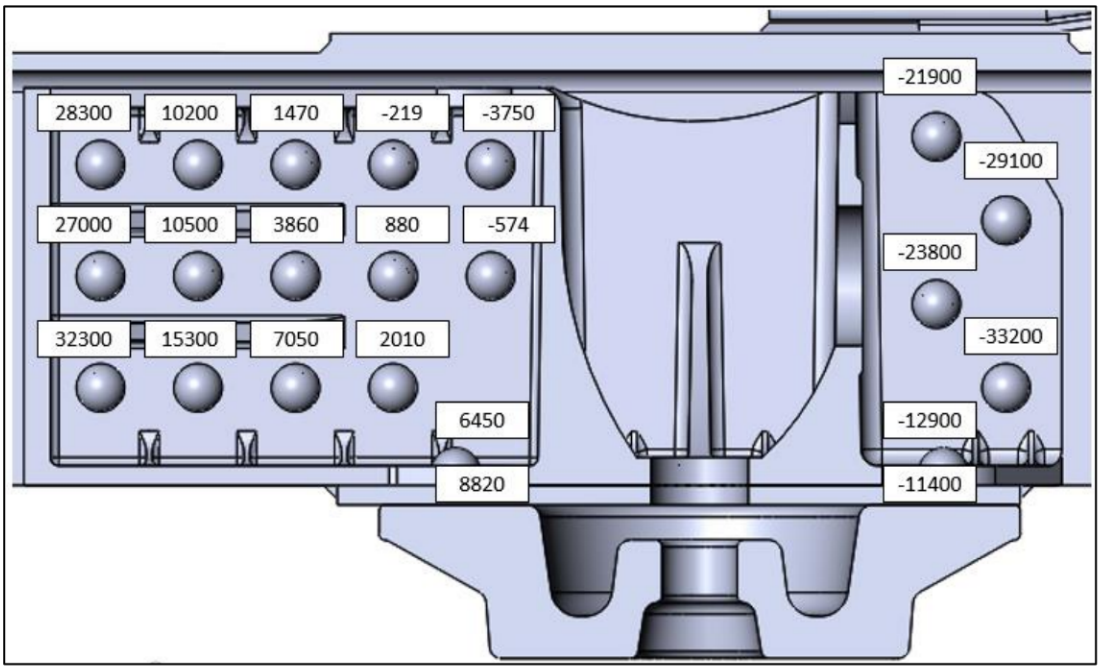

Figure 4.47 – Forces acting in a single-shear lap rivet connection in mode I (tension)

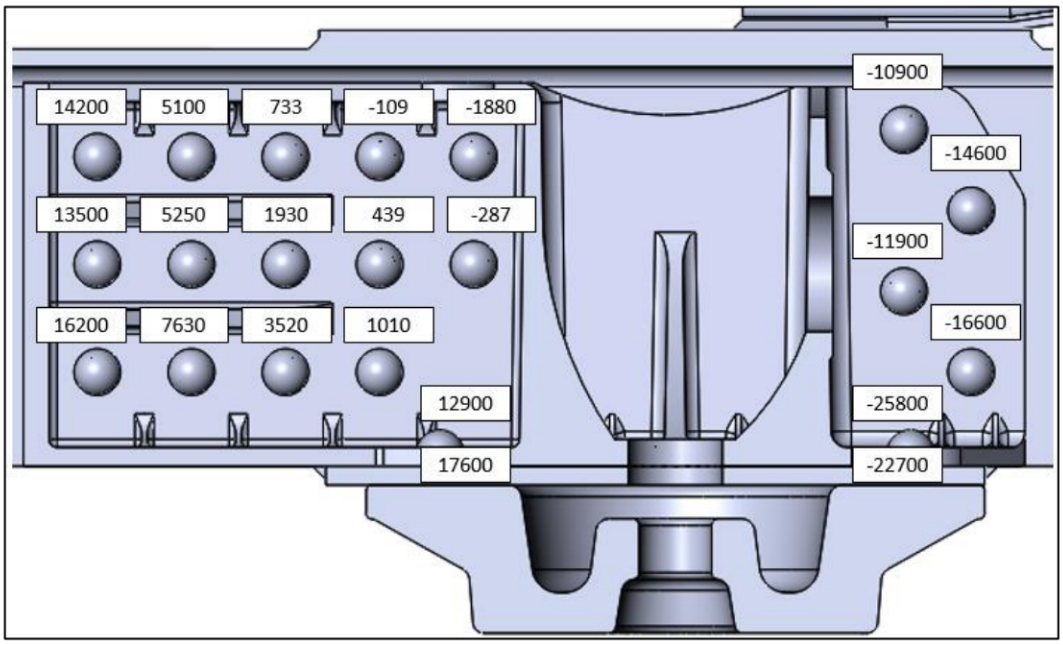

Figure 4.48 – Forces acting in a single-shear lap rivet connection in mode I (tension)

Let us consider the distribution of normal and contacting stresses on the center beam under the rivets from longitudinal tensile forces. The possible stress accumulation is assessed by comparing the obtained stresses with the endurance limit for normal stresses during a pulsating cycle σ_0=120 MPa.

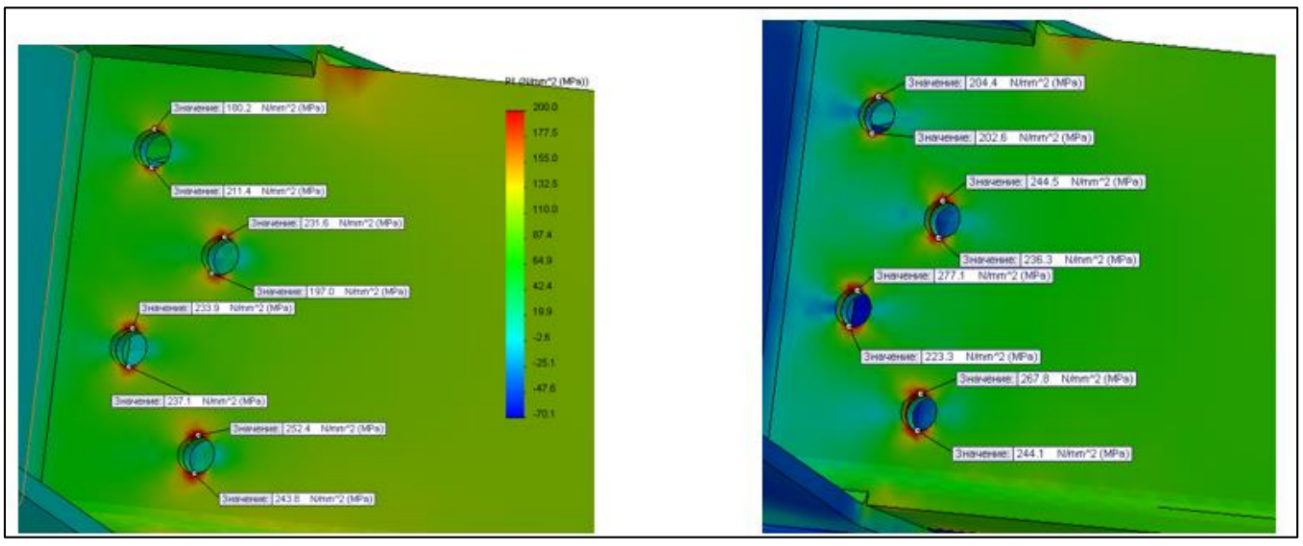

Figure 4.49 – Stress distribution on the center beam under the rivets due to longitudinal forces. Mode I (stretch 2.0 MN)

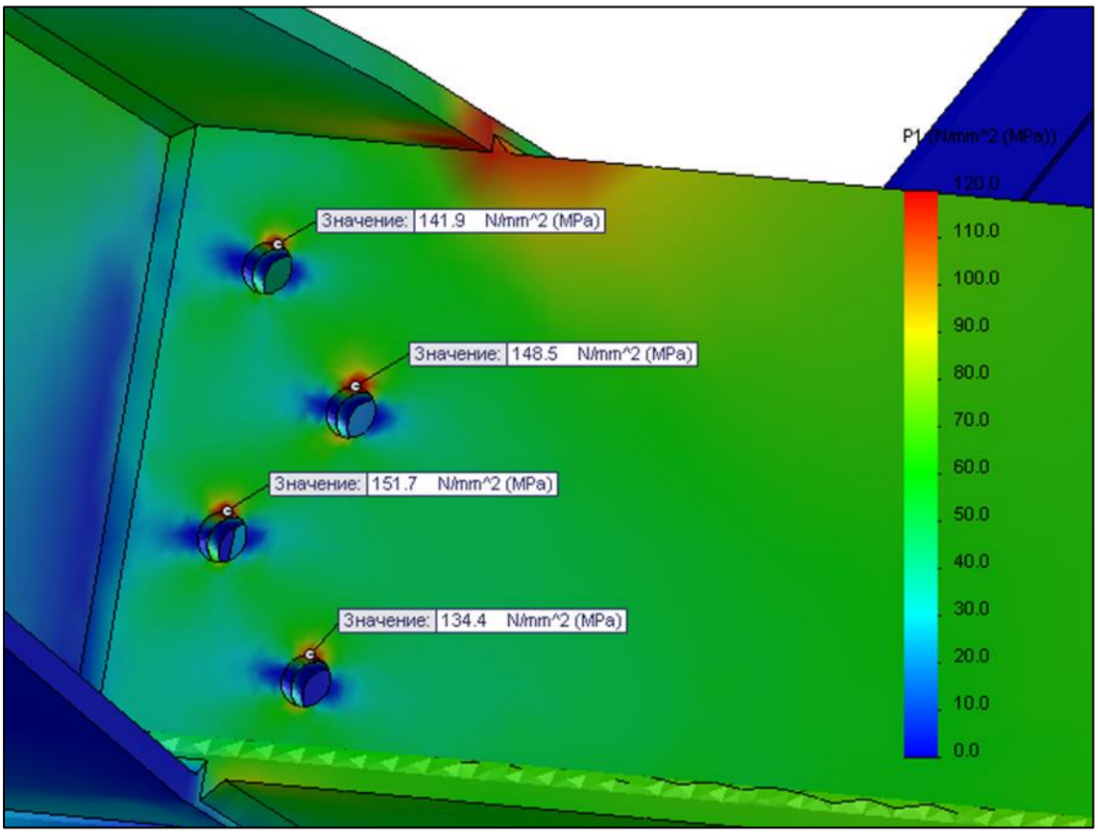

Figure 4.50 – Stress distribution on the center beam under the rivets due to longitudinal forces. Mode III (stretch 1.0 MN)

Based on the calculation results presented at 4.49 and 4.50, it can be concluded that fatigue damage accumulates in the center beam at a load of less than 1.0 MN. In this case, the crack will propagate vertically from the lower rivet hole at 151.7 MPa to the upper rivet hole at 141.9 MPa.

Thus, the jerk, mode I and mode III tensile modes are the main cause of fatigue cracks in the riveted joint area. Such significant stresses arise due to a sharp change in the stiffness of the connection.

4.5.5 Results of regulatory calculations for the grain wagon body modernization project

Robust calculations of the final version of the modernization of the grain wagon body were made on the basis of the constructed design diagrams with the addition of residual stresses in the amount of 20% of the yield strength.

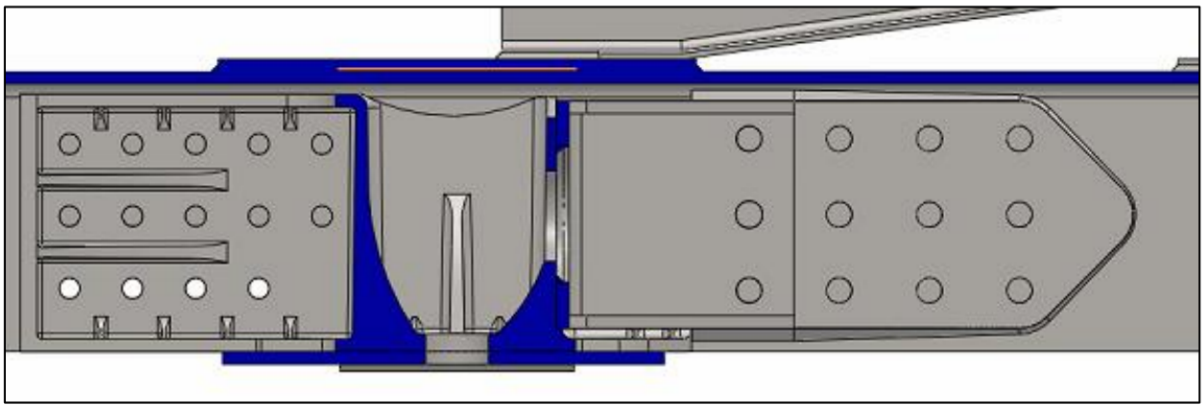

Figure 4.51 – Modernization of the grain wagon body

Since welded joints are used in modernization, those related to stress will be critical, since it is believed that the welded joint works for shear. Strength assessment is made by comparing the obtained stresses with permissible contact stresses for mode I [τ]=178 MPa, and for mode III [τ]=120 MPa. The possible stress accumulation is assessed by comparing the obtained stresses with the endurance limit for contacting stresses during a pulsating cycle τ-0=70 MPa.

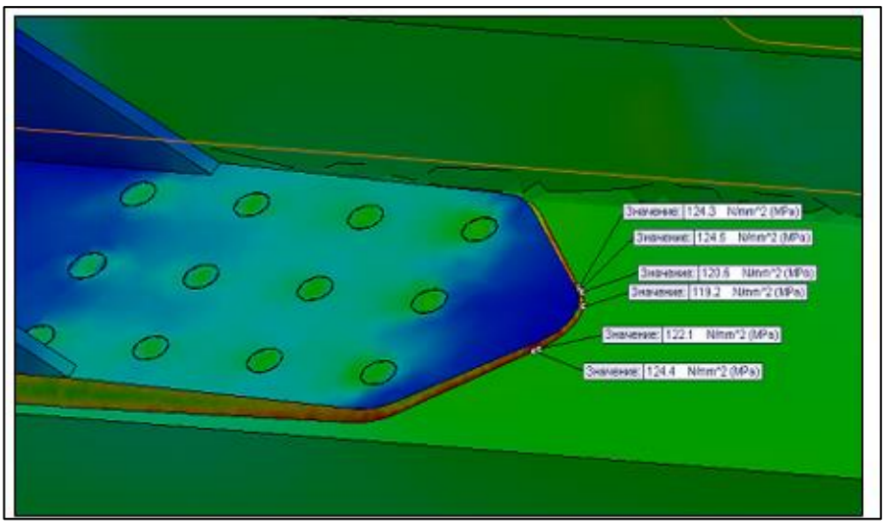

Figure 4.52 – Stress distribution of the final version on the center beam due to longitudinal forces. Mode III (stretch 1.0 MN)

The modernization meets the strength requirements, the highest stresses do not exceed the endurance limits for contact stresses for a pulsating cycle of 62.3 MPa < [70 MPa].

4.5.6Checking the effectiveness of the completed upgrade by conducting control tests and determining the service life

The purpose of conducting control tests of modernized grain wagons is to establish the effectiveness of the modernization performed and to determine the residual life after the modernization has been completed.

The purpose of the wedge drop test is to determine the stresses in the supporting structure elements of the body frame and bogie bolster.

The purpose of a typical contact strength test is to determine and evaluate dynamic stresses and deformations in the load-bearing structures of the wagon when standard impact forces are applied through the automatic coupling device.

The purpose of testing for life is to determine the appearance and development of damage and residual deformations in the load-bearing structures of the wagon under repeated exposure to longitudinal loads through the automatic coupling device, as well ascalculation of service life, which can be determined based on test results.



Figure 4.53 – Modernized covered hopper wagonfor grain model 19-752

4.5.6.1 Wedge release test

Determination of dynamic stresses in frame elements and bolsters is carried out based on the results of drop tests from wedges. According to the developed scheme of control points, strain gauges are installed on the bolster and the frame of the hopper wagon. Depending on the elements of the wagonbeing examined, wedges are installed under the wheels of the hopper wagon, and then the wagon is reset by rolling it onto the wedge. The wedge dimensions are height 21 mm, length 350 mm, width 50 mm.

A loaded hopper wagon is rolled onto wedges by a locomotive. The wedges are installed one by one (Table 3.4.1):

- under all the wheels of the wagon (imitation of bouncing);
- under the wheels of one side of one bogie and the other side of another bogie (imitation of twisting);
- to all wheels of one bogie (imitation of galloping);
- under the wheels of one side of the hopper (imitation of sideways rolling).

Table 4.18 – Scheme for installing wedges under the wheels of the wagon

No.	**Type of vibrations**	**Wheelset number**			
		1	**2**	**3**	**4**
1	Bouncing	■	■	■	■
		■	■	■	■
2	Body twisting	■	■		
				■	■
3	Galloping	■	■		
		■	■		
4	Lateral rolling	■	■	■	■

When dropping a wagon from the wedges, depending on the number of wedges used and their location from the corresponding wheels of the wagon bogies, the stress values are determined depending on the type of vibration.

Table 4.19 – Test results for wedge release

Salary no.	Bouncing, MPa	Salary no.	Torsion front right rear left, MPa	Salary no.	Torsion front left rear right, MPa
1	14	1	15	1	11
2	13	2	9	2	8
3	17	3	10	3	11
4	14	4	10	4	11
5	9	5	9	5	9
6	10	6	8	6	8
7	10	7	11	7	13
8	6	8	7	8	4
9	5	9	5	9	4
10	5	10	6	10	3
Salary no.	Galloping, MPa	Salary no.	Lateral pitching from the left, MPa	Salary no.	Lateral rolling on the right, MPa
1	15	1	10	1	13
2	14	2	10	2	9
3	12	3	9	3	12
4	9	4	11	4	10
5	6	5	10	5	10
6	9	6	8	6	11
7	16	7	12	7	13
8	5	8	3	8	5
9	3	9	3	9	4
10	4	10	5	10	7

Locations for installing strain gauges when testing drops from wedges:

- Points 1, 2, 3 – bolster;
- Points 4, 5 – pivot beam;
- Points 6,7, 8 – spinal beam;

- Points 9, 10 – modernization zone on the spine gully.

Before carrying out the “dumping from wedges” tests, the stress in the bolster from the mass of the load and the mass of the body with the frame was determined by lifting the body with jacks.



Figure 4.54 – Installation locations of strain gauges on the bolster, point 1, 2, 3



Figure 4.55 – Installation location of strain gauges on the pivot beam, point 4, 5



Figure 4.56 – Installation location of strain gauges on the center beam at points 6, 7

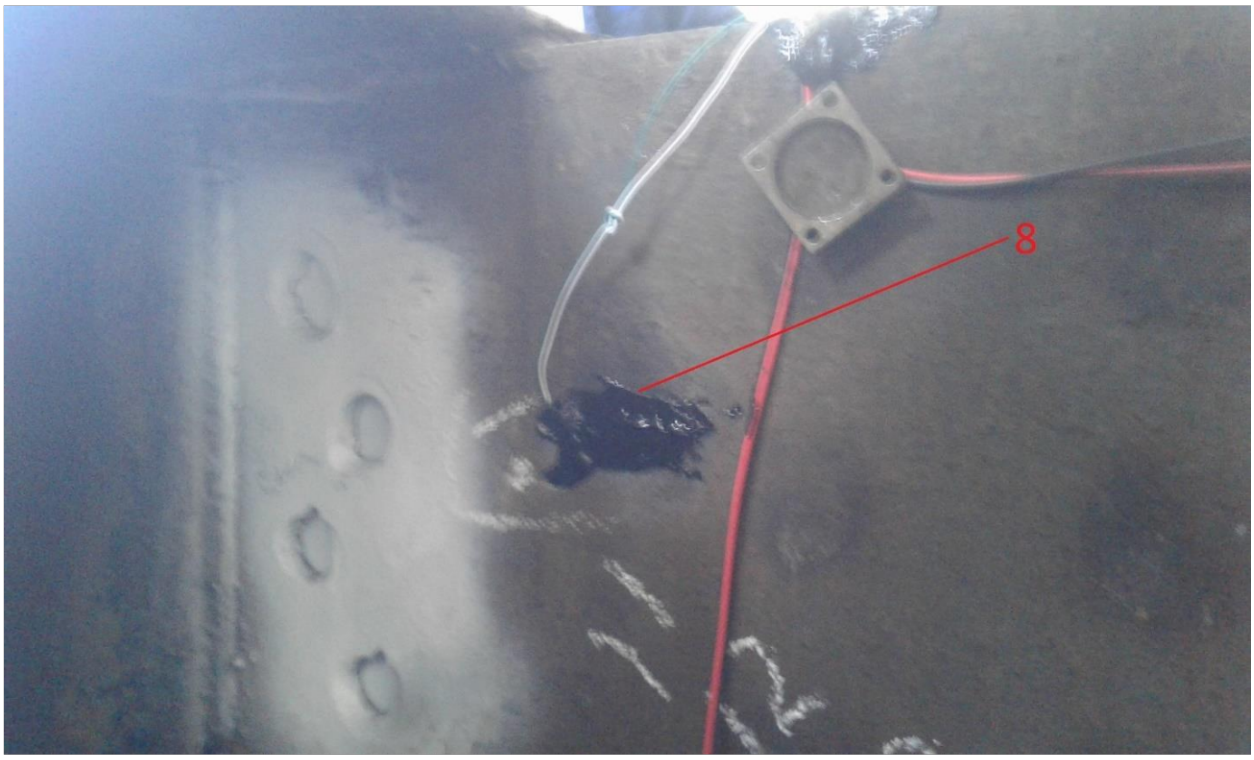

Figure 4.57 – Installation location of strain gauges on the center beam, point 8



Figure 4.58 – Place of installation of strain gauges in the modernization zone of points 9, 10

Experimental determination of the strength of a grain wagon during standard and life-long impact tests.

Test method.

When carrying out standard and life tests on an impact, the following indicators are measured:

- speed of attack of the striker wagon;
- impact force on the automatic coupler;
- number of cycles before failure or damage;
- voltage in the studied elements of the wagon.

To determine the longitudinal forces acting on the test wagon at the moment of impact, an automatic coupler-dynamometer was used (Figure 4.59), equipped with strain gauges and pre-calibrated with a static load on a stand with a force of up to 3.5 MN.



Figure 4.59 – Automatic coupler-dynamometer

Impact tests were carried out on a straight horizontal section of railway track using a locomotive.

In addition to the locomotive, the following equipment was used:

- Impact wagon weighing 91 tons;

- With a double-impact scheme, another hopper wagon model 19-752 is used, modernized No. 95378238 from one side, the track length is 140 m.

- Supporting equipment from three braked freight wagons with a total weight of 300 tons, the movement of which is limited by rail shoes and, taking into account the grain wagon No. 95378238, the weight is 390 tons.

To further speed up the testing, a two-impact scheme was used in one stroke of the striker wagon, in which the first impact is performed when the striker wagon is rolled onto the test wagon, and the second when the test wagon is rolled in conjunction with the striker wagon onto a fixed support.

Impacts were carried out by rolling a striker wagon onto the test wagon using a locomotive. Life tests were carried out in separate series of vessels, which in terms of the amount of damage corresponded to the impact of actions during the year of operation of the wagon. After each series of impacts, the technical condition of the wagon and its equipment was checked.

Impact tests were carried out with a single wagon, which hit a group of loaded wagons, braked by carriage shoes, standing on a straight section of the railway track.

When testing a single wagon, a loaded striker wagon was rolled onto a wagon installed in a group of wagons under test by a locomotive, which was uncoupled from the striker wagon, when it reached an approximately specified impact speed.

The statistical distributions of the maximum longitudinal forces acting on the wagon through the automatic coupler are taken as the initial (operational) spectrum of wagon loading. To calculate the test modes for the cyclic durability of the load-bearing elements of the wagon structure, we use generalized divisions of dynamic (impact) longitudinal forces, corrected by excluding forces with a quasi-static nature of action from the initial distributions.

Selection of test mode for life, processing and evaluation of test results of vinoconan based on:

- linear hypothesis of the amount of damage;

- stress fatigue curve: , where is the number of oscillation cycles with amplitude, t is the exponent.$\sigma_i^{nt} N_{i=const} N_i \sigma_i$

When determining the residual service life of the wagon, the vertical and longitudinal dynamic loads that arise during operation are taken into account. We make the calculation using the formula:

$$T_p = \frac{\left(\frac{\sigma_{a,N}}{[n]}\right)^m \cdot N_0}{N_{cI} \cdot \sum_j \left(\sigma_{aj}^I\right)^m \cdot P_j^I + N_{cII} \cdot \sum_k \left(\sigma_{aj}^{II}\right)^m \cdot P_k^{II}} \quad (4.8)$$

where T_p - is the estimated residual service life of the wagon, years;

$\sigma_{a,N}$ - endurance limit (in amplitude) for the control zone with a symmetrical cycle and the established load mode at the base number of cycles, MPa;

m - exponent in the fatigue curve equation. For welded structures made of rolled steel without strengthening treatment of seams in accordance with $m = 4$;

$[n]$the minimum acceptable safety factor for fatigue resistance for the selected area of the wagon $[n] = 1{,}5$;

N_0 - basic number of cycles;$N_0 = 10^7$

N_{cI} N_{cII} - number of cycles per 1 year of operation for each operational load (vertical and longitudinal);

$\sigma_{aj}^I, \sigma_{aj}^{II}$ – amplitudes of dynamic stresses reduced to a symmetrical cycle for each of the operational loads and their ranges, MPa;

P_j σ_{aj}- probability of occurrence of amplitude with level.

$$\sigma_{aN} = \bar{\sigma_{aN}}\left(1 - z_p\right) = 44{,}4 \cdot (1 - 1{,}645 \cdot 0{,}05) = 40{,}8\ MPa \quad (4.9)$$

where z_p – is the distribution quantile corresponding to a one-sided probability of 95%, $z_p = 1{,}645$;

υ – coefficient of variation of the fatigue threshold of the part:

- for welded frames and beams made of sheet and shaped steel during automatic welding under a layer of flux and inside a protective gas υ = 0.05;

- also for semi-automatic and manual welding υ=0.07;

– average calculated value of the endurance threshold:$\bar{\sigma}_{aN}$

$$\bar{\sigma}_{aN} = \frac{\bar{\sigma}_{-1}}{(\bar{K}_{\sigma})_k}, = \frac{200}{4{,}5} = 44{,}4 \text{ MPa}$$

$\bar{\sigma}_{-1}$– the average value of the endurance threshold of a smooth standard sample made of frame material with a symmetrical bending cycle on the base.N_0

$(\bar{K}_{\sigma})_k$ – the average value of the coefficient of reduction in the endurance threshold of the frame in relation to the endurance threshold of a smooth standard sample, .$(\bar{K}_{\sigma})_k = 4{,}5$

N_c – the number of cycles of vertical vibrations of a loaded wagon that occur during its service life of one year:

$$N_c = 365 \cdot f_{\epsilon} \frac{L_c \cdot 0.5 \cdot 10^3}{\bar{V}_T} \cdot T_{\text{к}} = 365 \cdot 3{,}08 \frac{162 \cdot 0{,}5 \cdot 10^3}{22{,}4} \cdot 1 = 4065000 \qquad (4.10)$$

T_k–design service life of the wagon after modernization;

L_c–design average daily mileage of the wagon (assuming 162 km);

$\bar{V}_T$– design average technical speed of the wagon is 22.4 m/s;

0,5– empty run coefficient;

f_ϵ–the effective frequency of the process of changing dynamic loads is determined by the formula.

$$f_\epsilon = \frac{a}{2\pi} \cdot \sqrt{\frac{g}{f}} = \frac{1.4}{2 \cdot 3.14} \cdot \sqrt{\frac{9.81}{0.05}} = 3{,}08 \text{ Гц.}$$

K_{di} – determined using formulas.

$$K_{di} = \frac{\overline{K_{di}}}{\omega} \sqrt{\frac{4}{\pi} ln \frac{1}{1 - P(K_{di})}} = \frac{0{,}185}{1{,}13} \sqrt{\frac{4}{3{,}14} ln \frac{1}{1 - 0{,}02 \cdot 0{,}35}} = 0{,}35$$

Where – the distribution parameter for a loaded wagon is 1.13.ω

The average possible value is determined by the formulas:$\overline{K_{di}}$

- At V≥15 m/s

$$\overline{K_{di}} = a + 3{,}6 \cdot 10^{-4} \cdot b \cdot \frac{V - 15}{f_{ст}} = 0.05 + 3{,}6 \cdot 10^{-4} \cdot 1 \cdot \frac{33{,}3 - 15}{0{,}05} = 0{,}181$$

- At V≤15 m/s

$$\overline{K_{di}} = a \cdot \frac{V}{15} = 0.05 \cdot \frac{13{,}75}{15} = 0{,}04$$

Where a is a coefficient equal to 0.5 for body elements;

b– coefficient taking into account the influence of the number of axles n in a bogie or group of bogies under one end of the carriage.

$$b = \frac{n+2}{2n};$$

V – design speed, m/s;

$f_{ст}$– static deflection of spring suspension, g.

The total estimated number of cycles during the estimated period of operation of the wagonfor the total mileage network is determined by the formula:

$$N_{заг}^{розр} = N_{zg}^{ud} \cdot T_{розр} \cdot K_{реж} \cdot K_{уд}, \qquad (4.11)$$

where N_{zg}^{ud} - the total number of cycles of impact longitudinal forces for 1 year of the average operating network on the structure of a wagon of this type, for distributions (without taking into account quasi-static forces) is:

- for freight wagons;$N_{zg}^{ud} \approx 20200$

T_{calc} - estimated period of operation of the wagon, (1 year);

K_{zr} - coefficient taking into account the influence of the empty run of the wagon when assessing the cyclic durability of load-bearing elements K_{zr} (for a grain wagon) $К_{em} = 0{,}5$;

$$K_{zr} = 1 - K_{em} \qquad (4.12)$$

$К_{ud}$- a coefficient that takes into account the asymmetry of the loading of the wagonstructure along its length during collisions and the uniformity of the application of impact forces to the automatic coupler at both ends of the wagon (when assessing the cyclic durability of the elements of the cantilever part of the wagon, it is recommended to take it equal to 0.6).

The choice of loading mode is carried out taking into account the ratio of the average daily mileage to the total network mileage.

For grain hopper wagons:

$$N_{fr}^{calc} = 20200 \cdot 1 \cdot 0{,}50 \cdot 0{,}6 \cdot \frac{162}{290} = 3393 \; in \; a \; 1 \; year$$

To study the influence of tensile forces on the strength of the rivet joint, tensile tests of 100 cycles were carried out after testing compressive impact loads of 300-400 blows, with recording of tensile force and stress indicators.

N_{ud}– the estimated number of collisions per year of wagon operation.

According to the single-impact scheme and; $F_{ekv} = 3{,}8$, F_{ekv}=3.4 MN; F_{ekv}=2.8 MN F_{ekv}=2.4 MN the basic number of cycles per one year of operation will be:

$$N_b = \frac{3393}{3{,}8^4} \cdot (0{,}25^4 \cdot 0{,}1258 + 0{,}6^4 \cdot 0{,}2852 + 1^4 \cdot 0{,}2802 + 1{,}4^4 \cdot 0{,}1832 + 1{,}8^4 \cdot 0{,}0772 + 2{,}2^4 \cdot 0{,}0359 + 2{,}6^4 \cdot 0{,}0208 + 3{,}0^4 \cdot 0{,}0023 + 3{,}4^4 \cdot 0{,}0003 + 3{,}7^4 \cdot 0{,}0001) = 68;$$

$$N_b = \frac{3393}{3{,}4^4} \cdot (0{,}25^4 \cdot 0{,}1258 + 0{,}6^4 \cdot 0{,}2852 + 1^4 \cdot 0{,}2802 + 1{,}4^4 \cdot 0{,}1832 + 1{,}8^4 \cdot 0{,}0772 + 2{,}2^4 \cdot 0{,}0359 + 2{,}6^4 \cdot 0{,}0208 + 3{,}0^4 \cdot 0{,}0023 + 3{,}4^4 \cdot 0{,}0003 + 3{,}7^4 \cdot 0{,}0001) = 107;$$

$$N_b = \frac{3393}{2{,}8^4} \cdot (0{,}25^4 \cdot 0{,}1258 + 0{,}6^4 \cdot 0{,}2852 + 1^4 \cdot 0{,}2802 + 1{,}4^4 \cdot 0{,}1832 + 1{,}8^4 \cdot 0{,}0772 + 2{,}2^4 \cdot 0{,}0359 + 2{,}6^4 \cdot 0{,}0208 + 3{,}0^4 \cdot 0{,}0023 + 3{,}4^4 \cdot 0{,}0003 + 3{,}7^4 \cdot 0{,}0001) = 230$$

$$N_b = \frac{3393}{2{,}4^4} \cdot (0{,}25^4 \cdot 0{,}1258 + 0{,}6^4 \cdot 0{,}2852 + 1^4 \cdot 0{,}2802 + 1{,}4^4 \cdot 0{,}1832 + 1{,}8^4 \cdot 0{,}0772 + 2{,}2^4 \cdot 0{,}0359 + 2{,}6^4 \cdot 0{,}0208 + 3{,}0^4 \cdot 0{,}0023 + 3{,}4^4 \cdot 0{,}0003 + 3{,}7^4 \cdot 0{,}0001) = 451;$$

With a 2-impact scheme, the first impact is made when the striker wagon is rolled onto the wagon being tested, and the second is when the wagon, tested alone or in conjunction with the striker wagon, is rolled onto the support wagons. With this scheme, impact forces are recorded on two tested automatic couplers of the wagon.

With a two-impact scheme with a force of the first impact F_1= 3.6 MN and the second impact $F_2 = 3{,}8MH$, the basic number of cycles per one year of operation will be:

$$N_{bII} = \frac{F_{ek.}^m N_б}{F_1^m + F_2^m} = \frac{3{,}8^4 \cdot 68}{(3{,}8^4 + 3{,}6^{4)}} = 38$$

With a two-impact scheme with a force of the first impact F_1= 3.4 MN and the second impact $F_2 = 3{,}6\,MH$, the basic number of cycles per one year of operation will be:

$$N_{bII} = \frac{F_{ek.}^{m} N_б}{F_1^m + F_2^m} = \frac{3{,}6^4 \cdot 107}{(3{,}6^4 + 3{,}4^4)} = 60$$

With a two-impact scheme with a force of the first impact F_1= 2.8 MN and the second impact $F_2 = 3{,}0\ MH$, the basic number of cycles per one year of operation will be:

$$N_{bII} = \frac{F_{ek.}^{m} N_б}{F_1^m + F_2^m} = \frac{3^4 \cdot 291}{(3^4 + 2{,}8^4)} = 628$$

Table 4.20 – Impact test results

No.	Strength (N), MH	Average force value (N), MH	The number of strokes is equal to the shock pattern	Number of strikes two strike pattern	Accumulated damage, MH^4
1	Less than 1	1	4	-	4
2	1.0-1.5	1.25	7	-	17
3	1.5-2.0	1.75	40	-	375
4	2.0-2.5	2.25	70	-	1794
5	2.5-3.0	2.75	60	-	3430
6	3.0-3.5	3.25	93	-	10375
7	More than 3.5	3.5	53	-	7953
8	3+2.6		-	78	9882
9	3.5+3		-	110	25410
10	3.8+3.2		-	67	20991
Total			582		80231

Table 4.21 – Results of life-long impact tests.

Dot	Strength, MN		
	2.5 MPa	3.0 MPa	3.5 MPa
1	35	41	57
2	21	34	72
3	55	82	93
4	29	28	31
5	19	25	26
6	16	23	29
7	19	23	38
8	60	68	87
9	68	79	91
10	58	70	86
11	27	33	77
12	28	31	62
13	37	67	80
14	12	22	39
15	41	52	36
16	55	66	95
17	10	17	29

In fact, 582 impacts were made during testing.

The operating time during the period of life tests was compared with the calculated operating time for the year of service of the grain truck. The operating time criterion is the sum of accumulated damage, determined by the formula:

$$\sum D = \sum P_i^4 \times n_i ,$$

where ∑ D is the sum of accumulated damage;

Pi – impact force;

n_i – number of impacts with force Pi.

The estimated amount of accumulated damage for a year of operation is determined by the formula:

$$D_p = P_{ek}^m \times n_б = 3{,}25^4 \times 102 = 11379 \text{ МПа}^4$$

As can be seen from the table, operating time accumulated damage during the period of impact life tests 80233 MH^4 and with the estimated amount of accumulated damage for the year of operation 11379 MH^4 answers:

$$T = \frac{\sum D}{D_p} = \frac{80231}{11379} = 7{,}05\ (year)$$

The service life of the covered grain hopper wagon model 19-752 after modernization is 7 years.

Based on the test data, the fatigue resistance safety factors of the wagons structural elements were calculated. Calculations were carried out according to the methodology set out in DSTU 7598-2014 “Freight wagons. General requirements for the calculations and design of new and modernized 1520 mm track wagons (non-self-propelled), It is assumed that the fatigue curve coefficient is m = 0.4, the concentration coefficient is 4.5, the average value of the endurance limit of the center and center beams is 210 MPa, the average daily mileage of the wagon is 2 km, design average speed – 22.4 m/s.

According to the calculation results, the smallest fatigue resistance safety factor is 1.9 with an acceptable value of 1.5.

CONCLUSIONS ON SECTION 4

General requirements for the mobile system have been formed and implemented to determine the quality and safety indicators for the movement of freight wagons with reduced tare in operation. This mobile system allows the running tests to be carried out without involving a laboratory wagon, which reduces the costs and time of such tests by 25.8%.

A method for in-depth processing of the results of rolling stock running tests is proposed. The essence is to perform a spectral analysis of dynamic processes for various elements of the load-bearing structures of a freight wagon in order to identify the relationships between the oscillatory processes of the load-bearing structures and the frequencies at which the interaction between them occurs. A software algorithm has been developed for in-depth assessment of experimental indicators of the quality of movement of lightweight wagons.

Based on the results of practical studies, it was established that a decrease in the tare weight indicator by more than 10% negatively affects the quality of movement of such wagons and a speed range of 60-70 km/h was identified, during which a sharp deterioration in movement dynamics was recorded in a number of experimental wagons.

A safe scheme for forming trains that include freight wagons with reduced tare is proposed. The values of compression forces obtained during running dynamic tests acting on the automatic coupling devices of wagons and reaching or exceeding critical values in the main and middle parts of the train according to such schemes. It is advisable to place empty wagons in the last third of the train.

As a result of the control tests of the hopper wagon model 19-752, which was modernized in accordance with the developed design and technological documentation, it was established that:

- stresses in the supporting structures of the wagon do not exceed permissible values (DSTU 7598-2014 “Freight wagons. General requirements for the calculations and design of new and modernized 1520 mm gauge wagons (non-self-propelled);
- No damage was detected in the area of modernization of the wagon frame in the form of deformations, cracks, breaks in the base metal and welds.
- During resource tests, 582 582 co-impacts with a force from 1 to 3.5 MN and more were made, which corresponds to a service life of 7 years.

SECTION 5
SYSTEM FOR MEASURING THE INTERACTION FORCES OF WHEELS AND RAILS ACCORDING TO THE CHARACTERISTICS OF THE STRESSED AND DEFORMED STATE

5.1 Determination of the deformation sensitivity zones of the wheel disc to force load

The placement of strain gauges on the wheel rims and the methods of their inclusion in the measuring circuit must be such that, while the circuit is sufficiently sensitive to the action of the measured force, the influence of a force in another direction is as small as possible. Therefore, studies to determine the zones on the surface of the wheel disk, the deformations of which are caused by the action of purely vertical and horizontal contact forces, are necessary to justify the equipping of wheel pairs with strain gauge schemes.

To carry out calculations of the stress-strain state of the wheel pair using the finite element method, 3D models of individual elements of the carriage wheel pair and P65 type rails were created, from which a general 3D model of the wheel pair installed on the rails was compiled (Fig. 5.1).

The deformation sensitivity zones of the wheel disk were determined based on the following design cases of wheel pair load:

- vertical load;
- load by vertical forces and forces from the action of the tare system (horizontal load).

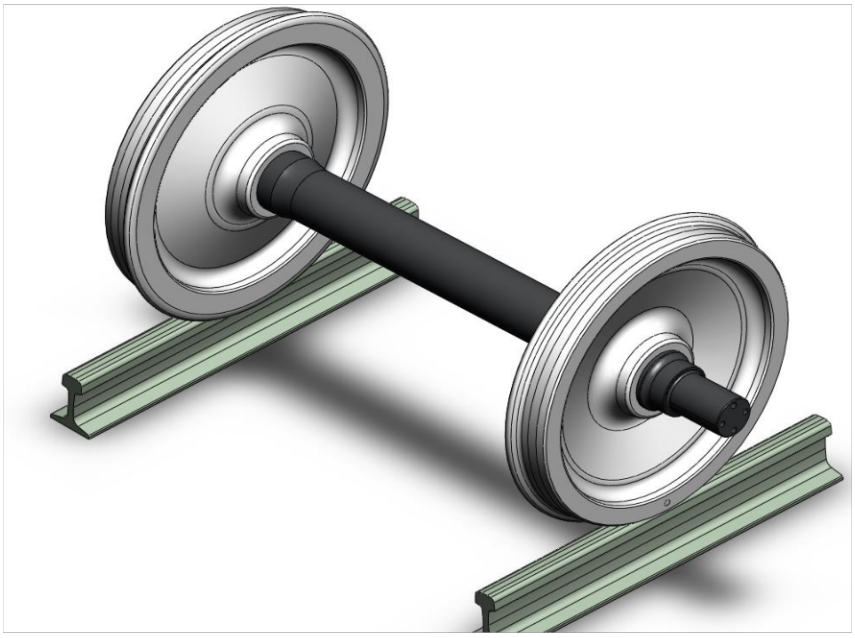

Figure 5.1 – 3D model of a wheelset

Vertical loading was specified based on the wagons mass of 52 tons. The side loading scheme simulated the application of horizontally directed forces from the loading device to the outer edge of the wheel above the contact with the rack. In the calculations, the magnitude of the lateral force was set at 50 kN.

Figure 5.2 shows the distribution of surface stresses of the wheel under vertical load (Fig. 5.2a) and the simultaneous action of vertical and lateral forces (Fig. 5.2b). As you can see, the greatest stresses in the wheel disk under vertical load occur in the zone of transition of the disk to the rim (zone I), as well as in the place adjacent to the hub (zone III). Under lateral load, near the zone adjacent to the hub, deformations spread to the middle part of the disk (zone II).

Thus, according to the results of calculations of the stress-strain state of the wheel disk, zone III turned out to be the most sensitive in terms of deformations to both vertical and lateral loads. Therefore, to measure lateral loads, zone II should be selected, which is practically sensitive only to lateral forces, and for measuring vertical loads, zone I should be selected.

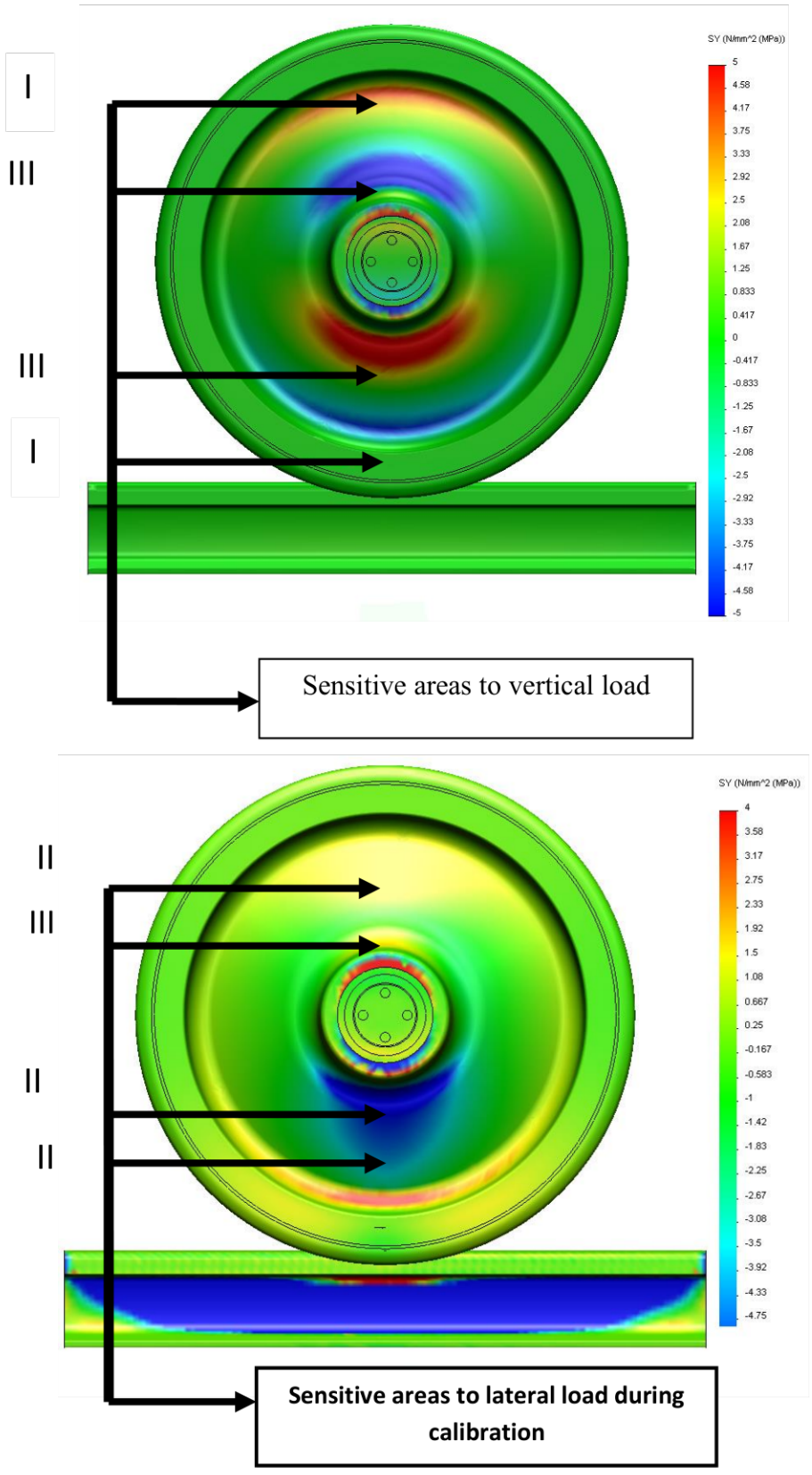

b)

Figure 5.2 – Diagrams of normal radial stress in a wheel disk under vertical (a) and combined (b) loads

5.1.1 Experimental determination of surface stresses of a wheel disk under the action of tare loads

The placement of strain gauges on the wheel pair disk and the methods of their inclusion in the measuring circuit must be such that, if the circuit is sufficiently sensitive to the measured force, the influence of a force of another direction on the circuit is excluded. Thus, in order to separately record the forces acting on the wheel pair, it is necessary to determine the placement of strain gauges, each of whichsensitiveonly up tostrength, acting in onedirection.

To clarify locations on the wheel rimpoints of sensitive areas to vertical and lateral loadsrelevant experimental studies were carried out. According to the scheme, strain gauges were placed on the wheel disk in the radial direction with a step commensurate with the base of the strain gauge. WITHThe diagram for placing strain gauges on the wheel disk is shown in Figure 5.3, and the coordinates of their location are in Figure 5.4.A total of 20 strain gauges were installed along the diametrical direction of the wheel (Fig. 5.5).

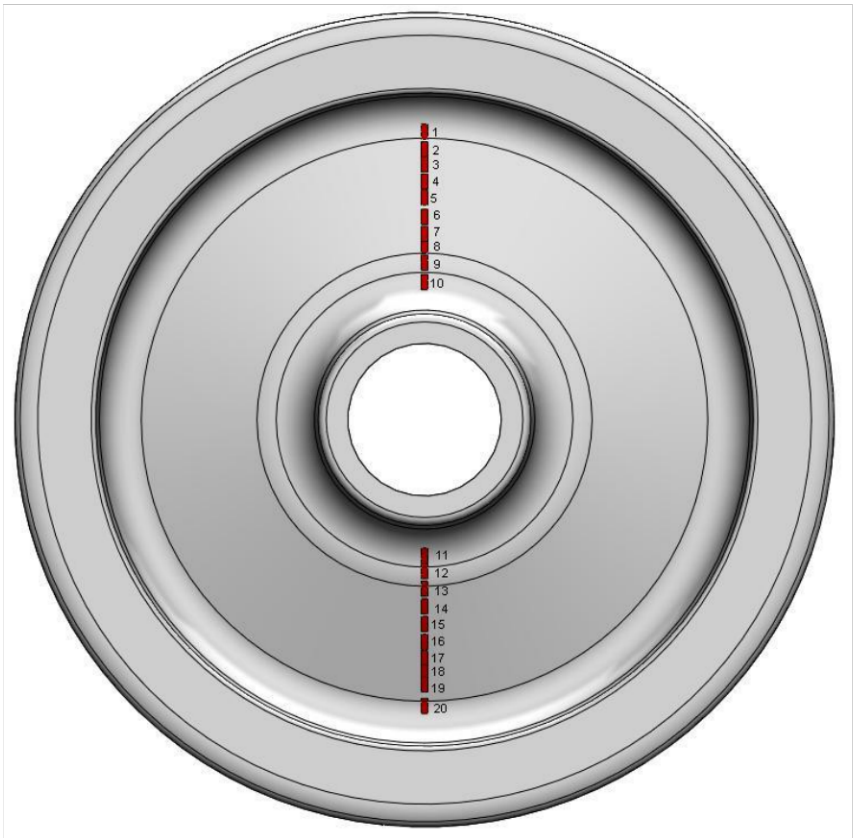

Figure 5.3 – Layout of strain gauges on the wheel of the measuring wheelset

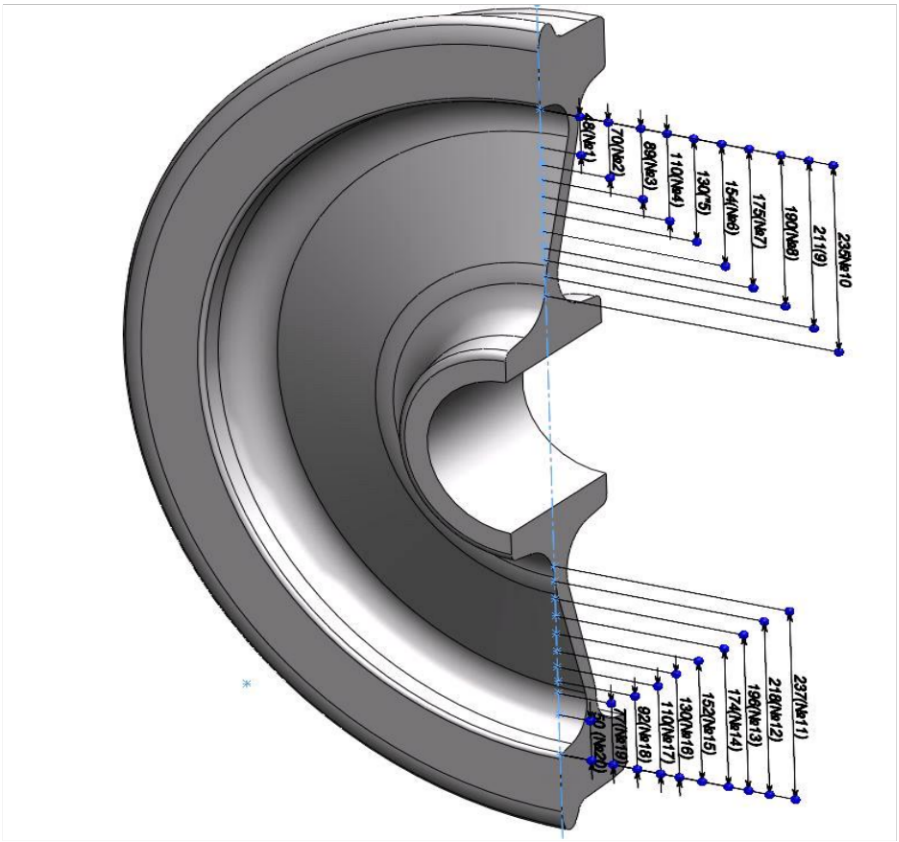

Figure 5.4 – Location of strain gauges on the wheel of the measuring wheelset

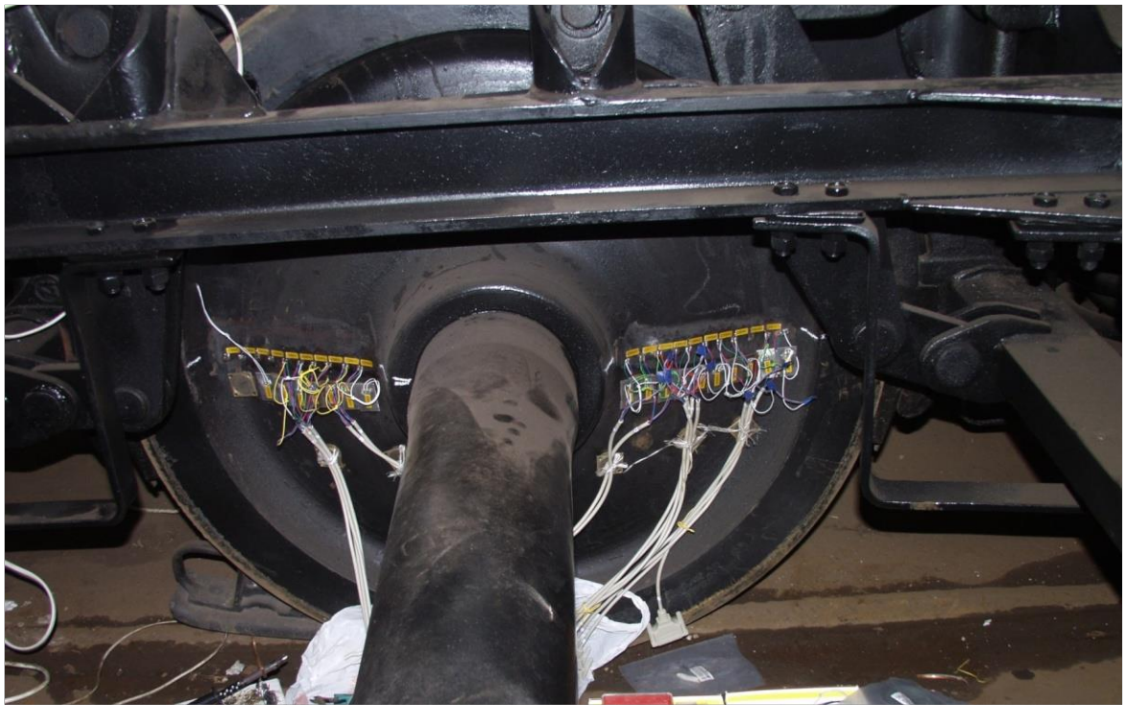

Figure 5.5– Placement of strain gauges on the inner surface of the wheel disk

The vertical loading of the wheel was created by the weight of the wagon body. Figure 5.6 shows the distribution of stresses from vertical loading of the wheel, measured three times at the locations of each strain gauge. Apparently, in this case, the greatest stresses occur at points 9 and 12. These points are located symmetrically relative to the center of the wheel. Areas near points 3, 4 and 17 are insensitive to vertical load.

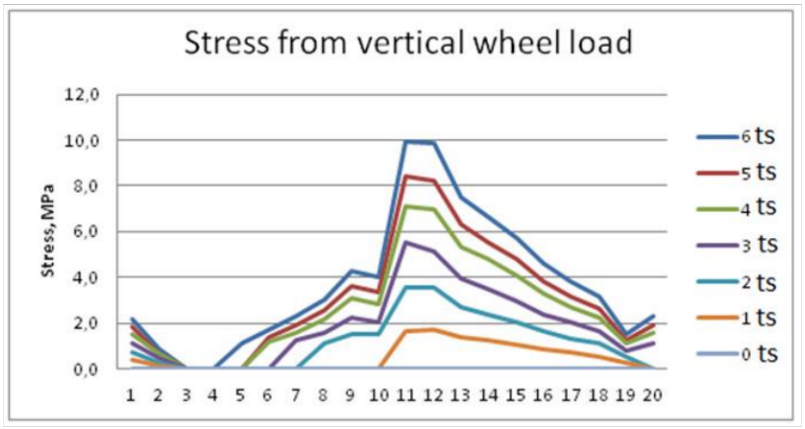

Figure 5.6 – Stress distribution on the wheel disk under vertical load

To load wheel pairs with horizontal transverse forces, a tare device is used.

The results of stress measurements when loading a wheel by lateral forces are presented in Figure 5.7. Here the stress distribution graphs correspond to power-law force values. Just as with a vertical load, in this case points 9 and 12 turned out to be the most sensitive. Point 3 and the zone between points 19 and 20 are insensitive to the action of lateral forces.

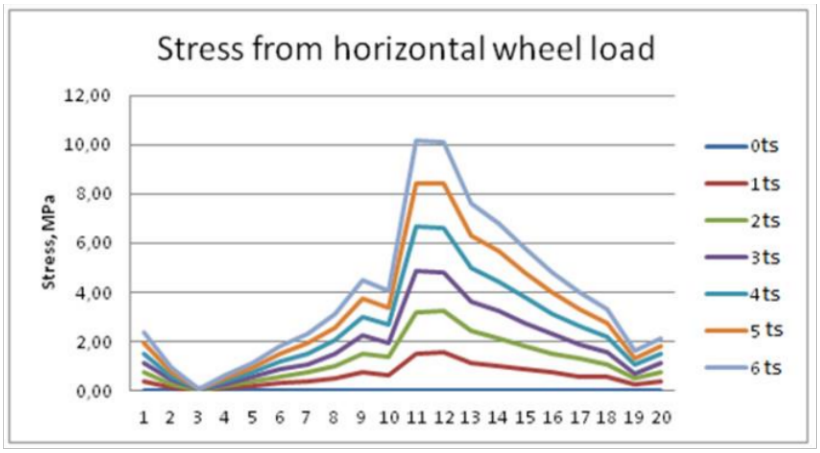

Figure 5.7 – Stress distribution on the wheel disk under horizontal load

The experimental data obtained make it possible to identify the zones of greatest stress that arise on the wheel disk under the action of lateral (horizontal) and vertical loads. Experimental data, taking into account the results of computer modeling of the wheel load, provide grounds for the development of a refined strain gauge scheme for direct measurements of the interaction forces between wheels and rails.

Table 5.1 – Stress value on the wheel disk under horizontal load

No. tensorezistor	Strain gauge readings, MPa						
	0	1 ts	2 ts	3 ts	4 ts	5 ts	6 ts
1	0	-0.35	-0.73	-1.10	-1.52	-1.95	-2.37
2	0	-0.15	-0.27	-0.43	-0.58	-0.76	-0.94
3	0	0.01	-0.01	-0.06	-0.09	-0.09	-0.09
4	0	0.10	0.20	0.28	0.40	0.50	0.61
5	0	0.19	0.37	0.56	0.75	0.93	1.12
6	0	0.34	0.57	0.91	1.16	1.49	1.79
7	0	0.36	0.75	1.09	1.52	1.92	2.34
8	0	0.49	1.02	1.48	2.04	2.57	3.10
9	0	0.73	1.48	2.22	2.97	3.72	4.47
10	0	0.60	1:35	1.91	2.66	3.40	4.07
11	0	-1.51	-3.19	-4.87	-6.67	-8.42	-10.14
12	0	-1.57	-3.26	-4.82	-6.62	-8.40	-10.13
13	0	-1.15	-2.42	-3.62	-4.98	-6.33	-7.62
14	0	-1.03	-2.15	-3.27	-4.42	-5.66	-6.81
15	0	-0.85	-1.83	-2.73	-3.82	-4.79	-5.80
16	0	-0.73	-1.53	-2.29	-3.14	-3.98	-4.80
17	0	-0.57	-1.30	-1.87	-2.61	-3.34	-4.01
18	0	-0.54	-1.09	-1.58	-2.18	-2.77	-3.33
19	0	-0.23	-0.52	-0.72	-1.07	-1.33	-1.65
20	0	0.38	0.77	1.11	1.50	1.84	2.11

Table 5.2 – Stress value on the wheel disk under vertical load

No. tensorezistor	Strain gauge readings, MPa						
	6 ts	5 ts	4 ts	3 ts	2 ts	1 ts	0
1	-2.20	-1.87	-1.53	-1.12	-0.75	-0.38	0
2	-0.84	-0.69	-0.65	-0.46	-0.27	-0.13	0
3	-0.01	-0.01	-0.01	0.00	0.00	-0.01	0
4	0.71	0.58	0.48	0.37	0.25	0.13	0
5	1.12	0.93	0.75	0.57	0.38	0.19	0
6	1.69	1:40	1:20	0.85	0.65	0.28	0
7	2.29	1.92	1.60	1.23	0.85	0.44	0
8	3.06	2.55	2.17	1.61	1.10	0.57	0
9	4:30	3.61	3.09	2.24	1.50	0.75	0
10	4.03	3:35	2.81	2.07	1.49	0.74	0
11	-9.93	-8.40	-7.09	-5.22	-3.55	-1.86	0
12	-9.89	-8.25	-6.97	-5.12	-3.55	-1.74	0
13	-7.51	-6.29	-5.34	-3.92	-2.69	-1.37	0
14	-6.68	-5.56	-4.78	-3.50	-2.38	-1.26	0
15	-5.71	-4.79	-4.10	-2.98	-2.05	-1.08	0
16	-4.60	-3.85	-3.28	-2.40	-1.64	-0.84	0
17	-3.82	-3.18	-2.72	-2.02	-1.32	-0.71	0
18	-3.17	-2.61	-2.25	-1.68	-1.12	-0.56	0
19	-1.49	-1.28	-1.12	-0.78	-0.56	-0.30	0
20	2.28	1.89	1.56	1.15	0.77	0.40	0

5.1.2 TTechnological implementation of a method for directly measuring the forces of interaction between wheels and rails

Based on the results of theoretical and experimental studies and analysis of existing systems for measuring forces acting on the running parts of rolling stock, it is recommended to measure contact forces using wheel deformations. In this case, strain gauges are installed on the inner surface of the disk.

The conducted studies have shown that the development of systems for directly measuring the forces of interaction between wheels and rails is based on the use of technologies that allow the installation of wheel sets of arbitrary configurations without interfering with the design and using wireless transmission of signals from strain gauge circuits.

The principal advantage of this method is that it makes it possible to measure the Y and Q forces continuously and close to the wheel-rack interface. It is also possible to measure high-frequency force processes. The measurement accuracy can be quite high (within 5-10%).

Based on the calculations and experimental data to determine the zones of deformation sensitivity of a standard carriage wheel disk to vertical and lateral loads, a layout of strain gauges for determining the contact forces of interaction between wheels and rails, shown in Figure 5.8, is recommended. Here, points 1-1', 5-5', 9-9' indicate the places where the greatest stresses arise. To measure lateral forces, points 2-2', 6-6', 10-10' are allocated, and for vertical forces - 3-3', 7-7', 11-11'. Measuring deformations at points 4-4', 8-8', 12-12' is intended to determine the instantaneous position of the wheel when the wagonis moving. The indicated points are located in the diametric directions A-A', B-B', C-C'. Corresponding strain gauge circuits are installed from strain gauges installed at certain points.

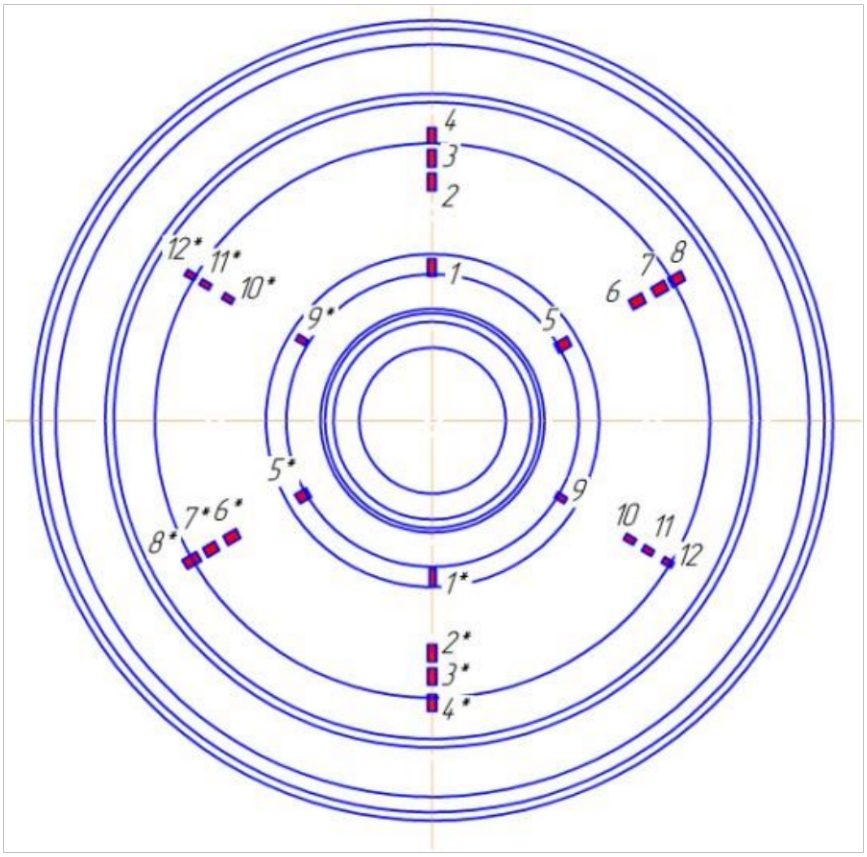

Figure 5.8 – Recommended arrangement of strain gauges on the surface of the wheel disk

Points 1-1*, 5-5*, 9-9* indicate the places where the greatest stresses occur. Points 2-2*, 6-6*, 10-10* are selected for measuring lateral forces, and 3-3*, 7-7*, 11-11* for vertical ones. Measurement of deformations at points 4-4*, 8-8*, 12-12* is intended to determine the momentary position of the wheel during the carriage movement.

To achieve accurate and reliable measurements, considerable care is required when installing the strain gauge circuits on the wheels of the measuring wheelset. Since the wheel set must operate under conditions of a wide range of dynamic loads, high humidity and significant temperature fluctuations, protection from water, oil and vibration is used to ensure reliable operation of the measuring circuits.

5.2 Theoretical studies of wheels dynamic loading of passenger wagons at high speeds

To assess the dynamic load of the wheels of a passenger wagon, a computer model of the dynamics of a passenger wagon was created.

Using the developed computer model of the dynamics of a passenger wagon, calculations were made to determine the forces of interaction between wheels and rails in terms of the level and nature of the change over time. The movement of a wagon along a straight track is considered with real inequalities at speeds of 36, 72, 108, 144 and 180 km/h.

Figures 5.9 – 5.24 show the obtained implementations of changes in time (oscillograms) of transverse horizontal (Fy_1l) and vertical (Fz_1l) interaction forces at a speed of V = 108 km/h.

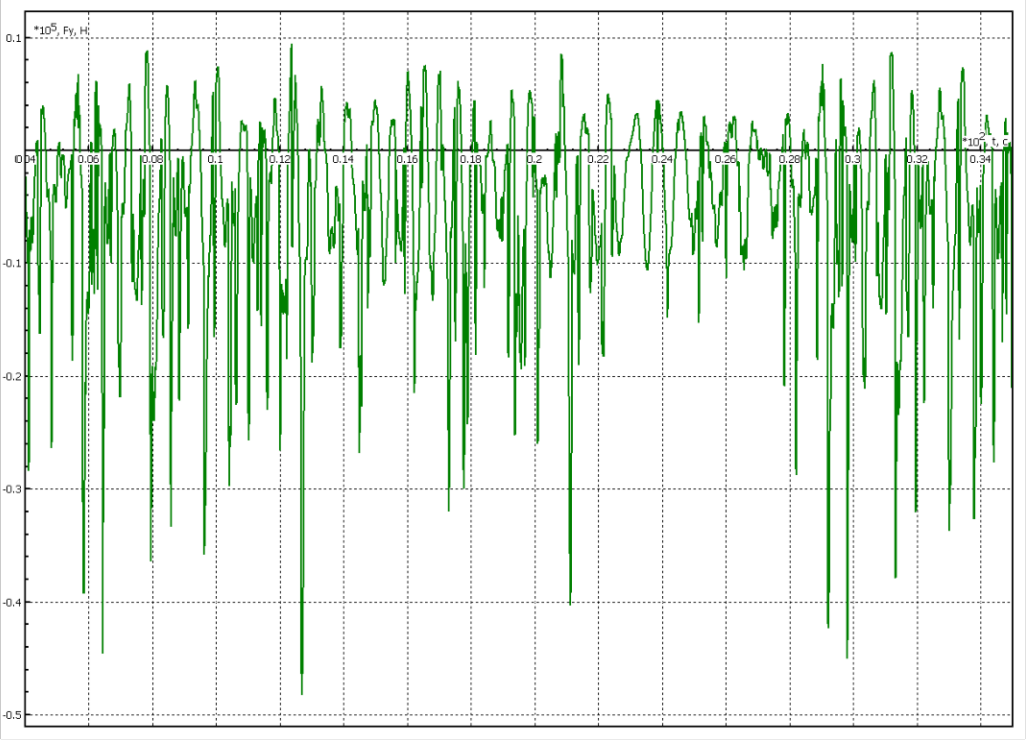

Figure 5.9 - Force oscillogram Fy_1l (left wheel of the first wheelset)

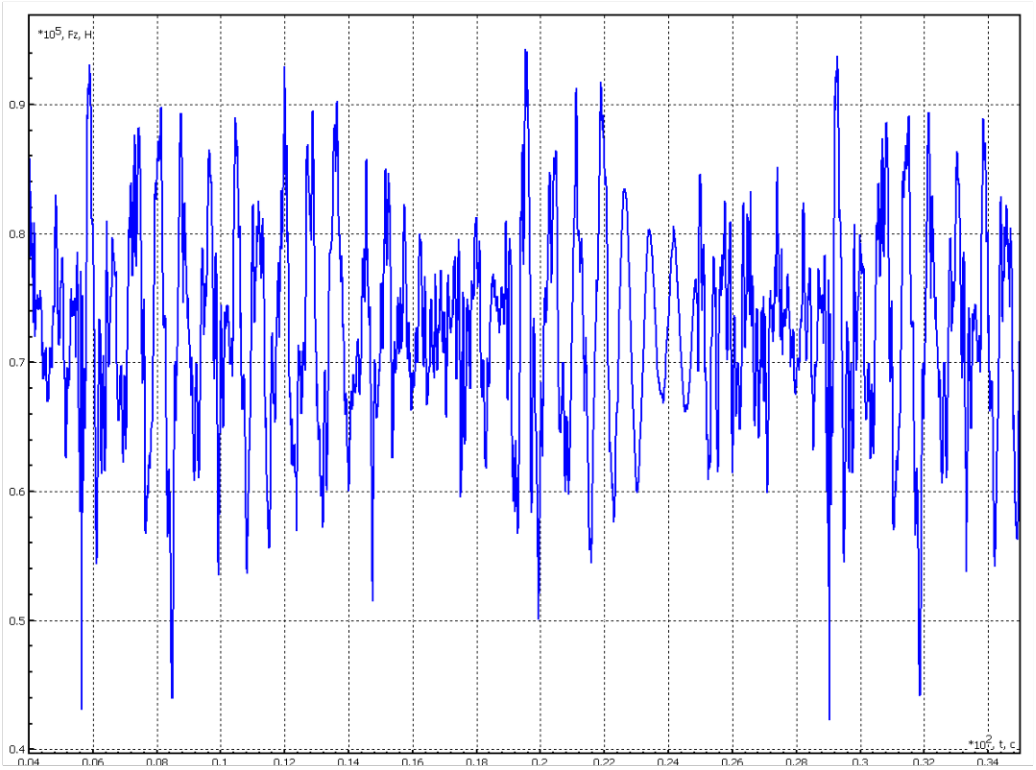

Figure 5.10 – Oscillogram of force Fz_1l (left wheel of the first wheelset)

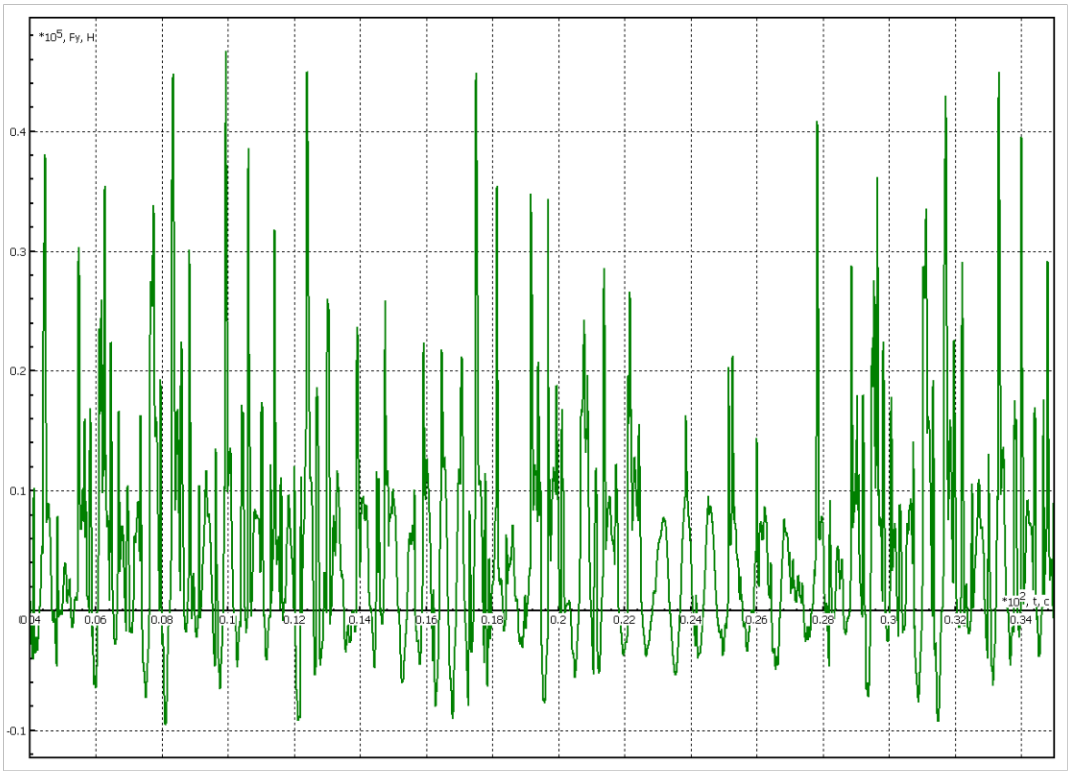

Figure 5.11 – Force oscillogram Fy_1r (right wheel of the first wheel pair)

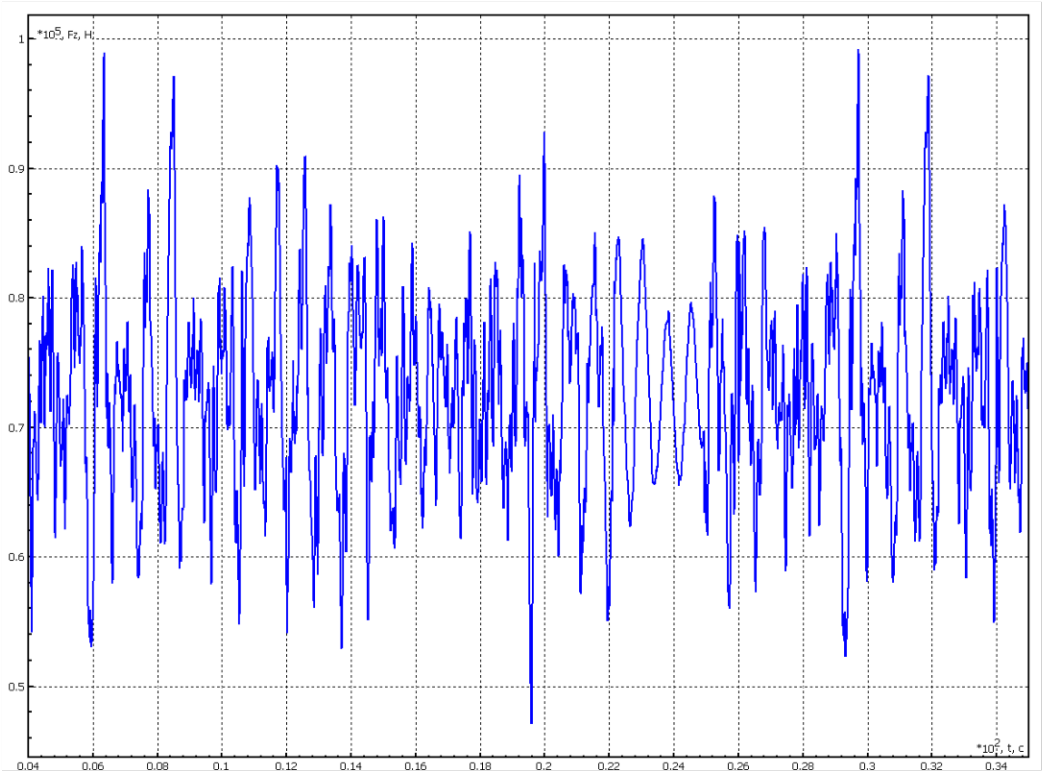

Figure 5.12 – Oscillogram of force Fz_1r (right wheel of the first wheel pair)

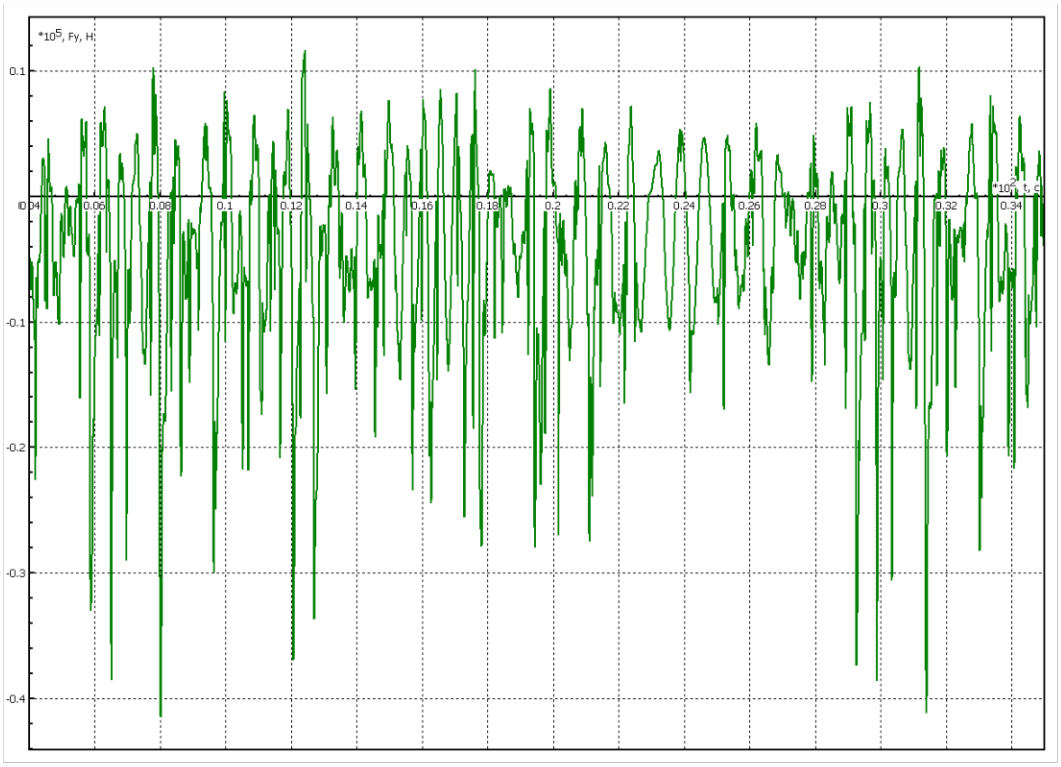

Figure 5.13 – Force oscillogram Fy_2l (left wheel of the second wheelset)

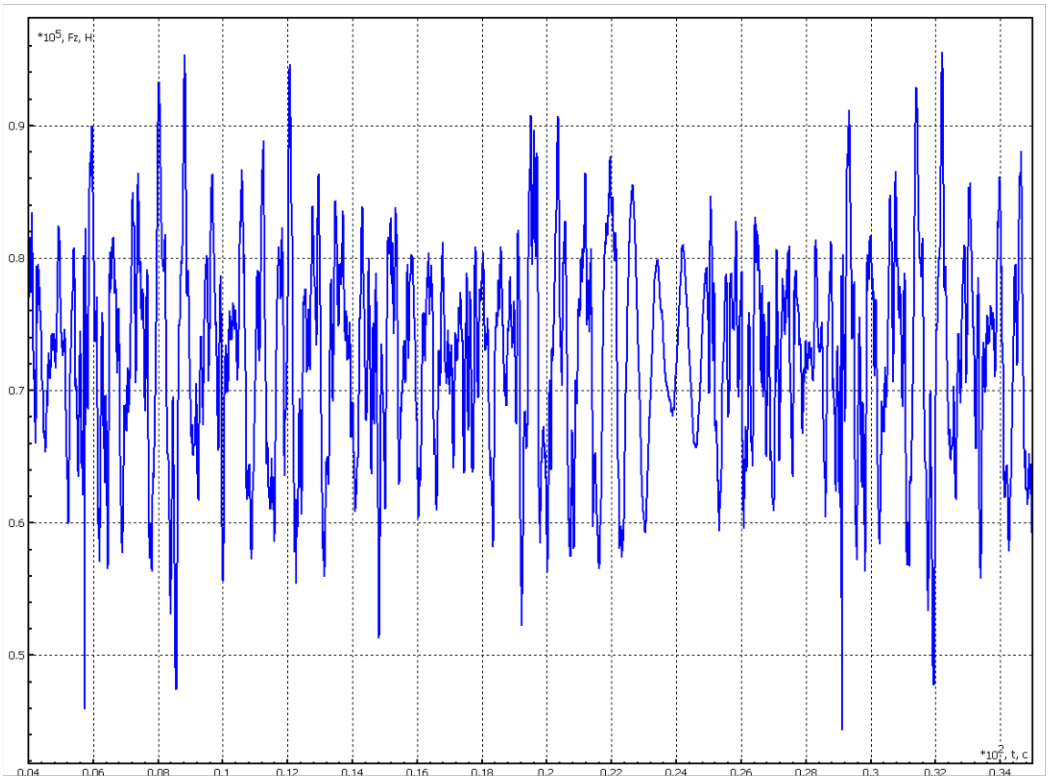

Figure 5.14 – Oscillogram of force Fz_2l (left wheel of the second wheelset)

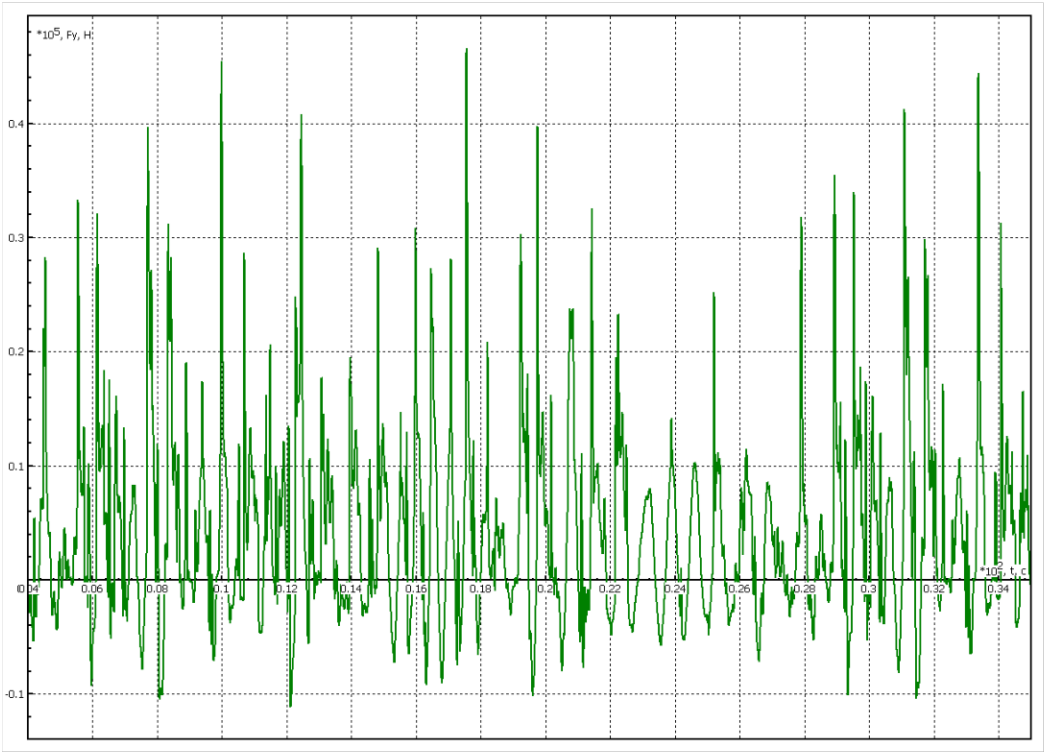

Figure 5.15 – Force oscillogram Fy_2r (right wheel of the second wheel pair)

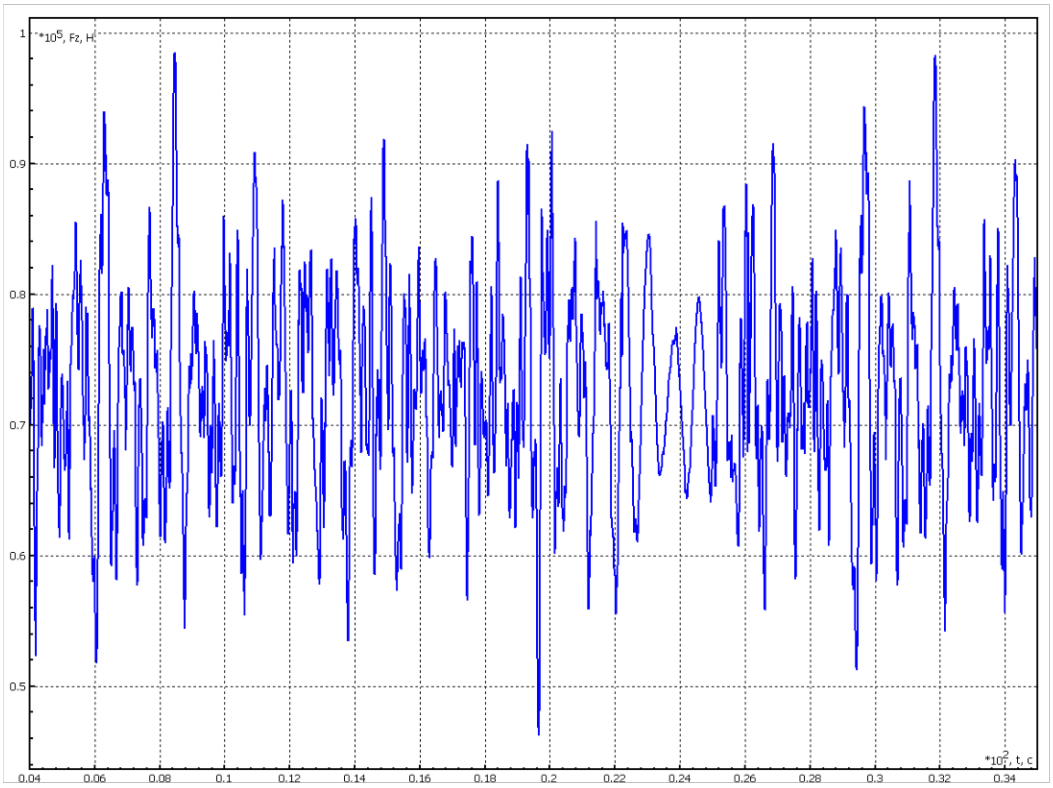

Figure 5.16 – Oscillogram of force Fz_2r (right wheel of the second wheel pair)

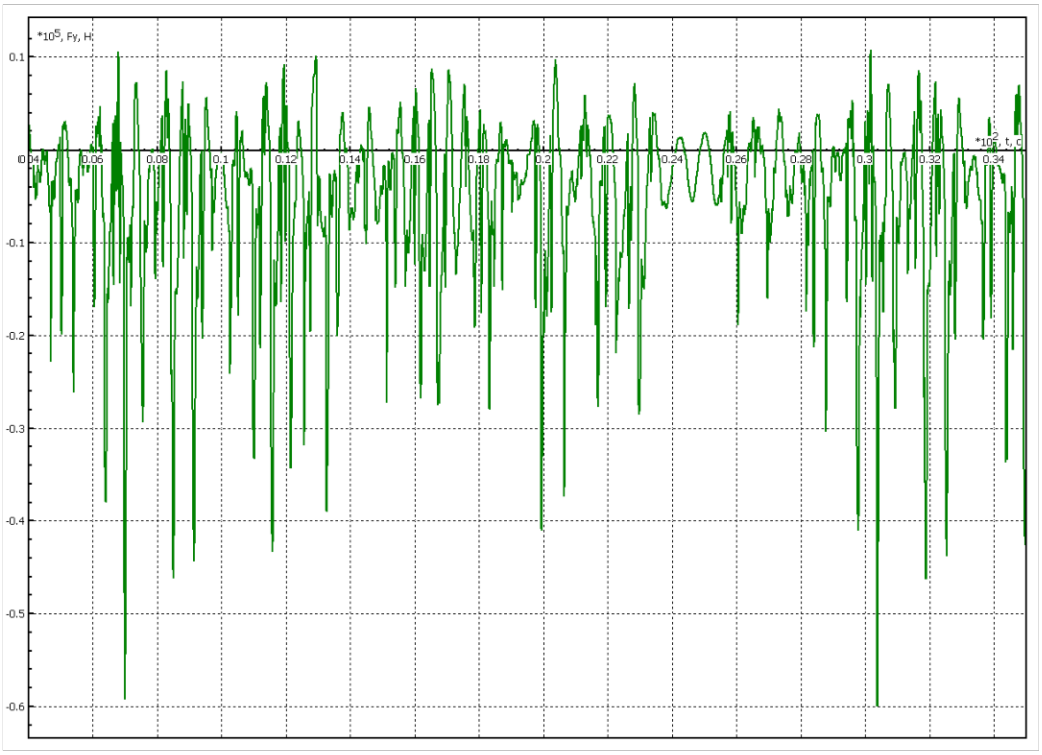

Figure 5.17 – Oscillogram of force Fy_3l (left wheel of the third wheel set)

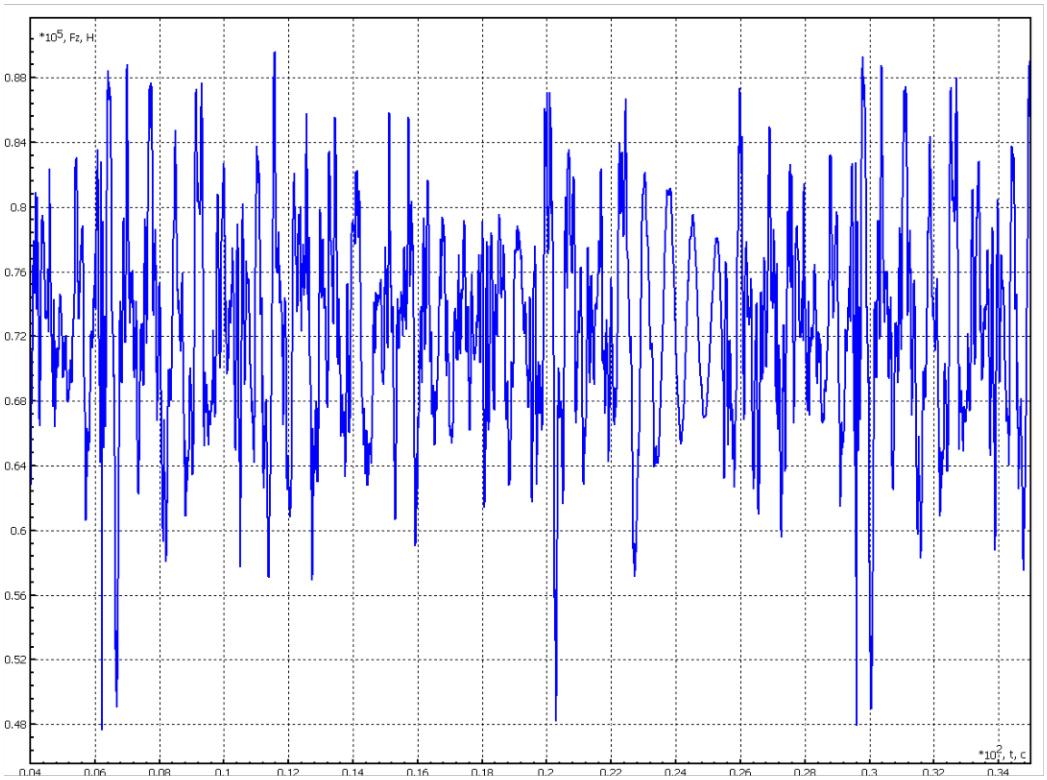

Figure 5.18 – Oscillogram of forces Fz_3l (left wheel of the third wheel set)

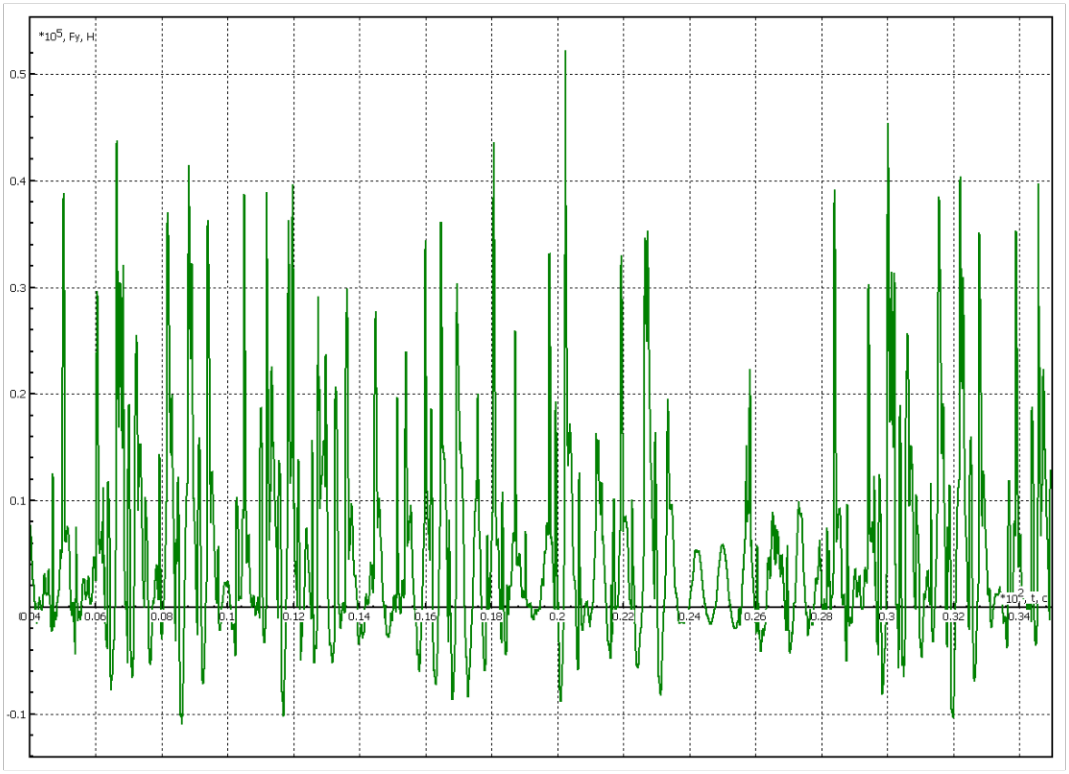

Figure 5.19 – Force oscillogram Fy_3r (left wheel of the third wheel set)

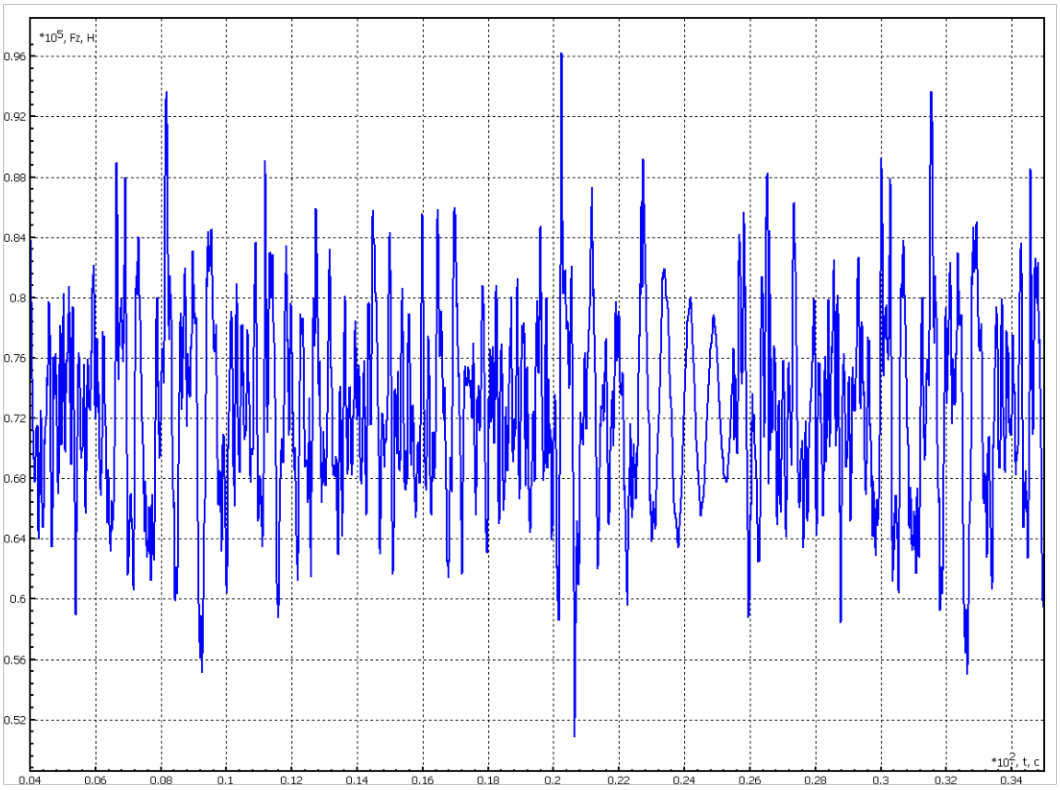

Figure 5.20 – Oscillogram of force Fz_3r (right wheel of the third wheel set)

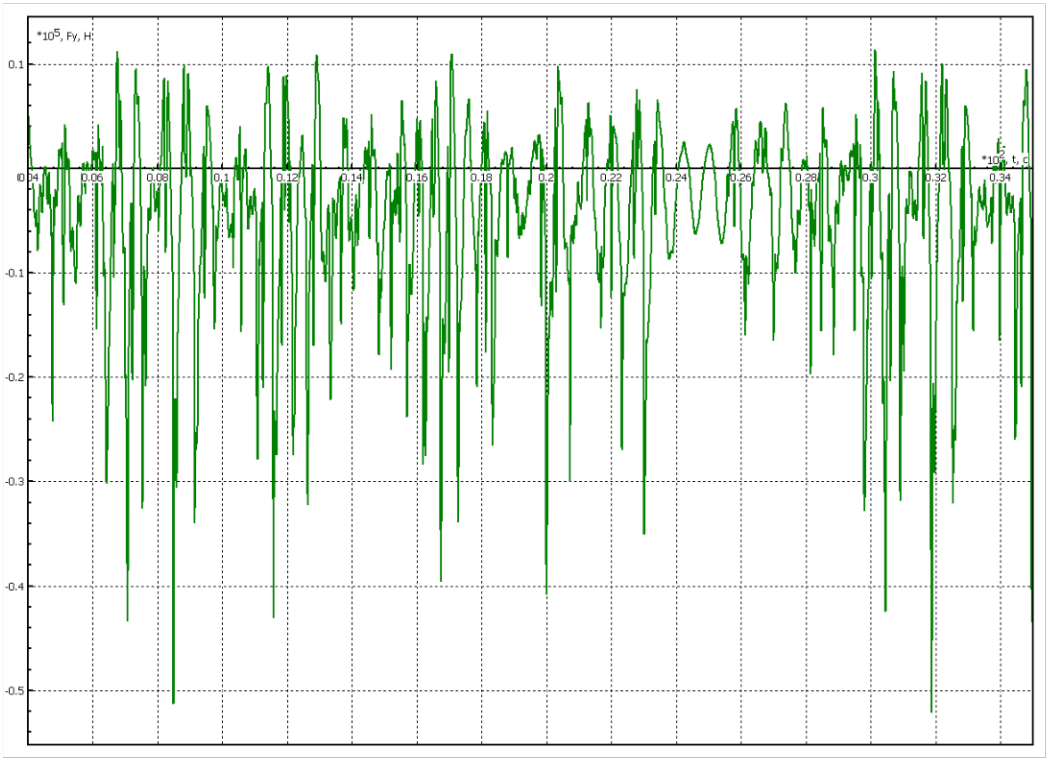

Figure 5.21 – Oscillogram of force Fy_4l (left wheel of the fourth wheel set)

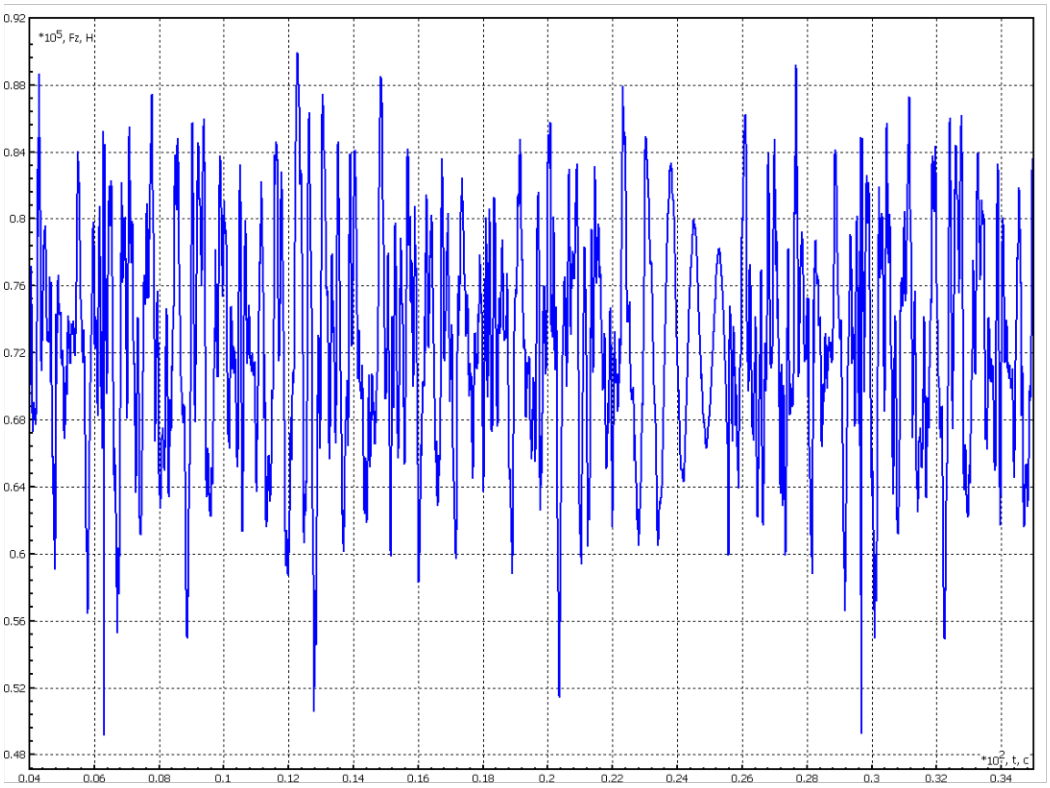

Figure 5.22 – Oscillogram of force Fz_4l (left wheel of the fourth wheel set)

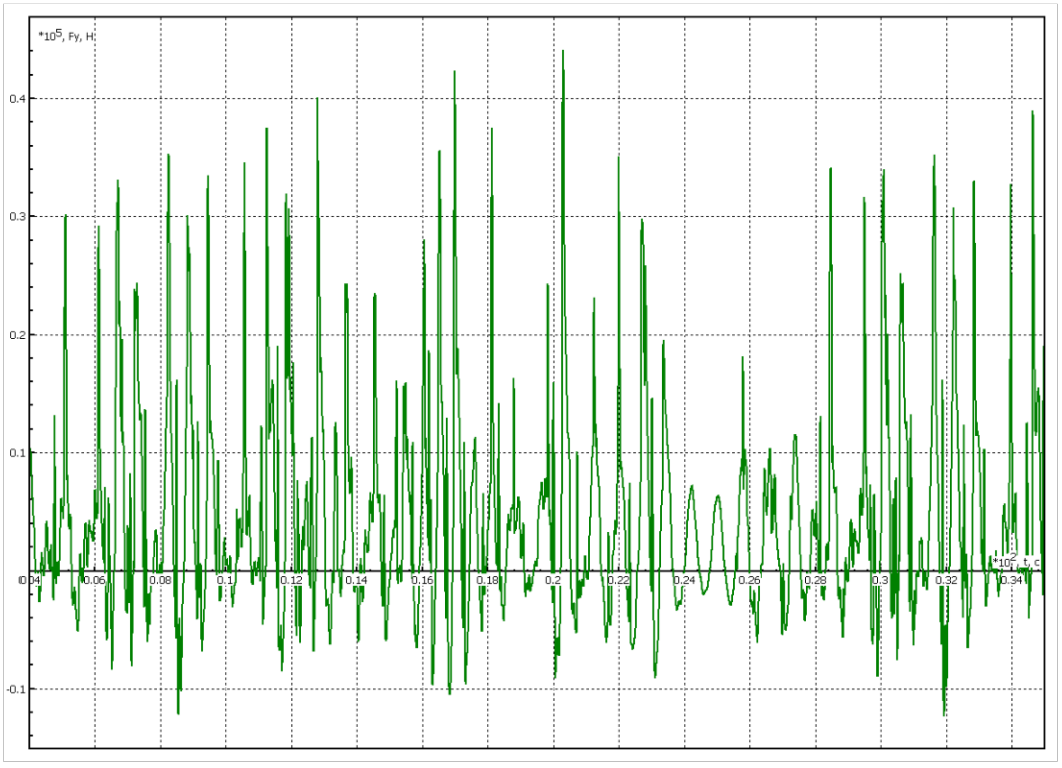

Figure 5.23 – Force oscillogram Fy_4r (right wheel of the fourth wheel set)

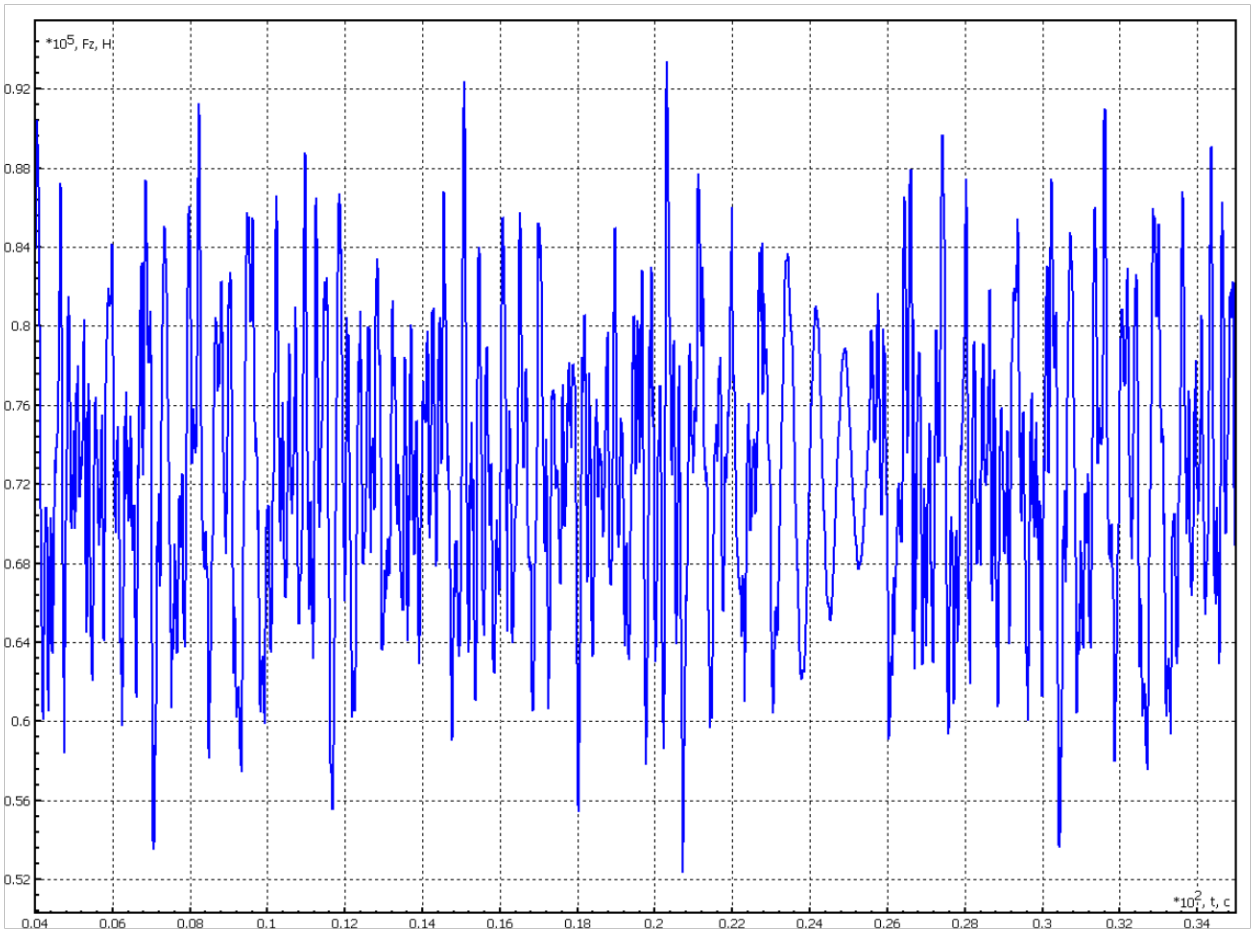

Figure 5.24 – Oscillogram of force Fz_4r (right wheel of the fourth wheel set)

Implementations similar to those given above were subjected to statistical processing. The results of statistical processing are summarized in tables 5.3 and 5.4.

Table 5.3 - Statistical characteristics of the transverse forces of interaction between wheels and rails

Pair of wheels	Wheel	Output ID	Standard deviations, kN / Mathematical hope, kN / Travel speed, km/h				
			36	72	108	144	180
CP No. 1	Lev	Fy_1l	4.93	5.75	8.44	17.15	19.58
			-3.4	-3.97	-5.08	-8.56	-9.18
	Right	Fy_1r	4.81	5.98	8.71	17.94	19.75
			3.42	3.97	5.04	8.80	9.22
CP No. 2	Lev	Fy_2l	3.24	4.51	7.87	19.38	22.87
			-2.34	-3.18	-4.29	-9.60	-11.47
	Right	Fy_2r	3.17	4.91	8.23	19.94	23.02
			2.34	3.20	4.26	9.67	11.37
CP No. 3	Lev	Fy_3l	4.87	5.16	9.31	17.85	19.47
			-3.20	-3.63	-5.23	-8.99	-8.89
	Right	Fy_3r	4.69	5.18	9.21	18.21	19.06
			3.17	3.66	5.23	9.14	8.90
CP No. 4	Lev	Fy_4l	3.23	3.84	8.57	20.17	22.45
			-2.25	-2.83	-4.40	-10.15	-10.76
	Right	Fy_4r	3.14	4.12	8.72	20.26	22.10
			2.30	2.80	4.45	10.18	10.60

Table 5.4 - Statistical characteristics of vertical forces of interaction between wheels and rails

Pair of wheels	Wheel	Output ID	Standard deviations, kN / Mathematical hope, kN / Travel speed, km/h				
			36	72	108	144	180
CP No. 1	Lev	Fz_1l	5.23	5.43	7.96	10.01	15.50
			72.45	72.51	72.53	72.49	72.58
	Right	Fz_1r	5.37	5.86	7.70	10.52	15.45
			72.68	72.64	72.58	72.75	72.68
CP No. 2	Lev	Fz_2l	4.25	4.52	7.78	11.45	17.43
			72.58	72.54	72.54	72.55	72.56
	Right	Fz_2r	4.28	4.99	7.87	12.08	17.57
			72.59	72.62	72.59	72.64	72.55
CP No. 3	Lev	Fz_3l	5.11	4.66	6.36	9.86	15.04
			72.48	72.48	72.53	72.52	72.51
	Right	Fz_3r	5.20	4.99	6.25	10.32	15.42
			72.64	72.65	72.62	72.63	72.66
CP No. 4	Lev	Fz_4l	4.18	4.92	6.66	11.27	16.61
			72.45	72.54	72.53	72.53	72.52
	Right	Fz_4r	4.31	5.25	6.92	11.92	17.40
			72.71	72.60	72.67	72.55	72.54

Maximum values of the studied quantities x_{max} are determined by the expression:

$$x_{max} = \bar{x} + k*s,$$

where $\bar{x}$ - expected value; s – standard deviation; k – coefficient depending on the specified confidence level. For the magnitudes of interaction forces between wheels and rails, which are important for assessing traffic safety, $k = 3$.

Tables 5.5 and 5.6 show the maximum values of the interaction forces between wheels and rails.

Table 5.5 – Maximum values of forces acting in the "wheel-rack" contact in the transverse direction

Pair of wheels	Wheel	Output ID	Maximum force value kN				
			Travel speed, km/h				
			36	72	108	144	180
CP No. 1	Lev	Fy_1l	18.19	21.22	30.4	60.01	67.92
	Right	Fy_1r	17.85	21.91	31.17	62.62	68.47
CP No. 2	Lev	Fy_2l	12.06	16.71	27.9	67.74	80.08
	Right	Fy_2r	11.85	17.93	28.95	69.49	80.43
CP No. 3	Lev	Fy_3l	17.81	19.11	33.16	62.54	67.3
	Right	Fy_3r	17.24	19.2	32.86	63.77	66.08
CP No. 4	Lev	Fy_4l	11.94	14.35	30.11	70.66	78.11
	Right	Fy_4r	11.72	15.16	30.61	70.96	76.9

Table 5.6 – Maximum values of forces acting in the "wheel-rack" contact in the vertical direction

Pair of wheels	Wheel	Output ID	Maximum force value kN				
			Travel speed, km/h				
			36	72	108	144	180
CP No. 1	Lev	Fz_1l	88.14	88.8	96.41	102.52	119.08
	Right	Fz_1r	88.79	90.22	95.68	104.31	119.03
CP No. 2	Lev	Fz_2l	85.33	86.1	95.88	106.9	124.85
	Right	Fz_2r	85.43	87.59	96.2	108.88	125.26
CP No. 3	Lev	Fz_3l	87.81	86.46	91.61	102.1	117.63
	Right	Fz_3r	88.24	87.62	91.37	103.59	118.92
No. 4	Lev	Fz_4l	84.99	87.3	92.51	106.34	122.35
	Right	Fz_4r	85.64	88.35	93.43	108.31	124.74

As can be seen from the data in Table 5.5, the level of horizontal forces of interaction between wheels and rails increases with increasing speed. At the same time, as V increases to 144 km/h, the values of horizontal forces approach the value of static overload from the wheel to the rail, and at V = 180 km/h the forces from the wheels of the second and fourth wheel pairs exceed this value.

The data in Table 5.6 shows that the dynamic additions of vertical forces of interaction between wheels and rails at V = 108 km/h amount to 30% of the static load, at V = 144 km/h – 50%, and at V = 180 km/h they reach 75%.

5.2.1 Calculations of the stress-strain state of wheels with determination of zones of sensitivity to the action of contact forces for the placement of strain gauges.

One of the important aspects in the system of direct measurement of contact interaction forces between wheels and rails is the determination of zones of deformation sensitivity of wheel disks from the action of vertical and lateral forces. From certain zones, it is important to localize such deformations in which they were a consequence of the action of forces in one direction.

To determine these zones, a finite element calculation was performed for three design schemes:

- vertical load of the wheel pair;
- loading by vertical forces and forces from the action of the loading system;
- loading of the wheel pair by vertical and horizontal forces when passing curved sections of the track.

Below are the results of calculations of the SSS characteristics for given wheel pair loading schemes.

Vertical load. Based on the research objective, in order to ensure greater clarity of the results, the maximum value in the diagram legend was reduced to 10 MPa, since these are the stresses that arise on the wheel disk.

Figure 5.25 shows the distribution of design stresses in the wheel pair elements under the action of a vertical load. Apparently, the greatest stresses arise in the wheel disk at the point of transition of the disk to the hub part of the wheel and amount to 7.78 MPa, as well as in the fillet transition between the neck and the pre-wrap part - 46 MPa.

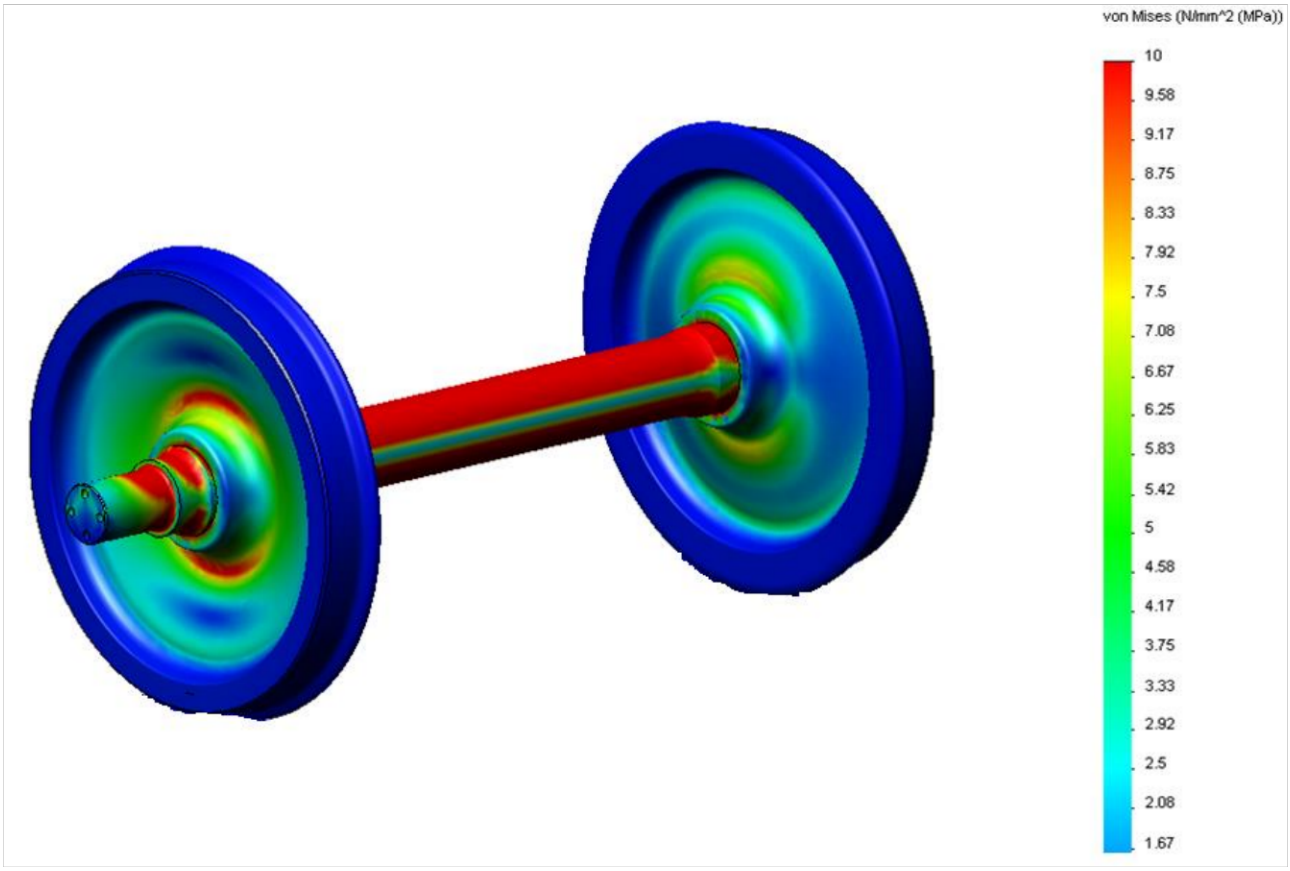

Figure 5.25 – Diagram of equivalent stresses, occurring in a wheel pair under vertical load

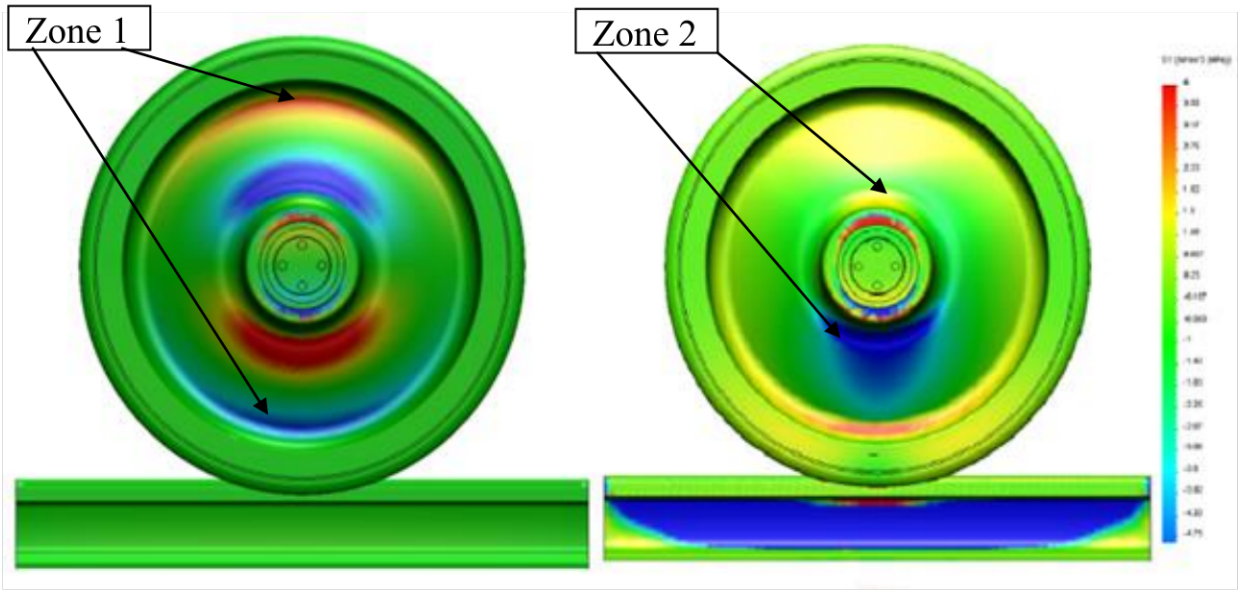

Figure 5.26 – Chart of wheel surface stresses under vertical load.

Figure 5.27 The graph of the surface stresses of the wheel under vertical load and under the simultaneous action of vertical and lateral forces.

The results of the calculation of the distribution of surface stresses of the wheel under vertical load (Fig. 5.26) and simultaneous action of vertical and lateral forces (Fig. 5.27) are presented. As can be seen, the greatest stresses in the wheel disc under vertical load occur in the transition zone of the disc to the rim (zone I), as well as in the place adjacent to the hub (zone III). In the case of lateral loading, deformations spread to the middle part of the disk (zone II) near the area of attachment to the hub.

Thus, according to the results of VAT calculations of the wheel disc, zone III was the most sensitive in terms of deformations to both vertical and lateral loads. Therefore, for lateral load measurement, zone II should be chosen, which is practically sensitive only to lateral forces, and zone I should be chosen for vertical load measurement.

5.3 Practical study of the direct measurement method of the interaction forces of the wheels with rails

Experiments on direct measurement of forces in the wheel-rack system were carried out on the wheel pair of a bogie of the KVN-TsNII-M type of a gauge-measuring wagon equipped on the basis of a passenger wagon (Fig. 5.28).



Figure 5.28 – Bogie type KVN-TsNII-M with experimental PKP

Experimental tests were carried out on the section of the track between the Kyiv-Pasazhyrsky and Kyiv-Volynsky stations (Figure 5.29). The position of the wagon on the site and the speed of movement were determined using GPS-Logger. GPS polling was carried out once per second.

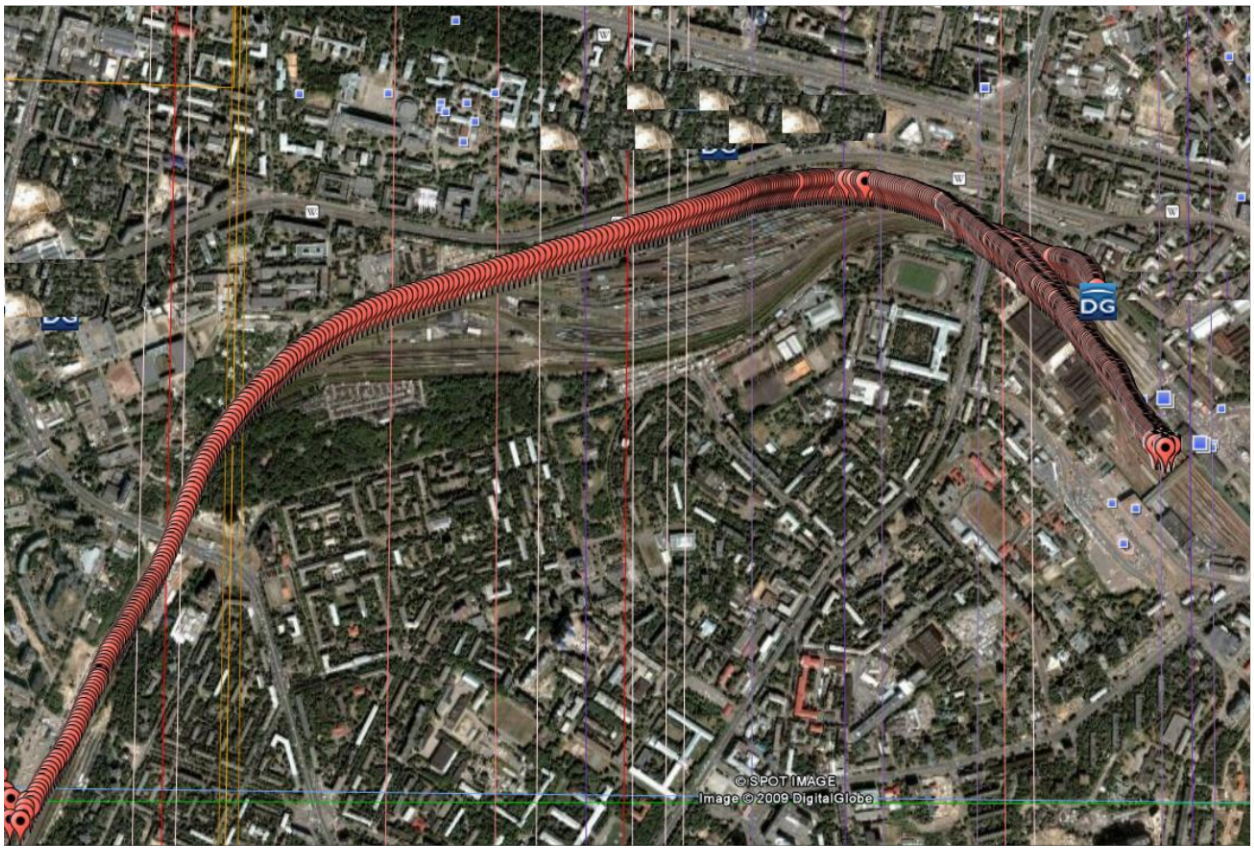

Figure 5.29 – Satellite view of the area where the experimental studies took place

On the wheel of the specified bogie, according to the diagram (Fig. 5.30), markings and installation of strain gauges were carried out. After installing the strain gauges on the wheel disk, the measuring circuits were installed and protected from external influences. Measuring equipment and batteries were installed on the wheelset axle using special fasteners.

To establish the relationship between the readings of the strain gauge circuits and the load in the vertical direction, the measuring system was calibrated.



Figure 5.30 – Installation of measuring circuits

The lateral load of the wheel pair was carried out using a hydraulic jack and a tipping device (Fig. 5.32).



Figure 5.32 – Taring with horizontal load

The position of the wagon on the site and the speed of movement were determined using GPS-Logger. GPS polling was carried out once per second.

Registration of strain gauge data was carried out using a software and hardware complex consisting of hardware based on the NI cRIO 9012 controller, an eight-day NI cRIO 9104 chassis with NI9237 modules and a software-virtual recorder developed in the LabView 8.6 software shell.

The software of the complex performs the following functions:

- configuration of measuring channels;
- selection of strain gauge connection diagram;
- autonomous recording of signals to an internal FLASH drive;
- writing data to a text file (for subsequent processing).

The signals were recorded onto a local FLASH drive. Figures 5.33 and 5.34 show a complete record of the forces that arose during the test trip.

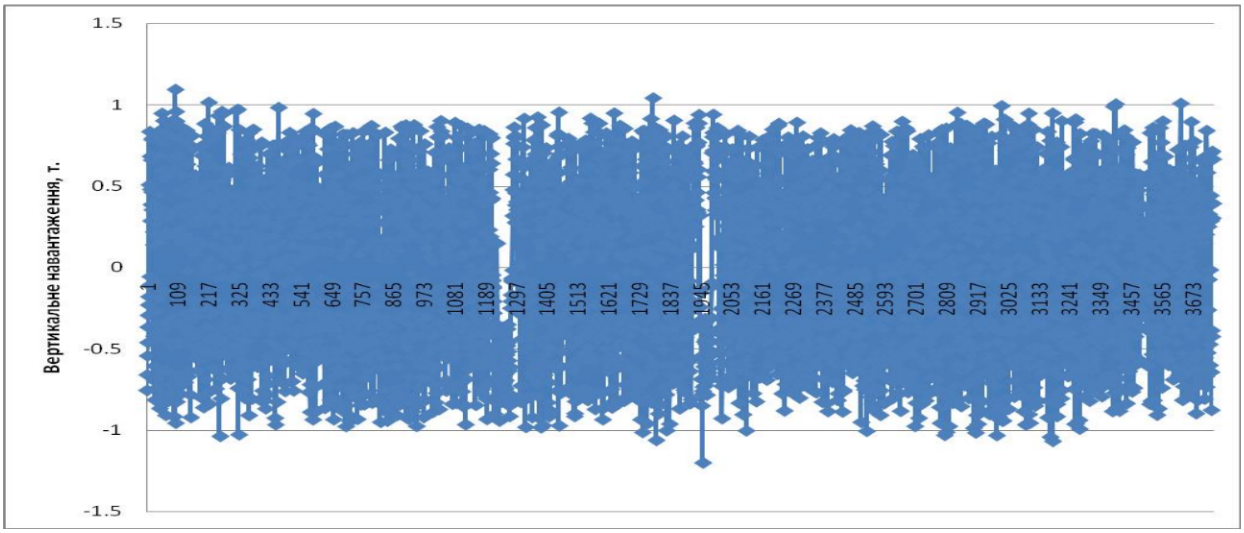

Figure 5.33 – Recording vertical forces

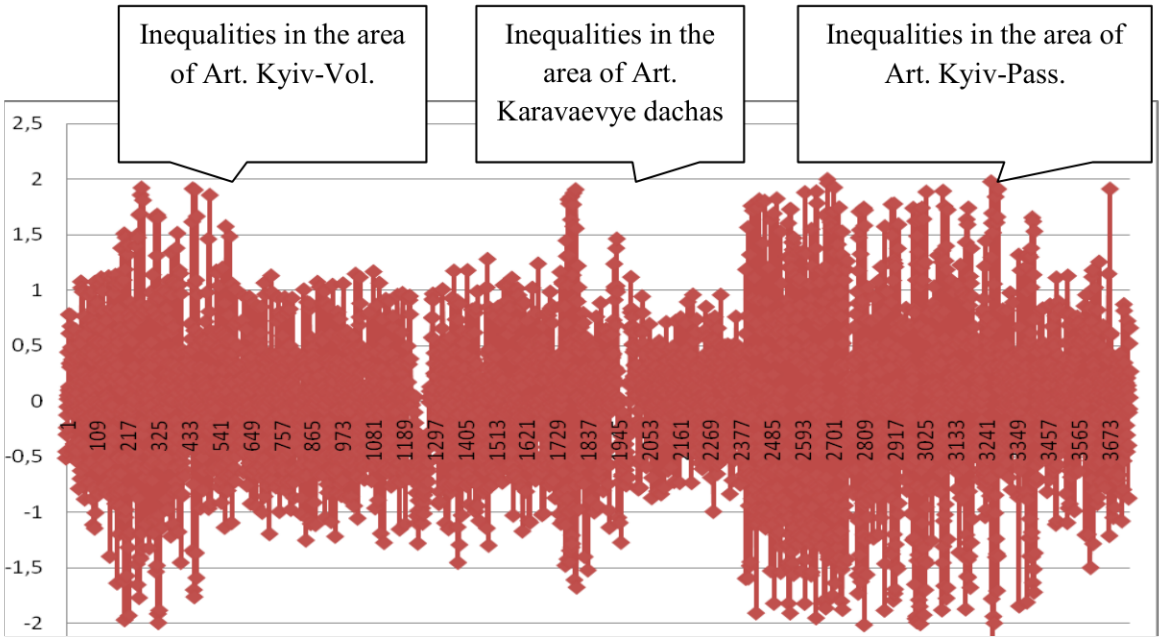

Figure 5.34 – Recording horizontal forces

Figures 5.35 and 5.36 show fragments of recording processes of vertical and lateral loads at a speed of 36 km/h.

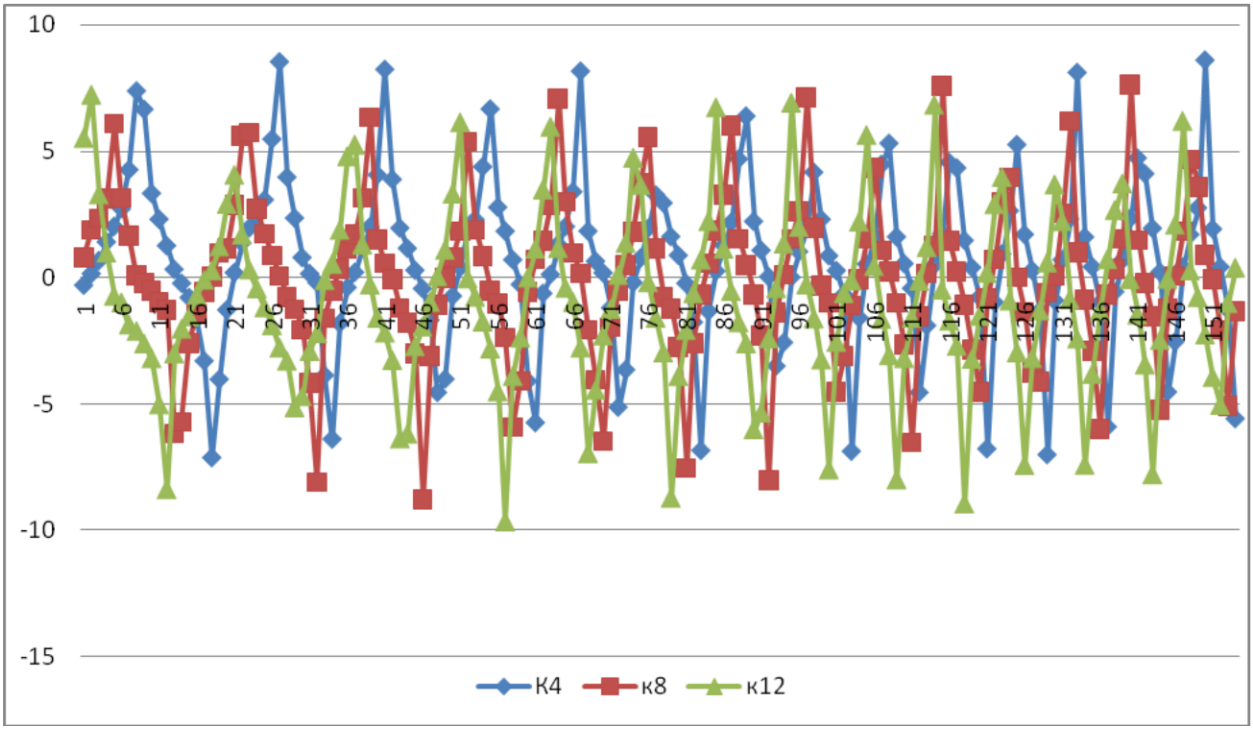

Figure 5.35 – Fragment of vertical load recording

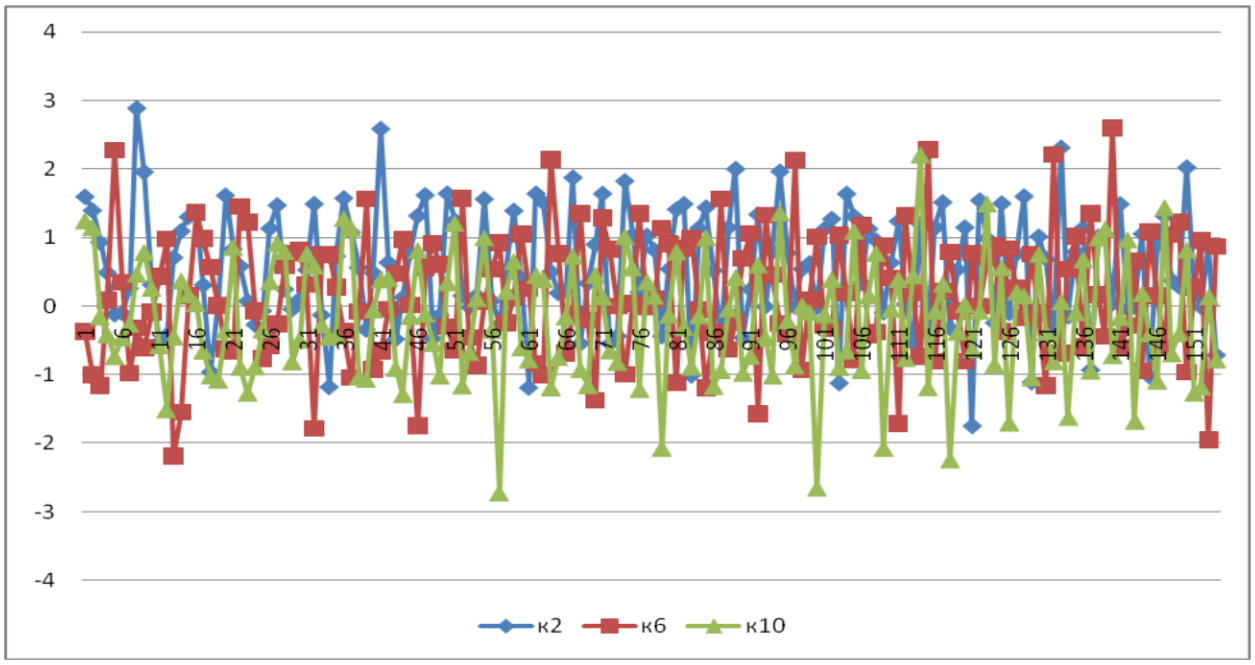

Figure 5.36 – Fragment of lateral load recording

Based on the results of calibration, calculations and experimental studies of the stress-strain state of wheel disks, the actual value of the interaction forces was determined from the readings of sensors that were in a vertical position relative to the track plan.

Based on the developed algorithm, the contact forces that arose during the experimental trip were obtained. Representative parts of records of dynamic processes at V = 36 km/h were subjected to statistical processing. The results of this processing are shown in Table 3.1. Here the maximum values of the studied quantity are determined by the expression:$\overline{x}_{max}$

$$\overline{x}_{max} = \overline{x} + ks, \qquad (5.1)$$

Where $\overline{x}$– arithmetic mean (mathematical expectation);

s – standard deviation (RMS);

k– coefficient depending on the given confidence level.

For quantities ΣY and Y/Q, which are important for assessing traffic safety, k=3, for other calculated values k = 2.2, except for quasi-static ones, for which k=0. Since the values of contact forces are important for assessing traffic safety, they are assumed to be equal to three.k

Table 5.7 – Results of statistical processing of contact force values

Estimation of magnitude	Q, transport	Y, transport
SLE	0.47	0.33
Maximum value	9.77	0.99

5.3.1 Determination of interaction forces by computer modeling of the motion dynamics of a track measuring wagon

Computer model of the dynamics of a passenger wagon, on the basis of which the wheel gauge is equipped, developed in the "Universal Mechanism" software package. The dynamic model of the wagon is represented by a spatial system of rigid bodies connected by elastic and dissipative elements. To develop graphic images of the wagons structural elements, 3D models of them were developed using the Compass package.

The wagons motion dynamics model was developed taking into account its design features and is a system composed of 41 rigid bodies, 24 linear, four contact, 20 bipolar and four special force elements simulating dry friction units. The hierarchical structure of the model made it possible to significantly simplify the process of its creation and at the same time avoid implicit errors when entering parameter values due to the use of similar identification of parameters in identical subsystems. The characteristic features of the model include the accuracy of conveying the geometry of the design of their analogues and advanced parameterization and identification of system elements.

The general model of the dynamics of a passenger wagon in structure (Fig. 3.37) consists of a body (K), two bolsters (NB) with boiler side (K) and non-boiler

side (NK) and two bogie subsystems - “Boiler side bogie” and “Non-boiler side bogie” sides." In turn, these subsystems include separate bodies of the bogie frame (RB), elements of the central cradle suspension (CLS) and the brake linkage (GVS), elastic-dissipative elements (EDE), as well as two subsystems of wheel pairs (WPS) with axle boxes. nodes (BV). The connections between the bodies are modeled by the corresponding force elements.

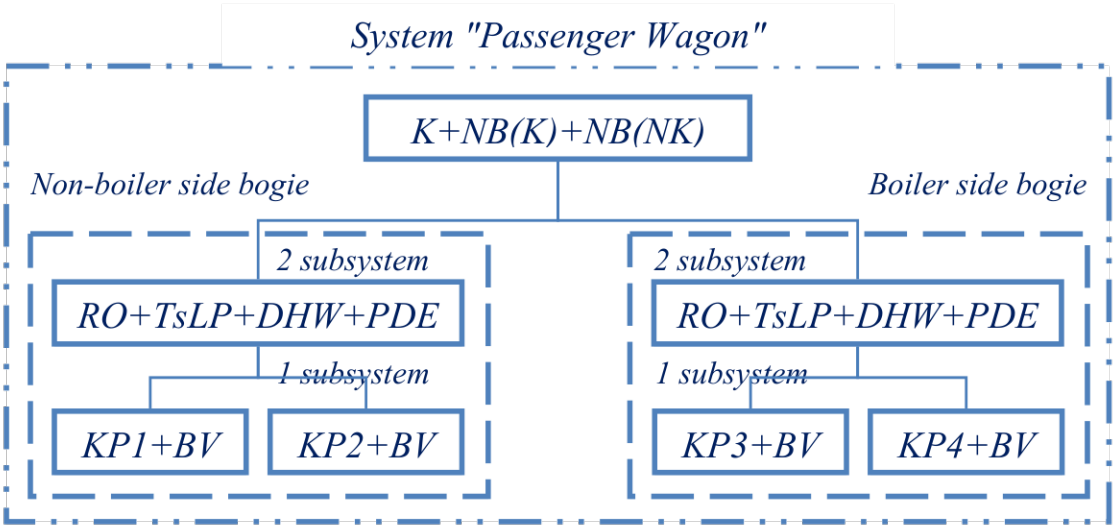

Figure 5.37 – Subsystems of a computer model of a passenger wagon:
K – body; RK – body frame; NB(K), NB(NK) – bolster of the boiler and non-boiler sides of the wagon, respectively; RO – bogie frame;
TsLP – central tube suspension; DHW – brake lever suspension;
PDE – elastic-dissipative elements; KP1,2,3,4 – wheel pairs;
BV – axle box units

Using the developed computer model of wagon dynamics, calculations were made to determine the forces of interaction between wheels and rails based on the level and nature of the change over time. The movement of a wagon along a straight track with real irregularities at speeds of 36, 72, 108, 144 and 180 km/h is considered. All obtained implementations were subjected to statistical processing. The processing results are summarized in Tables 5.8 and 5.9, where the numerator shows the values

of the hard currency coefficient, and the denominator shows the mathematical expectations.

Figures 5.38 and 5.39 show graphs of the dependence of the standard deviations (RMS) of the interaction forces between wheels and rails (Yi i Qi) on the speed of the wagon, constructed according to data from tables 5.8 and 5.9. Numbers 1...8 indicate wheel numbers.

Table 5.8 – Statistical characteristics of forces Y_i in kN

Pair of wheels	Wheel	Travel speed, km/h				
		36	72	108	144	180
CP No. 1	Lev	4.93	5.75	8.44	17.15	19.58
		-3.4	-3.97	-5.08	-8.56	-9.18
	Right	4.81	5.98	8.71	17.94	19.75
		3.42	3.97	5.04	8.80	9.22
CP No. 2	Lev	3.24	4.51	7.87	19.38	22.87
		-2.34	-3.18	-4.29	-9.60	-11.47
	Right	3.17	4.91	8.23	19.94	23.02
		2.34	3.20	4.26	9.67	11.37
CP No. 3	Lev	4.87	5.16	9.31	17.85	19.47
		-3.20	-3.63	-5.23	-8.99	-8.89
	Right	4.69	5.18	9.21	18.21	19.06
		3.17	3.66	5.23	9.14	8.90
CP No. 4	Lev	3.23	3.84	8.57	20.17	22.45
		-2.25	-2.83	-4.40	-10.15	-10.76
	Right	3.14	4.12	8.72	20.26	22.10
		2.30	2.80	4.45	10.18	10.60

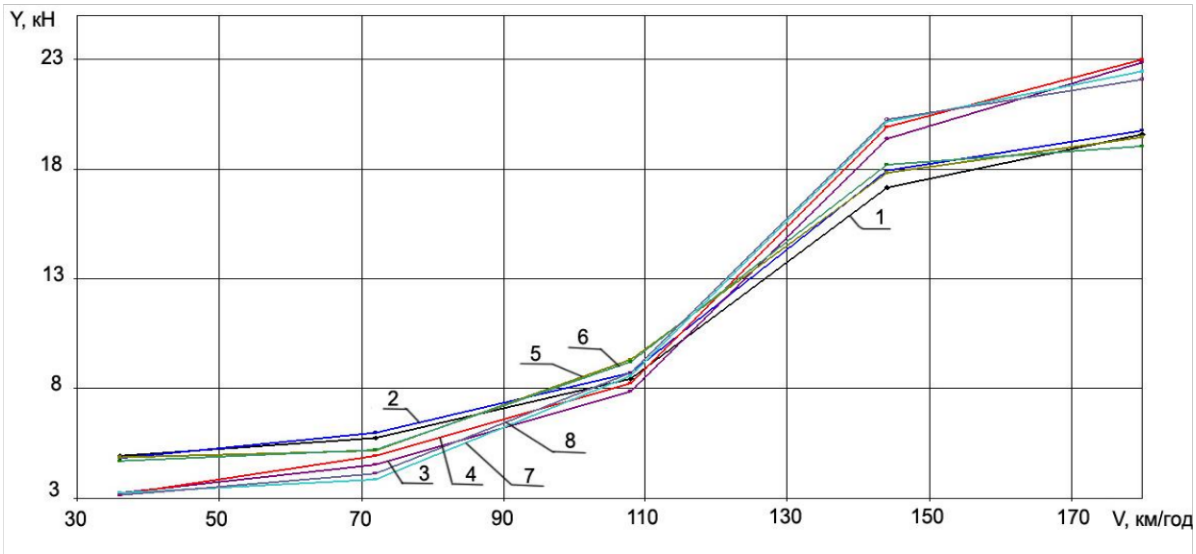

Figure 5.38 – SCR of horizontal interaction forces

Table 5.9 – Statistical properties of forces Qi in kN

Pair of wheels	Wheel	Travel speed, km/h				
		36	72	108	144	180
CP No. 1	Lev	5.23	5.43	7.96	10.01	15.50
		72.45	72.51	72.53	72.49	72.58
	Right	5.37	5.86	7.70	10.52	15.45
		72.68	72.64	72.58	72.75	72.68
CP No. 2	Lev	4.25	4.52	7.78	11.45	17.43
		72.58	72.54	72.54	72.55	72.56
	Right	4.28	4.99	7.87	12.08	17.57
		72.59	72.62	72.59	72.64	72.55
CP No. 3	Lev	5.11	4.66	6.36	9.86	15.04
		72.48	72.48	72.53	72.52	72.51
	Right	5.20	4.99	6.25	10.32	15.42
		72.64	72.65	72.62	72.63	72.66
CP No. 4	Lev	4.18	4.92	6.66	11.27	16.61
		72.45	72.54	72.53	72.53	72.52
	Right	4.31	5.25	6.92	11.92	17.40
		72.71	72.60	72.67	72.55	72.54

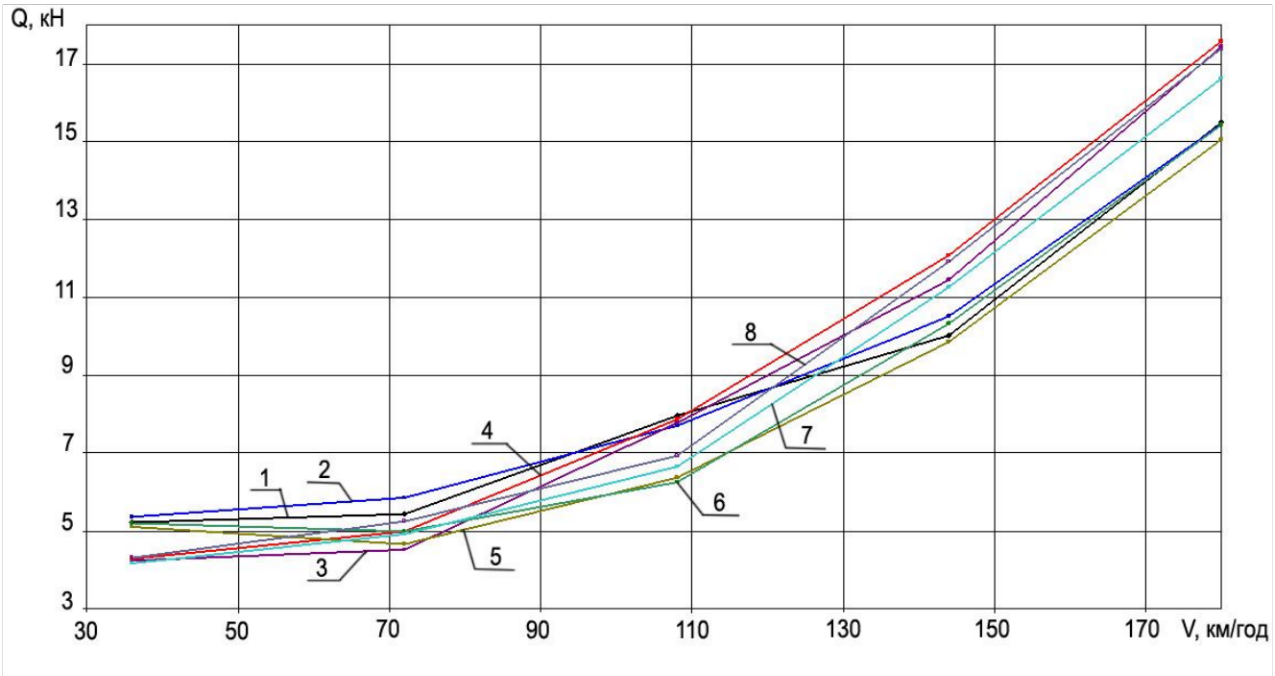

Figure 5.39 – SCR of vertical interaction forces

From the calculated data it follows that the SCR of horizontal forces intensively increases in the speed range of 108-144 km/h (Fig. 5.38), while the SCR of vertical forces (Fig. 5.39) smoothly increases with increasing speed of the wagon.

From a comparison of the SCR values obtained by computer modeling (Tables 5.8 and 5.9) and experiment (Table 5.7), it follows that the discrepancy for lateral load is 0.22%, and for vertical load – 9.34%. Thus, these data confirm, on the one hand, the reliability of the developed computer model, and on the other, the effectiveness of the proposed method for directly measuring the contact forces of interaction between wheels and rails.

Tables 5.10 and 5.11 show the maximum values of the interaction forces between wheels and rails, determined by expression (5.1).

Table 5.10 – Maximum values of forces Y_i, kN

Pair of wheels	Wheel	Travel speed, km/h				
		36	72	108	144	180
CP No. 1	Lev	18.19	21.22	30.4	60.01	67.92
	Right	17.85	21.91	31.17	62.62	68.47
CP No. 2	Lev	12.06	16.71	27.9	67.74	80.08
	Right	11.85	17.93	28.95	69.49	80.43
CP No. 3	Lev	17.81	19.11	33.16	62.54	67.3
	Right	17.24	19.2	32.86	63.77	66.08
CP No. 4	Lev	11.94	14.35	30.11	70.66	78.11
	Right	11.72	15.16	30.61	70.96	76.9

Table 5.11 – Maximum values of forces Q_i, kN

Pair of wheels	Wheel	Travel speed, km/h				
		36	72	108	144	180
CP No. 1	Lev	88.14	88.8	96.41	102.52	119.08
	Right	88.79	90.22	95.68	104.31	119.03
CP No. 2	Lev	85.33	86.1	95.88	106.9	124.85
	Right	85.43	87.59	96.2	108.88	125.26
CP No. 3	Lev	87.81	86.46	91.61	102.1	117.63
	Right	88.24	87.62	91.37	103.59	118.92
CP No. 4	Lev	84.99	87.3	92.51	106.34	122.35
	Right	85.64	88.35	93.43	108.31	124.74

According to estimates of the maximum values of the studied quantities, it follows that at v = 144 km/h the horizontal forces approach the value of the static load from the wheel on the rail (P0 = 64, kN), and at v = 180 km/h the forces Y2 and Y3 (from the wheels) second and fourth wheel pairs) exceed this value. Dynamic additions of vertical forces of interaction between wheels and rails at v = 108 km/h amount to 30% of the static load, at v = 144 km/h – 50%, and at v = 180 km/h they reach 75%.

5.4 Requirements for the system of direct measurement of the interaction forces of the wheel pairs with rails

During operation, rolling stock units, like any complex technical systems, are prone to failures, the reasons for which may be: violation of the manufacturing technology of individual elements, difficult operating conditions, non-compliance with the norms of technological processes for loading, unloading and transporting goods, aging and wear of components. Therefore, an important and urgent task is the introduction of periodic control tests and dynamic diagnostics of rolling stock units on the Ukrainian railways throughout their entire life cycle.

Modern trends in the development of measuring technology provide ample opportunities for the implementation of new instrumental approaches for assessing dynamic qualities, safety conditions for train traffic and promptly taking measures to prevent emergency situations. Taking into account the successful experience of implementing diagnostic systems for the undercarriage of passenger wagons and locomotives, there is a need to further improve the means and methods for experimental assessment of driving dynamics and safety indicators throughout the entire life cycle of rolling stock.

5.4.1 Characteristics and components of the mobile software and hardware complex

Development of a mobile software and hardware complex(hereinafter PAK)For control running tests and dynamic diagnostics of rolling stock units, it is based on a set of requirements formed based on the results of an analysis of the regulatory framework and modern measuring instruments used on the railways of European countries.

Mobile system for Determination of the dynamic load of rolling stock chassis in operation should consist of primary transducers, a global positioning system

receiver, analog signal transmission lines, subsystems for collecting measurement information, determination of traffic safety indicators in express processing mode, determination of the comfort level, determination of ride smoothness, determination of dynamic stress.

The primary transducers should be strain gauges, low-frequency accelerometers and displacement sensors. Analog signal transmission lines are cables that provide connection between primary transducers and recording devices with an operating voltage of up to 10 V and are components of the measuring system. Cables must be shielded, resistant to oils, have at least six cores, cable flexibility must correspond to class 1 or 2 and not change its properties at temperatures from minus 40°C to plus 80°C.

The mobile system must provide the ability to autonomously conduct control tests of dynamic diagnostics of rolling stock units in order to determine the load of the running gear, as the main component of checking the quality of capital repairs (CVR), assessing the residual life of load-bearing structures, and performing control tests as part of work to extend the assigned period service and determination of the load of chassis under operating conditions of rolling stock.

During control sea trials, the following quantities are recorded: dynamic applications of vertical movements occurring in the central and axle box suspension; vertical and horizontal transverse accelerations of bogie frames and wagonbody; dynamic application of stresses in dangerous sections of the body frame and bogie frames under different driving modes.

The mobile system should consist of hardware based on the CompactRIO platform and software written in the graphical programming language G in the LabVIEW (Laboratory Virtual Instrumentation Engineering Workbench) software package from National Instruments (USA). The software consists entirely of the following subsystems:

a) collecting measurement information;

b) determining the level of comfort;

c) determination of smoothness;

d) determination of traffic safety indicators in express processing mode.

5.4.2 Hardware

A mobile system for control road tests and dynamic diagnostics of rolling stock units based on the National Instruments CompactRIO platform allows you to solve a wide range of problems related to monitoring the technical condition of vehicles both under test conditions and in normal operating modes.

The system implements two functional options: assessing strength and safety indicators in real time, as well as performing measurements of physical quantities (displacement, acceleration, deformation) in an offline black box mode with subsequent statistical processing (Fig. 5.40). In addition, to analyze the influence of movement speed on changes in controlled parameters, obtain precise time signals and determine current coordinates, data obtained using a GPS receiver module with a sampling frequency of up to 8 Hz is used.

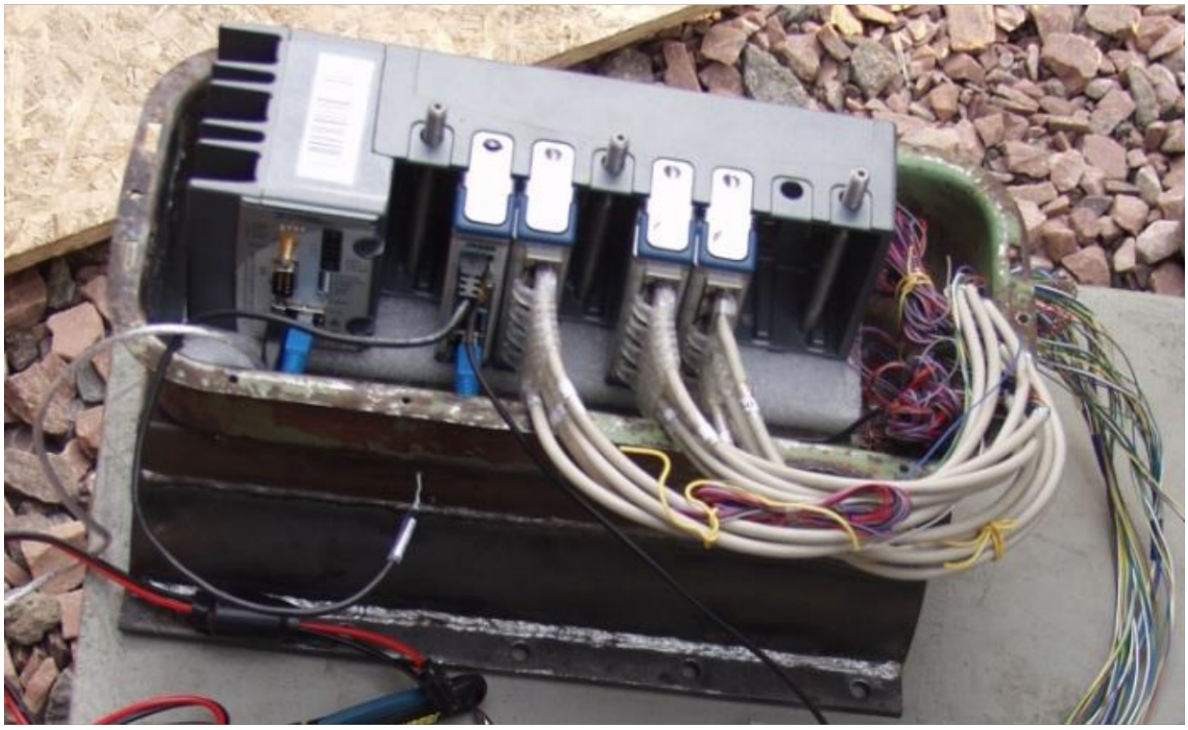

Figure 5.40 – Using the mobile system in offline mode

The general block diagram of the mobile system is shown in Figure 5.41.

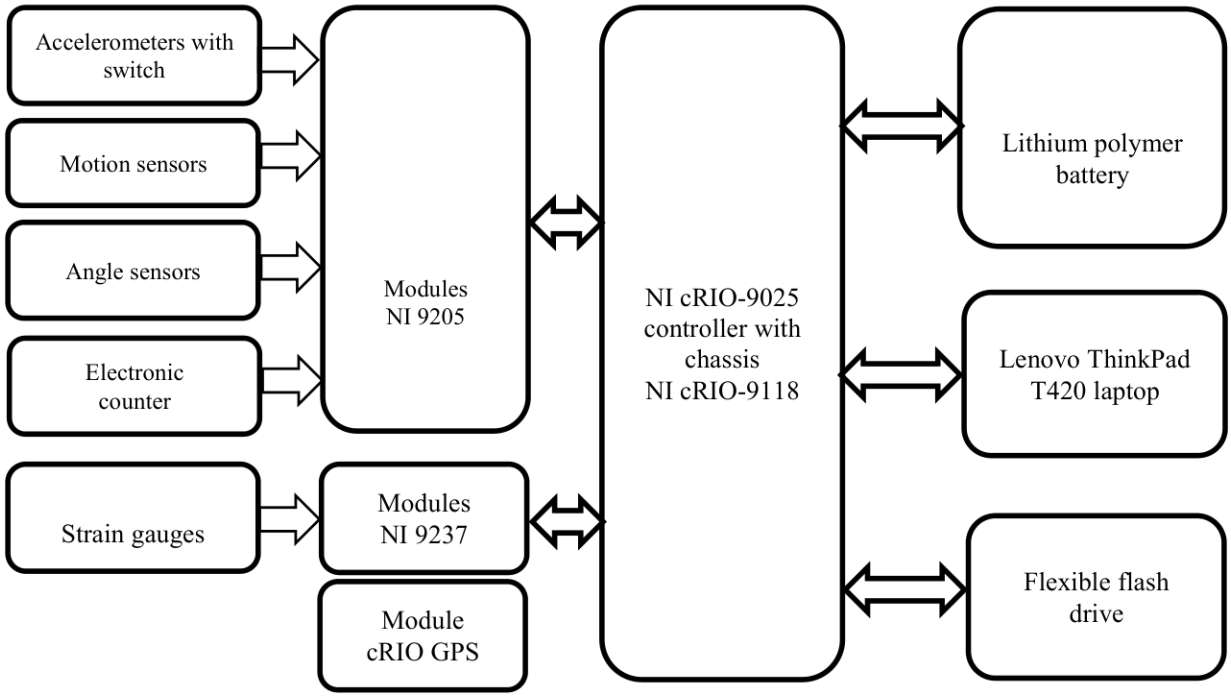

Figure 5.41 – Block diagram of the mobile system

5.4.3 Primary converters

In order to measure and evaluate the dynamic load of the rolling stock crew, a low-frequency accelerometer of the experimental type UM was created. In order to use this accelerometer when measuring accelerations on rolling stock, a cubic-shaped housing has been developed. The choice of this accelerometer housing design is determined by its ease of use. An accelerometer has been created - this accelerometer has dimensions of 35x35x31 mm. It consists of a housing, a cover, a board with a microcircuit and an electrical connector, as well as fasteners (magnet, bolts, washers, nuts).

The case has a cutout in which a board with an ADXL 278 chip is placed on one side and an UZNTs 05-7/12VP111 connector is installed on the other. The cover and electrical connector are filled with epoxy glue. The general view of the accelerometer is shown in Figure 5.42.

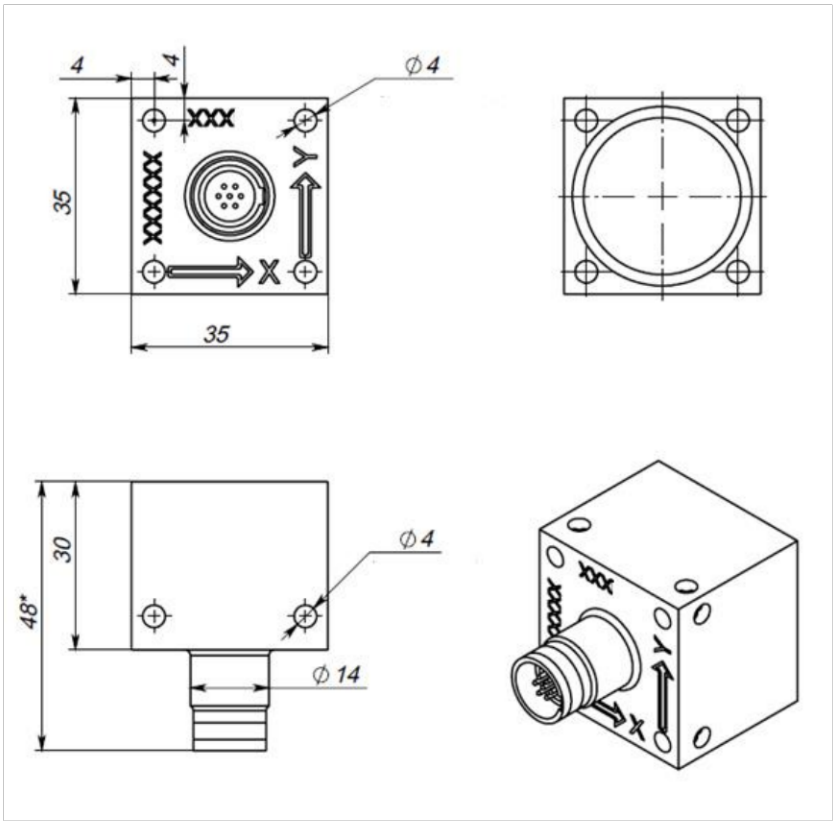

Figure 5.42 – Experimental low-frequency accelerometer

The board includes an Analog Devices ADXL 278 microcircuit. The wiring diagram is shown in Figure 5.43.

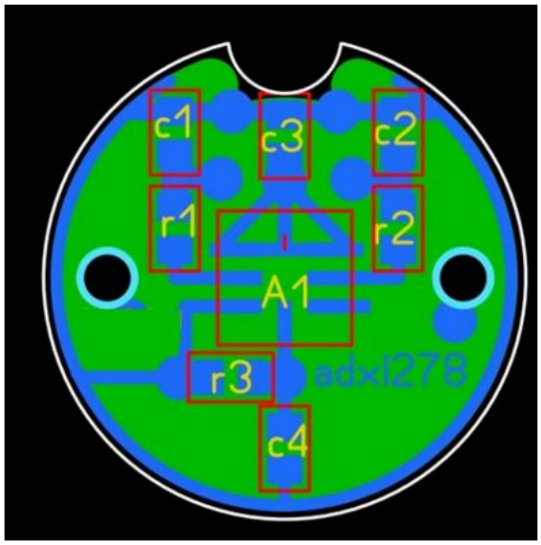

Figure 5.43 – Board with ADXL 278 chip

The manufacture of the board together with the microcircuit was completely carried out in accordance with the technical requirements of the manufacturer of the ADXL 278 microcircuit (temperature and soldering profile), defined in the passport.

Table 5.12 shows the general technical requirements for accelerometers that must be used when conducting running dynamic strength tests to determine the dynamic load of the chassis under operating conditions of rolling stock.

Table 5.12 – General technical requirements for accelerometers

No.	Accelerometer installation area		Recommended range, m/s2	Operating frequency range (microcircuit sensitivity), Hz	Additional requirements
1	Axle box unit		+/- 500	0…100 (0…250)	a) general frequency transmission in the range of 0.4 Hz ±0.5 dB; b) nonlinearity and hysteresis: – ≤ 0.3% measuring range; c) sensitivity of ordinary axes: ≤ 0.05 (m/s)2; d) temperature effect: - for ≤ 3% of the measuring range; - with sensitivity ≤ 5.10% – 4.0/0C.
2	Bogie	with single-stage spring suspension	+/- 100	0…100 (0…250)	
		with two or more degrees of suspension	+/- 50	0…40 (0…100)	
3	Body		+/- 15	0…20 (0…50)	

The measured accelerations can be used as indicators of the quality of track geometry and to detect local geometric deviations affecting the dynamic behavior of rolling stock. These measurements should be used in combination with basic parameter measurements.

Acceleration measurements should be made at specific locations on the body and bogies, depending on the need for a specific assessment. Thus, vertical accelerations of axle boxes are measured to identify rail surface defects and isolated geometric irregularities. The lateral accelerations of the bogie serve to detect irregularities with short waves. Transverse and vertical accelerations of the body reveal track defects that affect the dynamic characteristics of comfort.

The sampling frequency must be at least 2.5 times the cutoff frequency applied to the signal. Measurement of bogie and body accelerations should be carried out in the operating speed range for the line within a tolerance of +/-10%.

In order to measure movements and evaluate dynamic qualities, cable displacement sensors are used (Fig. 5.44). Rope sensors measure linear movement using a steel cable. In this case, the cable drum is connected to a sensitive element, which converts the movement of the cable into a linear output signal. The measurement is carried out with high accuracy and dynamics.

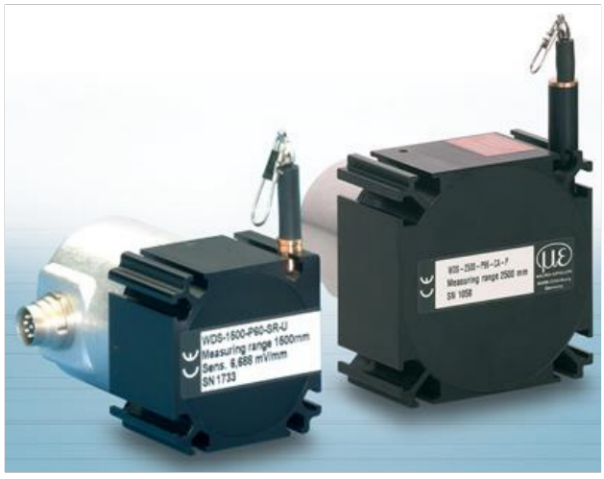

Figure 5.44 – Cable-type displacement sensors

Based on the comparative characteristics of the static deflections of bogies of four types Y-32, GP-200, KVN TsNII, 68-7007, displacement sensors with the following measurement ranges were determined to be optimal: 300 mm for measuring displacements in the primary suspension stage, 625 mm for the secondary stage.

CONCLUSIONS ON SECTION 5

A new method for measuring contact forces has been proposed: through the deformation of the wheel disks of wheelsets, its high efficiency and promise have been confirmed through experimental and theoretical studies.

Technical proposals and recommendations have been developed for the method of directly measuring the forces of interaction between wheels and rails:

- based on the results of modeling and experiment, a scheme for placing strain gauges on the inner surface of the wheel disk was developed. This scheme includes points that are most sensitive to vertical and lateral loads; recommended connection diagrams for strain gauges;

- technical proposals were provided for installing strain gauges on the surface of the wheel disk and mounting measuring equipment on the wheel pair;

- recommendations and technical proposals for carrying out tare work were provided: for tare in the vertical direction it was recommended to use the wheel-by-wheel weighing technique, and for tare in the horizontal direction a set of equipment was proposed that ensures the load of the wheel.

General recommendations have been developed for recording and filtering parameters, statistical processing of measured values (Y, Q) and calculated values ($\Sigma Y2m$, $Y/Q2m$).

The proposed method for measuring contact forces allows you to directly measure contact forces, thereby assessing real traffic safety indicators for a given type of rolling stock, in contrast to the existing methodology: measurement by deformations of bogie frames, which gives only an indirect assessment and does not apply to the traffic conditions of passenger trains above 140 km/h.

SECTION 6
MOBILE SYSTEM FOR DETERMINING THE DYNAMIC LOAD OF THE ROLLING PARTS OF THE ROLLING STOCK IN OPERATION

6.1 General requirements for software and hardware complex

A mobile system for determining the dynamic load of rolling stock undercarriages in operation must consist of primary transducers, a global positioning system receiver, analog signal transmission lines, subsystems for collecting measurement information, determining traffic safety indicators in express processing mode, determining the level of comfort, and determining the smoothness of the ride. , determination of dynamic stresses

The primary transducers should be strain gauges, low-frequency accelerometers and displacement sensors. Analog signal transmission lines are cables that provide connection between primary transducers and recording devices with an operating voltage of up to 10 V and are components of the measuring system. Cables must be shielded, resistant to oils, have at least six cores, cable flexibility must correspond to class 1 or 2 and not change its properties at temperatures from minus 40°C to plus 80°C.

The mobile system must provide the ability to autonomously carry out control tests of dynamic diagnostics of rolling stock units in order to determine the load of the running gear, as the main component of checking the quality of capital repairs, assessing the residual life of load-bearing structures, performing control tests as part of work to extend the designated service life and determining loads of chassis under operating conditions of rolling stock.

6.2 Measurement information collection subsystem

The measurement information collection subsystem collects, stores and visualizes changes in information signals from displacement sensors, vibration accelerations and mechanical deformations. In addition, GPS receiver data is used to analyze the influence of movement speed on changes in controlled parameters, obtain precise time signals and determine current coordinates. The generalized structure of the measurement information subsystem is shown in Figure 6.1.

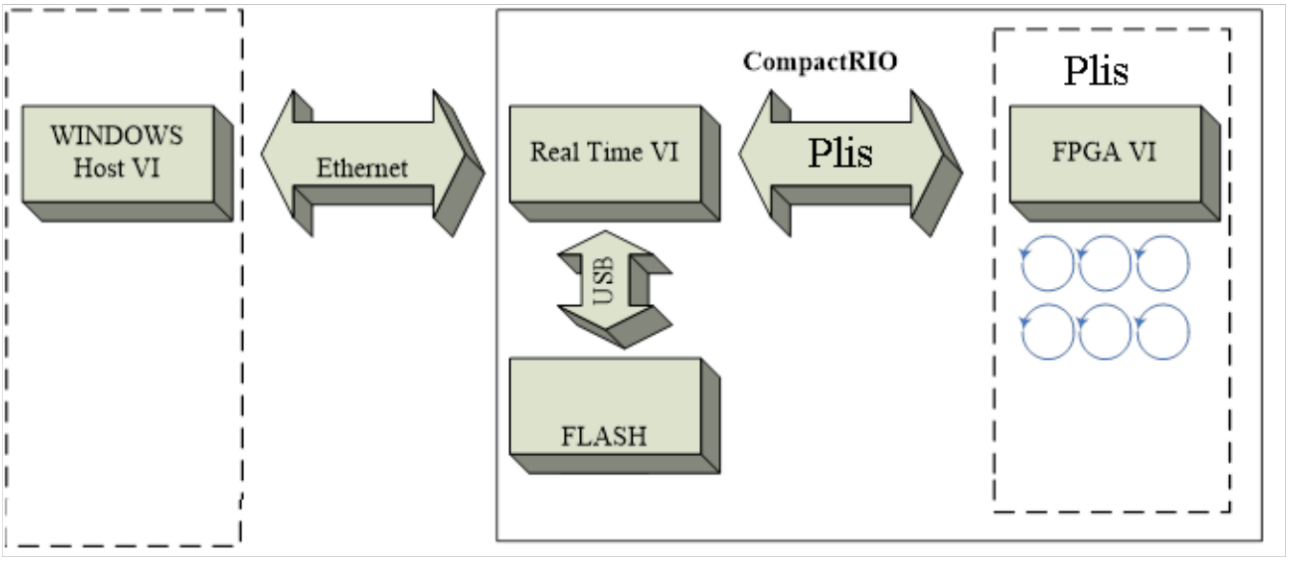

Figure 6.1 – Software structure

The developed acquisition subsystem provides operation of a CompactRIO controller with an 8-module chassis with a built-in programmable logic integrated circuit (FPGA) and two universal 9205 ADC modules with a maximum sampling frequency of 250 kHz and

five 9237 strain gauge modules with a maximum frequency of 50 kHz per channel, a GPS signal receiver module.

Thanks to the built-in FPGA, CompactRIO has the ability to implement measurement data processing algorithms at the hardware level with a deterministic execution time of 25 ns without transferring the load to the controller's central processor. A typical CompactRIO device includes a controller running a PharLab or VxWorks real-time operating system, a chassis, and I/O modules. The chassis carries an FPGA core that is directly connected to universal or specialized input/output modules that have built-in means for matching and processing information signals. There are different chassis models that have different numbers of slots for modules and differ in the characteristics of FPGA chips.

Thanks to its autonomy, hardware and weight-size characteristics, as well as the ability to operate in adverse conditions, CompactRIO can be used to solve a wide range of problems in collecting measurement information and controlling processes.

Most software for CompactRIO is developed according to a scheme that provides for its conditional division into three levels: the HOST VI virtual instrument on a control PC running Windows OS, RT VI on a controller with a real-time OS, and FPGA VI on an FPGA that does not have its own OS, since the logic The program's operation was implemented directly at the hardware level. Each of the presented levels has its own specific functionality and implements individual functions of the system as a whole.

Common tasks performed using HOST VI on a Windows computer:

- saving data on a computer and accessing databases;
- integration with external information systems;
- interface organization.

Typical tasks performed in RT VI on a real-time controller:

- data processing;
- management;
- saving data in the built-in memory of the controller and external media.

Typical tasks performed in FPGA VI on FPGA:

- input-output operations;

- hardware clocking and control of the process of interaction with equipment;
- low-level processing of measuring signals.

An FPGA is a chip whose functionality is determined by programming or "configuration", which is the more common term when working with this class of integrated circuits. The LabView FPGA Module package is an addition to the LabView software environment that allows you to specify the logical operation of the FPGA as a regular virtual device instead of programming using a specialized VHDL language. This package allows you to create programs with synchronous and asynchronous parallel loops running in hardware, and provides time-deterministic data collection and analysis.

The LabVIEW FPGA Module software package completely takes care of the multi-step process of converting a virtual device into FPGA binary code. At the first stage, the virtual device is converted into text code in the VHDL language, after which it is compiled into binary form by the standard industrial compiler Xilinx ISE. During the compilation process, the code is optimized for execution speed and the number of logic gates involved.

The result of compilation is a binary file (bitstream file) that completely defines the FPGA configuration. When the program starts, the binary file is loaded onto the chassis, that is, the FPGA configuration process occurs. The binary file can be written to the built-in flash memory and automatically loaded when the system is turned on. The configuration is not saved when the power is turned off, so the binary file must be downloaded again when power is turned on again. With appropriate configuration settings, it can be loaded automatically from the flash memory of the FPGA device or by a program using the controller.

FPGA VI virtual instruments can be produced completely, independently of other system components, and remain operational even if the controller fails. Moreover, a buffer can be organized on the FPGA to prevent data loss in such a situation.

The FPGA is designed primarily for clocking, synchronization, control, data acquisition and preliminary digital processing of information signals, control of each input/output module.

A virtual device for a CompactRIO controller typically includes two or more loops: a critical priority loop, which implements control and data processing algorithms, and a normal priority loop, which is responsible for data safety, a remote web interface, and communication over an Ethernet network or RS bus. 232.

The CompactRIO platform provides three paths to elevate data from modules to the real-time controller level: through front panel elements, through a mechanism known in LabView as Local Variables, and through a DMA FIFO buffer. The first two approaches are relatively simple in terms of implementation, but suboptimal in terms of efficiency. At the same time, the DMA FIFO method allows you to receive data obtained at high sampling rates from a large number of modules without delay. One of the advantages of DMA mode is that data transfer occurs regardless of the central processor.

FPGA devices that support DMA FIFO buffers have direct memory access, unlike other methods that require the CPU. Direct memory access is implemented by capturing the PCI bus (bus mastering) by the FPGA device, in which it gains access to bus control, and therefore access to memory, bypassing the processor.

The DMA FIFO buffer consists of two sections: one part is located in the FPGA memory, the other in the controller memory. The FPGA can write or read from the buffer element by element using the FIFO Read and FIFO Write methods, and the controller can write or read samples of elements. The two parts of the buffer are connected using a hardware-software DMA controller. Thus, from a software point of view, they look like a single FIFO buffer.

The FPGA VI virtual device, located on the FPGA, implements the functionality of initialization, clocking, polling of data acquisition modules and subsequent loading of the received samples into the DMA FIFO buffer. To ensure a deterministic sequence of command execution, the programming language structure in LabView

Flat Sequence Structure is used, which contains elements for polling modules and writing to a buffer.

The DMA FIFO buffer is cyclically polled at intervals set by a timer at the real-time controller level, after which the samples obtained in the form of integers according to the dynamic range and bit capacity of the acquisition module are normalized by the values of acceleration and deformation. The received data is fed to a virtual device, which processes and stores it on an external drive connected via a USB bus.

CompactRIO controllers have a built-in USB 2.0 controller, but not all drives support this standard, which can lead to significant write delays, which, in turn, lead to DMA FIFO buffer overflow and incorrect operation of the system as a whole.

The presented system does not have a virtual control device located on a personal computer, but instead uses the LabView Remote Panel mechanism. This function implements the so-called Client-Server model, where the controller is the server, and the client is any computer with LabView installed. By default, CompactRIO is licensed for one external connection, but the number can be expanded. To activate the Remote Panel on the controller, you need to activate the Web server in the project settings and select the virtual devices to which you want to allow remote access. This feature can significantly reduce the time required to develop HOST VI, but can create a load on the data network.

In addition to the acquisition modules, to synchronize time and acquire current speed and coordinates, a GPS receiver is also connected to the controller, installed on the chassis in the same way as standard modules. Because the receiver is manufactured by a third party, the LabView Real Time Module does not have a standard means of acquiring GPS data, so it uses a set of separately installed virtual devices to communicate with it. In addition, to ensure correct functioning of the module as part of the project, the SubVIs supplied with the module should also be added to the FPGA VI. If initialization is successful, the GPS data is presented as a

cluster or directly in text format, which can be used to configure software or perform other tasks.

6.3 A system for determining the level of comfortable movement

The subsystem for determining the comfort level is based on the requirements of the DSTU UIC 513 standards. These documents provide for the assessment of the comfort of passengers in mainline railway wagons, in which passengers normally occupy a “sitting” or “standing” position.

According to the accepted methodology, the comfort index is calculated based on the accelerations of: a) the body in the middle part, above the pivot points in three directions (according to the simplified method - NMV); b) effective accelerations at floor level, on the seat cushion in the vertical and transverse directions; on the back of the chair for sitting in the longitudinal direction (full volume method in the sitting position - NVA); c) the wagon body at floor level in three directions (full-volume method in the “standing” position - NVD).

To exclude high-frequency components in the range of the output signal and select for analysis the frequency band corresponding to the vibrations of the wagon, digital signal filtering is used in the process of data preprocessing. Depending on the acceleration axis and the location of the accelerometer, three types of filtering with different amplitude-frequency characteristics are used.

For statistical processing of vertical accelerations measured by an accelerometer placed at floor level or in seating areas, filters are used, the amplitude-frequency characteristic of which is described by formulas (6.1) and (6.2), and for accelerations measured on the back of seats in the longitudinal direction and filters are used on the cushion in the transverse direction according to − (6.1) and (6.3):

$$H_A(s)=\frac{s^2\cdot 4\pi^2\cdot f_2^2}{\left(s^2+\frac{2\pi\cdot f_1}{Q_1}\cdot s+4\pi^2 f_1^2\right)\left(s^2+\frac{2\pi\cdot f_2}{Q_1}\cdot s+4\pi^2 f_2^2\right)}, \quad (6.1)$$

$$H_B(s)=\frac{(s+2\pi\cdot f_3)\left(s^2+\frac{2\pi\cdot f_5}{Q_3}\cdot s+4\pi^2 f_5^2\right)}{\left(s^2+\frac{2\pi\cdot f_4}{Q_2}\cdot s+4\pi^2 f_4^2\right)\left(s^2+\frac{2\pi\cdot f_6}{Q_4}\cdot s+4\pi^2 f_6^2\right)}\cdot\frac{2\pi\cdot Kf_4^2\cdot f_6^2}{f_3\cdot f_5^2}, \quad (6.2)$$

$$H_C(s),H_D(s)=\frac{(s+2\pi\cdot f_3)}{\left(s^2+\frac{2\pi\cdot f_4}{Q_2}\cdot s+4\pi^2 f_4^2\right)}\cdot\frac{2\pi\cdot Kf_4^2}{f_3}. \quad (6.3)$$

Expressions (6.1), (6.2) and (6.3) indicate: HA(s) – transfer function of the bandpass filter; HB(s) – transfer function of the weighted filter of vertical accelerations; NS(s), HD(s) – transfer function of the weighted filter of longitudinal and transverse accelerations; f1, f2, Q1 – filter coefficients characterizing band boundaries; *f3, f4, f5, f6, Q2, Q3, Q4, K* – filter coefficients characterizing the parameters of the transfer function.

Table 6.1 presents the filter coefficients in accordance with the requirements of the UIC 513 standard. The amplitude-frequency characteristics of the filters used are presented in Figure 6.2.

During processing, instead of formulas (6.1 – 6.3), without significantly affecting the results, you can use a simplified representation of the amplitude-frequency characteristic:

$$F_0(f)=\begin{cases}0.4 & 0{,}4\le f<2\\ 0.2\cdot f & 2\le f<5\\ 1 & 5\le f<16\\ 16/f & 16\le f<f_{max}\end{cases} \quad (6.4)$$

$$F_c^*(f) = \begin{cases} 1 & 0.4 \le f < 8 \\ 8/f & 8 \le f \le f_{max} \end{cases} \quad (6.5)$$

$$F_d^*(f) = \begin{cases} 1 & 0.4 \le f < 2 \\ 2/f & 2 \le f \le f_{max} \end{cases} \quad (6.6)$$

Where $H_A(s)$ Compliant $F_b(f)$, $H_B(s)$ according $F_c^*(f)$, A $H_C(s)$, $H_D(s)$ - $F_d^*(f)$.

Table 6.1 – Filter coefficients

Strip boundaries			Parameters of the amplitude-frequency function							
f_1 (Hz)	f_2 (Hz)	Q_1	f_3 (Hz)	f_4 (Hz)	f_5 (Hz)	f_6 (Hz)	Q_2	Q_3	Q_4	K
0.4	100	0.71	-	-	-	-	-	-	-	-
0.4	100	0.71	16	16	2.5	4	0.63	0.8	0.8	0.4
0.4	100	0.71	8	8	-	-	0.63	-	-	1.0
0.4	100	0.71	2	2	-	-	0.63	-	-	1.0

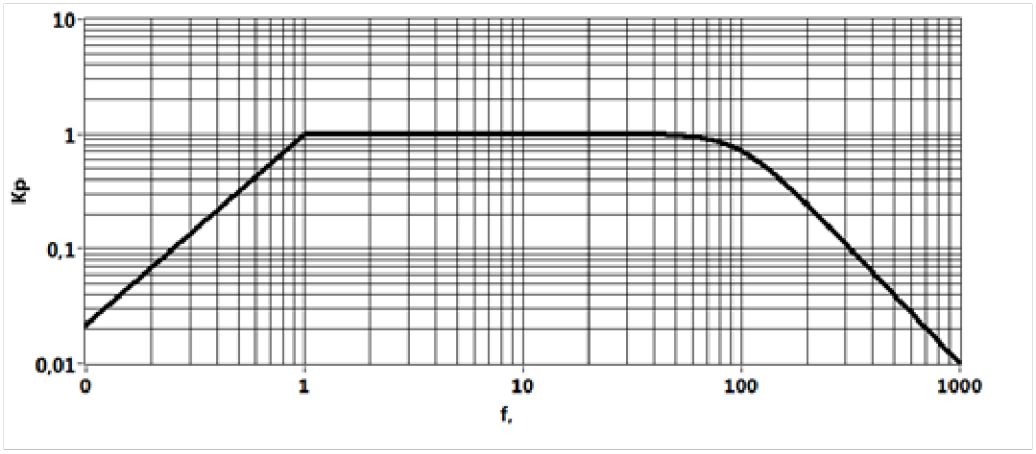

a)

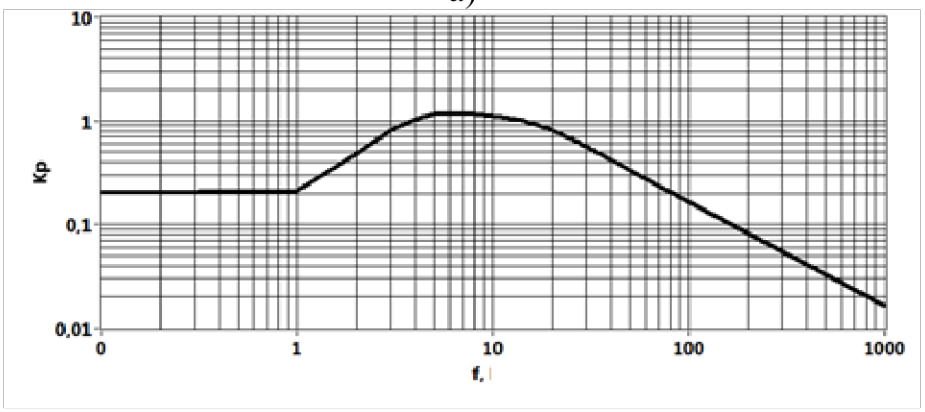

b)

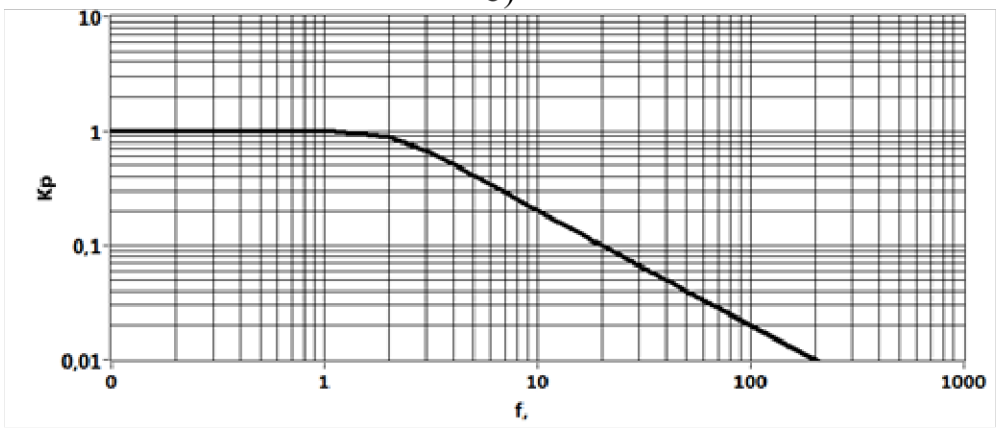

v)

Figure 6.2 – Amplitude-frequency response of the digital filters used: a) $H_A(s)$; b) $H_B(s)$; v) $H_C(s), H_D(s)$

Figure 6.3 shows the results of filtering a signal received from an accelerometer located on the floor of a passenger wagon moving at a speed of 70 km/h, before (Fig. 6.3a) and after (Fig. 6.3b) passing the filter.

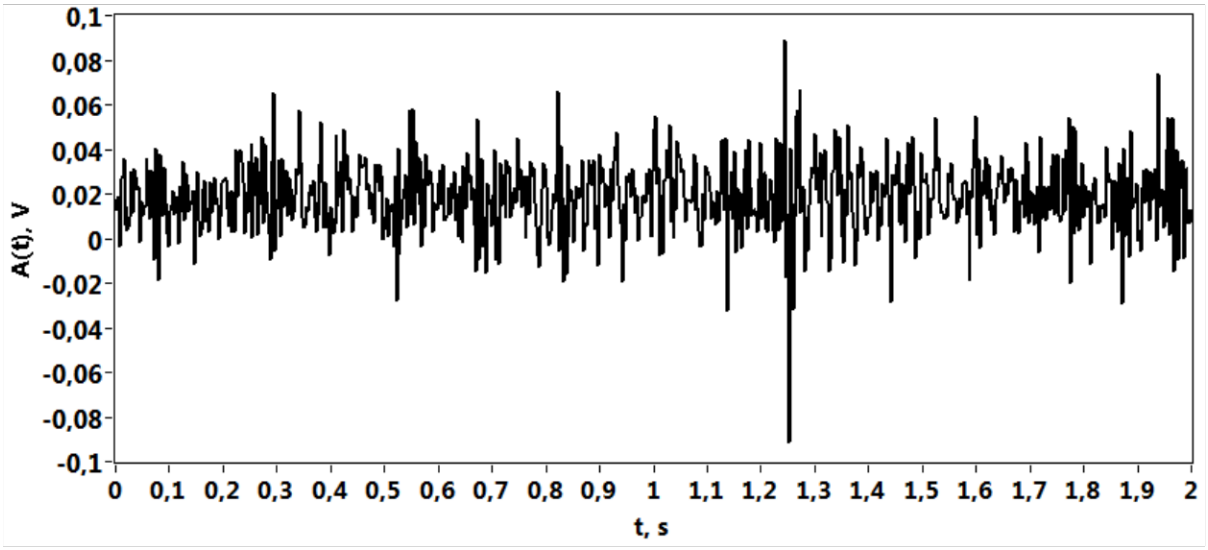

a)

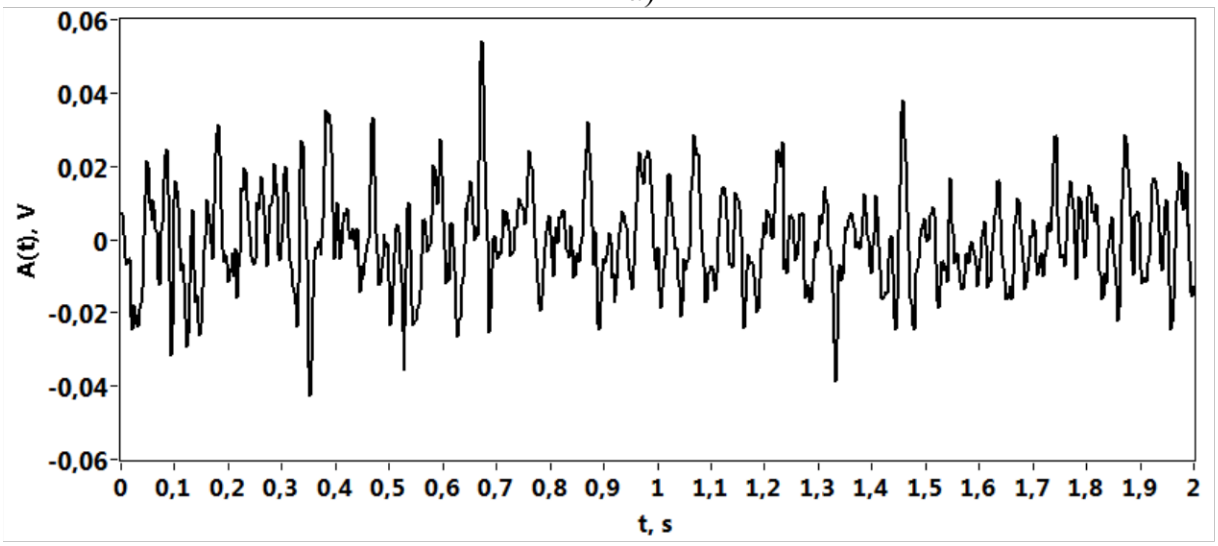

b)

Figure 6.3 – Filtered signals

In accordance with the requirements of the UIC 513 standard, a comfort index is calculated, which is assessed on the following scale: $N<1$ – very good comfort; $1<N>2$ – good comfort; $2<N>4$ – average comfort; $4<N>5$ – poor comfort; $N>5$ – unacceptable comfort.

The technical implementation of the subsystem is based on the results of sea trials of the model 62-7067 wagon. The calculated values of the comfort index NMV are compared with the limit value [N] = 4.0. The calculation results are shown in Table 6.2.

Based on the tabular data, graphs of the dependence of comfort indices on driving speed were constructed (Fig. 6.4). Apparently, comfort conditions deteriorate noticeably in the driving speed range of 120-140 km/h.

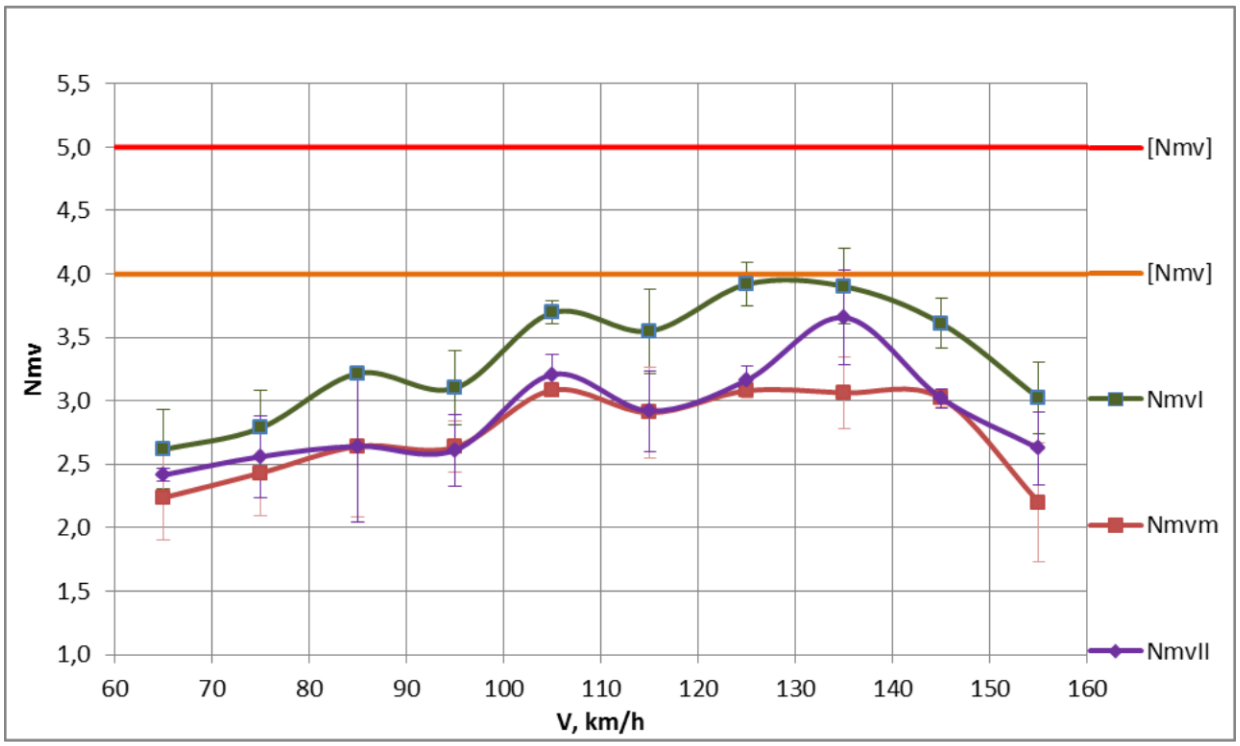

Figure 6.4 – Comfort indices for the wagon model 62-7067 of a two-system electric train on the Kyiv-Kharkov line

(NmvI, NmvII – comfort indices in the area of pivots I and II; Nmvm – comfort index in the middle of the body)

Table 6.2 – Comfort index of the wagon model 62-7067 of a two-system electric train on the Kyiv-Kharkov line

Index	Travel speed, km/h	Average value	SLE	Percentage of the limit value, %
NMVI (comfort index in the zone and pivot)	61-70	2.6	0.3	65.4
	71-80	2.8	0.3	69.7
	81-90	3.2	0.1	80.4
	91-100	3.1	0.3	77.5
	101-110	3.7	0.1	92.4
	111-120	3.6	0.3	88.8
	121-130	3.9	0.2	98.0
	131-140	3.9	0.3	97.5
	141-150	3.6	0.2	90.2
	151-160	3.0	0.3	75.6
NMVm (comfort index inside the body)	61-70	2.2	0.3	55.9
	71-80	2.4	0.3	60.8
	81-90	2.6	0.6	66.0
	91-100	2.6	0.2	65.9
	101-110	3.1	0.1	77.1
	111-120	2.9	0.4	72.7
	121-130	3.1	0.1	77.0
	131-140	3.1	0.3	76.6
	141-150	3.0	0.1	75.5
	151-160	2.2	0.5	55.0
NMV1I (comfort index in zone II of the pivot)	61-70	2.4	0.1	60.4
	71-80	2.6	0.3	64.0
	81-90	2.6	0.6	66.1
	91-100	2.6	0.3	65.3
	101-110	3.2	0.2	80.2
	111-120	2.9	0.3	73.0
	121-130	3.2	0.1	79.1
	131-140	3.7	0.4	91.4
	141-150	3.0	0.1	75.5
	151-160	2.6	0.3	65.6

6.4 System for determining traffic safety indicators

The subsystem for determining the smoothness of the ride is based on the requirements of the standard for the requirements for the smoothness of movement of railway rolling stock SOU MPP 45.060-204:2007. This standard is intended to assess ride comfort by checking the compliance of the wagons smoothness indicator Wz with the standards provided for in the technical documentation for the wagons. The smoothness indicator depends on the intensity and spectral composition of accelerations of the wagon body.

According to the accepted methodology, the ride comfort characteristics Wz are calculated from body accelerations above the pivot assemblies at the output of the "physiological filter". In accordance with this, the smoothness indicators in the vertical (W_{zv}) and horizontal (W_{zg}) directions are calculated. The general view of block diagrams is presented in Figure 6.5.

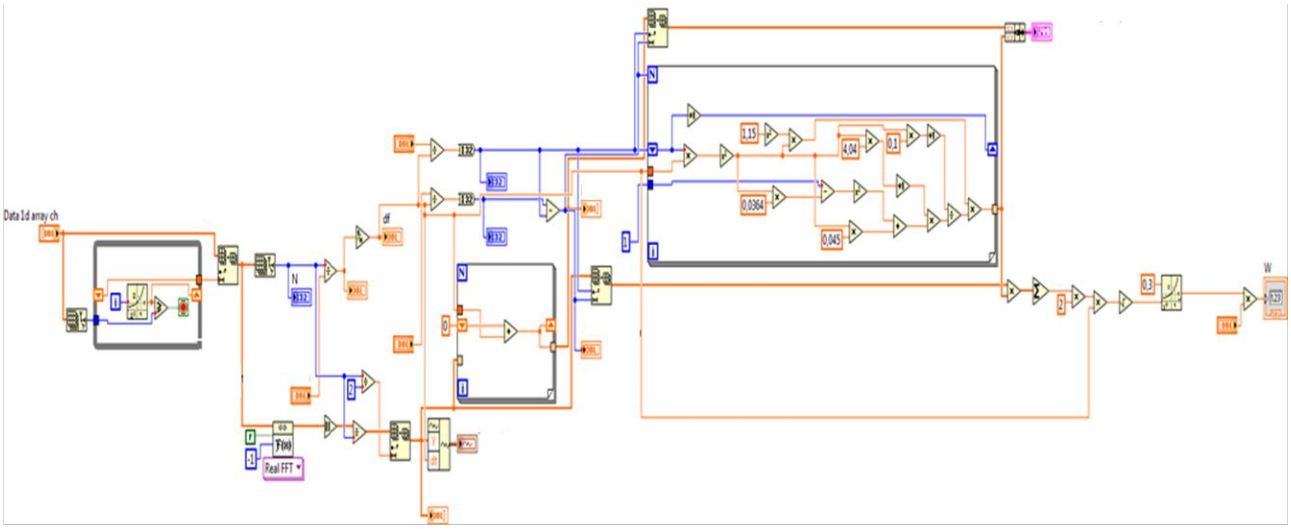

Figure 6.5 – General view of the block diagram

The data in Table 6.3 characterizes the assessment of the ride characteristics.

Table 6.3 – Assessment of the driving performance of the wagon based on the smoothness indicator Wz

Assessment of carriage performance	Wz value
Very good	2
Good	2 – 2.5
Sufficient for passenger carriages	2.5 – 3
Limit for passenger wagon	3 – 3.25
Sufficient for a locomotive	3.25 – 3.5
Limit for a locomotive	3.5 – 3.75
Sufficient for freight wagon	3.6 – 4
Limit for freight wagon	4 – 4.25
Limit for humans from a physiological point of view	4.5
Dangerous from the point of view of derailment of rolling stock	5

The calculation of smoothness indicators is carried out according to the following algorithm: the size of the block for calculations is determined; the size of the input block is determined by the logarithm to base two, and using the built-in LABVIEW function, a Fourier transform is performed to construct the power spectrum; based on the Fourier transform, frequency arrays and data arrays are generated in a given frequency range from 0.5 to 20 Hz; the value of the normalized amplitude-frequency characteristic of the correction filter is calculated according to expression (6.7). Block diagram shown in Figure 6.6.

$$q_н(f) = 1.15 \cdot \sqrt{\frac{(1+0{,}1 \cdot f^2)}{(1+4{,}04f^2) \cdot ((1+0{,}0364f^2)^2 + 0{,}045f)}}, \quad (6.7)$$

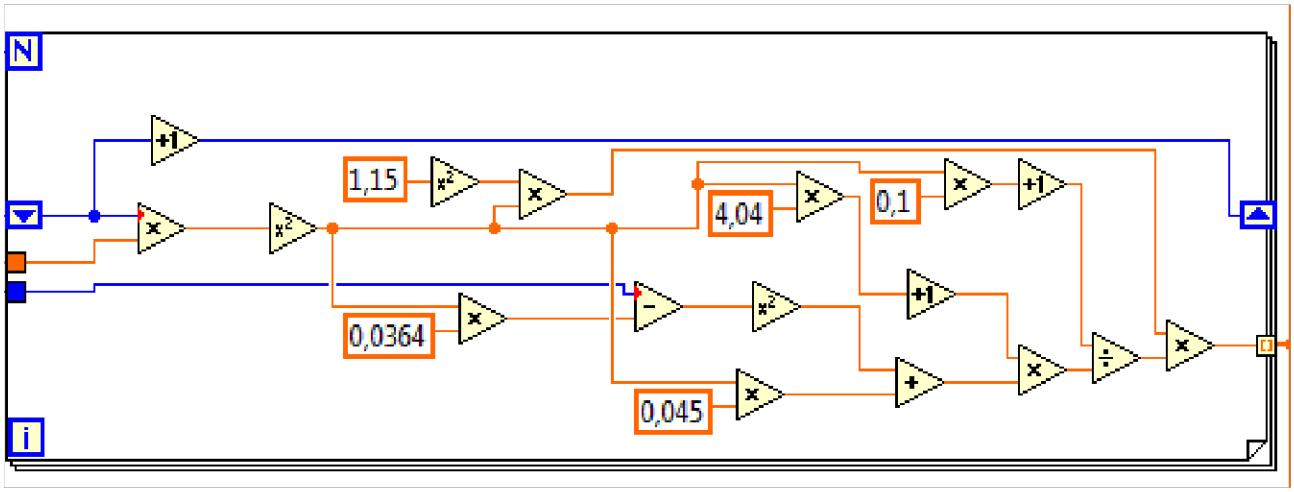

Figure 6.6 – Block diagram of the correction filter

The final smoothness indicator Wz for the data array is calculated using the formula:

$$W = a \cdot \widetilde{a}_k^{0,3}, \tag{6.8}$$

Where α=4.346 – for vertical vibrations; α=4.676 – for horizontal (transverse) vibrations; $\widetilde{a}_k^{0,3}$ – root mean square value of vibration accelerations at the output of the correction filter.

An example of the smoothness assessment results is shown in Figure 6.7. The obtained values of smoothness indicators compared to the permissible limit value [Wz] = 3.75.

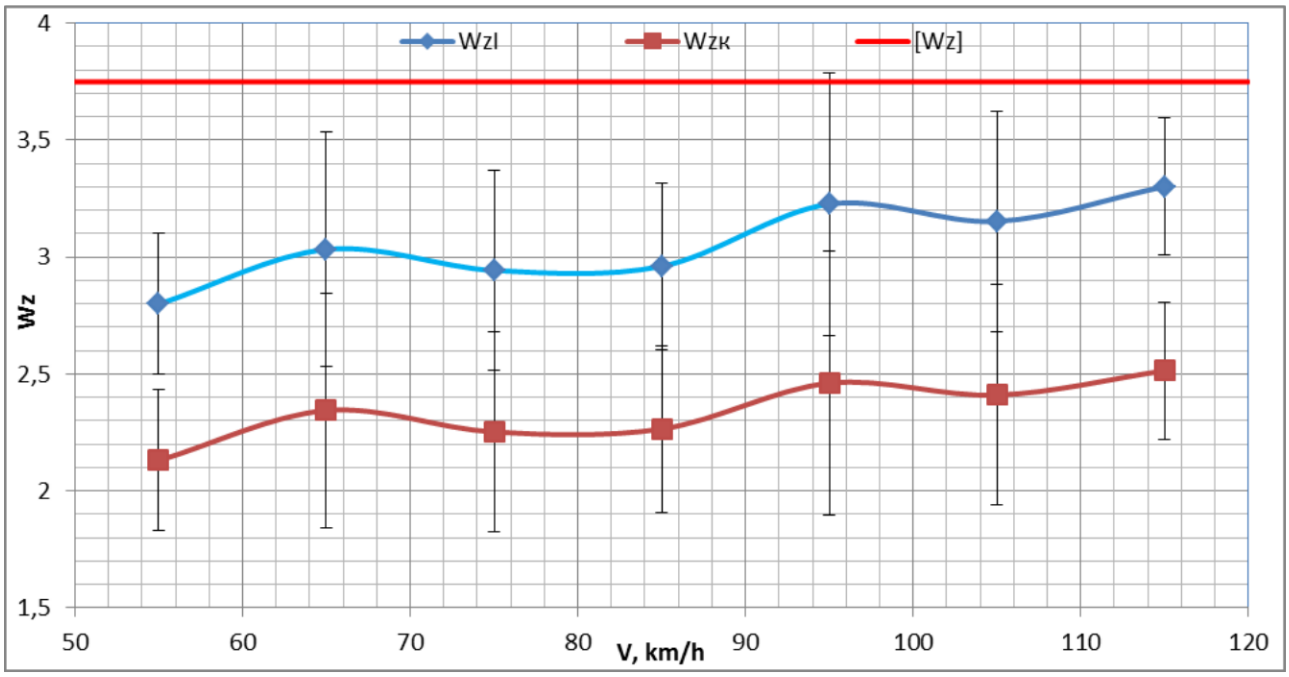

Figure 6.7 – Smoothness indicators in the vertical direction (WzI – smoothness indicator in the pivot section; Wzk – smoothness indicator)

6.5 System for determining traffic safety indicators

The subsystem for determining safety indicators is designed to work in express processing mode. This subsystem is a software package installed on a PC and implements the determination and display of safety indicators in real time with a result update interval of once every two seconds or once per 100 meters of the distance traveled.

According to the current methods of full-scale testing on 1520 mm railways, it is expected to determine traffic safety indicators based on the so-called “frame forces” acting from the frame structures of the chassis on the wheel pairs. However, due to the fact that these characteristics do not provide a direct picture of the force interaction of wheels with rails, this leads to a decrease in the reliability of the results obtained in the process of running research.

On the railways of EU countries, the assessment of traffic safety indicators of high-speed rolling stock is regulated by standards establishing the following test methods:

- normal method: measuring contact interaction forces in the horizontal transverse (Y) and vertical (Q) directions;

- simplified method: measurement of lateral force (H) and body acceleration in the transverse () and vertical () directions;$\ddot{y}^*\ddot{z}^*$

- simplified method: measurement of transverse accelerations of the bogie frame () and body accelerations in the transverse () and vertical () directions.$\ddot{y}^+\ddot{y}^*\ddot{z}^*$

In order to introduce modern approaches to assessing traffic safety indicators, work has been done on the technical implementation of a simplified test method based on measuring accelerations $(\ddot{y}^+, \ddot{y}^*, \ \ddot{z}^*)$.

After filtering, the mathematical expectation (x) and standard deviation (s) are calculated to subsequently determine the maximum possible acceleration values ($X_{\max}$) according to the following formula:

$$X_{\max} = \bar{x} + k \cdot s, \qquad (6.9)$$

where k is a coefficient depending on the given confidence level (to determine safety indicators $k = 3$).

The values determined in this way are compared with the maximum permissible values specified by the UIC 518 standard as follows: for vertical body acceleration = 3 m/s2; for lateral accelerations of the body –= 3 m/s2 when moving straight and in curves of large radius, = 2.8 $(\ddot{z}_s^*)_{lim}(\ddot{y}_s^*)_{lim}(\ddot{y}_s^*)_{lim}$ m/s^2 - in curves with radius 400 ≤ R ≤ 600 m, = 2.6$(\ddot{y}_s^*)_{lim}$m/s2 – in curves with a radius of 250 ≤ R ≤ 400 m. For lateral accelerations of the bogie frame, the maximum permissible accelerations are determined as follows:

$$((\ddot{y}_s^+)_{lim})\text{lim} = 12 - \text{Mb}\ /5, \qquad (6.10)$$

where Mb is the mass of the bogie in tons.

The pilot implementation of the subsystem was carried out based on the results of sea trials of the model 68-7041 wagon along the Kharkov-Kyiv, Kyiv-Donetsk and Lviv-Kyiv routes.

Figure 6.8 shows the root-mean-square deviations (RMS) of the horizontal transverse accelerations of the bogie frame, recorded during the movement of the experimental train along the Lviv-Kyiv route. Based on the fact that the weight of the model 68-7041 bogie is 6.68 tons, the value $(\ddot{y}_s^+)_{lim}$=5.33 m/s2. As can be seen from the presented results, the largest standard deviations of acceleration are at least two times lower than the maximum permissible value, which indicates a significant margin of resistance of the wagon from the east of the rails.

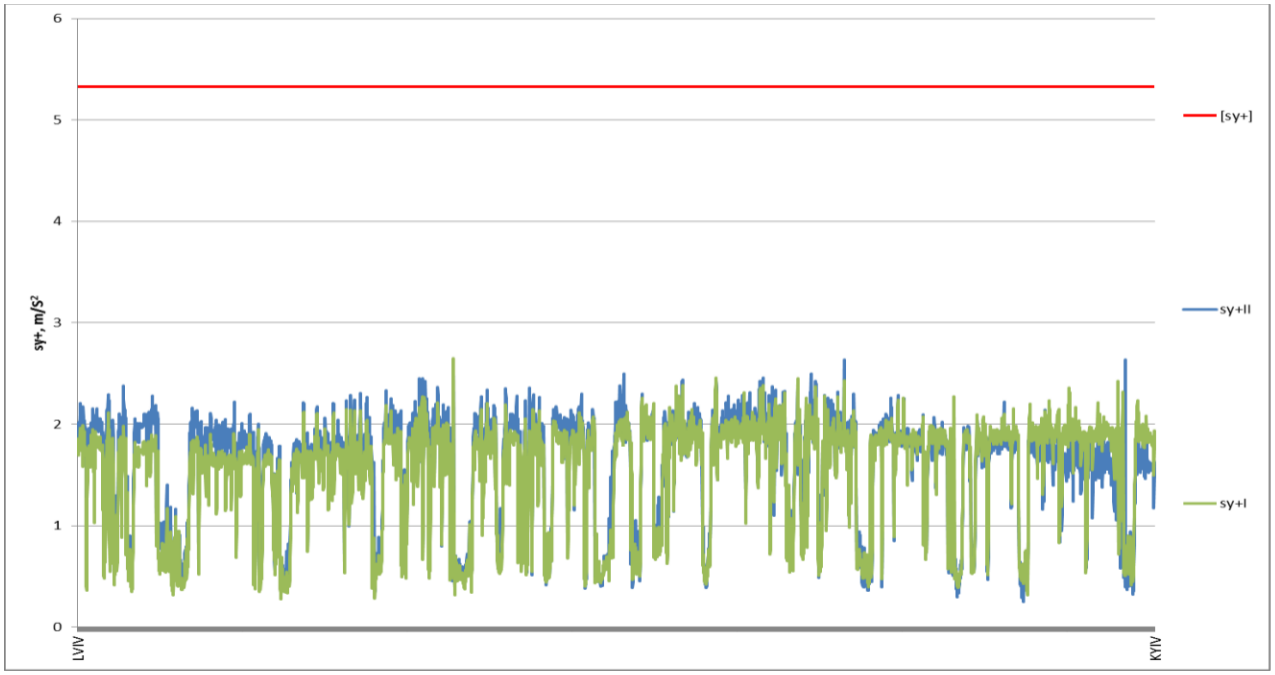

Figure 6.8 – RMS of horizontal lateral accelerations of the bogie frame, measured during a test trip on the Lviv-Kyiv line

6.6 A system for determining the indicators of the interaction of the pantograph and contact network

In this work, the basic criteria of the process of the pantograph and overhead line interaction of railway rolling stock are considered. An analysis of the causes and consequences of impaired current collection was also performed. The analysis of existing systems and technical means for determining the qualitative and quantitative indicators of the pantograph and overhead line interaction was carried out and their classification was carried out according to the location, the principle of obtaining information and controlled parameters. Based on the results of research, the main quantitative and qualitative indicators of the interaction of current collectors with the overhead line in the conditions of operation on the railways of Ukraine, which should be subject to control, have been established. Field tests were also conducted to determine such indicators in real operating conditions of railway rolling stock. According to the results of the research, an experimental complex was developed to determine the indicators of the interaction of current receivers of various types of rolling stock with the contact network in operating conditions.

6.6.1 Formulation of the problem

Increasing the speed and safety of rail transportation is becoming a more urgent issue. In the work, a review and criterion analysis of the basic processes of the interaction of the pantograph and the contact network of railway rolling stock, which is operated on the railways of Ukraine, is carried out. Factors that have a negative effect on current collection have been determined, including: the amount of wear of the pantograph lining, the frequency of separation of the pantograph from the contact wire, the range of oscillations of the pantograph rail, the pressure of the pantograph on the contact wire and the acceleration of the pantograph rail in operation. An analysis of the causes and consequences of impaired current collection was carried

out. Current international scientific works on the process of interaction of the pantograph and contact network were studied.

It was concluded that these works, to a greater extent, are aimed at the development of mathematical models of the interaction of the pantograph and contact network, analyzes of malfunctions of the pantograph in operation and wear of the graphite insert of the pantograph. At the same time, this work is aimed at the development of an autonomous mobile system for determining the indicators of the interaction of current receivers with the contact network, which is not sufficiently described in existing scientific works.

The analysis of the existing complexes for determining the qualitative and quantitative indicators of the interaction of the pantograph and contact network was performed. It was established that the existing complexes are multi-component in terms of control methods, difficult to operate, expensive, and are installed stationary on railway rolling stock and railway infrastructure objects. In contrast to those, the proposed system is autonomous, mobility placed on any locomotive or motorcar mobile unit, which allows to reduce the costs of operation and the complexity of installation.

The proposed mobile system allows you to detect not only the indicators that characterize the current draw, but also the faults of the contact network itself, such as: contact network sagging and contact wire exiting the working surface of the pantograph.

6.6.2 Basic criteria for the interaction of the pantograph and overhead line

The main criteria of the current collection process include:

- values of wear of the contact pair, separation of the current collectors from the wire, the range of oscillations of the slide and contact pressure
- coefficients of reliability of contact operation and efficiency of current collection, as well as minimum annual operating costs
- reliability and economy of current collection.

The amount of wear of dynamic contact pairs in operation is the most objective criterion for evaluating their performance. Wear can be used as a comparative indicator for the materials of the contact pair and the amount of current. It characterizes the work of a dynamic system. However, the process of wear of the contact wire proceeds slowly, for several years, during which the weather conditions will change repeatedly, as well as the types of rolling stock (hereinafter referred to as ERS) and current collectors with different characteristics, currents, and speeds of movement. Other factors will also affect it, for example, the height of the resulting wear of the wire sections. Therefore, the results of the contact wire wear analysis can be obtained only after a significant period has passed.

The current collector plates wear out much faster. Their service life is the mileage before replacement. But a specific current collector will wear out when driving on a traction shoulder (or shoulders) with specific profiles in weather conditions that change over several days, in different manners of driving trains by drivers and train situations (current, speed), depletion of lubricants, etc. However, the most important for operation are the statistical data on the average specific wear of the wires and the consumption of the plates, correlated to the ERS mileage.

The separation of current collectors from the contact wire is a criterion that can be used during inspection trips. They give an instant assessment of the reliability of current collection, although they do not consider the possibility of pressing the wire. During visual assessment (using a voltmeter), the number of breaks is considered, when they are registered with an oscilloscope or other devices - their duration. A variant of this assessment is the deviation coefficient K_s, which represents the percentage ratio of the sum of the deviation times to the observation period T.

$$K_s = \frac{\sum t_s}{T} \cdot 100\%. \qquad (6.11)$$

The range of oscillations of the skid relative to the level of the rail head (or the wire squeeze by the current collector) is determined by the dynamic component of the contact pressure of the current collector and is calculated according to the formula:

$$2\Delta P_{co} = P_{co\,max} - P_{co\,min}. \tag{6.12}$$

The coefficient of unreliability of the contact characterizes its susceptibility to damage (pressure or drops). To determine it, it is necessary to set the values of permissible minimum and maximum pressures. The sum of the number of cases where the contact pressure in the span exceeds the permissible values gives the unreliability coefficient:

$$k_r = n_{max}k_d + n_{min}k_d, \tag{6.13}$$

where: k_d– risk factor.

One of the main criteria for the quality of current collection is the pressure in the sliding contact (contact pressure), which shows whether the contact suspension for a given type of current collector can provide a normal mode of current collection at a given speed.

6.6.3. Existing systems for controlling the interaction of the pantograph and overhead line.

The optimal amount of contact pressure allows to ensure reliable current collection and minimal wear of contacting elements.

To register the pressure of the current collector on the contact wire, special measuring strips are used, which can be classified (Fig. 6.10):

- by construction: frame, beam and lamellar
- by type of measuring elements - tensometric, pneumatic
- optical and spring
- by the number of used measuring elements - with one sensor,
- with two sensors, three or more

- if possible, remove traction current - current collectors and measuring devices.

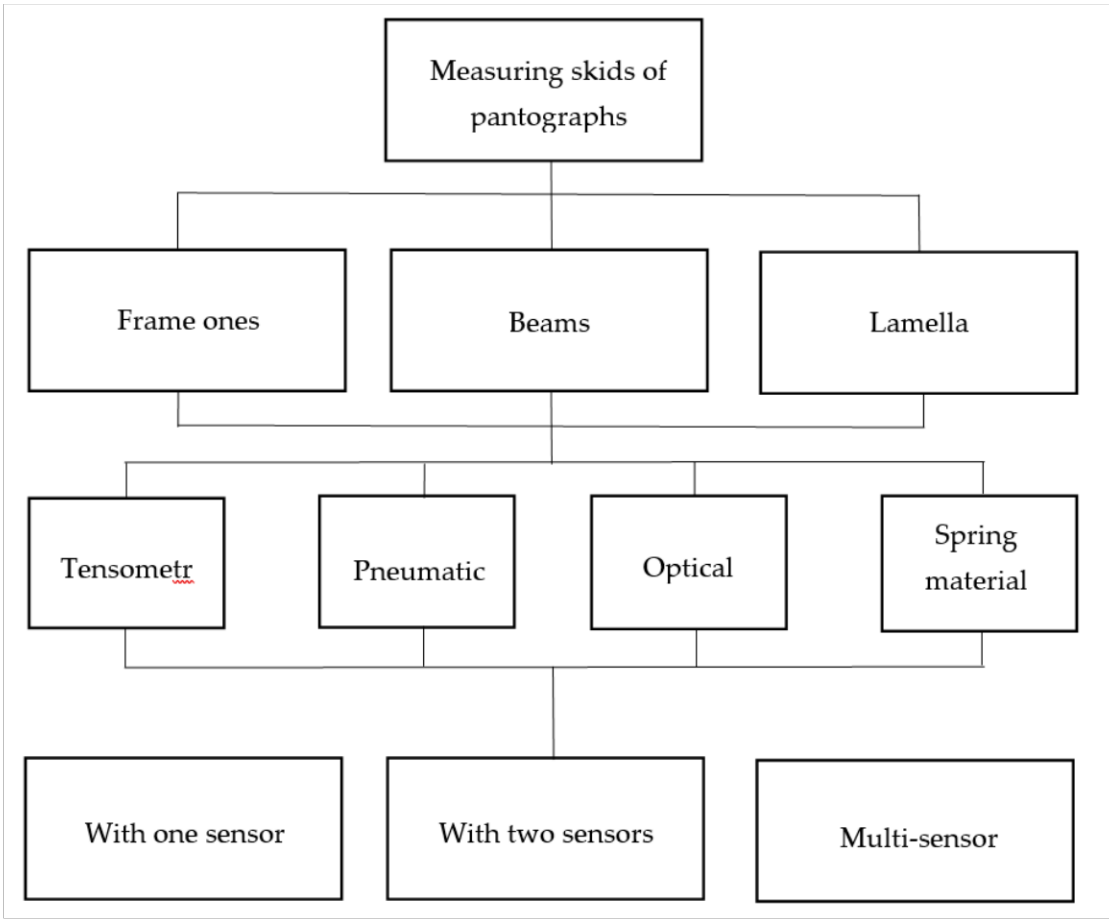

Figure 6.10 – Classification of measuring skids.

From the analysis of the known measuring rails of current collectors, it can be concluded that they are mainly installed on the inspection rolling stock and cannot be used as a replacement for standard current-carrying devices. In addition, when conducting tests at high speeds of movement, measuring current collectors, like ordinary ones, are in difficult conditions (mechanical abrasion, electrical erosion, heating by current, action of transverse and vertical forces, etc.), so their design must ensure high strength. The structure should not have extra elements, it should have the same aerodynamic characteristics and mass as standard current collector skids.

The most perfect and convenient of them is the beam measuring skid of the current collector SSS87 from Siemens (Figure 6.11). This skid is designed to adequately assess the interaction of the pantograph with the contact suspension in real

conditions due to the possibility of measuring the value of the contact pressure of the pantograph, the acceleration of its plane-parallel movements and torsional vibrations, the temperature of the contact elements of the skid and the current taken by the current collector.

The main advantage of such a measuring skid is that it is designed for the flow of traction current during full-scale tests without reconstruction of the main units and with a change in the minimum number of elements of the current collector.

The measuring skid of the current collector of the Siemens company allows: to register the following parameters of the interaction of the current collector and the contact suspension during full-scale:

- the amount of contact pressure of the current collector on the contact wire (measurement range of the sensor ±50 kg)
- acceleration of plane-parallel (vertical, horizontal, transverse) movements and torsional oscillations of the current collector slide from -4 to +5 g
- the current flowing through the current receivers is up to 2000 A
- the temperature of the contact plates of the current collector in the range from 0 to +600 °C.

Two ZFA 50 kg strain gauges, which have a low error and a sufficient measurement range, are used to measure the amount of contact pressure of the current collector.

With the help of two-axis accelerometers Analog Devices ADXL JCP-320 REEL, accelerations of plane-parallel (vertical, horizontal, transverse) movements and torsional oscillations of the current collector skid are determined to correct readings taken from strain gauges in order to obtain more accurate and reliable information about the amount of contact pressure of the current collector skid taking into account the inertial forces acting on it during the movement of electric rolling stock, especially at high speeds.

The signal from the acceleration sensors can also be used to infer abnormal modes of operation of the current collector, collisions with obstacles on the contact

hinge, malfunctions of components and assemblies of the current collector itself, which is necessary for accident prevention.

The heating temperature of the contact elements of the current collector can be measured by temperature sensors (thermocouples) 11 type THK - 0001.

Table 6.4 shows the classification of modern systems used to control the quality of current collection.

Table 6. – Classification of control systems

System	**By location**	**According to the principle of obtaining information**	**According to the controlled parameter**
Automatic Pantograph Inspection system	On the infrastructure	Video control	Geometric parameters
Sicat PMS	On the infrastructure	Mechanical control	Displacement
PantoInspect	On the infrastructure	Video control	Geometric parameters
PANTOBOT	On the infrastructure	Video control	Geometric parameters
Pantograph Damage Monitoring System	On the rolling stock	Mechanical control	Acceleration
Automatic Pantograph Monitoring of Carbon Strips	On the infrastructure	Video control	Geometric parameters
The control system of the laboratory wagon of "NIIEFA-ENERGO" LLC	On the rolling stock	Video control, mechanical control	Geometric parameters, acceleration, displacement
System " YZNOS"	On the rolling stock	Video control	Geometric parameters



Figure 6.11 – An example of the Sicat PMS control system of the Siemens company.



Figure 6.12 – An example of the Pantograph Damage Monitoring System

6.6.4 The results of the study on the determination of quantitative and qualitative indicators of the interaction of the current collector with the overhead line

In the process of interaction of the current collector with the overhead line, complex dynamic and physical processes occur, which can be evaluated by several indicators, the measurement and control of which is proof of the safety and quality of the current collection system.

Based on syllogistic studies, the following qualitative and quantitative indicators of the interaction of current receivers with the overhead line were determined (Figure 6.13).

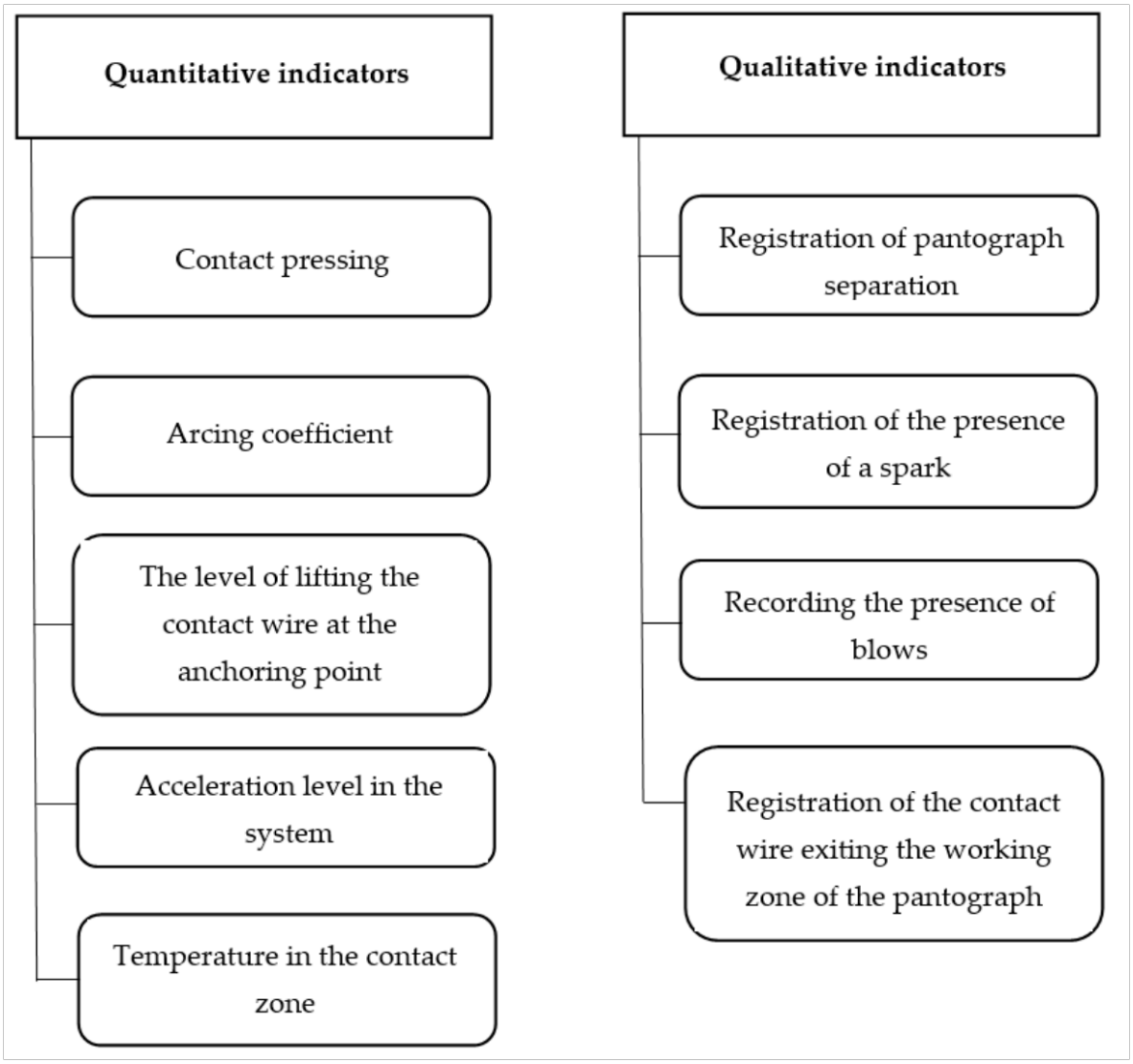

Figure 6.13 – Qualitative and quantitative indicators of the interaction of current collectors with the overhead line.

Quantitative indicators of the interaction of current collectors with the overhead line:

• contact pressure - a vertical force exerting pressure on the contact wire through the current collector. Contact pressure is the sum of forces from all contact points of the current collector.

• percentage coefficient of arc formation

• the level of acceleration in the " current collection - overhead line " system

• the level of lifting of the contact wire at the anchoring point when passing the current collector

• temperature in the contact zone.

Qualitative indicators of the interaction of current receivers with the overhead line:

• registration of disconnections of the current collections from the overhead line

• registration of the presence of sparking

• registration of the presence of blows

• registration of the exit of the contact wire beyond the working zone of the pantograph.

In addition, to the above-mentioned qualitative and quantitative indicators, when monitoring the interaction of current collectors with the overhead line, operational conditions (speed of the train, its location) and environmental conditions (rain, ice, temperature, wind, tunnel) should be considered, as well as the layout (characteristics and placement of current collectors, type of contact suspension) during measurements. This additional data ensures reproducibility of measurements and comparability of measurement results.

6.6.5 Full-scale tests on determining the index of interaction of the pantograph and contact network (measurement of accelerations)

To register readings, a software-hardware complex is used, which consists of a NI 9012 cRIO controller with an NI 9205 ADC module and software developed in the LabVIEW software package. The speed of the train and its position on the route were determined using the SEA cRIO Gxxx Mobile GPS receiver module with a sampling frequency of 8 Hz, and vibration accelerations were recorded using an NI9205 ADC with a frequency of 500 Hz. Three-axis accelerometers with a measurement range of ± 50 m/s^2 were used to record acceleration readings. The arrangement of accelerometers on the pantograph is shown in Figure 6.14.

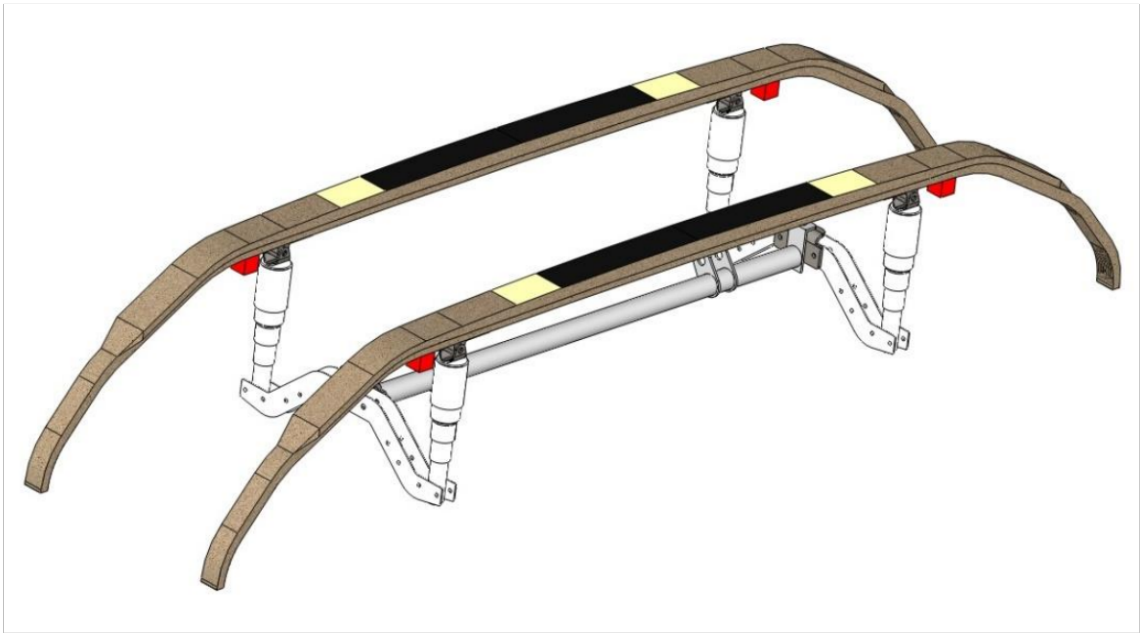

Figure 6.14 – Scheme of placement of accelerometers on the pantograph.

The general view of the installed system on the rolling stock is shown in Figure 6.15.



Figure 6.15 – General view of the measuring system on the pantograph.

As a result of the tests carried out on some sections of the experimental route, excess accelerations of the pantograph skids were recorded, which indicates malfunctions in the overhead line. Recorded data, acceleration, and location, are immediately transmitted to the server and enable the relevant services to quickly eliminate malfunctions. An example of recorded malfunctions is shown in Figure 6.16—6.18.

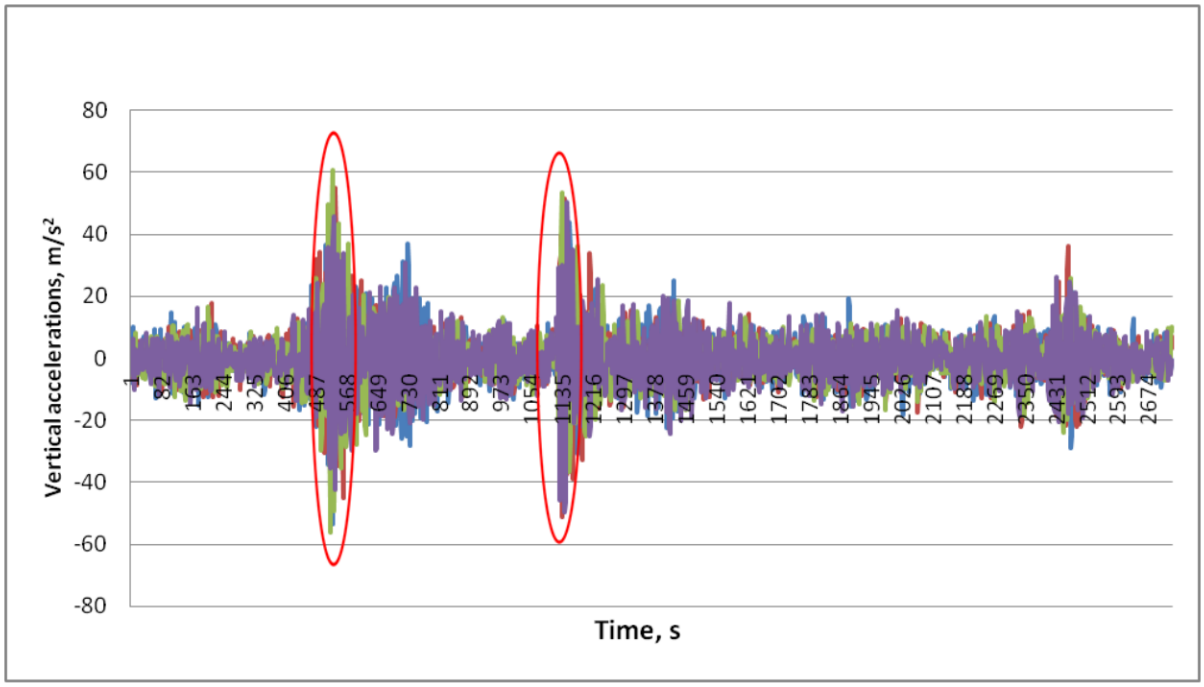

Figure 6.16 – Vertical accelerations of the pantograph bottom bracket

St. Gogoleve - St. Matyashivka (+ 604 m from Gogoleve station).

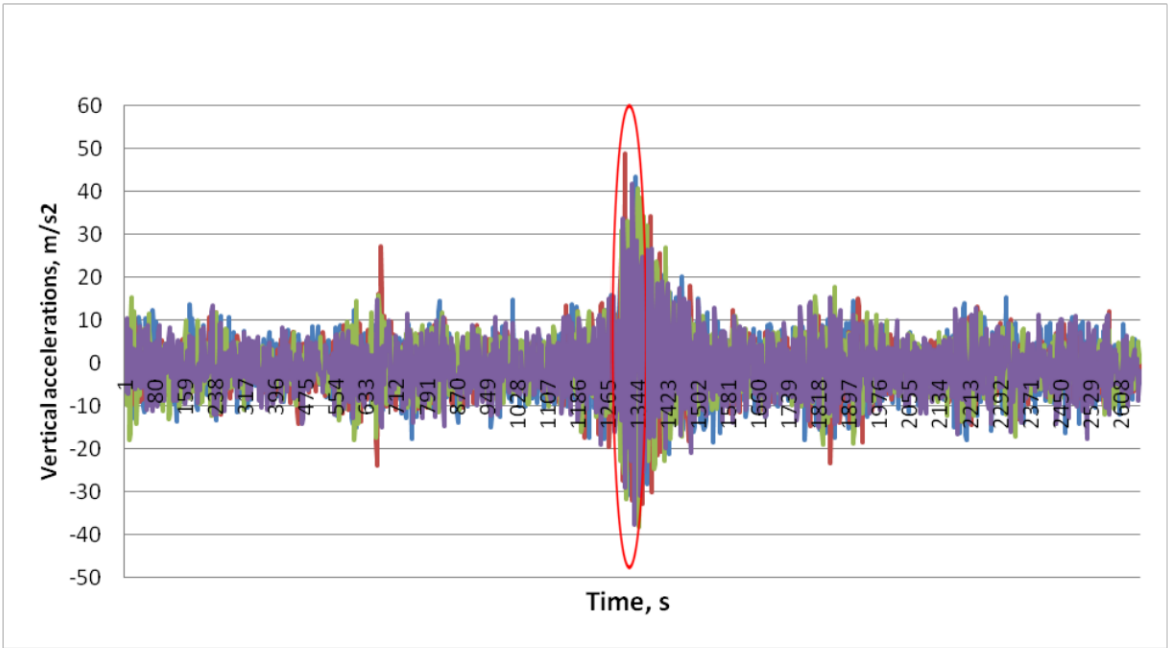

Figure 6.17 – Vertical accelerations of the pantograph bottom bracket St. Paris Commune – St. Petrovska Sloboda (+1.14 km from Paris Commune station).

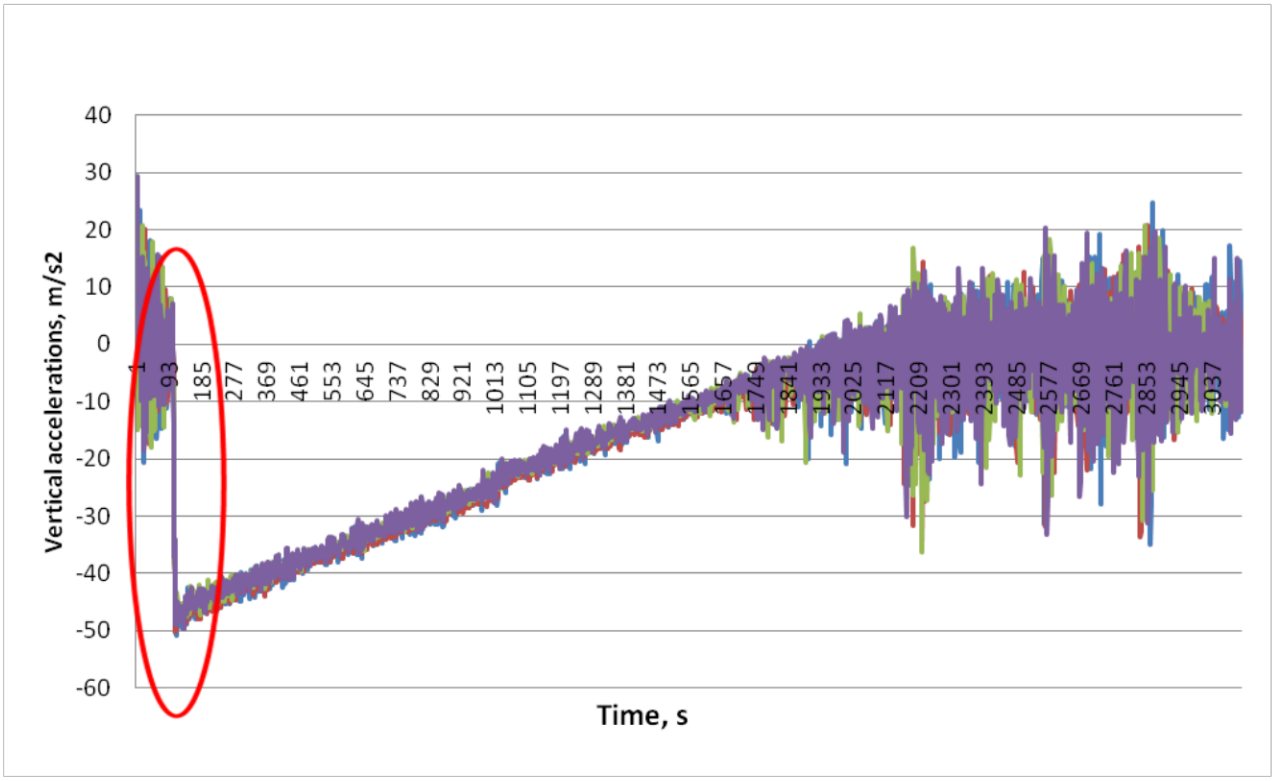

Figure 6.18 – Accelerations of the pantograph bottom bracket St. Pharmaceutichna - St. Forestry (+981 m from the station Pharmaceutichna).

6.6.6 Discussion

According to the results of the analysis of the consequences of impaired current collection, it was established that the most rational way to solve problems with the interaction of the current collector and overhead line can be considered the improvement of current collectors, as well as in-depth studies of current collection processes in steady and transient modes.

In steady state, unsatisfactory current collection can lead to:

a) to the catastrophically increasing wear of contacting elements (at the same time, the movement of trains may last for some time)

b) damage with delay of trains; separation, which lead to annealing and re-annealing of the wire; to circular fire on the collectors of traction engines; to an unacceptable increase in radio and television interference; as well as to detachment, accompanied by shocks, which cause a decrease in the reliability of fastening parts; to periodic increase in contact pressure, etc.

Thus, in the stable mode, the economic (with little wear) and reliable (without damage) current collection process becomes the decisive factor. Current collection problems in this case are solved by improving the characteristics of contact suspensions and improving current collectors. Each path also includes improving the antifriction properties of contact materials.

In transient modes, an unsatisfactory process of current collection leads not only to the burning of wires, but also to the breakdown of elements of current collectors and contact suspensions due to the short-term appearance of vertical and horizontal longitudinal and transverse forces, to unacceptable changes in the characteristics and parameters of nodes during operation, etc.

The causes of such damage can be:

- horizontal forces from the contact wire
- collisions when lifting and lowering the current collector.
- collisions against obstacles on the contact wire
- insufficient current collector lowering time and knot strength.

- side wind
- lack of proper control in operation
- vertical and transverse vibrations of the body.

As a result of the analysis of the existing current collection quality control systems, they can be classified according to the following parameters.

According to the location, the existing systems can be conditionally divided into those installed on rolling stock – passenger wagons, laboratory wagons, and those installed on infrastructure elements - under overpasses, overhead line supports, and other fixed structures located near the track.

According to the controlled parameters, the existing systems can be conditionally divided into those that control:

- geometric parameters of the interaction between the pantograph and the contact wire
- geometric parameters of graphite inserts
- temperature characteristics of the contact area
- accelerations occurring in the pantograph - contact wire system.
- moving the contact wire.

According to the principles of obtaining information, systems can be divided into those based on the principles of video control, thermographic control, and mechanical control.

Video control involves the use of a video camera as the primary source of information, which allows you to receive images with a high frequency (more than 30 frames/sec) and a resolution sufficient to reliably distinguish the overhead line, pantograph parts, suspension elements, etc. Processing of the received information takes place in a computer system using specific software that implements various methods of image processing using machine vision methods. This approach allows you to "recognize" the contact wire, the suspension, the characteristic points of the pantograph, which in turn can be used to build a profile of the movements of the

contact wire relative to the pantograph, fix the exit of the contact wire outside the optimal zone of contact with the pantograph, register vertical and horizontal movements pantograph, etc.

Processing can take place both in real time with the simultaneous issuance of control results to the operator (if the control system is located based on the laboratory wagon) and after set time intervals.

The number of video cameras may differ in different systems. The simplest options involve the use of only one camera placed both directly and against the direction of movement of the wagon. More complex ones can have 2 or more cameras. The increase in the number of sources of primary video information makes it possible to evaluate the geometric characteristics of the interaction of the pantograph with the contact wire in a larger number of geometric dimensions.

Thermographic control is like video control in many ways. In this case, a thermal imager is used as the primary source of data, which captures the temperature change in the area of the point of contact between the wire and the pantograph. An increase in temperature can indirectly indicate the quality of the current and indicate the presence of an electric arc. Video information from the thermal imager can be used to determine the geometric position of the contact wire relative to the pantograph, to track the movement of the pantograph.

Mechanical control involves the registration in various ways of mechanical vibrations that occur during the interaction of the pantograph with the contact wire during movement. As primary converters can accelerometers recording pantograph acceleration, wear sensors, strain gauges, etc. should be used.

Based on the results of the analysis conducted, an experimental measuring complex was developed to determine the indicators of the interaction of the pantograph with the overhead line (measurement of vibration accelerations of the pantograph). The complex consists of a NI 9012 cRIO controller with an NI 9205 ADC module and software developed in the LabVIEW software package. The speed of the train and its position on the route were determined using the SEA cRIO Gxxx

Mobile GPS receiver module with a sampling frequency of 8 Hz, and vibration accelerations were recorded using an NI9205 ADC with a frequency of 500 Hz. Three-axis accelerometers with a measurement range of ± 50 m/s2 were used to record acceleration readings. The results of the experimental studies showed the efficiency of this complex and the recorded data make it possible to determine problem areas in the overhead line on the route of the experimental trip with a location accuracy of ±9.6 m.

CONCLUSIONS ON SECTION 6

General requirements for the software and hardware complex are formulated to determine the dynamic load of the chassis under operating conditions of the rolling stock.

Technical solutions have been implemented regarding the means of conducting running tests of rolling stock to determine the dynamic load of the running gear under operating conditions, which increases the efficiency of predicted assessments and increases the efficiency of testing.

A set of software subsystems has been developed to collect measurement information, determine the level of ride comfort, smoothness and safety indicators of rolling stock using simplified schemes.

The following conclusions were made based on the conducted research on the determination of quantitative and qualitative indicators of the interaction of current collectors with the overhead line in operating conditions:

- Based on syllogistic studies of the experience of other countries in the technical diagnosis of the overhead line and its interaction with the pantograph, a classification of existing systems was developed with an analysis of the main principles of operation, and quantitative and qualitative

indicators of the interaction of the current collector with the overhead line were determined.

- Modern systems used to control the quality of current collection in most cases are combined and combine mechanical and telemetric approaches to measuring the required values.
- An experimental measuring complex has been developed to determine the basic indicators of the interaction of the pantograph with the overhead line (measurement of vibration accelerations of the pantograph) in operating conditions, which allows in real time with an accuracy of ± 9.6 m to determine deviations from the norms of maintenance of the overhead line, which in turn, allows promptly appropriate services to eliminate detected malfunctions.

GENERAL CONCLUSIONS

1. The scientific and technical materials aimed at determining and evaluating movement quality indicators were reviewed and analyzed, the problems of wagon operation were analyzed, and the problems of experimental evaluation of movement quality and safety indicators were analyzed. An analysis of research and existing systems for evaluating indicators of traffic quality and safety was carried out, a review of technical solutions that improve indicators of quality and safety of traffic of freight wagons was carried out. The need for the development of scientifically based recommendations regarding direct measurements of the forces of interaction between wheels and rails to determine the actual margin of stability of wheel pairs from derailment was noted.

2. A method for in-depth processing of the results of rolling stock running tests is proposed. The essence is to perform a spectral analysis of dynamic processes for various elements of the load-bearing structures of a freight wagon in order to identify the relationships between the oscillatory processes of the load-bearing structures and the frequencies at which the interaction between them occurs. A software algorithm has been developed for in-depth assessment of experimental indicators of the quality of movement of freight wagons with reduced tare.

3. The general requirements for the mobile system for determining the quality and safety indicators of the movement of freight wagons with reduced tare in operation have been formulated and implemented. This mobile system allows running tests without involving the laboratory wagon, which reduces costs and time for conducting such tests by 25.8%.

4. According to the results of practical studies of freight wagons with reduced tares, it was established that a decrease in the tare mass index by more than 10% negatively affects the indicators of the quality of movement of such wagons, and a

speed range of 60-70 km/h was revealed, during which a sharp deterioration of traffic dynamics indicators was recorded in a number of experimental wagons.

5. A safe scheme of train formation, which includes freight wagons with reduced tare, is proposed. Obtained during running dynamic tests, the values of compressive forces acting on autocoupling devices of wagons and reaching or exceeding critical values in the main and middle parts of the train according to the following schemes. It is advisable to place empty wagons in the last third of the train.
6. A new method for measuring contact forces has been proposed: through the deformation of the wheel disks of wheelsets, its high efficiency and promise have been confirmed through experimental and theoretical studies. Technical proposals and recommendations have been developed for the method of directly measuring the forces of interaction between wheels and rails:

- based on the results of simulation and experiment, a scheme for placing strain gauges on the inner surface of the wheel disc was developed. This scheme includes points that are most sensitive to vertical and lateral loads; connection schemes of strain gauges are recommended;

- technical proposals for installing strain gauges on the surface of the wheel disc and mounting the measuring equipment on the wheel pair are provided;

- recommendations and technical proposals for carrying out tare work are provided: for tare in the vertical direction, it is recommended to use the wheel-by-wheel weighing method, and for tare in the horizontal direction, a set of equipment is proposed that ensures the load on the wheels of the wheel pair.

7. The proposed method of measuring contact forces makes it possible to directly measure contact forces, thereby evaluating real traffic safety indicators for a given type of rolling stock, in contrast to the existing method: measurement by deformations of bogie frames, which gives only an indirect assessment and does not apply to the conditions of passenger train traffic above 140 km/h

8. The general requirements for the software and hardware complex for determining the dynamic load of running parts in the conditions of operation of the

rolling stock are formulated. Technical solutions have been implemented regarding the means of running tests of rolling stock to determine the dynamic loading of running parts in operating conditions, which increases the effectiveness of forecasted assessments and increases the efficiency of testing.

9. A complex of software subsystems for collecting measurement information, determining the level of driving comfort, smoothness of movement and safety indicators of rolling stock according to simplified schemes has been developed.

10. The following conclusions were made based on the conducted research on the determination of quantitative and qualitative indicators of the interaction of current collectors with the overhead line in operating conditions:

- Based on syllogistic studies of the experience of other countries in the technical diagnosis of the overhead line and its interaction with the pantograph, a classification of existing systems was developed with an analysis of the main principles of operation, and quantitative and qualitative indicators of the interaction of the current collector with the overhead line were determined.
- Modern systems used to control the quality of current collection in most cases are combined and combine mechanical and telemetric approaches to measuring the required values.
- An experimental measuring complex has been developed to determine the basic indicators of the interaction of the pantograph with the overhead line (measurement of vibration accelerations of the pantograph) in operating conditions, which allows in real time with an accuracy of ± 9.6 m to determine deviations from the norms of maintenance of the overhead line, which in turn, allows promptly appropriate services to eliminate detected malfunctions.

REFERENCES

1. Marye G. Interaction of track and rolling stock. Marye G. - M.: Goszheldorizdat, 1933. - 338.

2. Nadal MJ Locomotives a Vapeur Collection Encyclopedia Scintifique Biblioteque de Mecanique Applique et Genie, Vol. 186, (Paris), 1908.

3. Mishchenko K.N. The current state of the issue of re-attaching the wheel to the rail. K.N. Mishchenko. Proceedings of DIIT. 1950. Issue. XX. pp. 53-67.

4. Bromberg E.M. Interaction between track and rolling stock. EAT. Bromberg, M.F. Verigo, V.N. Danilov, M.A. Frishman; Under general ed. M.A. Frishman. M.: Gostranszheldorizdat, 1956. 280 p.

5. Verigo M.F. Interaction between track and rolling stock. M.F. Verigo, A.Ya. Kogan. M.: Transport, 1986. 559 p.

6. Verigo M.F. Issues of interaction between track and rolling stock and issues of track calculation. M.F. Verigo. Proceedings of the Central Research Institute of Railways. 1963. Issue. 286. 125s.

7. Vershinsky S.V. Dynamics of a car: a textbook for railway universities. transport. S.V. Vershinsky, V.N. Danilov, I.I. Chelnikov. M.: Transport, 1978. 352 p.

8. Masliev V.G. Dynamics of a locomotive with a device for radial installation of wheel pairs in curves. V.G. Masliev. Newsletter of Skhidnoukr. national. university Technical sciences. Transport series. 2002. No. 6(52). With. 69-74.

9. Verigo M.F. Modernization of spring suspension of bogies type MT-50. M.F. Verigo, L.O. Gracheva, P.S. Anisimov. VNIIZHT. 1968. VIP. 372. 112 p.

10. Kondratyev V.F. About the derailment of a wheel. V.F. Kondratiev. VNIIZHT Newsletter. 1980. No. 6. pp. 23-25.

11. Pogorelov D.Y. A criterion for assessing the danger of rolling stock derailing by rolling a wheel onto the rail head. D.Y. Pogorelov, V.A. Simonov. Rolling stock of the 21st century: ideas, requirements, projects. 2009. pp. 136-138.

12. Pogorelov D.Yu. An indicator for assessing the danger of rolling stock derailing by rolling a wheel onto the rail head. .YU. Pogorelov, V.A. Simonov. Newsletter of the Eastern Ukrainian National University named after V. Dahl. 2010. No. 5(147). Part I. pp. 64-70.

13. Azovsky A.P. On assessing the stability margin of a wheel against rolling onto the rail head. A.P. Azovsky, V.N. Koturanov M.N. Ovechnikov, I.V. Plotnikov. Collection of articles from the international conference “Train Safety”. M.: MIIT. 2007. P.VI-1-VI-2.

14. Koturanov V.N. Methodology for calculating the stability margin of a wheel against derailment. V.N. Koturanov, D.V. Ivanov, A.G. Petrov et al. Proceedings of the conference “Traffic Safety”. M.: MIIT. 2010. P.7-24.

15. Kogan A.Ya. The relevance of the construction of a high-speed railway passenger line in St. Petersburg. Moscow (St. Petersburg Conference). 2004.

16. Trofimov A.N. On the stability of rolling stock against derailment. A.N. Trofimov. Proceedings of DIIT. 1983. Vol. 228/25. pp. 23-26.

17. Vinnik L.V. Notes on the use of the Nadal criterion when assessing derailment safety. L.V. Vinnik, G.P. Buchak. Newsletter of the Eastern Ukrainian National University named after V. Dahl. 2005. No. 8(147). Part 1. pp. 108-113.

18. Ishizawa M. Car bogies of the New Tokaido Line and the results of their use. M. Ishizawa, N. Mitsui, S. Otsuka. Monthly newsletter of the MAJK. 1969. No. 2. pp. 3-27.

19. Elkins J. New Criteria for Flange Climb Derailment. J. Elkins, Wu. Huimun. 2000 ASME/IEEE Joint Railroad Conference, April 4-6. 2000. P. 1-7.

20. Weistock H. Whell Climb Derailment Criteria for Evaluation of Rail Vehicle Safety. Paper no 84 – WA/RT – 1, ASME Winter Annual Meeting. 1984. P. 34-42.

21. Klokova N.P. Strain gauges: Theory, calculation methods, development. M.: Mechanical Engineering, 1990. - 224 p.

22. Fomin O.V., Prokopenko P.M. Theoretically - experimentally determined the coefficient of stability of a flat car in storage due to operational-degradative changes in packaging. Newsletter of SNU im. V. Dahl. Severodonetsk. 2018. No. 2(243). pp. 225-232

23. Fomin O.V., Prokopenko P.M., Fomina A.M. Experimental evaluation of the indicators of the ductility of the flat car in the minds of operation. Collection of scientific works of the State University of Infrastructure and Technology, series "Transport systems and technologies. 2018. No. 32 volume 1. Kiev. pp. 126-134.

24. Oleksij Fomin, Juraj Gerlici, Alyona Lovska, Mykola Gorbunov, Kateryna Kravchenko, Pavlo Prokopenko, Vladimir Hauser. The improved hatch cover construction for universal open box-type wagon from the strength and durability point of view. Manufacturing Technology. 2019. Vol. 19. No. 2. R 216-221. (The data is indexed in the Scopus database).

25. Fomin O.V., Prokopenko P.M., Gorbunov M.I., Fomina A.M. Evaluation of the performance of the hull of passenger cars in the train warehouse. Newsletter of SNU im. V. Dahl. Severodonetsk. 2019. No. 2(250). pp. 103-109

26. Fomin O.V., Prokopenko P.M., Sapronova S.Yu., Fomina A.M. Experimental evaluation of the indicator of durability coefficient of pull-out cars in operation. Collection of scientific works of the State University of Infrastructure and Technology, series "Transport systems and technologies. Kyiv. 2019 No. 33 volume 1. pp. 144-155.

27. Fomin Oleksij, Lovska Alyona, Daki Olena, Bohomia Volodymyr, Tymoshchuk Olena and Prokopenko Pavlo. The substantiation of the concept of creating containers with viscous-elastic connections in fitting. ARPN Journal of Engineering and Applied Sciences. VOL. 14 No. 15. 2019. R 2771-2776. (The data is indexed in the Scopus database).

28. Fomin A.V., Prokopenko P.N., Gorbunov N.I., Sova S.S. A method for assessing the quality indicators of the movement of lightweight empty cars. Collection of scientific works of the State University of Infrastructure and Technologies. Series “Transport systems and technologies”. Kyiv. 2020. No. 35. pp. 44-51.

29. Fomin O.V., Kara S.V., Prokopenko P.M., Gorbunov M.I., Fomin V.V. Assessment of the dynamic components of the ruk of re-equipped hopper cars after normal operation. Collection of scientific works of the State University of Infrastructure and Technologies. Series “Transport systems and technologies”. Kyiv. 2020. No. 36. pp. 33-42.

30. Fomin O.V., Kara S.V., Prokopenko P.M., Gorbunov M.I., Fomin V.V. Investigation of the dynamics indicators of empty passenger cars from the restoration of operational indicators. Newsletter of SNU im. V. Dahl. No. 20. 2021. pp. 22-32.

31. Fomin O.V., Prokopenko P.M. Theoretical aspects of testing platform cars with operational-boundary modified packaging. Collection of scientific proceedings of the VIII International Scientific and Practical Conference “Transport and Logistics: Problems and Solutions” May 23-25, 2018 m. Odessa. Skhidnoukrainsk National University named after V. Dahl. 2018. pp. 132-134.

32. Fomin O.V., Prokopenko P.M. Experimentally determined the coefficient of durability of a platform car in operation. Collection of scientific papers from the scientific and practical conference “Logistics management and safety in transport” November 16-17, 2018. Kyiv. 2018. pp. 229-231.

33. Fomin O.V., Prokopenko P.M., Fomina A.M. Experimental assessment of the ductility of passenger vans. Current problems of daily coverage: realities and prospects. Materials of the All-Ukrainian Conference of Students and Workers of the Western Military District. Abstracts of testimonies from conference participants. Mariupol College DVNZ "Azov State Technical University", May 17, 2019 Mariupol. 2019. pp. 124-125.

34. Fomin O.V., Prokopenko P.M., Sova S.S., Fomina A.M. Theoretical assessment of the excess resource of a testing car. Collection of the Proceedings of the All-Ukrainian Scientific and Practical Conference "Transport Technologies and Road Safety" 14–15 April 2020. Zaporizhzhya. 2020. pp. 47-49.

35. Kara S.V., Petrenko V.O. Prokopenko P.M. Carrying out periodic control testing of trailer cars in order to improve their efficiency. The 7th International scientific and practical conference "Science, society, education: topical issues and development prospects" (June 7-9, 2020) SPC "Sci-conf.com.ua", Kharkiv. 2020. pp. 328 – 330.

36. Fomin O.V., Lovska A.O., Gerlici. J., Fomina Yu.V., Fedosov-Nikonov D.V., Prokopenko P.M. Determination of the patterns of dynamic influence of the non-propelled structure of a closed car when operating from a new fire at a horizontal plane. International scientific and technical conference "Energy efficiency in transport", Kharkiv, November 18-20, 2020: Abstracts of evidence. UkrDUZT. Kharkiv. 2020. pp. 52-53.

37. Fomin A.V., Prokopenko P.M., Gorbunov N.I., Kara S.V. Fomin V.V. Assessment of the dynamic qualities of the car under operating conditions. Collection of the VII international scientific and practical conference "Science and education in the modern world: challenges of the 21st century." October 22, 2020 Nur-Sultan (Kazakhstan). 2020. pp. 105-108.

38. Fomin O.V., Kara S.V., Prokopenko P.M., Gorbunov M.I., Fomin V.V. Inflow into intermodal container transportation of wagons with operational-border changed packaging. Collection of materials from the international scientific and practical conference "Dnieper Readings-2020". Breast 23, 2020, m. Kiev. 2020. pp. 186-189.

39. Kelrikh M.B., Fomin A.V. Prokopenko P.N. Assessment of the dynamic qualities of the platform under operating conditions. Materials of the X International Scientific and Practical Conference "Problems of Transport Safety". Part 5.

"Belarusian State University of Transport". November 26-27, 2020. Republic of Belarus, Gomel. 2020. pp. 73-74.

40. Prokopenko P.M., Technical diagnostics of hopper cars for transporting waste products and agglomerates with the term of service that exceeds the normative ones. Collection of scientific works - Young scientist: State University of Infrastructure and Technologies. Kyiv. 2018. No. 2. pp. 57-61.

41. Fomin O.V., Prokopenko P.M. Assessing the excess resource of trailer cars in terms of service, which exceeds the standard. Transport transport in Ukraine. Kyiv. 2018. No. 4. P. 37-48

42. Kelrikh M.B., Braykovska N.S., Fomin O.V., Prokopenko P.M. Features of the testing of the tank car for unsafe installations. Scientific journal – Newsletter of the Shidnoukrainian National University named after Volodymyr Dahl. Severodonetsk. 2019. No. 3(251). pp. 77-83.

43. Fomin O.V., Prokopenko P.M., Burlutsky O.V., Fomina A.M. Control testing of a tank car with a method of assessing the excess life of load-bearing structures. "Vcheni notes of the Tavria National University named after V.I. Vernadsky. Series: Technical Sciences. Kyiv. Volume 30 (69) Part 2 No. 5. 2019. P. 154-159.

44. Kelrikh M.B., Fomin O.V., Prokopenko P.M., Sova S.S. Theoretical aspects of the allocation of excess resource of a tank car for unsafe vehicles. Newsletter of the Ukrainian National University named after Volodymyr Dahl. Severodonetsk. No. 5 (261). 2020. pp. 5-9.

45. Fomin O.V., Gorbunov M.I., Kara S.V., Prokopenko P.M., Grindey P.O. Upgrading of cast parts of heavy-duty vans based on the results of significant global accidents. Newsletter of the Ukrainian National University named after Volodymyr Dahl. Severodonetsk. No. 19. 2020. pp. 1-7.

46. Fomin O.V., Prokopenko P.M. Gorbunov M.I., Kara S.V., Fomin V.V. Assessment of the value of the non-structural structures of a trailer car with the

treatment of their degradation changes. Newsletter of the Ukrainian National University named after Volodymyr Dahl. Severodonetsk. No. 19. 2020. pp. 8-16.

47. O.V. Fomin, P.M. Prokopenko, A.O. Lovsky. Technical diagnosis of surfaces with a terminal service which remains a semiconductor from a normative. Abstracts of the international scientific and technical conference “Technologies and infrastructure for transport”. Kharkiv. May 14-16, 2018. pp. 512-513.

48. Kelrikh M.B., Braykovska N.S., Fomin O.V., Prokopenko P.M. Features of the testing of a tank car for unsafe installations. Collection of scientific proceedings of the IX International Scientific and Practical Conference “Transport and Logistics: Problems and Solutions” May 22-24, 2019. Odessa. 2019. pp. 76-79.

49. Fomin O.V., Prokopenko P.M. Investigation of load-bearing systems of cars with a method of assessing their excess resource. Materials of the 79th International Scientific and Practical Conference “Problems and prospects for the development of urban transport” 16-17 May 2019. Dnipro. 2019 pp. 88-89.

50. Fomin O.V., Prokopenko P.M., Fomina A.M. Technical assessment of the excessively fragile metal structure of the car. Collection of reports from the 2nd Regional Scientific and Practical Conference “Transport systems and technologies: problems and prospects for development” 12th quarter 2019. Zaporizhzhya. 2019. pp. 24-26.

51. Kelrich M., Braikovskaya N., Fomin O., Prokopenko P. Features of research results of liquid cargo in a railway cister during movement.Globalization of scientific and educational space. Innovations of transport. Problems, experience, prospects: thesis, 5-10 May 2020. Georgia. 2020. P. 27-30.

52. M. Kelrykh, O. Fomin, J. Gerlici, P. Prokopenko, K. Kravchenko and T. Lack. Features of tank car testing for dangerous cargoes transportation. IOP Conf. Series: Materials Science and Engineering. No. 659. 2019.

53. Musij Kelrykh, Oleksij Fomin, Juraj Gerlici, Pavlo Prokopenko, Kateryna Kravchenko, Tomas Lack. Tank car testing for dangerous cargoes transportation. Book of Abstracts for the 9th International Scientific Conference [on]

Research and Development of Mechanical Elements and Systems, IRMES 2019, 5-7 September 2019. Kragujevac, Serbia. 2019. R. 226-227.

54. Oleksij Fomin, Angela Shvets, Vladimir Hauser, Pavlo Prokopenko. Transversal displacement of freight wagons bogies. Proceedings abstracts for the international scientific conference dynamics of rigid and deformable bodies. October 9-11. 2019. Estí nad Labem, Czech Republic. 2019.

55. Fomin O.V., Prokopenko P.M., Krisenko N.M., Sova S.S. Control testing of a tank car with a method of assessing the excess life of load-bearing structures. Materials of the third all-Ukrainian practical-cognitive online conference "Scientific thought of reality and the future" 29 leaf fall - 5 breast. 2019. Ivano-Frankivsk. pp. 52-55.

56. Fomin O.V., Prokopenko P.M., Borovich R.O., Litvinenko A.S. Theoretical features of the allocation of excess resource to non-human structures of a vantage car with a service line that overrides the significance. Materials of the third all-Ukrainian practical-cognitive online conference "Scientific thought of the present and the future." 2019. 29 leaf fall - 5 breasts. 2019. pp. 55-58.

57. Fomin O.V., Prokopenko P.M., Gorbunov M.I., Sova S.S. Assessment of the excess resource of load-bearing structures of a passenger car beyond the boundaries assigned to the term of service. Logistics management and safety in transport: a collection of scientific works of scientific and practical conference, June 14-16, 2019. Severodonetsk. SNU im. V. Dahl. Liman. 2019. pp. 160-164.

58. Kelrikh M.B., Braikovskaya N.S. Prokopenko P.N. Features of conducting research to extend the designated service life of tank cars for the transportation of light powdery cargo. Materials of the IX international scientific and practical conference "Problems of transport security". Part 1. "Belarusian State University of Transport". Republic of Belarus, Gomel. 2019. pp. 158-160.

59. Fomin O.V., Gorbunov M.I., Kara S.V., Prokopenko P.M. The upgrading of cast parts for vantage carriages will lead to the development of systems for diagnosing the largest vantage areas. The 1st International scientific and practical

conference “Science and education: problems, prospects and innovations” (October 7-9, 2020) CPN Publishing Group. Kyoto, Japan. 2020. pp. 472 – 477.

60. Dyomin Yu.V., Chernyak G.Yu. Fundamentals of wagon dynamics: Study guide. - K.: KUETT, 2003. - 270 p.

61. Fomin, O.V. Optimization design of elements of railway semi-car bodies and organization of their production: monograph/ O.V. Fomin. – Donetsk: DonIZT UkrDAZT, 2013. – 251 p.

62. Fomin, O.V. Study of defects and damage of the bearing systems of railway half-cars: monograph/ O. V. Fomin. - Kyiv: DETUT, 2014. - 299 p.Theoretical foundations for conceptually new rolling stock modules. Part 1: monograph / Gorbunov M. I, Fomin O. V, Kovalenko V. V, Domin R. Yu. ; Volodymyr Dahl East Ukrainian National University. – Dnipro : Akcept PP, 2017. – 100 p. https://www.researchgate.net/publication/336835679_THEORETICAL_FOUNDATIONS_FOR_CONCEPTUALLY_NEW_ROLLING_STOCK_MODULES_Part_1

63. Theoretical aspects of applied transport mechanics. part 1:monograph / O.V. Fomin, M. I. Gorbunov, O. V. Burlutski, end other. – Sievierodonetsk: Volodymyr Dahl East Ukrainian National Universit, 2019. – 198 p http://dspace.snu.edu.ua:8080/jspui/handle/123456789/2876

64. Fomin, O., Lovska, A.; Fomin, O. (Ed.) (2020). Concept of freight wagons made of round pipes. Tallinn: Scientific Route, 72. doi: https://doi.org/10.21303/978-9916-9516-3-7 http://monograph.route.ee/rout/catalog/book/16

65. Fomin, O.V. et al. (2021). Controlled heat straightening for the rolling stock structures to restore their serviceability // Monograph. – Ostrava, Czech Republic. Hlučín: Anisiia Tomanek OSVČ. – 2021. – 119 p. ISBN 978-80-908088-7-4 DOI 10.47451/book2021-09-01 http://tuculart.eu/store/books/2021-09-01/

66. O.V. Fomin, A.O. Lovska. Dynamics and durability of freight wagons with nominal(drawing) dimensions and taking into account abrading action:

Monograph. Riga, Latvia : Baltija Publishing,2021. 212 p.. DOI 10.30525/978-9934-26-156-5 http://baltijapublishing.lv/omp/index.php/bp/catalog/book/203

67. Fomin, O., & Lovska, A. (2022). Improved models and constructs of structural interaction in railway container transportation // Monograph. – Ostrava, Czech Republic. Hlučín: Tuculart Edition. – 2022. – 114 p DOI: 10.47451/book2022-02-01 (http://tuculart.eu/store/books/2022-02-01/)

68. Fomin, O., and A. Lovska. Temperature effects on railway rolling stock components (Part 1). Dallas, USA: Primedia eLaunch LLC, 2022. 144 p. DOI 10.36074/teorrsc-monograph.2022 https://publishing.logos-science.com/index.php/primedia/article/view/285

69. Fomin, O. Determination of vertical dynamics for a standard ukrainian boxcar with Y25 bogies / O.V. Fomin, A. O. Lovska // Scientific Bulletin of National Mining University. 2021, Issue 5, p.67-72 https://doi.org/10.33271/nvngu/2021¬5/067 http://www.nvngu.in.ua/index.php/en/archive/on-the-issues/1870-2021/content-5-2021/5990-67

70. Samsonkin V.M., Chernyak G.Yu. Before assessing the risks of building a dry warehouse with slats on a computer modeling stand. Transport transport in Ukraine. 2012. No. 2. P.39–42.

71. Mostovich A.V. Improvement of methods and methods of experimental evaluation of indicators of the safety of the roller and the smoothness of the run of a wet roller warehouse. Dissertation for the development of the scientific level of a candidate of technical sciences for the specialty 05.22.07 - dry goods warehouse, climbing and train traction: stolen 05.30.2016, approved by the decisions of the attestation board of the Ministry of Education and Science of Ukraine 09.29.2016. Skhidnoukrainsk National University named after Volodymyr Dahl, Severodonetsk, 2016. 276 p.

72. Fomin, O.V. A software-calculating complex for determining the optimal characteristics of warehouse elements of vans. Collection of scientific works of the Donetsk Institute of Health Transport of the Ukrainian State Academy of Health Transport. Donetsk: DonIZT, 2013. VIP. 34. pp. 105-112.

73. Fomin, O.V. The theoretical foundations of the software complex are designed and developed for mathematical models of warehouse vans. Scientific journal "Bulletin of the Kremenchutsk National University named after Mikhail Ostrogradsky." Kremenchuk: KDPU, 2013.Vip. 6(83). pp. 87-91.

74. Vinokurov, M.V. Studies of vibrations and stability of cars. Dnepropetrovsk 1939. Issue. 12. 392 p.

75. Verigo, M.F., A.Ya. Kogan. Interaction between track and rolling stock. Transport. 1986. 559 p.

76. Verigo, M.F. Interaction of track and rolling stock in small radius curves and combating lateral wear of rails and wheel flanges. PKTB CPU MPS. 1997. 207 p.

77. M.F. Verigo, G.I. Petrov, V.V. Khusidov. Simulation modeling of interaction forces between the crew and the track. Bulletin OS D. No. 6. 1995. P. 3-8.

78. Kalnitsky, L.A. The influence of nonlinearity of elastic elements of spring suspension on the driving performance of railway cars. Abstract of dissertation. Dr. Tech. Sci. 1969. 41 p.

79. Pogorelov D.Yu. Modeling of mechanical systems with a large number of degrees of freedom. Numerical methods and algorithms. Abstract of dissertation. Doctor of Physics mat. Sci. Bryansk. 1994. 26p.

80. Pogorelov D.Yu., A.E. Pavlyukov, T.A. Yudakova Development of a mathematical model of a railway carriage in software for automated synthesis of equations of motion. Information technologies in modeling and control: collection. scientific Proceedings of the II International Scientific and Practical Conference, June 20-22, 2000. St. Petersburg 2000. pp. 298-300.

81. Chernyak A.Yu., Diomin Yu.V., Zakhovaiko O.P., Shevchuk P.A. Computer modeling of the dynamics of rack transport vehicles. News of the National News. tech. University of Ukraine "Kiev Polytechnic Institute". Machine-building series. 2014. – 94-98.

82. Chernyak A.Yu. Application of computer modeling to determine the probable causes of derailment of freight cars. Railway transport of Ukraine. No. 3,

2009. – P. 49 -52.

83. Chernyak A.Yu. Computer model for prompt determination of the probable causes of derailment of freight cars. News of Skhidnoukrain. national univer. im. V. Dahl. Sci. zhur. No. 5(147) Part. 1, 2010. – P. 40 - 46.

84. Samsonkin V.M., Chernyak G.Yu. Before assessing the risks of building a dry warehouse from slats on a computer modeling stand, Zalizny Transport. Ukraine. – 2012. – No. 2. – P.39–42.

85. Chernyak G.Yu. The method of assessing the significance of factors in the risk of creating a dry warehouse with slats. News of Skhidnoukrain. national univer. im. V. Dahl. Sci. zhur. No. 5(176) Part. 2, 2012. – P. 190 – 194.

86. Chernyak G.Yu., Shcherbina Yu.V. Principles of developing computer models of the dynamics of a dry warehouse (on the example of an electric locomotive of the ChS7 series) // Railway transport of Ukraine. – 2011. – No6. – S. – 47-51.

87. Chernyak A.Yu. Modeling of random disturbances in the “rail vehicle-track” system // Bulletin of Skhidnoukrainsk University. V. Dahl. Tech. Sciences. Ser. Transport 1. – 2003. – No9 (67). - pp. 173-177.

88. Instructions for settling and reducing the number of infections in Ukraine CPU 0269 / E.I. Danilenko, A.M. Orlovsky, M.B. Kurgan, V.O. Yakovlev and others. – K.: TOV “NVP Poligrafservis”, 2012. – 456 p.

89. Cooper J., McGillen K. Probabilistic methods for analyzing signals and systems: Transl. from English M., Mir. 1989.

90. Vorlesungsskript: Technische Mechanik 2 Lecture Notes on Applied Mechanics, Part 2 https://www.researchgate.net/publication/325486028_Vorlesungsskript_Technische_Mechanik_2_Lecture_Notes_on_Applied_Mechanics_Part_2

91. Vorlesungsskript: Technische Mechanik, Teil 3 Lecture Notes Applied Mechanics, Part 3 https://www.researchgate.net/publication/325485861_Vorlesungsskript_Technische_Mechanik_Teil_3_Lecture_Notes_Applied_Mechanics_Part_3

92. Manashkin L.A., Myamlin S.V. On the measurement of vertical forces in freight car bogies. XI International Conference “Problems of transport mechanics”. Theses of the testimony. – Dnipropetrovsk. 2004. P. 115.

93. Licciardello RV Introduction to the Experimental Evaluation of the Dynamics of Railway Vehicles. Rail vehicle dynamics and associated problems. Gliwice: Silesian University of Technology. 2005. P. 89-113.

94. E.P. Blokhin, L.A. Manashkin, E.L. Stambler et al.; Ed. E.P. Blokhina. Calculations and tests of heavy trains. M.: Transport. 1986. 263 p.

95. Bogomaz G.I. Dynamics of railway tank cars. K. Science. thought. 2004. 224 p.

96. Lazaryan V.A., Danovich V.D. Differential equations of plane vibrations of a four-axle rail vehicle moving along a beam lying on an inertial base. In the book: Dynamics and strength of high-speed ground transport. Sci. Dumka, 1976. – P.142-148.

97. Mathematical modeling of vibrations of rail vehicles. V.F. Ushkalov, L.M. Reznikov, V.S. Ikkol et al.; Ed. V.F. Ushkalova. – K.: Science. thought. 1989. 240 p.

98. Pogorelov D. Simulation of Rail Vehicle Dynamics with Universal Mechanism Software. Rail vehicle dynamics and associated problems. Gliwice: Silesian University of Technology, 2005. P. 13-58.

99. V.S. Kossov, V.F. Rudenko, D.Yu. Pogorelov, V.A. Simonov, V.N. Languages. Assessing the safety of train traffic using the Universal Mechanism PC. Transport transport in Ukraine. 2007. No. 3. P.26-29.

100. Cherniak A.Yu. Operational definition of the possible causes of the derailment of freight cars. Prace naukowe Politechniki Warszawskiej. Transport, z. 98. 2013. R. 109-116.

101. Yu.V. Demin, R.Yu. Demin, A.Yu. Chernyak. Mathematical modeling and dynamics of railway rolling stock. Transport transport in Ukraine. 2007. No. 4. P.3–8.

102. Zenkevich O. Finite element method / Transl. z eng. B.E. Win. M.: Mir. 1975. 541 p.

103. Alyamosky A.A. COSMOSWorks. Fundamentals of structural strength calculations in the SolidWorks environment. M.: DMK Press. 2010. 784 p.

104. Alyamosky A.A. Engineering calculations in SolidWorks Simulation. M.: DMK Press. 2011. 464 p.

105. Alyamosky A.A. SolidWorks Simulation. How to solve practical problems. SPb.: BHV-Petersburg. 2012. 448 p.

106. Alyamosky A.A. SolidWorks Simulation. Engineering analysis for professionals: tasks, methods, recommendations. M.: DMK Press. 2014. 562 p.

107. A. Glagovsky, I. D. Piven. Electrical resistance strain gauges. B. Ed. 2nd, revised and additional Leningrad Energy. 1972. 86 p.

108. 85. R. L. Hannah, S. E. Reed. Strain Gage Users'Handbook. London: Chapman&Hall. 1992. 476 p.

109. Blum P. LabVIEW: programming style. Per. from English Ed. Mikheeva P. M. DMK Press. 2008. 400 p.

110. 8LabVIEW for everyone. Kring D. Travis D. Per. from English Ed. P. Mikheeva M. DMK Press. 2011. 904 p.

111. Vasiliev A.S., Lashmanov O.Yu. Basics of programming in the LabVIEW environment. SPb: ITMO University. 2015. 82 p.

112. J. Bendat, A. Piersol. Applied analysis of random data. M: Peace. 1989. 540 p.

113. Dynamic loads of the chassis of freight cars. Ed. N.N. Kudryavtseva. Proceedings of VNIIZhT, vol. 572. M. Transport. 1977. 143 p.

114. V.P. Fedosov, A.K. Nesterenko.Digital signal processing in LabVIEW. M. DMK Press. 2007. 427 p.

115. Yu.V. Demin, L.A. Dlugach, M.L. Korotenko, O.M. Markova. Self-oscillations and stability of movement of rail vehicles. K.: Science. Dumka, 1984. 160 p.

116. Lazaryan V.A., Dlugach L.A., Korotenko M.L. Stability of movement of rail vehicles. K.: Science. thought. 1972. – 200 p.

117. Lazaryan V.A. Vehicle Dynamics: Fav. tr. – K.: Science. Dumka, 1985. – 528 p.

118. Demin Yu.V. Chassis of freight cars and train traffic safety. Transport in Ukraine. 1998. No. 2-3. pp. 13-16.

119. K. Bladon, D. Rennison, G. Izbinsky, R. Tracy, T. Bladon. Predictive condition monitoring of railway rolling stock. Conference On Railway Engineering, Conference Proceedings. Darwin, 2004. P. 22.1-22.12.

120. UIC Code 518.Testing and approval of railway vehicles from the point of view of their dynamic behaviour.Safety – Track fatigue – Ride quality.– International Union of Railways. – September 2009. – 119 p.

121. UIC Code 519.Method for determining the equivalent conicity. – 1st edition, 2004.

122. Code UIC 430-4 OR. Wagons. Circulation entre des réseaux à écartement de 1435 mmet des réseaux à écartement de 1520 mm. Prescriptions techniques et conditions d'homologation. 1re édition, Mai 2004.

123. Code UIC 430-5 O – Regulations for the exchange and use of new generation freight wagons between railways with gauges of 1435 mm and 1520 mm; 1st edition, November 2003.

124. Code UIC 505 - 1 OR. Railway transport stock - Rolling stock construction gauge.

125. Code UIC 510-3 O. Wagons - Essais de résistance au banc des bogies à 2 essieuxet 3 essieux. 1re éditiondu 01.01.89 - Nouveautiragedu 01.07.94.

126. Code UIC 535-2 O - Standardisation and positioning of steps, end platforms, gangways, handrails, tow hooks, automatic coupler and brake valve controls on wagons in connection with the fitting of the automatic coupler of the UIC Member Railways and OSJD Member Railways 3rd edition of 1.1.78 and 7 Amendments.

127. Code UIC 577 OR Wagon stresses* 105 3rd edition, May 2004.

128. CodeUIC581 OR. Wagons – Lifting – Rerailing.1st edition of 1.1.83 and 1 Amendment.

129. EN 12663–2. Railway applications - structural requirements of railway vehicle bodies – Part 2: Freight wagons. B., 2010. 54 c.

130. European Standard 14363. Railway applications – Testing for the acceptance of running characteristics of railway vehicles – Testing of running behaviour and stationary tests. – June 2005. – 113 p.

131. DSTU 7598:2014 Freight wagons. General requirements for calculations and design of new and modernized wagons of 1520 mm gauge (non-self-propelled)

132. DSTU 7774:2015 Main line passenger cars of locomotive traction. General technical standards for calculating and designing the mechanical part of wagons

133. DSTU 7773:2015 Main line passenger cars of locomotive traction. General technical requirements.

134. DSTU GOST 33211:2017 (GOST 33211-2014, IDT) Freight wagons. Requirements for strength and dynamic qualities.

135. DSTU B V.2.3-29-2011 Approximate dimensions of buildings and railway rolling stock, track 1520 (1524) mm. (GOST 9238-83, MOD)

136. DSTU B GOST 9720:2011 Approximate dimensions of buildings and railway rolling stock of gauge 750 mm. (GOST 9720:76, IDT).

137. DSTU EN 15273-2:2018 Railway transport. Dimensions Part 2. Rolling stock (EN 15273-2:2013 + A1:2016, IDT).

138. DSTU EN 15273-3:2018 (EN 15273-3:2013+A1:2016, IDT). Railway transport. Dimensions Parts 3. Construction dimensions.

139. DSTU 7571:2014 Railway rolling stock. Norms of permissible impact on a railway track with a width of 1520 mm.

140. DSTU 7776:2015 Dump wagons (dump trucks). General requirements for calculations and design of new and modernized railway dump trucks with a gauge of 1520 mm.

141. DSTU 3445-96 (GOST 10674-97). Tank wagons of main railways gauge 1520 mm. General technical conditions.

142. DSTU 7530:2014. Two-axle carts of freight wagons of main railways with a gauge of 1520 mm. General technical conditions. – Kyiv, SE UkrNDNC, 2015.

143. DSTU 7776:2015. Dump wagons (dumpcars). General requirements for calculations and design of new and modernized railway dump trucks with a gauge of 1520 mm.

144. DSTU GOST 32700:2016 (GOST 32700-2014, IDT) Railway rolling stock. Methods of controlling adhesion.

145. DSTU GOST 31846:2016 (GOST 31846:2012, IDT) Special rolling stock. Requirements for the strength of load-bearing structures and dynamic qualities.

146. DSTU GOST 15.902:2017 System of development and approval of products for production. Railway rolling stock. Procedure for development and production approval (GOST 15.902-2014, IDT).

147. DSTU UIC 513:2004 Mainline passenger cars. Guidelines for assessing passenger comfort depending on vibration.

148. Standards for the calculation and design of 1520 mm gauge railway carriages of the Ministry of Railways (non-self-propelled). – M.: GosNIIV-VNIIZhT, 1996. 354 p. 146

149. Standards for calculating and assessing the strength of load-bearing elements, dynamic properties and the impact on the track of the undercarriage of locomotives on 1520 mm gauge railways. 1998. 127 p.

150. Standards for calculating and assessing the strength of load-bearing elements and dynamic qualities of the undercarriage of multi-unit rolling stock of the

1520 mm gauge railways of the Ministry of Railways of the Russian Federation. M., 1997. 147 p.

151. RD 24.050.37-95 Freight and passenger cars. Test methods for strength and driving performance. M.: GosNIIV, 1995. 102 p.

152. Recommendations for the expansion and direct modification of the forces of interaction between the wheels and racks to ensure the safety margin of the wheel set when leaving the racks by increasing the safety of the wheel Hello Confirmed and put into effect by order of Ukrzaliznytsia No. 004 dated 01/05/2009.

153. Built-in intelligent real-time controller CompactRIO. CompactRIO 9012/9014 Operating Instructions and Specifications. USA, Texas, Austin: National Instruments. 2007. 19 p.

154. Installation instructions. CompactRIO Reconfigurable embedded system. Chassis with RIO-9111/9112/9113/9114/9116/9118. USA, Texas, Austin: National Instruments. 2009. 19 p.

155. Operation Instructions and Safety Guidelines cRIO GPS Modules. Germany, Troisdorf: Datentechnik GmbH, 2011 28 p.

156. Ukrainian patent for useful model No. 130258, IPC (2018.01) B61D 3/00, Solid-bottomed passenger car. Fomin O.V., Gorbunov M.I., Prokopenko P.M., Tsymbalyuk A.V., Fomina A.M., (Ukraine); Vlasnik: author – No. u 2018 07212; application 06/26/2018; publ. November 26, 2018, Bulletin No. 22.

157. Ukrainian patent for useful model No. 129972, IPC (B61D 5/06 (2006.01)) Liquid tank. Gorbunov M.I., Fomin O.V., Prokopenko P.M., Kara S.V., Fomina A.M., Lebedev V.S. (Ukraine); Vlasnik: SNU im. V. Dahl. – No. u201804502; application 04/24/2018; publ. 26.11.2018, Bulletin No. 22/2018.

158. Patent of Ukraine for the useful model No. 129971, IPC (B61D 5/06 (2006.01)) Liquid tank. Gorbunov M.I., Fomin O.V., Prokopenko P.M., Kara S.V., Fomina A.M., (Ukraine); Vlasnik: SNU im. V. Dahl. – No. u201804500; application 04/24/2018; publ. 26.11.2018, Bulletin No. 22/2018.

159. Ukrainian patent for useful model No. 129970, IPC (B61D 5/06 (2006.01)) Liquid tank. Gorbunov M.I., Fomin O.V., Prokopenko P.M., Kara S.V., Fomina A.M., (Ukraine); Vlasnik: SNU im. V. Dahl. – No. u201804499; application 04/24/2018; publ. 26.11.2018, Bulletin No. 22/2018.

160. Ukrainian patent for useful model No. 131586, IPC (2006): B61D 7/00, B61D 17/00, Critical hopper car for transporting grain. Fomin O.V., Gorbunov M.I., Prokopenko P.M., Tsymbalyuk A.V., Fomina A.M., (Ukraine); Vlasnik: author – No. u 2018 07208; application 06/26/2018; publ. 01/25/2019, Bulletin No. 2/2019.

161. Ukrainian patent for useful model No. 131587, IPC (2016) B61D 7/00, B61F 1/14 (2006.01) Critical hopper car for transportation of mineral goods. Fomin O.V., Gorbunov M.I., Prokopenko P.M., Tsymbalyuk A.V., Fomina A.M., (Ukraine); Vlasnik: author – No. u 2018 07209; application 06/26/2018; publ. 01/25/2019, Bulletin No. 2/2019.

162. Ukrainian patent for useful model No. 134401, IPC (2006), B61D 3/00, Solid-bottomed passenger car. Fomin O.V., Prokopenko P.M., Obukhovsky V.V., Fomina A.M. (Ukraine); Vlasnik: author – No. u2018 12990; application 12/27/2018; publ. 05/10/2019, Bulletin. No. 9.

163. Ukrainian patent for the useful model No. 134983, IPC B61D 3/08 (2006.01) Universal flat car. Fomin O.V., M.I. Gorbunov, Prokopenko P.M., O.O. Evseeva, O.V. Burlutsky, Fomina A.M. (Ukraine); Vlasnik: author – No. u 201900302; application 01/11/2019; publ. 06/10/2019, Bulletin. No. 11.

164. Ukrainian patent for useful model No. 134986, IPC (2006) B61D 7/00 B61D 17/00, Critical hopper car for transporting grain. Fomin O.V., M.I. Gorbunov, Prokopenko P.M., O.O. Evseeva, O.V. Burlutsky, Fomina A.M. (Ukraine); Vlasnik: author – No. u 201900306; application 01/11/2019; publ. 06/10/2019, Bulletin. No. 11.

165. Ukrainian patent for useful model No. 135500, IPC (2006): B61D 17/00, B61D 17/04, Method for increasing the structural value of the center beam of a pull-down car. Zaytsev Volodymyr Oleksandrovich, Petrenko Vyacheslav

Oleksandrovich, Braslavets Yuriy Volodymyrovych, Kara Sergey Vitaliyovich, Prokopenko Pavlo Mykolayovich, Koshel Oleksiy Oleksandrovich, Yatsenko Lyudmila Fedorivna (Ukraine). Vlasnik:Branch "Scientific Research and Design and Technology Institute of Transport Transport" PJSC "Ukrzaliznytsia". No. u201811317;application 01/11/2019; publ. 07/10/2019, Bulletin. No. 13.

166. Ukrainian patent for useful model No. 135562, IPC (2006): B61D 7/00, B61D 17/00, Critical hopper car for transportation of mineral goods.Fomin O.V., M.I. Gorbunov, Prokopenko P.M., O.O. Evseeva, O.V. Burlutsky, Fomina A.M. (Ukraine); Vlasnik: author – No. u201900308; application 01/11/2019; publ. 07/10/2019, Bulletin. No. 13.

167. Patent of Ukraine for the useful model No. 138162, IPC (2006.01) B61D 3/20, (2006.01) Flatbed car. Fomin O.V., Gorban A.V., Prokopenko P.M., Sklyarenko I.Yu. (Ukraine); Vlasnik: State University of Infrastructure and Technology – No. u 2019 03964; application 04/16/2019; publ. November 25, 2019, Bulletin No. 22.

168. Ukrainian patent for useful model No. 139756, IPC 5/06 (2006.01) Liquid tank. Fomin O.V., M.I. Gorbunov, Prokopenko P.M., O.O. Evseeva, O.V. Burlutsky, Fomina A.M. (Ukraine); Vlasnik: author – No. u 2019 00309; application 01/11/2019; publ. 01/27/2020, Bulletin No. 2.

169. Ukrainian patent for useful model No. 142162, IPC (2006.01) B61D 3/00, B61D 3/18 (2006.01). 4th spring dump car. Fomin Oleksiy Viktorovich, Sklyarenko Inna Yuriivna, Levchenko Olga Viktorivna, Fomina Anna Mykolaivna; Prokopenko Pavlo Mykolayovich. (Ukraine); Vlasnik: State University of Infrastructure and Technology – No. U201907841, application 07/11/2019; publ. 05/25/2020, Bulletin No. 10.

170. Ukrainian patent for useful model No. 142163, IPC (2006.01) B61D 3/00, B61D 3/18 (2006.01). 4th spring dump car. Fomin Oleksiy Viktorovich, Sklyarenko Inna Yuriivna, Skok Pavlo Oleksandrovich, Fomina Anna Mykolayivna, Prokopenko Pavlo Mykolayovich. (Ukraine); Vlasnik: State University of

Infrastructure and Technology – No. U201907841, application 07/11/2019; publ. 05/25/2020, Bulletin No. 10.

171. Ukrainian patent for useful model No. 146774, IPC (2006.01) B61D 3/00, B61D 3/18 (2006.01). Kritia hopper car for transporting cement. Fomin Oleksiy Viktorovich, Sklyarenko Inna Yuriivna, Prokopenko Pavlo Mykolayovich, Fomina Anna Mykolayivna, Tymoshchuk Olena Mykolayivna (Ukraine); Vlasnik: State University of Infrastructure and Technology – No. U202006035, application 09.21.2020; publ. 03/17/2021, Bulletin No. 11.

172. Ukrainian patent for useful model No. 146775, IPC (2006.01) B61D 3/00, B61D 3/18 (2006.01). 8-spring carriage. Fomin Oleksiy Viktorovich, Sapronova Svitlana Yuriivna, Skok Pavlo Oleksandrovich, Prokopenko Pavlo Mykolayovich, Fomina Anna Mykolayivna (Ukraine) Vlasnik: National University of Infrastructure and Technology – No. U202006036, application 09/21/2020 ; publ. 03/17/2021, Bulletin No. 11.

ADDITION A

PATENT DEVELOPMENTS FOR IMPROVING WAGON TRAFFIC SAFETY INDICATORS

A.1. 4-SPRING DUMP WAGON

The utility model relates to carriage building and can be used for rail freight transportation of bulk cargo that does not require protection from precipitation and their mechanical unloading.

The 4-way dump wagon model 31-638 is known; the wagon is an all-metal self-unloading car with a body structure that tilts during unloading. The wagon consists of a carriage module containing two biaxial bogies, an automatic coupler module, a braking equipment module, a lower frame module with two buffer walls, two pivot beams, four cylindrical beams and an upper frame module containing side walls and two ends. unloading It is characterized by mechanized loading into the body and unloading from outside the rails by tilting the body with pneumatic cylinders.

The disadvantages of this design are as follows: dump wagons of this model are characterized by unreasonably insufficient load-carrying capacity and a reduced service life due to unsatisfactorily lower dynamic and strength load resistance indicators, which determines their operation on railway and vehicle networks. and imposes additional restrictions on the transportation of cargo volumes.

The utility model is based on the task of improving the dump wagon by having hinged elements in its design instead of existing fixed elements (solid beams, welded joints), namely the presence of a hinged element in the middle part of the spinal beam, the presence of hinged elements at the junction of the spinal beam with: buffer walls, pivot and cylindrical beams. The introduction of new features in interaction with known ones ensures the appearance of additional degrees of freedom of the design and implements in it the principle of adaptive perception of operational loads in a loaded or unloaded state, which, as a consequence, improves the dynamics and strength of a dump vehicle, reduces material consumption and, accordingly, increases the load capacity. dump wagon services.

The task is achieved by the fact that in a dump wagon containing bogies, automatic coupling devices, braking equipment, a body including an upper frame with side sides, end walls, an unloading mechanism and a lower frame with a center beam, buffer walls, pivot and cylindrical beams, a model with a hinged element in the middle part of the spinal beam; There are hinge elements at the junction of the center beam with: buffer walls, pivot and cylindrical beams.

The advantages of the proposed technical solution are the improvement of the dynamics and strength of the dump wagon, the increase in the carrying capacity and service life of the wagon.

The essence of the utility model is explained by illustrative material, where in FIG. Fig. 1 shows a dump wagon containing bogies 1, braking equipment 2, automatic coupling devices 3, upper frame 4, lower frame 5; Fig. 2 shows the lower frame of a dump wagon with a spinal column (with a central hinge in the middle part 6), buffer, pivot beams 8 and cylindrical beams 9, which are connected pivotally 10, also in Fig. 3 shows the hinge connection 11 with the center beam

The proposed dump wagon works as follows.

During movement, vertical and horizontal forces from the upper frame are transmitted to the lower frame, which includes a center beam with a central hinge element, which is hingedly connected to the buffer walls, pivot and cylindrical beams (Fig. 2, Fig. 3), which partially absorb vibration energy , impacts and improve the dynamics and strength of the dump wagon. The movement of the dump wagon is ensured using bogies 1 (Fig. 1). The brake of the dump wagon is provided by braking equipment 2. The connection of the dump wagon with other wagons or locomotives is provided by automatic coupling devices 3.

The use of the proposed technical solution will improve dynamics and strength, increase the load capacity of the dump wagon and service life.

Utility model formula

A dump wagon containing bogies, automatic coupling devices, braking equipment, an upper frame with side walls, end walls and an unloading mechanism, a lower frame with a spinal, buffer walls, pivot, cylindrical beams, characterized in that in the middle part of the spinal beam; There are hinge elements at the junction of the center beam with: buffer walls, pivot and cylindrical beams.

Essay

Utility model object: 4-way dump wagon.

Scope of application: railway transport, the utility model can be used in the design of a 4-valve dump wagon.

The essence of the utility model: A dump wagon containing bogies, automatic couplers, braking equipment, an upper frame containing side walls, two end walls and an unloading mechanism, a lower frame with two buffer walls, two pivots, four cylindrical beams in which the fixed connection is replaced. to the swivel joint.

Technical result: improved dynamics and strength indicators, increased load capacity and service life of a 4-wheel dump wagon.

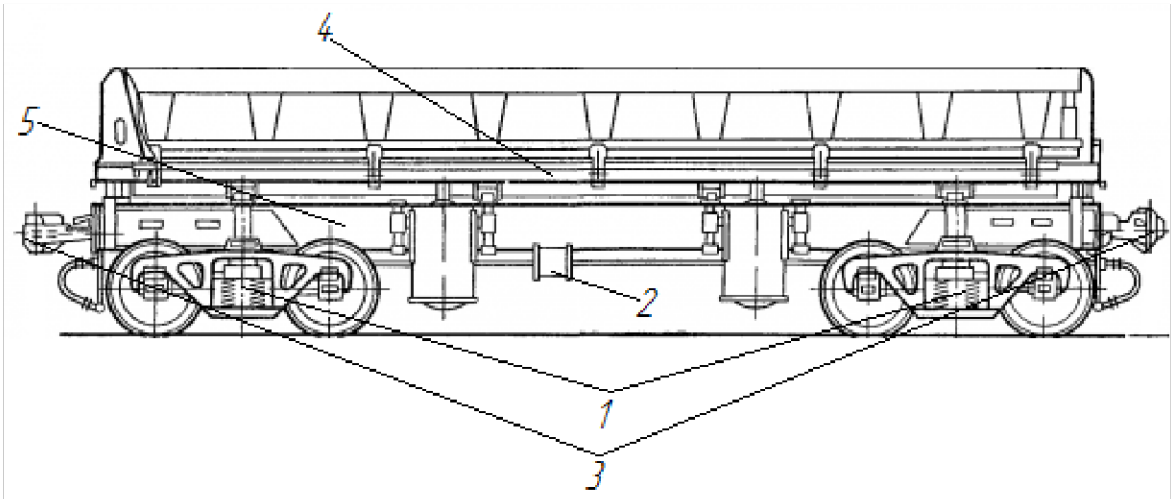

Fig. 1 – 4 spring wagon dump truck

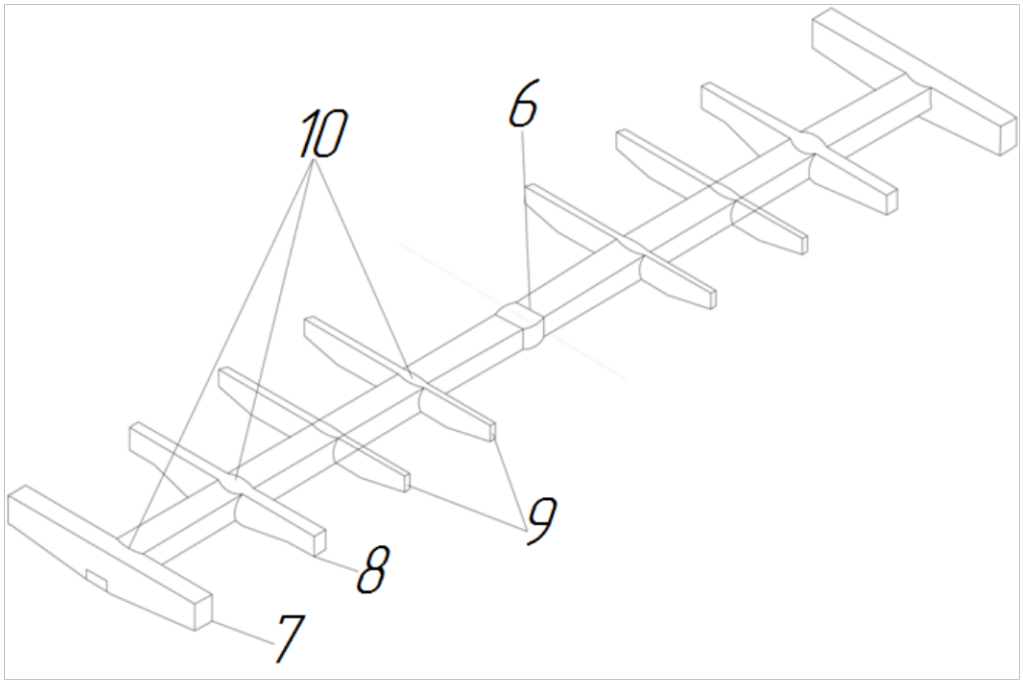

Fig. 2 – 4 spring wagon dump truck

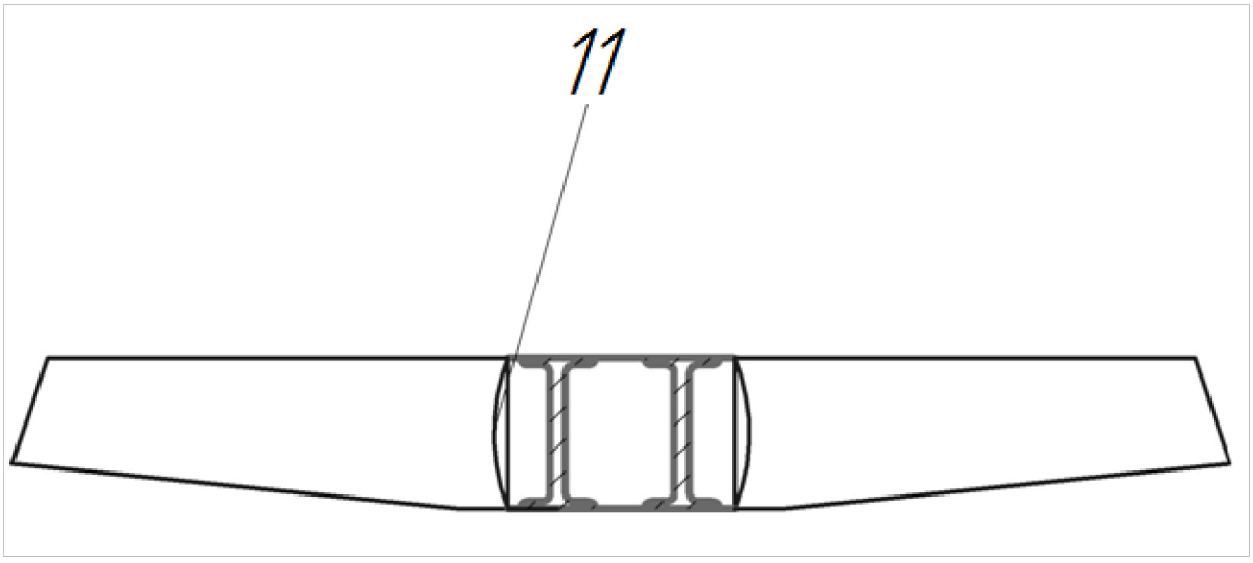

Fig. 3 – 4 spring wagon dump truck

A.2. UNIVERSAL COVERED WAGON

The utility model relates to carriage building and can be used for freight rail transportation that requires protection from precipitation.

A universal covered car for the transportation of goods that require protection from precipitation, model 11-217, is known; the all-metal wagon has an outer metal lining and a wooden inner lining, the design of which consists of a carriage module containing two biaxial bogies and an auto module. equipment, a frame module with a centerline, two end, two pivot, two main and seven intermediate weft beams and a body module containing two side walls with sheathing and a frame, including vertical posts, two end walls with sheathing and a frame. , including resistant intermediates and an all-metal roof. Characterized by loading through side doors, sunroofs and unloading through side doors.

The disadvantages of this design are as follows: the universal box wagon of this model is characterized by an unreasonably insufficient load capacity and a reduced service life due to unsatisfactorily lower dynamic and strength loads, which causes an increase in the cost of cargo transportation during their operation on railway networks. railway transport and imposes additional restrictions on the transportation of cargo volumes.

The utility model is based on the task of improving a universal covered wagon by using hinged elements in its design instead of existing fixed elements (solid beams, welded joints), namely the presence of a hinged element in the middle part of the center beam, the presence of hinged elements at the junction of the end beams, pivot and main beams, the presence of hinge elements at the junction of the side wall posts with the lower skin and at the junction of the roof with the side wall posts. The introduction of new features in interaction with the known ones ensures the appearance of additional degrees of freedom of the design and implements in it the principle of adaptive perception of operational loads in a loaded or unloaded state,

which, as a consequence, improves the dynamics and strength of a universal covered wagon, ensures a reduction in material consumption and, accordingly, increases the load capacity. increases the service life of the wagon.

The task is achieved by the fact that in a universal covered wagon containing bogies, automatic coupling devices, braking equipment, a body including a frame with a center beam, end beams, main beams and a roof, according to the utility model, there is a hinge element in the middle part of the center beam; existing hinge elements at the junction of the center beam with: end, pivot and main beams; There are hinge elements at the junction of the side wall pillars with the bottom trim and at the junction of the roof with the side wall pillars.

The advantages of the proposed technical solution are the improvement of the dynamics and strength of the universal covered wagon, the increase in the carrying capacity and service life of the wagon.

The essence of the utility model is explained by illustrative material, where in FIG. 1 shows a universal covered wagon containing bogies 1, braking equipment 2, automatic coupling devices 3, a body 4, a universal covered wagon includes a frame with a vertebral (with a hinged connection in the middle part 5), end 6, pivot beams 7 and main beams that are pivotally connected 9 (Fig. 2), hinge elements at the junction of the side racks with the lower frame 10 (Fig. 3) and at the junction of the roof with the racks of the side walls 11 (Fig. 4).

The proposed universal box wagon works as follows.

During movement, vertical and horizontal forces from the body are transmitted to the center beam with a hinged element, which is pivotally connected to the end, pivot, and main beams, which in turn are pivotally connected to the racks of the side walls, which in turn are pivotally connected. with a wagon roof (Fig. 2, Fig. 3, Fig. 4), partially absorbing vibration energy and improving the dynamics and strength of a universal covered wagon. The movement of the universal covered wagon is ensured with the help of trolleys 1 (Fig. 1). The brake of a universal covered wagon is

provided by braking equipment 2. The connection of a universal covered wagon with other wagons or locomotives is provided by automatic coupling devices 3.

The use of the proposed technical solution will improve the dynamics and strength, increase the carrying capacity of a universal covered wagon and its service life.

Utility model formula

A universal covered wagon containing bogies, automatic couplers, braking equipment, a body, a frame with center, end, pivot, and main beams, characterized in that there is a hinge element in the middle part of the center beam; existing hinge elements at the junction of the center beam with: end, pivot and main beams; There are hinge elements at the junction of the side wall pillars with the bottom trim and at the junction of the roof with the side wall pillars.

Essay

Utility model object: a universal covered wagon for transporting goods that require protection from precipitation.

Scope of application: railway transport, the utility model can be used in the design of a universal covered carriage.

The essence of the utility model: A universal covered wagon containing bogies, automatic coupling devices, braking equipment, a body including a frame with an articulated center beam, end beams, pivot beams, main beams in which the fixed connection is replaced by a hinge connection, existing hinge elements. at the junctions of the side wall posts with the bottom trim and at the junctions of the roof with the side wall posts.

Technical result: improved dynamics and strength indicators, increased load capacity and service life of a universal covered wagon.

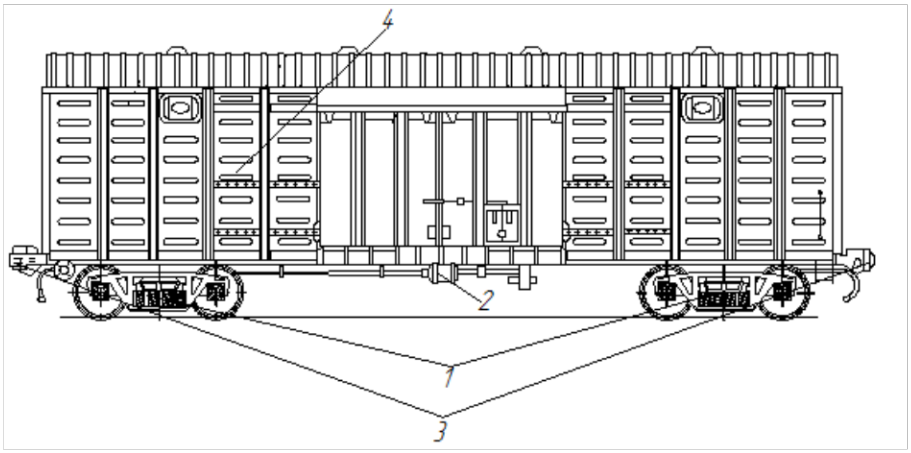

Fig. 1 – Universal covered wagon

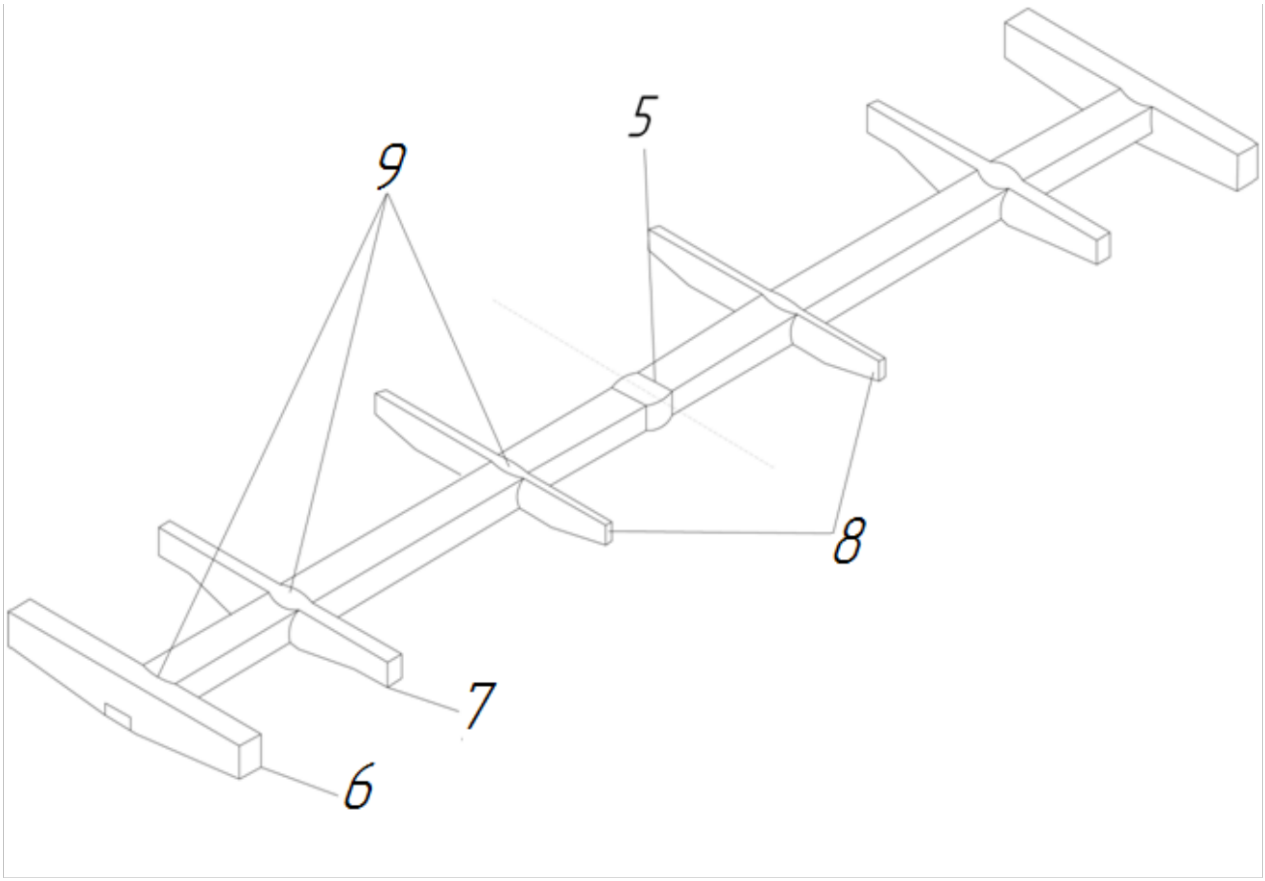

Fig. 2 – Universal covered wagon

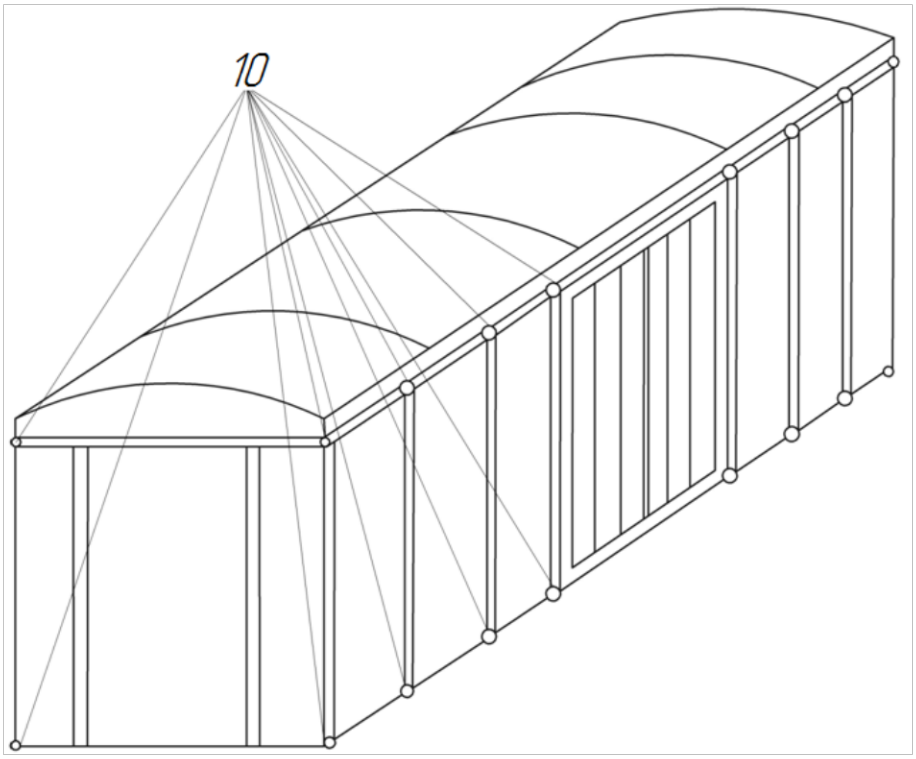

Fig. 3 – Universal covered wagon

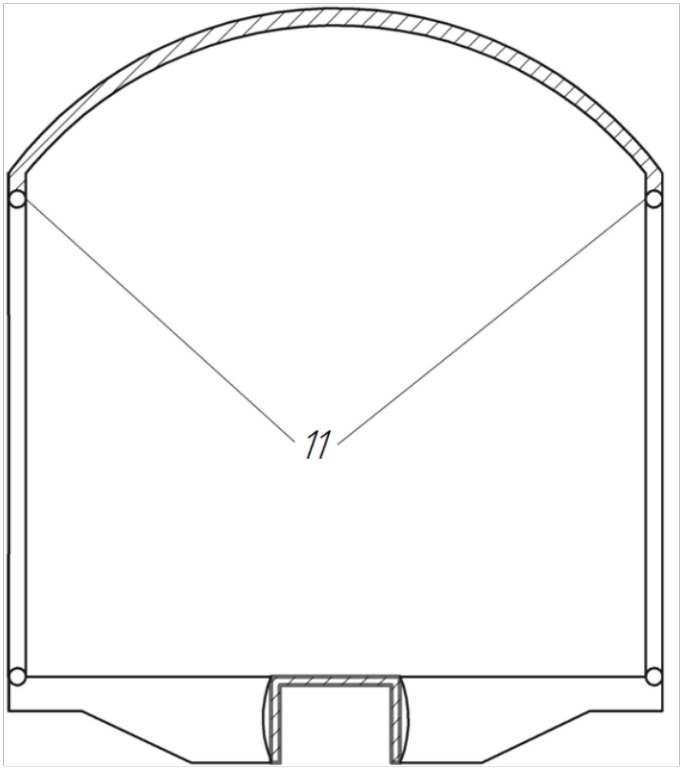

Fig. 4 – Universal covered wagon

A.3. RAILWAY TANK STATION

The utility model relates to railway transport, namely railway tanks, and can be used for the transportation of liquid cargo.

A railway tank is known, containing bogies, a frame, braking equipment, automatic coupling devices, a boiler, fastening the boiler to the frame and supports of the boiler on the frame.

The disadvantage of this design is that when transporting liquid cargo, the dynamics of the railway tank are worse than most other types of wagons, which in turn imposes additional features and restrictions regarding train transportation.

The utility model is based on the task of improving the railway tank by replacing the supports located between the boiler and the frame with rubber-metal elements that absorb vibration energy, which, as a result, improves the dynamics of the railway tank.

The objective is achieved by the fact that in a railway tank containing bogies, a frame, braking equipment, automatic couplers, a boiler, fastening the boiler to the frame and boiler supports on the frame, according to the utility model, the boiler supports on the frame are made in the form of rubber-metal elements.

The advantages of the proposed technical solution are the improvement of the dynamics of the railway tank.

The essence of the utility model is explained by illustrative material, where in FIG. Figure 1 shows a railway tank containing bogies 1, frame 2, braking equipment 3, automatic couplers 4, boiler 5, fastening the boiler to the frame (not indicated), supports 6 of the boiler on the frame, which are made in the form of rubber-metal elements (Fig. 2).

The proposed railway tank works as follows.

During movement, vertical and horizontal forces from the boiler 5 are transmitted to the frame 2 partially through the fastening and through the supports 6,

which are made in the form of rubber-metal elements that partially absorb vibration energy and improve the dynamics of the railway tank. The movement of the railway tank is ensured with the help of bogies 1. The brake of the railway tank is provided by braking equipment 3. The connection of the railway tank with other wagons is provided by automatic couplers 4.

The use of the proposed technical solution will improve the dynamics of the railway tank.

Utility model formula

A railway tank containing bogies, a frame, braking equipment, automatic couplers, a boiler, fastening the boiler to the frame and boiler supports on the frame, characterized in that the boiler supports on the frame are made in the form of rubber-metal elements.

Essay

Utility model object: railway tank.

Scope of application: railway transport, the utility model can be used in the design of a railway tank for transporting liquid cargo.

The essence of the utility model: in a railway tank containing bogies, a frame, braking equipment, automatic coupling devices, a boiler, fastening the boiler to the frame and boiler supports on the frame, the boiler supports on the frame are made in the form of rubber-metal elements.

Technical result: improving the dynamics of a railway tank.

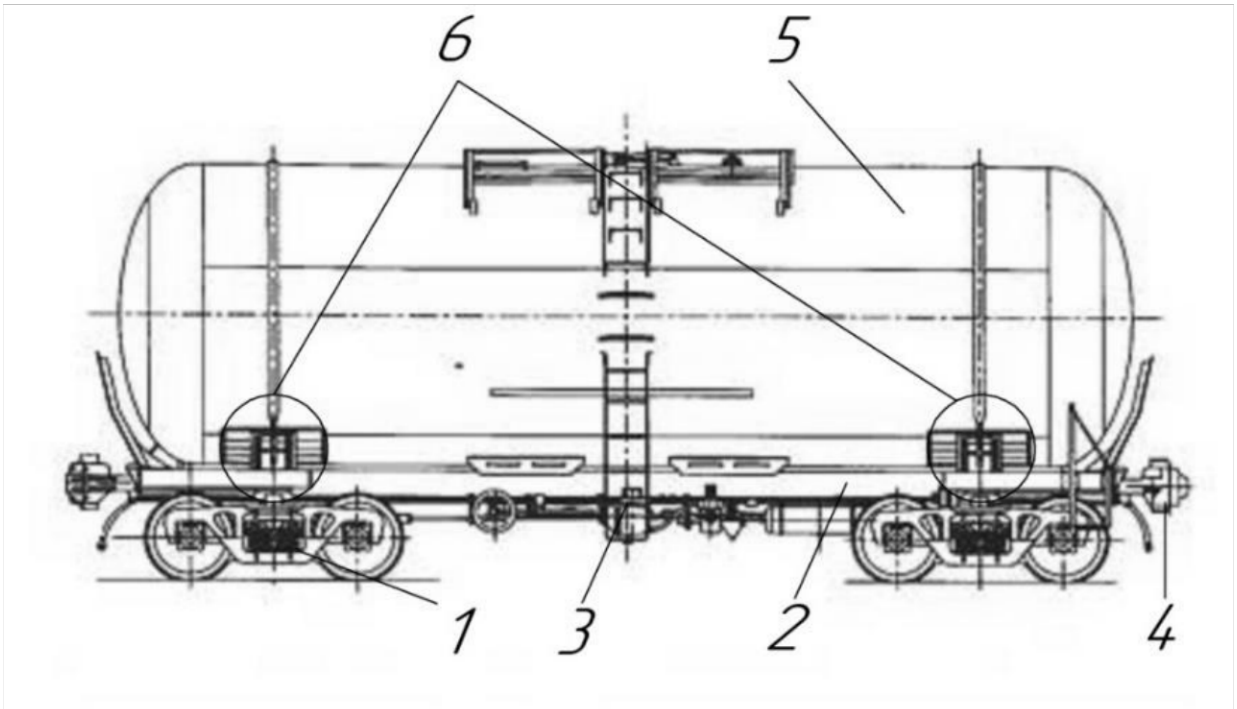

Fig. 1 – Railway tank

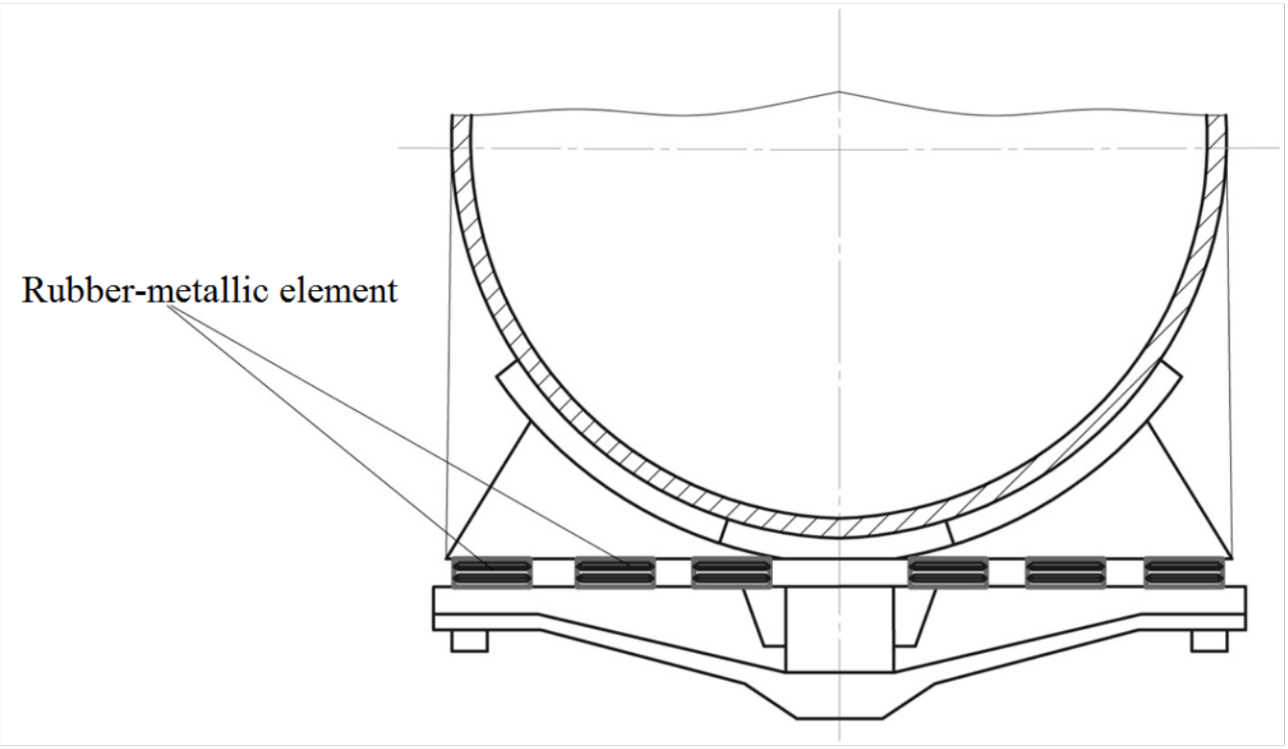

Fig. 2 – Railway tank

A.4. 6 SPRING RAILWAY TANK STATION

The utility model relates to railway transport, namely railway tanks, and can be used for the transportation of liquid cargo.

A 6-spring railway tank is known, containing bogies, a frame, braking equipment, automatic couplers, a boiler, a boiler mount and boiler supports on the frame.

The disadvantage of this design is that when transporting liquid cargo, the dynamics of the railway tank are worse than most other types of wagons, which in turn imposes additional features and restrictions regarding train transportation.

The utility model is based on the task of improving a 6-axle railway tank by replacing the supports that are located between the boiler and the frame with leaf springs that absorb vibration energy, which, as a result, improves the dynamics of the railway tank.

The objective is achieved by the fact that in a 6-axle railway tank containing bogies, a frame, braking equipment, automatic couplers, a boiler, a boiler mount and boiler supports on the frame, according to the utility model, the boiler supports on the frame are made in the form of leaf springs.

The advantages of the proposed technical solution are the improvement of the dynamics of a 6-axle railway tank.

The essence of the utility model is explained by illustrative material, where in FIG. Figure 1 shows a 6-spring railway tank containing bogies 1, frame 2, braking equipment 3, automatic couplers 4, boiler 5, boiler mounting (not indicated), boiler supports 6 on the frame, which are made in the form of leaf springs (Fig. 2).

The proposed 6-spring railway tank works as follows.

During movement, vertical and horizontal forces from the boiler 5 are transmitted to the frame 2 and partially through the supports 6, which are made in the form of leaf springs, partially absorbing vibration energy and improving the

dynamics of the 6-axle railway tank. The movement of a 6-axle railway tank is ensured with the help of bogies 1. The braking of a 6-axle railway tank is provided by brake equipment 3. The connection of a 6-axle railway tank with other wagons is provided by automatic couplers 4.

The application of the proposed technical solution will improve the dynamics of a 6-axle railway tank.

Utility model formula

A 6-spring railway tank containing bogies, a frame, braking equipment, automatic couplers, a boiler, a boiler mount and boiler supports on the frame, characterized in that the boiler supports on the frame are made in the form of leaf springs.

Essay

Utility model object: 6-spring railway tank.

Scope of application: railway transport, the utility model can be used in the design of a 6-axle railway tank for transporting liquid cargo.

The essence of the utility model: in a 6-axle railway tank containing bogies, a frame, braking equipment, automatic couplers, a boiler, the boiler is mounted and the boiler supports on the frame, the boiler supports on the frame are made in the form of leaf springs.

Technical result: improving the dynamics of a 6-way railway tank.

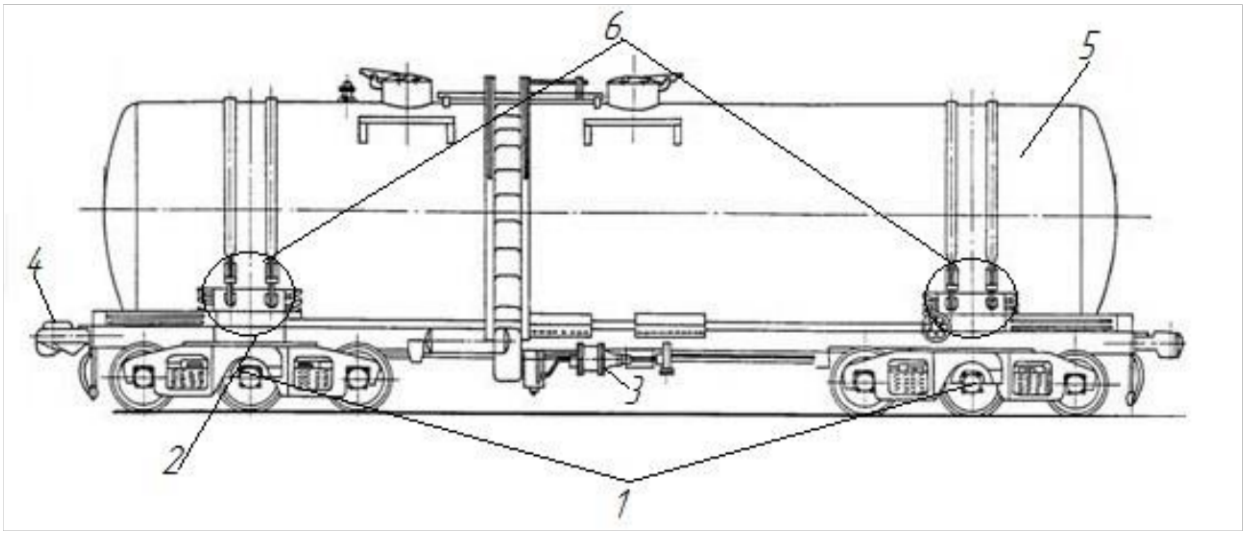

Fig. 1 – 6 spring railway tank

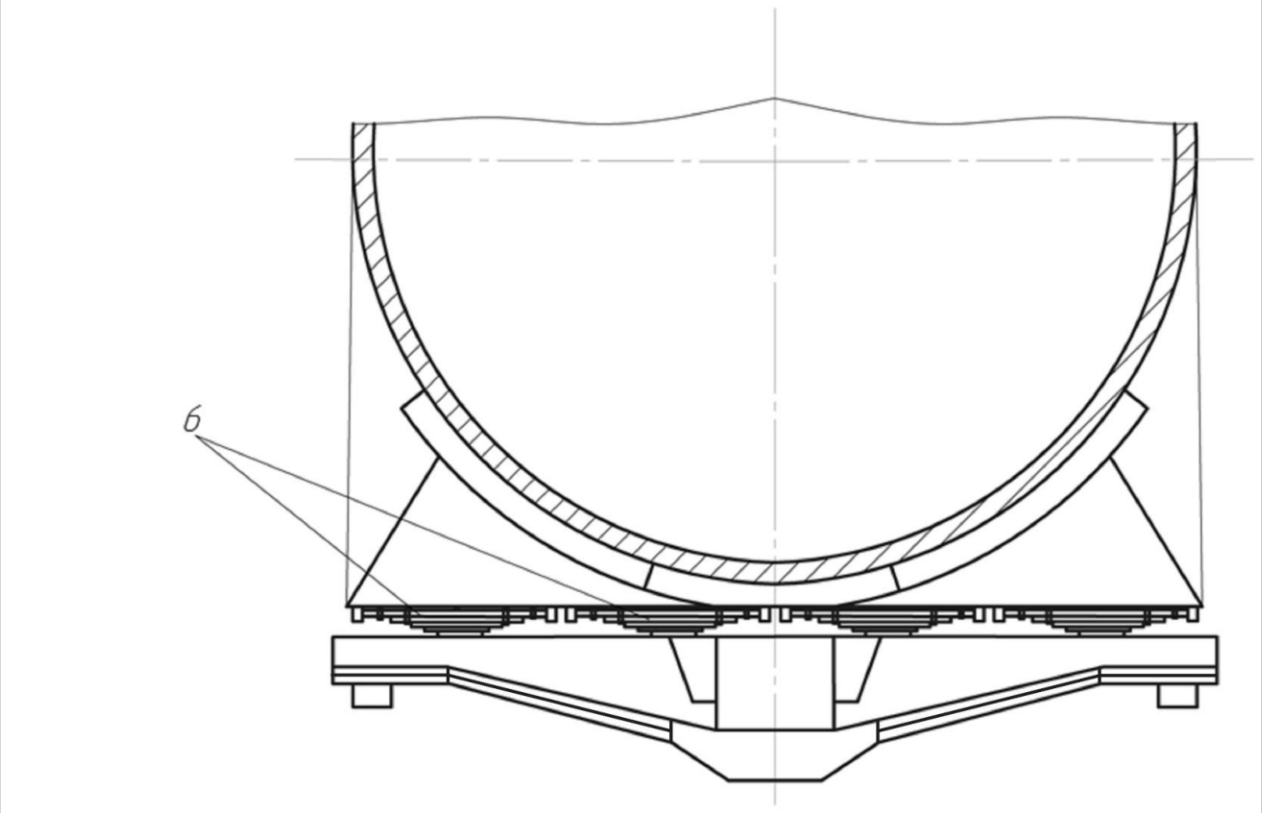

Fig. 2 – 6 spring railway tank

A.5. VERTEBRAL BEAM OF FREIGHT WAGON

The utility model belongs to railway transport, namely to repair, modernization, construction and operation of freight wagons and can be used for technical control and improving the safety of movement of freight wagons, namely the center beam of a freight wagon at the junction with the rear stops, including after repairs in these areas.

A known center beam of a freight wagon contains longitudinal non-sewing profiles, connection points with automatic coupling equipment, bogies, and transverse beams.

The disadvantage of such a center beam of a freight wagon, according to an analysis of strength calculations and failures of the load-bearing structures of wagons, is that the junction of the center beam with the rear stops in certain models of wagons, including hopper wagons for transporting grain of the model 19-752, has stress concentrators in which cracks occur.

There is a known method for repairing center beams, which consists in the fact that when a crack occurs in the center beam, an overlay is installed on the area with the crack by welding. “Instructions for welding and surfacing during the repair of freight wagons and containers” - Instruction TsV-0019).

The disadvantage of this repair method is that it cannot be used at riveted joints, at the edges of the center beam and areas with changes in geometric parameters, as well as the impossibility of further monitoring the stress level.

There is also a known method for repairing center beams, which consists in the fact that if a crack occurs, it is repaired by welding (Wagons of freight railways of Ukraine track 1520 (1524) mm. Manual for depot repair. VND UZ 32.2.04.037-2014).

The disadvantage of this repair method is that after welding, residual stresses appear at the site of destruction of the spinal beam and it is impossible to further control the stress levels.

A prototype design for the center beam of a freight wagon with the ability to further control stress levels has not been found.

The utility model is based on the task of improvement center beam of a freight wagon by introducing into the design a diagnostic module for the most dangerous zone.

The task is achieved by the fact that center beam of a freight wagon, containing longitudinal non-seeding profiles, connection points with automatic coupling equipment, bogies, cross beams**,** according to the utility model, at the junction of the center beam with the rear stops, which are the zone of combination of longitudinal non-seeding profiles with automatic coupling equipment, a diagnostic module is installed, consisting of strain gauges, a protective coating and output connectors for connecting test equipment.

The advantages of the proposed technical solution are the possibility of constant or periodic monitoring of the level of dynamic stresses and oscillation frequencies of the hazardous area center beam of a freight wagon (junction of the center beam with the rear stops) which is especially important for wagons after long-term operation or after repairs and upgrades.

The essence of the utility model is presented in Fig. 1, which shows a diagram center beam of a freight wagon. The spinal beam of a freight wagon contains longitudinal non-sewing profiles 1, connection points with automatic coupling equipment 2, connection points with bogies and transverse beams (not marked in the image). The area where the longitudinal non-seeding profiles 1 connect with the automatic coupling equipment 2 contains a dangerous zone - the junction of the center beam with the rear stops (zone A). Additionally the general outline of the wagon is shown using the example of grain wagon 3. In zone A at the junction of the center beam with the rear stops, a diagnostic module is installed, consisting of strain

gauges 4, a protective coating 5 and output connectors 6 for connecting test equipment.

Spinal beam of a freight wagon works as follows.

Vertical and horizontal forces from the body of wagon 3 are transmitted to the upper parts longitudinal non-sewing profiles 1 and at the junction with the transverse beams. After this, vertical and horizontal forces are transmitted from longitudinal non-seeding profiles 1 to the points of connection with the automatic coupling equipment 2 and the points of connection with the bogie.

Longitudinal forces from the train are transmitted through the junction of the center beam with automatic coupling equipment 2.

The forces from the contact of the wheels with the tracks are transmitted through the junction of the center beam with the bogies.

When connecting the testing equipment, strain gauges 4 through output connectors 6 provide control of the deformation of the test (dangerous) zone of the spinal beam of a freight wagon, which makes it possible to evaluate the levels of dynamic stresses and vibration frequencies. The protective coating 5 is designed to protect the strain gauges 4 from damage and the environment.

The use of the proposed technical solution will make it possible to constantly or periodically monitor the level of dynamic stresses and oscillation frequencies of the dangerous zone.center beam of a freight wagon (junction of the center beam with the rear stops)which is especially important for wagons after long-term operation or after repairs and upgrades.

Utility model formula

The spinal beam of a freight wagon contains longitudinal non-sewing profiles, points of connection with automatic coupling equipment, bogies, transverse beams, which is characterized by the fact that at the junction of the center beam with the rear stops, which are the zone of combination of longitudinal non-sewing profiles with

automatic coupling equipment, a diagnostic module consisting of strain gauges, protective coating and output connectors for connecting test equipment.

Essay

Utility model object: center beam of a freight wagon.

Application area: railway transport, may be useful used in the repair, modernization, construction and operation of freight wagons.

The essence of the utility model: in the center beam of a freight wagon, containing longitudinal non-sewing profiles, connection points with automatic coupling equipment, bogies, transverse beams, at the connection points of the center beam with the rear stops, which are the zone of combination of longitudinal non-sewing profiles with the automatic coupler. , a diagnostic module is installed, consisting of strain gauges, a protective coating and output connectors for connecting test equipment.

Technical result: possibility constantly or periodically monitor the level of dynamic stresses and vibration frequencies of the hazardous area center beam of a freight wagon (junction of the center beam with the rear stops)which is especially important for wagons after long-term operation or after repairs and upgrades.

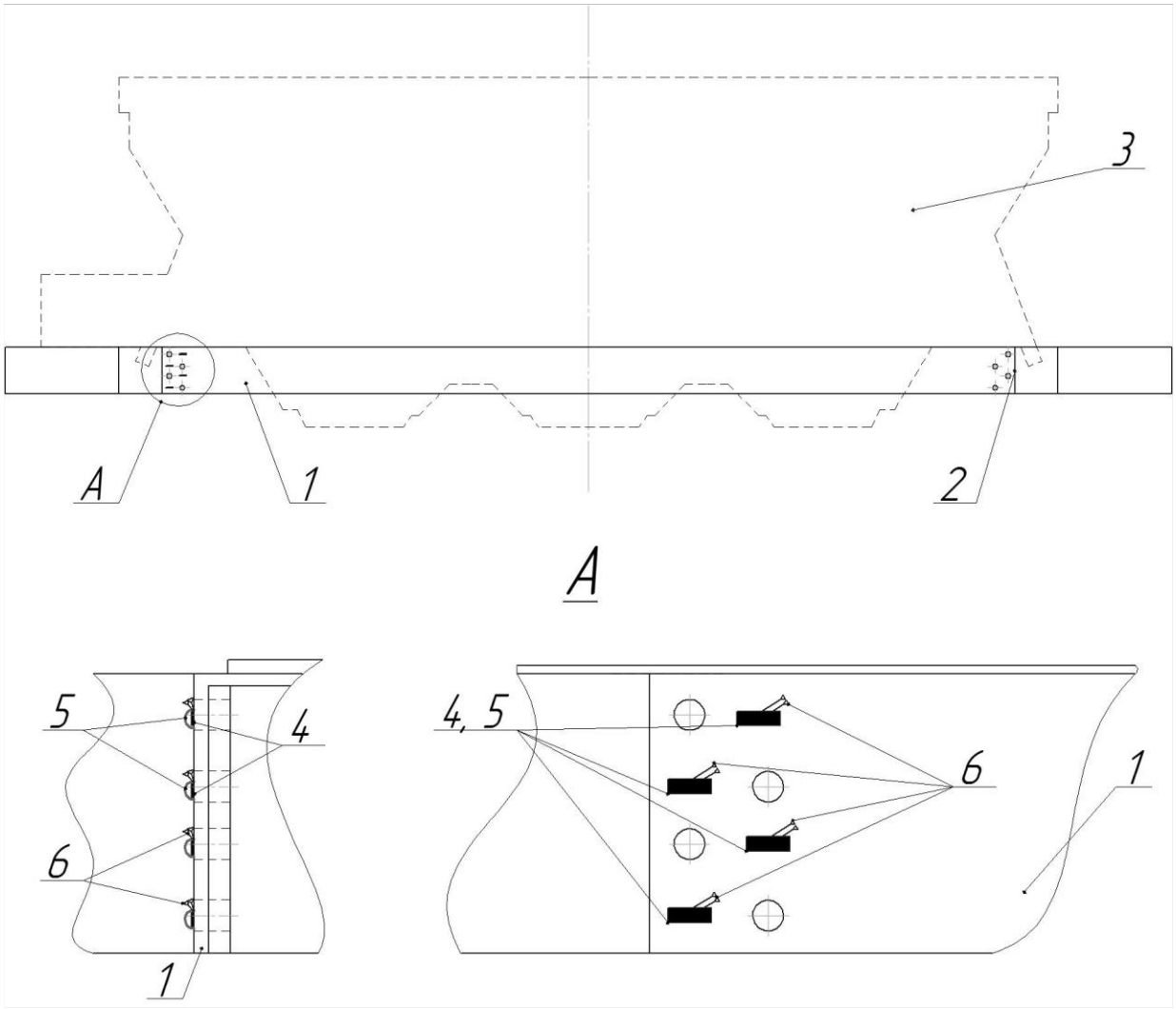

Fig. 1 – Spinal beam of a freight wagon

A.6. UNIVERSAL PLATFORM WAGON

The utility model relates to carriage building and can be used for rail transportation of wheeled and tracked vehicles, long, artificial, timber and other cargo, containers and equipment that does not require protection from atmospheric influences.

A universal platform wagon is known, the design of which consists of a carriage module containing two biaxial bogies, an automatic coupler module, a braking equipment module, a frame module including a frame with vertebral, end, pivot and main transverse beams.

The disadvantages of this design are as follows: universal platform wagon this model is characterized by an unreasonably insufficient load-carrying capacity and a reduced service life due to unsatisfactorily lower dynamic and strength load resistance indicators, which, when used on railway networks, causes an increase in the cost of cargo transportation and a decrease in the profitability of the load and restrictions on the profitability of work and the competitiveness of railway cargo transport.

The utility model is based on the task of improvement universal flat wagon by using hinge elements in its design instead of existing fixed elements (solid beams, welded joints), namely, installing a hinge element in the middle part of the spine beam, installing hinge elements at the junction of the end beams, pivot beams and main transverse beams. The introduction of new features in interaction with known ones ensures the appearance of additional degrees of freedom of the structure and implements in it the principle of adaptive perception of operational loads in a loaded or unloaded state, which, as a consequence, improves dynamics and strength indicators universal platform wagon ensures a reduction in material consumption and,

accordingly, increases the carrying capacity and increases the service life of the wagon.

The goal is achieved by the fact that in universal flat wagon, containing bogies, automatic coupling devices, braking equipment, a frame with spinal, end beams and main transverse beams, according to the utility model, a hinge element is installed in the middle part of the spinal beam; Hinge elements are installed at the junction of the center beam with: end, pivot and main transverse beams.

The advantages of the proposed technical solution are improved dynamics and strength universal flat wagon, increasing the load capacity and service life of the flat wagon.

The essence of the utility model is explained by illustrative material, where in FIG. 1 pictured universal flat wagon, which contains bogies 1, braking equipment 2, automatic coupling devices 3, frame 4, while universal flat wagon includes (Fig. 2) a frame with a vertebral (with a hinged connection in the middle part, position 5), end 1, pivot beams 2 and main transverse beams 3 which are handedly connected 4 also connected to (Fig. 3) hinged with 1 main transverse beam with a spinal beam.

Proposed universal flat wagon works as follows.

During movement, the vertical and horizontal forces of the frame are transmitted to the center beam with a hinge element, which is handedly connected to the end, pivot and main transverse beams (Fig. 2, Fig. 3), which partially absorb vibration energy and improve dynamics and strength universal flat wagon. Movement universal flat wagon is provided using bogies 1 (Fig. 1). Braking universal flat wagon provided with braking equipment 2.universal flat wagon with other wagons or locomotives, it is equipped with automatic coupling devices 3.

The use of the proposed technical solution will improve dynamics and strength, and increase load capacity universal flat canard service life.

Utility model formula

Universal flat wagon, containing bogies, automatic coupling devices, braking equipment, a frame with spinal, end, pivot and main transverse beams, characterized in that a hinge element is installed in the middle part of the spinal beam; Hinge elements are installed at the junction of the center beam with: end, pivot and main transverse beams.

Essay

Utility model object: universal flat wagon.

Scope of application: railway transport, utility model can be used in construction universal flat wagon.

The essence of the utility model: universal flat wagon, containing bogies, automatic coupling devices, braking equipment, a frame with an articulated center beam, end, pivot and main transverse beams, in which the fixed connection is replaced by a hinge connection.

Technical result: improved dynamics and strength, increased load capacity and service life universal flat wagon.

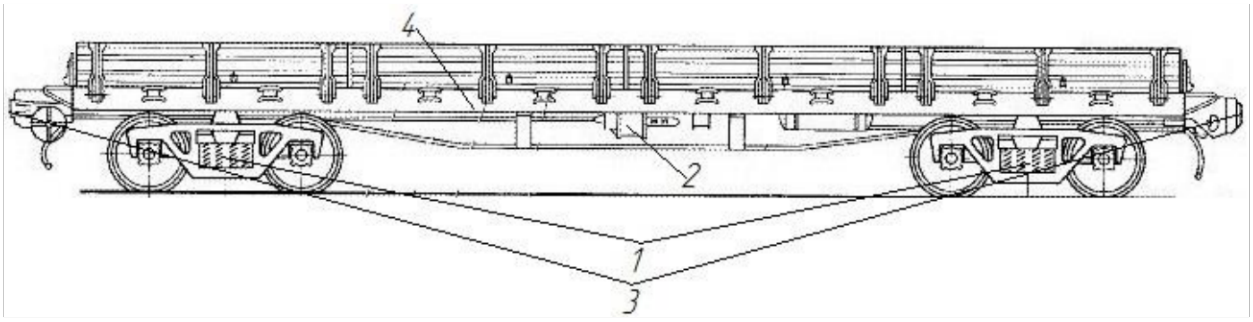

Fig. 1 – Universal flat wagon

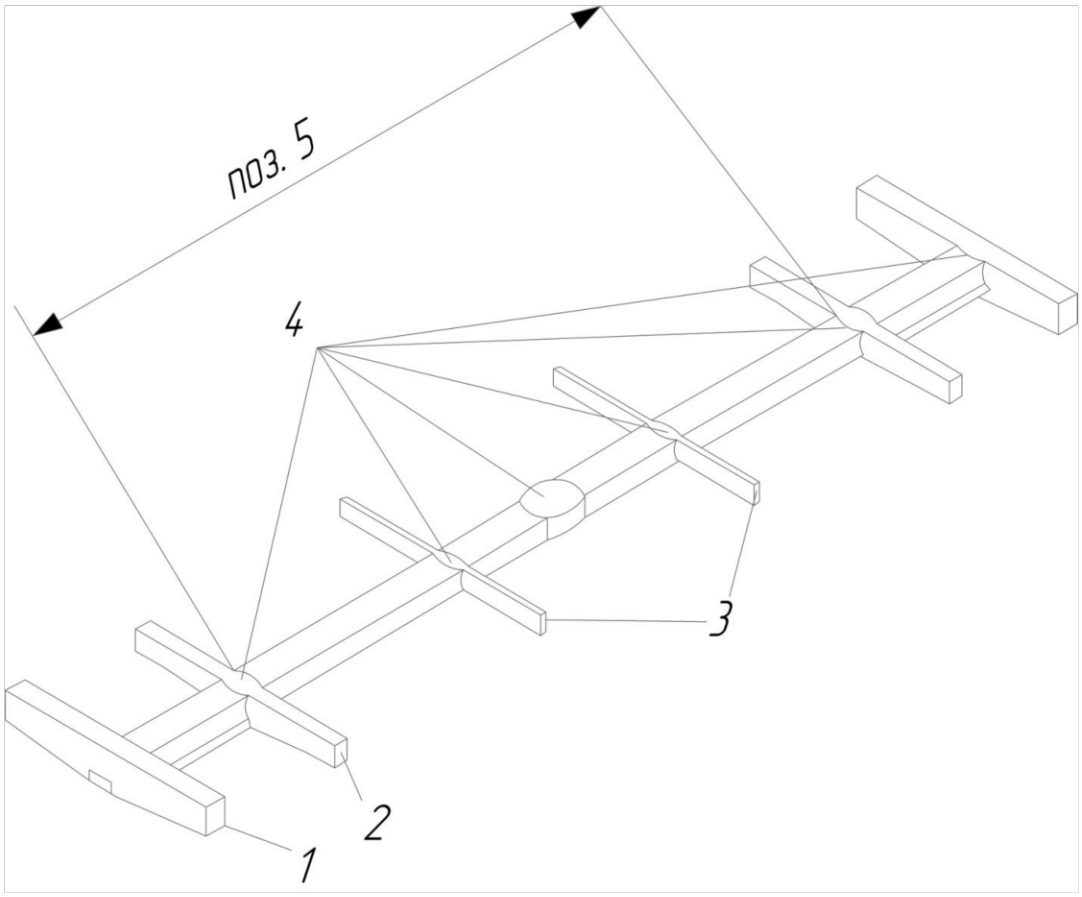

Fig. 2 – Universal flat wagon

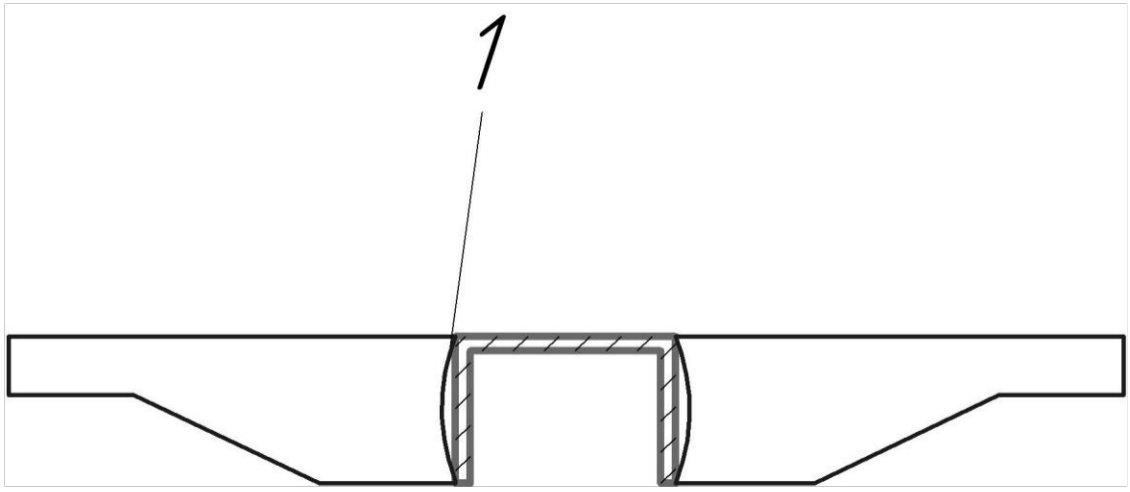

Fig. 3 – Universal flat wagon

A.7. HOPPER WAGON FOR TRANSPORTATION OF PELLETS

The utility model relates to wagon building and can be used for rail freight transportation of bulk cargo that does not require protection from precipitation, in particular pellets.

A known bunker-type hopper wagon for transporting pellets, model 20-4015-01, the wagon is an all-metal self-unloading, bunker-type wagon, the design of which consists of a carriage module containing two biaxial bogies, an automatic coupler module, a brake module, two end and two pivot , two intermediate beams and a body module containing two side walls having a skin and a frame including vertical posts, and two end walls having a skin and a frame including resistant intermediate ones.

The disadvantages of this design are as follows: hopper wagons for transporting pellets of this model are characterized by unreasonably increased material consumption and insufficient load capacity and reduced service life due to lower dynamic and strength indicators, which determines their operation on railway transportation networks. operation and competitiveness of railway transport and imposes additional restrictions on the transportation of cargo volumes.

The utility model is based on the task of improving a hopper wagon for transporting pellets by making the middle part of the center beam, end beams, intermediate beams and vertical pillars of the side walls and intermediate pillars of the end walls in the form of leaf springs. The introduction of new features, when interacting with known ones, ensures the absorption of vibration energy, which, as a consequence, improves the dynamics and strength of the hopper wagon for transporting pellets, reduces material consumption and, accordingly, increases the load capacity and increases the service life of the wagon.

The objective is achieved by the fact that in a hopper wagon for transporting pellets, containing bogies, automatic coupling devices, braking equipment, a body which includes a frame with a spine, end beams, intermediate beams, vertical pillars

of the side walls, intermediate pillars of the end walls, according to the utility model, the middle part of the center beam, end beams and intermediate beams of the frame, vertical pillars of the side walls, intermediate pillars of the end walls are made in the form of leaf springs.

The advantages of the proposed technical solution are improving the dynamics and strength of the hopper wagon for transporting pellets, increasing the carrying capacity and service life of the wagon.

The essence of the utility model is explained by illustrative material, where in FIG. Figure 1 shows a hopper wagon for transporting pellets, containing bogies 1, braking equipment 2, automatic coupling devices 3, a body 4, including a frame (Fig. 2) with a spinal column (middle part 6), end beams 7, intermediate beams 8, which are made in in the form of leaf springs 9 (Fig. 3, section of the end and intermediate beams), the racks of the side walls 5 (Fig. 1) and the intermediate racks of the end walls 10 (Fig. 4) are made in the form of leaf springs.

The proposed hopper wagon for transporting pellets works as follows.

During movement, vertical and horizontal forces from the body 4 are transmitted to the center beam with pivot beams, end beams 7, intermediate beams 8 (Fig. 2), side wall posts 5 (Fig. 1), intermediate posts of end walls 10 (Fig. 4), which are made in the form of leaf springs, which additionally absorb vibration energy and improve the dynamics and strength of the hopper wagon for transporting pellets. The movement of the hopper wagon for transporting pellets is ensured using bogies 1 (Fig. 1). Braking of the hopper wagon for transporting pellets is provided by braking equipment 2. The connection of the hopper wagon for transporting pellets with other wagons or locomotives is provided by automatic coupling devices 3.

The use of the proposed technical solution will improve dynamics and strength, reduce material consumption, increase the load capacity of a hopper wagon for transporting pellets and increase its service life.

Utility model formula

A hopper wagon for transporting pellets, containing bogies, automatic coupling devices, braking equipment, a body, a frame with vertebral, end, pivot, intermediate beams, characterized in that the middle part of the vertebral beam, end beams and intermediate beams of the frame, vertical pillars of the side walls, The intermediate racks of the end walls are made in the form of leaf springs.

Essay

Utility model object: hopper wagon for transporting pellets.

Scope of application: railway transport, the utility model can be used in the design of a hopper wagon for transporting pellets.

Essence of the utility model: A hopper wagon for transporting pellets, containing bogies, automatic couplers, braking equipment, a body including a frame with the middle part of the center beam, end beams and intermediate beams of the frame, vertical pillars of the side walls, intermediate pillars of the end walls are made in the form of sheets. springs

Technical result: improved dynamics and strength, reduced material consumption of the hopper wagon for transporting pellets, increased load capacity and service life.

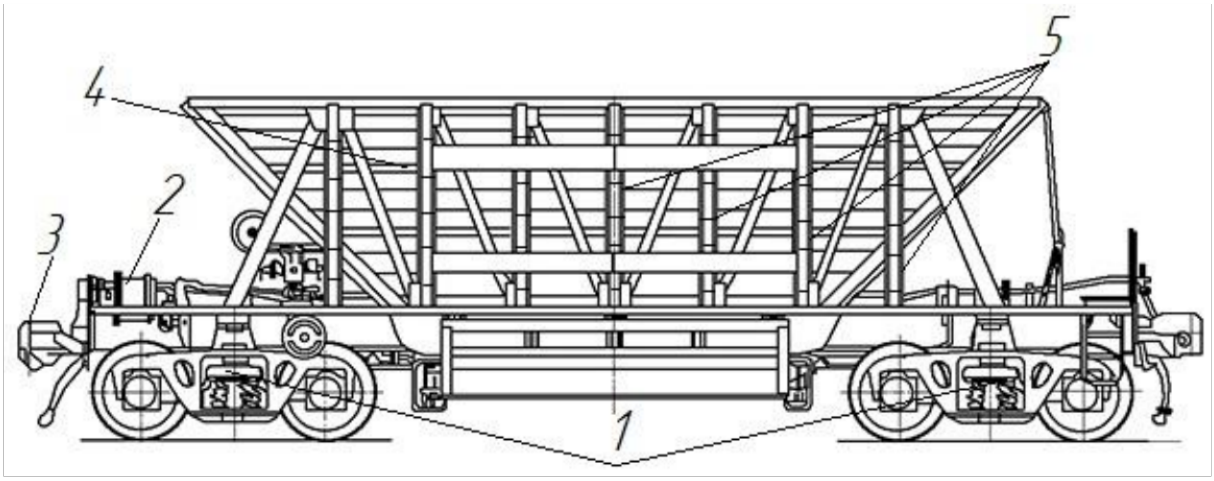

Fig. 1 – Hopper wagon for transporting pellets

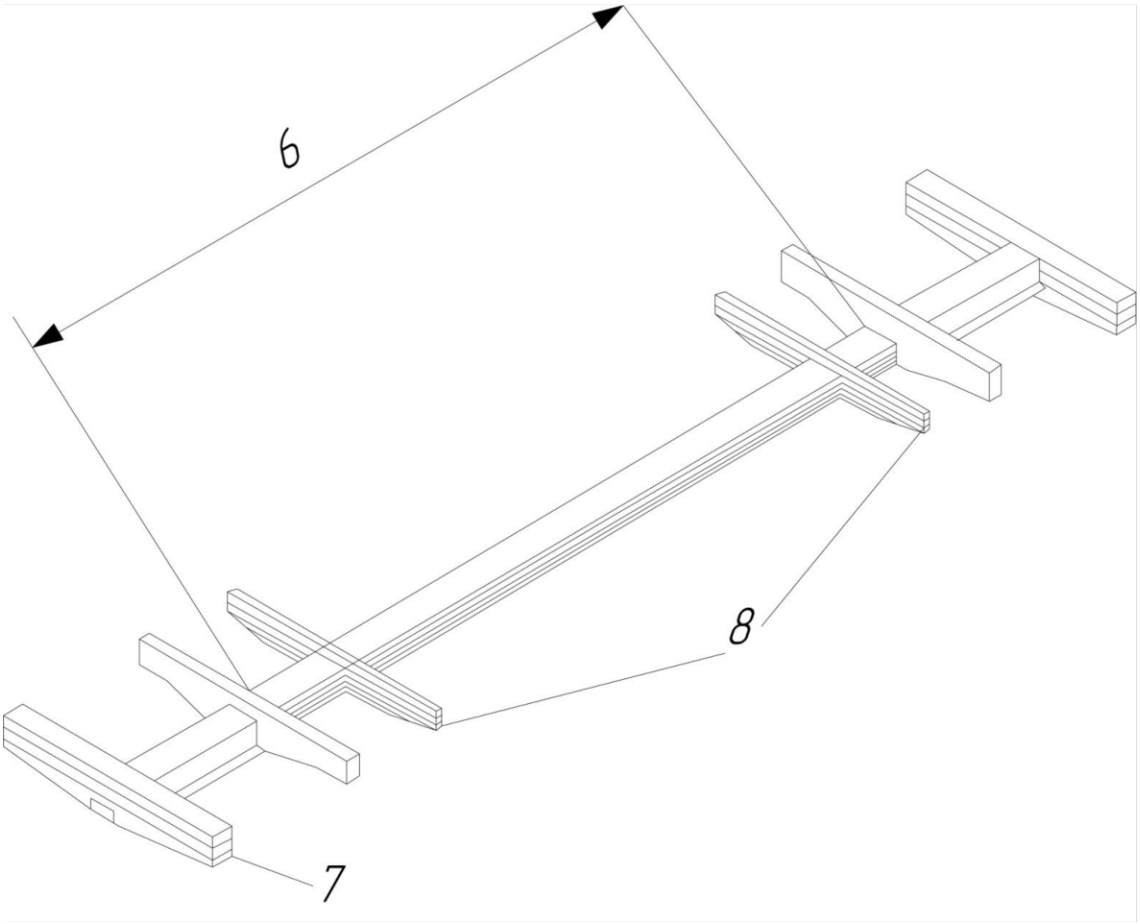

Fig. 2 – Hopper wagon for transporting pellets

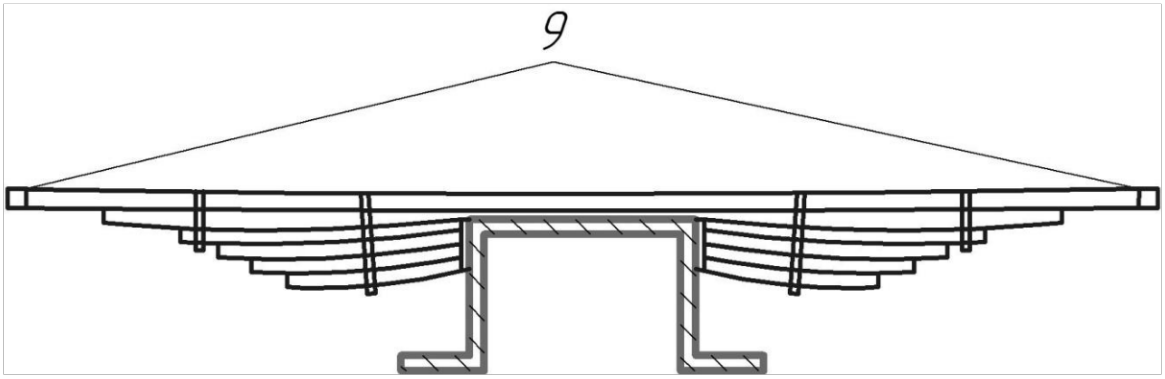

Fig. 3 – Hopper wagon for transporting pellets

A.8. COVERED HOPPER WAGON FOR TRANSPORTATION OF PELLETS

The utility model relates to wagon building and can be used for rail freight transportation of bulk cargo that does not require protection from precipitation, in particular pellets.

A covered bunker-type hopper wagon for transporting pellets, model 20-4015-01, is known. The wagon is an all-metal self-unloading, bunker-type wagon, the design of which consists of a carriage module containing two biaxial bogies, an automatic coupler module, a spindle module, two end modules, two pivot beams, two intermediate beams and a body module containing two side walls with sheathing and a frame including vertical posts, and two end walls with sheathing and a frame including resistant intermediate ones.

The disadvantages of this design are as follows: hopper wagons for transporting pellets of this model are characterized by unreasonably insufficient load capacity and reduced service life due to unsatisfactorily lower dynamic and strength loads for possible load resistance indicators, which determines their operation on railway transportation networks operation and competitiveness of railway transport and imposes additional restrictions on the transportation of cargo volumes.

The utility model is based on the task of improving a hopper wagon for transporting pellets by using hinged elements in its design instead of existing fixed elements (solid beams, welded joints), namely the presence of hinged elements at the junctions of end, pivot and intermediate beams. The introduction of new features in interaction with known ones ensures the appearance of additional degrees of freedom of the design and implements in it the principle of adaptive perception of operational loads in loaded or unloaded states, which, as a consequence, improves the dynamics and strength of the hopper wagon for transporting pellets, reduces material

consumption and, accordingly, increases the carrying capacity and increases the service life of the wagon.

The objective is achieved by the fact that in a hopper wagon for transporting pellets, containing bogies, automatic coupling devices, braking equipment, a body that includes a frame with a spinal column, end beams, intermediate beams, according to the utility model, there are hinge elements at the junctions of the spinal column. beams with: end, pivot and intermediate beams.

The advantages of the proposed technical solution are improving the dynamics and strength of the hopper wagon for transporting pellets, increasing the carrying capacity and service life of the wagon.

The essence of the utility model is explained by illustrative material, where in FIG. Figure 1 shows a hopper wagon for transporting pellets, containing bogies 1, braking equipment 2, automatic coupling devices 3, a body 4, while the hopper wagon for transporting pellets includes (Fig. 2) a frame with a spinal column, end beams 5, pivot beams 6 and intermediate beams 7, which are connected by a hinge 8, are also shown in (Fig. 3) a hinged connection 9 of the intermediate beam with the center beam.

The proposed hopper wagon for transporting cement works as follows.

During movement, vertical and horizontal forces from the body are transmitted to the center beam, which is handedly connected to the end, pivot and intermediate beams (Fig. 2, Fig. 3), which partially absorb vibration energy and improve the dynamics and strength of the wagon hopper for transporting pellets. The movement of the hopper wagon for transporting pellets is ensured using bogies 1 (Fig. 1). Braking of the hopper wagon for transporting pellets is provided by braking equipment 2. The connection of the hopper wagon for transporting pellets with other wagons or locomotives is provided by automatic coupling devices 3.

The use of the proposed technical solution will improve the dynamics and strength indicators, increase the load capacity of the hopper wagon for transporting pellets and increase the service life.

Utility model formula

A hopper wagon for transporting pellets, containing bogies, automatic couplers, braking equipment, a body, a frame with spinal, end, pivot, and intermediate beams, characterized in that there are hinge elements at the junction of the spinal beam with the end, pivot beams. and intermediate beams.

Essay

Utility model object: hopper wagon for transporting pellets.

Scope of application: railway transport, the utility model can be used in the design of a hopper wagon for transporting pellets.

The essence of the utility model: A hopper wagon for transporting pellets, containing bogies, automatic coupling devices, braking equipment, a body including a frame with a center beam, end beams, pivot beams and intermediate beams, in which the fixed joint is replaced by a hinge joint.

Technical result: improved dynamics and strength indicators, increased load capacity and service life of a hopper wagon for transporting pellets.

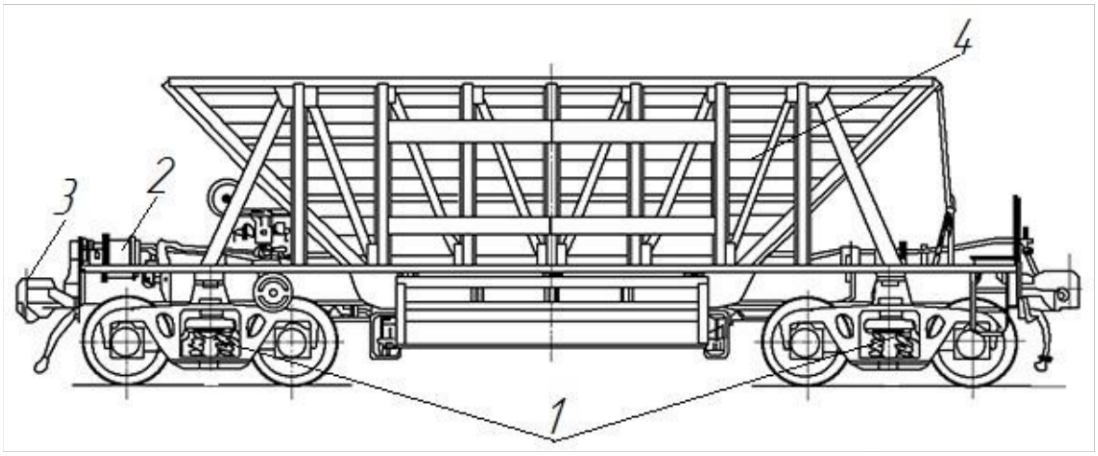

Fig. 1 – Hopper wagon for transporting pellets

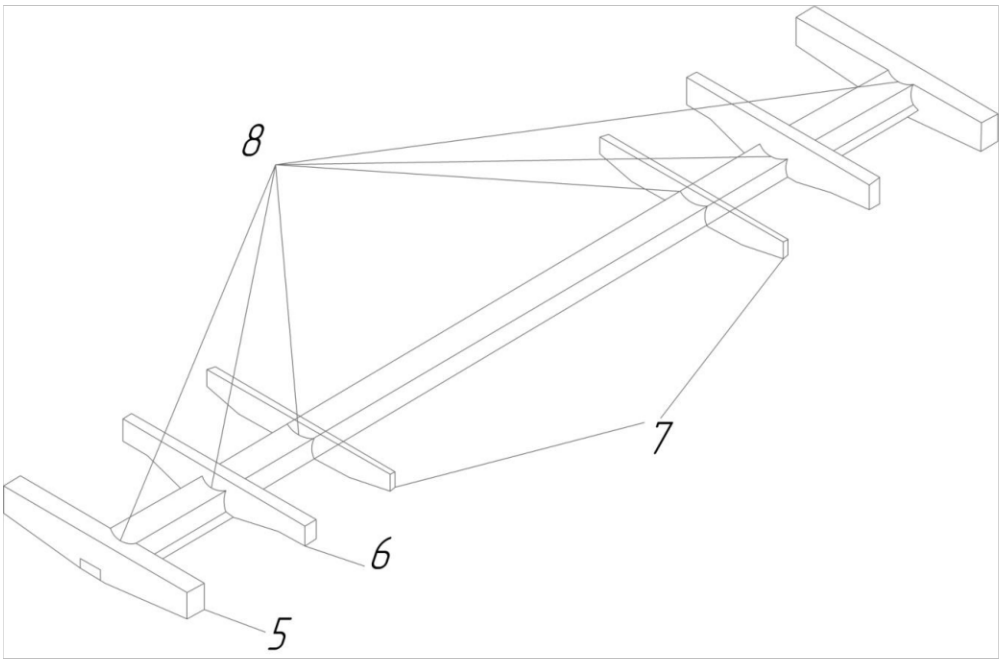

Fig. 2 – Hopper wagon for transporting pellets

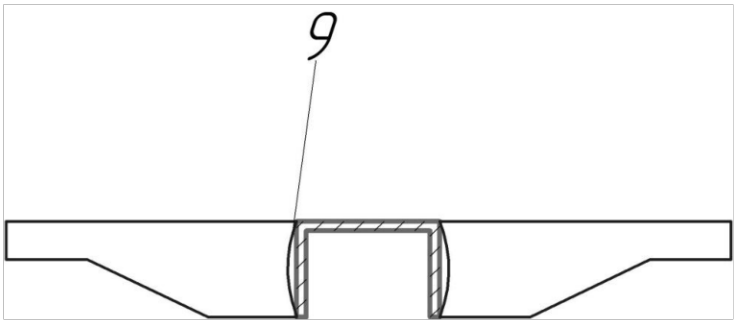

Fig. 3 – Hopper wagon for transporting pellets

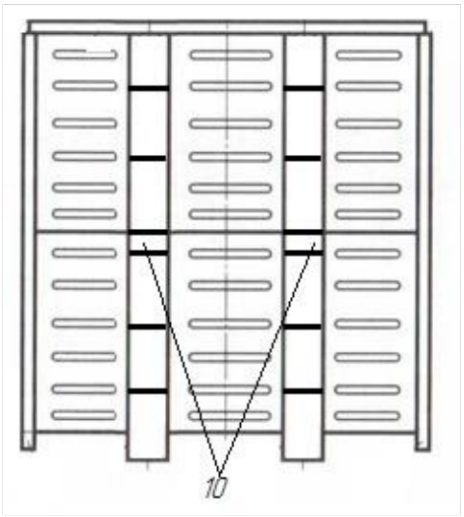

Fig 4 – Hopper wagon for transporting pellets

A.9. PLATFORM WAGON

The invention relates to carriage building and can be used for rail transportation of wheeled and tracked vehicles, artificial, timber and long cargo, boxed cargo, containers and other cargo that does not require protection from precipitation.

A known flat wagon model 13-4012, the design of which contains bogies, automatic couplers, braking equipment, a body, a frame with vertebral, end, pivot, and transverse beams.

The disadvantages of this design are as follows: flat wagons of this model are characterized by unreasonably insufficient load-carrying capacity and a reduced service life due to lower dynamic and strength characteristics, which, when operating on railway networks, causes an increase in the cost of cargo transportation and a decrease in the profitability of work, and the competitor imposes additional restrictions on transportation of cargo volumes.

The utility model is based on the task of improving the flat wagon by making the middle part of the spine beam, transverse and end beams in the form of leaf springs. The introduction of new features, when interacting with known ones, ensures the absorption of vibration and impact energy, which, as a consequence, improves the dynamics and strength of the platform wagon, reduces material consumption, and, accordingly, increases the load capacity and increases the service life of the wagon.

The objective is achieved by the fact that in a flat wagon containing bogies, automatic coupling devices, braking equipment, a body, a frame with vertebral, end, pivot, intermediate beams according to the utility model, the middle part of the spinal beam, end, pivot, transverse beams are made in the form of sheets springs

The advantages of the proposed technical solution are the improvement of the dynamics and strength of the flat wagon, the increase in the carrying capacity and service life of the wagon.

The essence of the utility model is explained by illustrative material, where in FIG. Figure 1 shows a flat wagon containing bogies 1, braking equipment 2, automatic coupling devices 3, body 4, frame 5 (Fig 2) with vertebral (including the middle part 4), end 1, pivot 2 transverse beams 3, which are made in in the form of leaf springs 5 (Fig. 3).

The proposed platform wagon works as follows.

During movement, vertical and horizontal forces from the body (4) are transmitted to the center beam with pivot, end transverse beams (Fig. 2) are made in the form of leaf springs, which partially absorb vibration energy and improve the dynamics and strength of the flat wagon. The movement of the platform wagon is ensured with the help of bogies 1. The braking of the platform wagon is provided by braking equipment 2. The connection of the platform wagon with other wagons is provided by automatic coupling devices 3.

The use of the proposed technical solution will improve the dynamics and strength indicators, increase the load capacity of the flat wagon and service life.

Utility model formula

A flat wagon containing bogies, automatic couplers, braking equipment, a body, a frame with spinal, end, pivot, and transverse beams, characterized in that the middle part of the center beam, end, pivot, and transverse beams are made in the form of leaf springs.

Essay

Utility model object: flat wagon.

Scope of application: railway transport, the utility model can be used in the design of a flat wagon for transporting wheeled and tracked vehicles, artificial, timber and long cargo, cargo in boxes, containers and other cargo that does not require protection from precipitation.

The essence of the utility model: A flat wagon containing bogies, automatic couplers, braking equipment, a body including a frame with a center beam, end, pivot, and transverse beams, which are made in the form of leaf springs.

Technical result: improved dynamics and strength of the flat wagon, increased load capacity and service life.

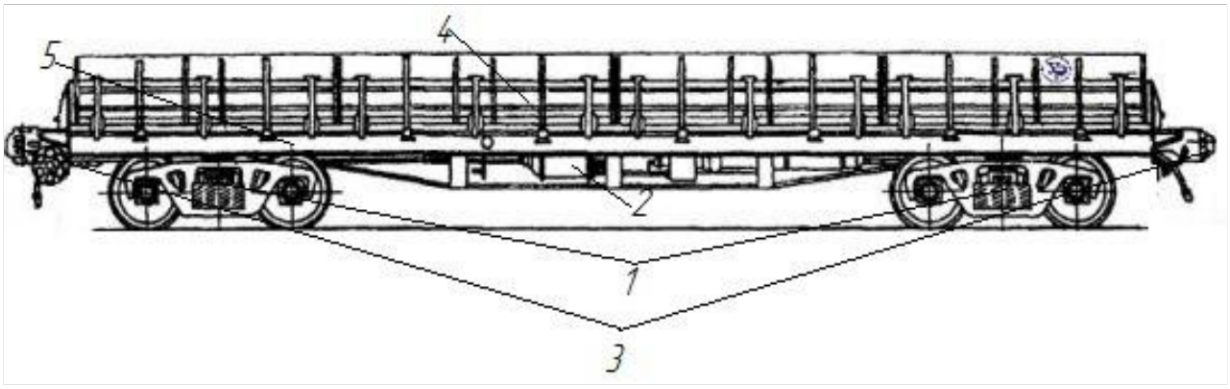

Fig. 1 – Flat wagon

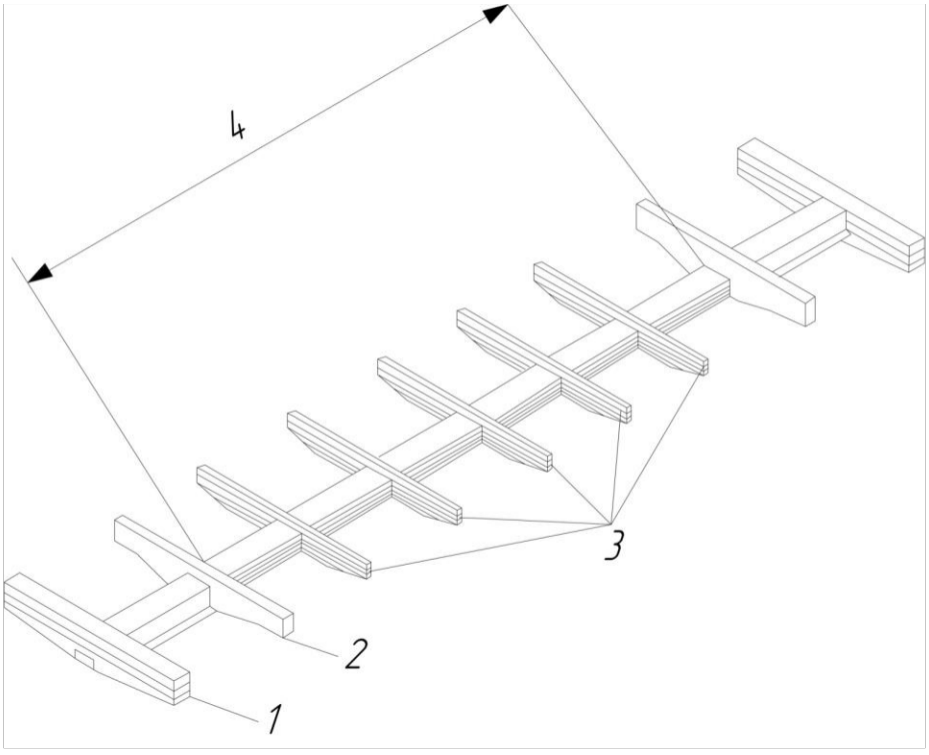

Fig. 2 – Flat wagon

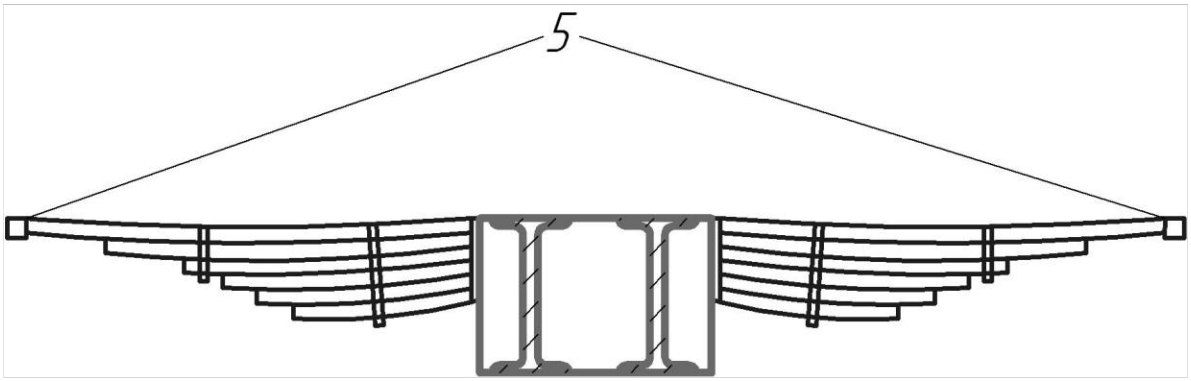

Fig. 3 – Flat wagon

A.10. HOPPER WAGON FOR GRAIN TRANSPORTATION

The utility model relates to carriage building and can be used for rail freight transportation of bulk cargo that requires protection from precipitation, in particular grain.

A well-known hopper wagon for the transportation of grain, model 19-752, is an all-metal self-unloading, bunker type, the design of which consists of a carriage module containing two biaxial bogies, an automatic coupler module, a braking equipment module, a frame module with x two pivots, two middle intermediate beams and a body module containing two side walls having a sheathing and a frame, including an upper frame and vertical posts, and two end walls, having a sheathing and a frame consisting of a frame. upper, side and intermediate pillars. There are also loading hatches in the roof of the wagon, and six unloading bins, three on each side, in the floor of the wagon.

The disadvantages of this design are as follows: a hopper wagon for transporting grain of this model is characterized by an unreasonably insufficient load capacity and a reduced service life due to unsatisfactorily lower dynamic and strength loads for possible load resistance indicators, which causes an increase in the cost of cargo during their operation on railway networks operation and competitiveness of railway transport and imposes additional restrictions on the transportation of cargo volumes.

The utility model is based on the task of improving the technical and economic indicators of a hopper wagon for transporting grain by making parts of the body module in a stamped way, namely making the side walls and intermediate pillars of the side walls in a solid, stamped way, with additional stiffeners; making end walls and end posts in a continuous, stamped manner, with additional stiffening ribs; execution of the wagon roof in a continuous stamped manner with additional stiffening ribs. The introduction of new features in interaction with the known ones

ensures the appearance of damping in the body module structure, which implements in it the principle of adaptive perception of operational loads in loaded or unloaded states, which, as a consequence, improves the dynamics and strength of a hopper wagon for transporting grain and reduces weight. material for the manufacture of a hopper wagon for transporting grain, simplifying the technological process of manufacturing a hopper wagon for transporting grain, increasing the carrying capacity and its service life.

The objective is achieved by the fact that in a hopper wagon for transporting grain containing bogies, automatic couplers, braking equipment, a frame module, a body module with side and end walls, side wall posts, end walls and a roof according to the utility model, side walls and intermediate posts the side walls are made in a continuous, stamped manner, with additional stiffening ribs; The end walls and end pillars are made in a solid, stamped manner, with additional stiffening ribs, and the roof is made in a solid, stamped manner with additional stiffening ribs.

The advantages of the proposed technical solution are improving the dynamics and strength of a hopper wagon for transporting grain, reducing the mass of material for the manufacture of a hopper wagon for transporting grain, simplifying the technological process of manufacturing a hopper wagon for transporting grain, increasing the load capacity and service life of the wagon.

The essence of the utility model is explained by illustrative material, where in FIG. Figure 1 shows a hopper wagon for grain transportation, containing bogies 1, braking equipment 2, automatic coupling devices 3, frame module 4, body module 5, while the body module (Fig. 2) includes: a stamped side wall 6 with side wall posts 7 and transverse corrugations 8 (also shown in Fig. 3), a stamped end wall 9 with end wall racks 10, a stamped solid roof with additional stiffeners 11. In Fig. Figure 3 shows a cross-section of a stamped side wall 6 with side wall posts 7, a reinforcing lining of the side wall post 12, which provides the necessary rigidity of the structure.

The proposed hopper wagon for grain transportation works as follows. To form a freight railway train, a hopper wagon for transporting grain is connected to the rear

wagon and the front wagon (or locomotive) through the automatic coupler 3 and to the brake line of the train through the brake equipment 2 (Fig. 1). As a result of loading the body module with cargo, the corresponding loads are transferred to the frame module 4(figure 1) and then on the axis of the wheel pairs of two biaxial bogies 1 (Fig. 1). In this case, the bulk cargo is also distributed and acts on the side walls and intermediate racks of the side walls, on the end walls and end racks and on the roof of the wagon, which made in a continuous stamped manner with additional stiffening ribs. During the movement of a freight train, the greatest loads on the structural elements of a hopper wagon for transporting grain occur in extreme situations. For example, significant inertial loads during emergency braking acting on the front end wall with the pillars of the body module.

The use of the proposed technical solution will improve the dynamics and strength of a hopper wagon for transporting grain, reducing the mass of material for the manufacture of a hopper wagon for transporting grain, simplifying the technological process of manufacturing a hoper wagon for transporting grain, increasing the carrying capacity and service life of the wagon.

Utility model formula

A hopper wagon for transporting grain, containing bogies, braking equipment, automatic couplers, a frame module, a body module, characterized in that the side walls and intermediate pillars of the side walls are made solid, stamped, with additional stiffeners; The end walls and end pillars are made in a solid, stamped manner, with additional stiffening ribs, and the roof is made in a solid, stamped manner with additional stiffening ribs.

Essay

Utility model object: hopper wagon for grain transportation.

Scope of application: railway transport, the utility model can be used in the design of a hopper wagon for transportation of bulk cargo that requires protection from precipitation, in particular grain.

The essence of the utility model is that in a grab wagon for transporting grain, containing bogies, braking equipment, automatic coupling devices, a frame module, a body module in which the side walls and intermediate pillars of the side walls are made solid, stamped, with additional stiffeners; The end walls and end pillars are made in a solid, stamped manner, with additional stiffening ribs, and the roof is made in a solid, stamped manner with additional stiffening ribs.

Technical result: improving the dynamics and strength of a hopper wagon for transporting grain, reducing the mass of material for the manufacture of a hopper wagon for transporting grain, simplifying the technological process of manufacturing a hopper wagon for transporting grain, increasing the load capacity and service life of the wagon.

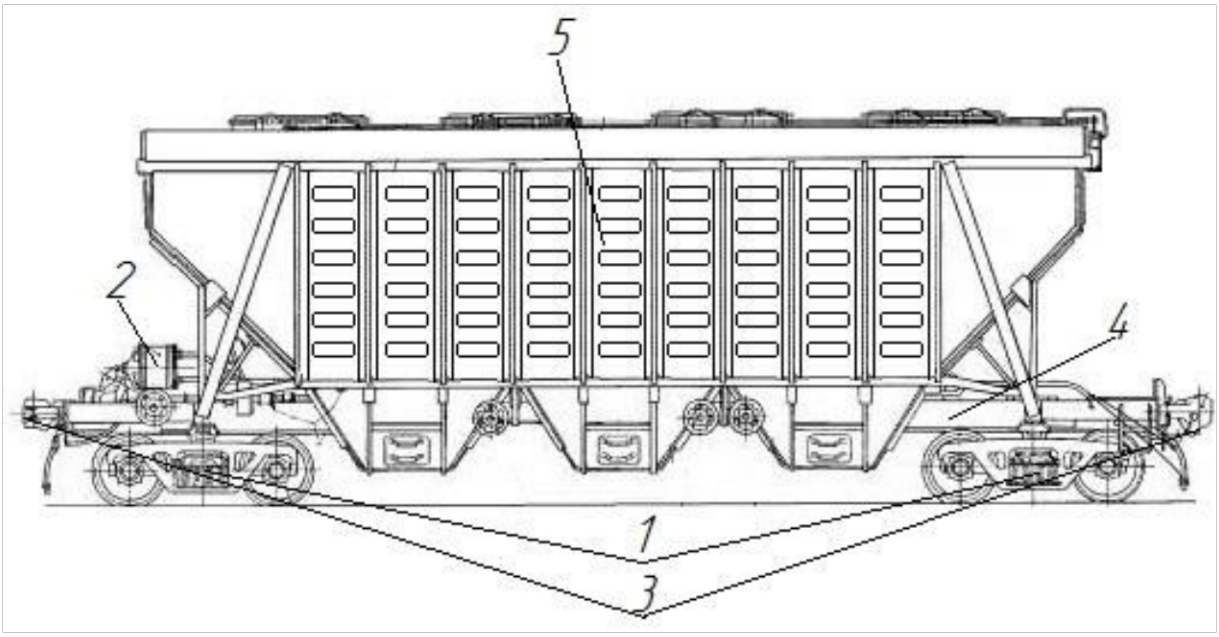

Fig. 1 – Hopper wagon for transporting grain

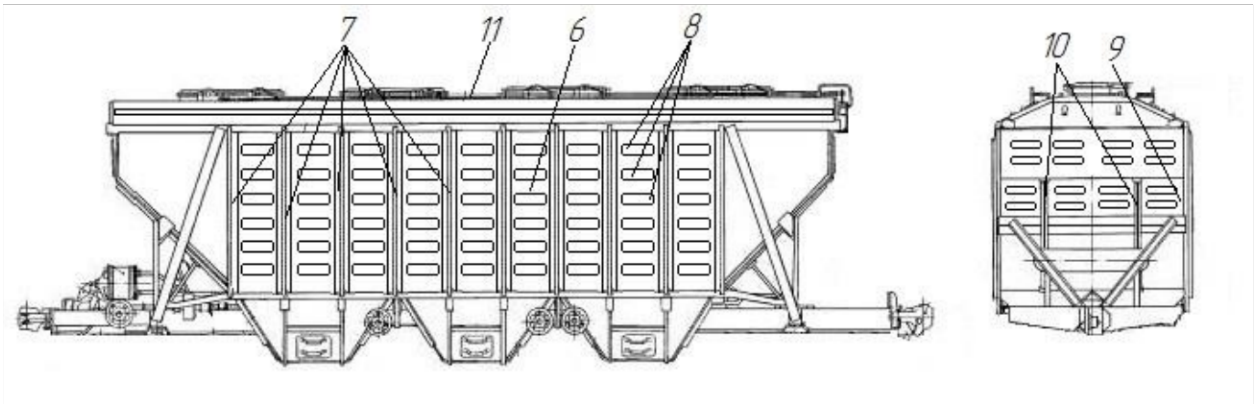

Fig. 2 – Hopper wagon for transporting grain

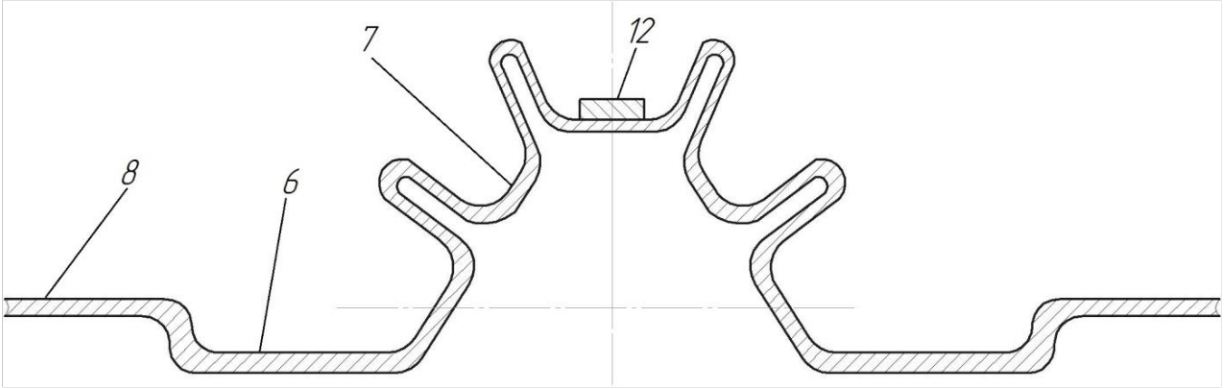

Fig. 3 – Hopper wagon for transporting grain

A.11. UNIVERSAL COVERED WAGON

The utility model relates to carriage building and can be used for freight rail transportation that requires protection from precipitation.

A universal covered wagon for the transportation of goods requiring protection from precipitation, model 11-217, is known; the all-metal wagon has an outer metal lining and a wooden inner lining, the design of which consists of a carriage module containing two biaxial bogies, a brake equipment module, a frame module with a vertebral , two end, two pivot, two main and seven intermediate weft beams and a body module, which contains two side walls with sheathing and a frame including vertical posts, two end walls and a frame including resistant intermediate ones and a solid metal roof. Characterized by loading through side doors, sunroofs and unloading through side doors.

The disadvantages of this design are as follows: the universal box wagon of this model is characterized by an unreasonably insufficient load capacity and a reduced service life due to unsatisfactorily lower dynamic and strength loads, which causes an increase in the cost of cargo transportation during their operation on railway networks. railway transport and imposes additional restrictions on the transportation of cargo volumes.

The basis of the utility model is the task of improving the technical and economic indicators of a universal covered wagon by making parts of the body module in a stamped way, namely, making the side walls and intermediate pillars of the side walls in a solid, stamped way, with additional stiffeners; making end walls and end posts in a continuous, stamped manner, with additional stiffening ribs; execution of the wagon roof in a continuous stamped manner with additional stiffening ribs. The introduction of new features in interaction with known ones ensures the appearance of damping in the body module structure, which implements

in it the principle of adaptive perception of operational loads in loaded or unloaded states, which, as a consequence, improves the dynamics and strength of a universal covered wagon, reducing the mass of material for the manufacture of a universal covered wagon , simplification of the technological process of manufacturing a universal covered car, increasing the carrying capacity and its service life.

The task is achieved by the fact that in a universal covered wagon containing bogies, automatic coupling devices, braking equipment, a frame module, a body module with side, end walls, side wall posts, end walls and a roof according to the utility model, side walls and intermediate side wall posts are completed continuous, stamped method, with additional stiffening ribs; The end walls and end pillars are made in a solid, stamped manner, with additional stiffening ribs, and the roof is made in a solid, stamped manner with additional stiffening ribs.

The advantages of the proposed technical solution are improving the dynamics and strength of a universal covered wagon, reducing the mass of material for the manufacture of a universal covered wagon, simplifying the technological process of manufacturing a universal box wagon, increasing the carrying capacity and service life of the wagon.

The essence of the utility model is explained by illustrative material, where in FIG. Figure 1 shows a universal covered wagon containing bogies 1, braking equipment 2, automatic couplers 3, frame module 4, body module 5, while the body module (Fig. 2) includes: a stamped side wall 6 with side wall posts 7 and transverse corrugations 8 (also shown in Fig. 3), a stamped end wall 9 with end wall racks 10, a stamped solid roof with additional stiffeners 11. In Fig. Figure 3 shows a cross-section of a stamped side wall 6 with side wall posts 7, a reinforcing lining of the side wall post 12, which provides the necessary rigidity of the structure.

The proposed universal box wagon works as follows. To form a freight railway train, a universal covered wagon is connected to the rear wagon and the front wagon (or locomotive) through the automatic coupler 3 and to the brake line of the train through the braking equipment 2 (Fig. 1). As a result of loading the body module

with cargo, the corresponding loads are transferred to the frame module 4(figure 1) and then on the axis of the wheel pairs of two biaxial bogies 1 (Fig. 1). In this case, the bulk cargo is also distributed and acts on the side walls and intermediate racks of the side walls, on the end walls and end racks and on the roof of the wagon, which made in a continuous stamped manner with additional stiffening ribs. During the movement of a freight train, the greatest loads on the structural elements of a universal covered wagon occur in extreme situations. For example, significant inertial loads during emergency braking acting on the front end wall with the pillars of the body module.

The use of the proposed technical solution will improve the dynamics and strength of a universal covered wagon, reduce the mass of material for the manufacture of a universal covered wagon, simplify the manufacturing process for a universal covered wagon, increase the load capacity and service life of the wagon.

Utility model formula

A universal covered wagon containing bogies, braking equipment, automatic couplers, a frame module, a body module, characterized in that the side walls and intermediate pillars of the side walls are made solid, stamped, with additional stiffeners; The end walls and end pillars are made in a solid, stamped manner, with additional stiffening ribs, and the roof is made in a solid, stamped manner with additional stiffening ribs.

Essay

Utility model object: universal carriage.

Scope of application: railway transport, the utility model can be used in the design of a universal covered wagon for transporting goods that require protection from atmospheric influences.

The essence of the utility model is that in a universal covered wagon containing bogies, braking equipment, automatic couplers, a frame module, a body module in

which the side walls and intermediate pillars of the side walls are made solid, stamped, with additional stiffeners; The end walls and end pillars are made in a solid, stamped manner, with additional stiffening ribs, and the roof is made in a solid, stamped manner with additional stiffening ribs.

Technical result: improving the dynamics and strength of a universal covered wagon, reducing the mass of material for the manufacture of a universal covered wagon, simplifying the technological process of manufacturing a universal covered wagon, increasing the carrying capacity and service life of the wagon.

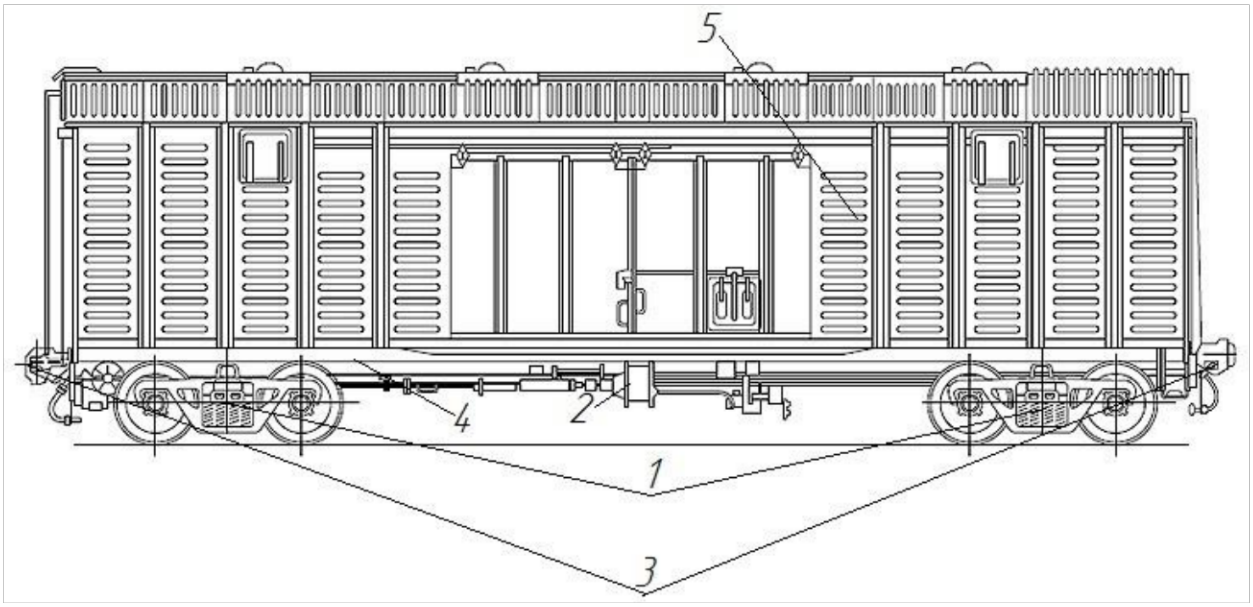

Fig. 1 – Universal covered wagon

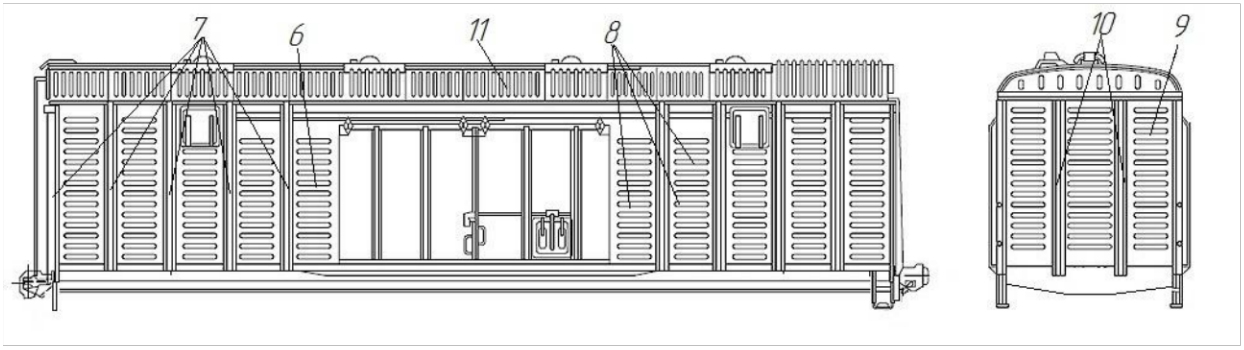

Fig. 2 – Universal covered wagon

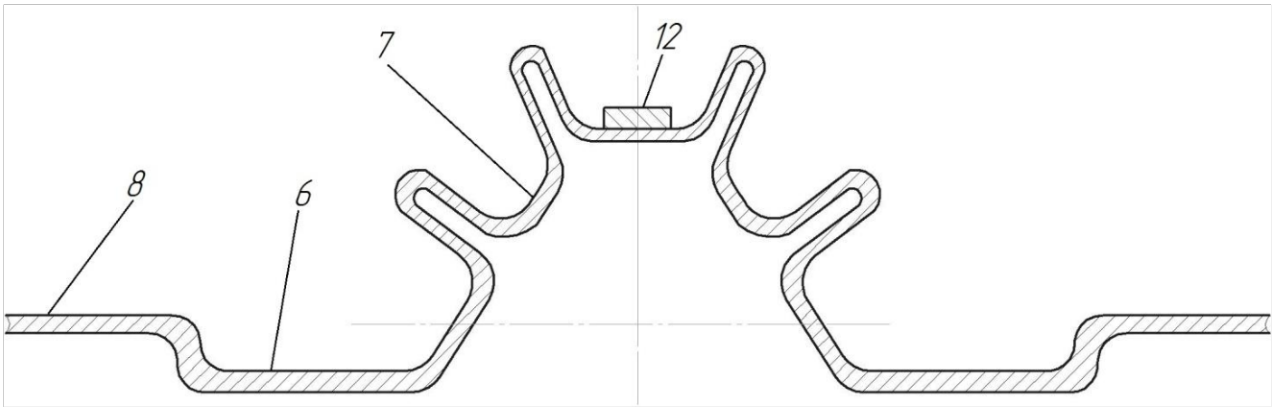

Fig. 3 – Universal covered wagon

A.12. RAILWAY TANK WAGON

The utility model relates to railway transport, to the modernization, construction and operation of freight wagons and can be used for technical control and improving the safety of carriage movement.

A railway tank is known, containing bogies, a frame, braking equipment, automatic coupling devices, a boiler, fastening the boiler to the frame and supports of the boiler on the frame.

The disadvantages of this design are as follows: a railway tank for liquid cargo is characterized by unreasonably reduced overhaul intervals, unsatisfactory motion dynamics and a reduced service life due to unsatisfactorily lower dynamic and strength load resistance indicators, which determines their operation on networks. decrease in the profitability of operation and competitiveness of railway transport and imposes additional restrictions on the transportation of cargo volumes

The utility model is based on the task of improving a railway tank for the transportation of liquid cargo by having an autonomous module for diagnosing the quality of movement of the wagon, introducing hinged elements into supporting structures instead of existing fixed elements (solid beams, welded joints), namely the presence of a hinged element in the middle part spinal beam; the presence of hinge elements at the junction of the end and pivot beams. The introduction of new features in interaction with known ones provides the opportunity to constantly diagnose traffic quality indicators that characterize the technical condition of the wagon and track; the appearance of additional degrees of freedom of the design and implements in it the principle of adaptive perception of operational loads in loaded or unloaded states, which, as a consequence, improves the dynamics and strength of a railway tank for the transportation of liquid cargo, ensures a reduction in material consumption and, accordingly, increases the load capacity for liquid cargo.

The task is achieved by the fact that in a railway tank wagon for the transportation of liquid cargo, containing bogies, automatic couplers, braking equipment, a frame with vertebral, end and pivot beams according to the utility model, an autonomous module for diagnosing indicators of the quality of movement of the wagon is installed, consisting of a recorder - transmitter, accelerometers (which are installed on the unsprung and sprung parts of the wagon), GPS transmitter and power module with an articulated piezoelectric element; existing hinge element in the middle part of the spinal beam; the existing hinge element at the junction of the center beam with: end and pivot beams.

The advantages of the proposed technical solution are the constant diagnosis of the technical condition of the wagon, improvement of the dynamics and strength of the railway tank for the transportation of liquid cargo, increase in carrying capacity and service life.

The essence of the utility model is explained by illustrative material, where in FIG. Figure 1 shows a railway tank wagon for the transportation of liquid goods, containing bogies 1, a frame 2, a boiler 3, accelerometers 4, a recorder-transmitter 5, while the railway tank wagon for the transport of liquid goods includes (Fig. 2) a frame with a vertebral (with a hinged eso-element in the middle part 6), end 7 and pivot beams 8, in which there are hinge joints 9.

The proposed railway tank for liquid cargo operates as follows.

During movement, vertical and horizontal forces from the boiler are transmitted to a center beam with a hinged piezoelectric element, which is handedly connected to the end and pivot beams (Fig. 2, Fig. 3), which partially absorb vibration energy and improve dynamics and strength railway tank for transporting liquid cargo, in turn, the vibrations of the articulated piezoelectric element converts the vibration energy into electrical energy and accumulates in the power module of the autonomous diagnostic module (Fig. 1). When moving, accelerometers 4 and a recorder-transmitter 5 record indicators of the wagon's movement dynamics and provide constant monitoring of the technical condition of the wagon and track.

The use of the proposed technical solution will make it possible to constantly diagnose indicators of the quality of wagon movement that characterize the technical condition of the wagon and track, improve dynamics and strength indicators, increase the carrying capacity of a railway tank for transporting liquid cargo, which is especially important for wagons after long-term operation or after repairs and upgrades.

Utility model formula

A railway tank for the transportation of liquid cargo, containing bogies, automatic coupling devices, braking equipment, a boiler, a frame with vertebral, end, pivot beams, characterized in that the existing autonomous module for diagnosing indicators of the quality of movement of the wagon, consisting of a recorder-transmitter, accelerometers (installed on unsprung and sprung parts of the wagon), GPS transmitter and power module with a hinged piezoelectric element; existing hinge element in the middle part of the spinal beam; the existing hinge element at the junction of the center beam with: end and pivot beams.

Essay

Utility model object: railway tank wagon.

Scope of application: railway transport, the utility model can be used in the design of a railway tank wagon for the transportation of liquid cargo.

The essence of the utility model: A railway tank car for the transportation of liquid cargo, containing bogies, automatic couplers, braking equipment, a boiler, a frame with an articulated center beam, end, pivot beams, in which the fixed joint is replaced by a hinged joint and an existing autonomous module for diagnosing quality indicators carriage movement

Technical result: constant diagnosis of traffic quality indicators characterizing the technical condition of the tank wagon and track, improvement of dynamics and strength indicators, increased load capacity and service life of the railway tank wagon for the transportation of liquid goods.

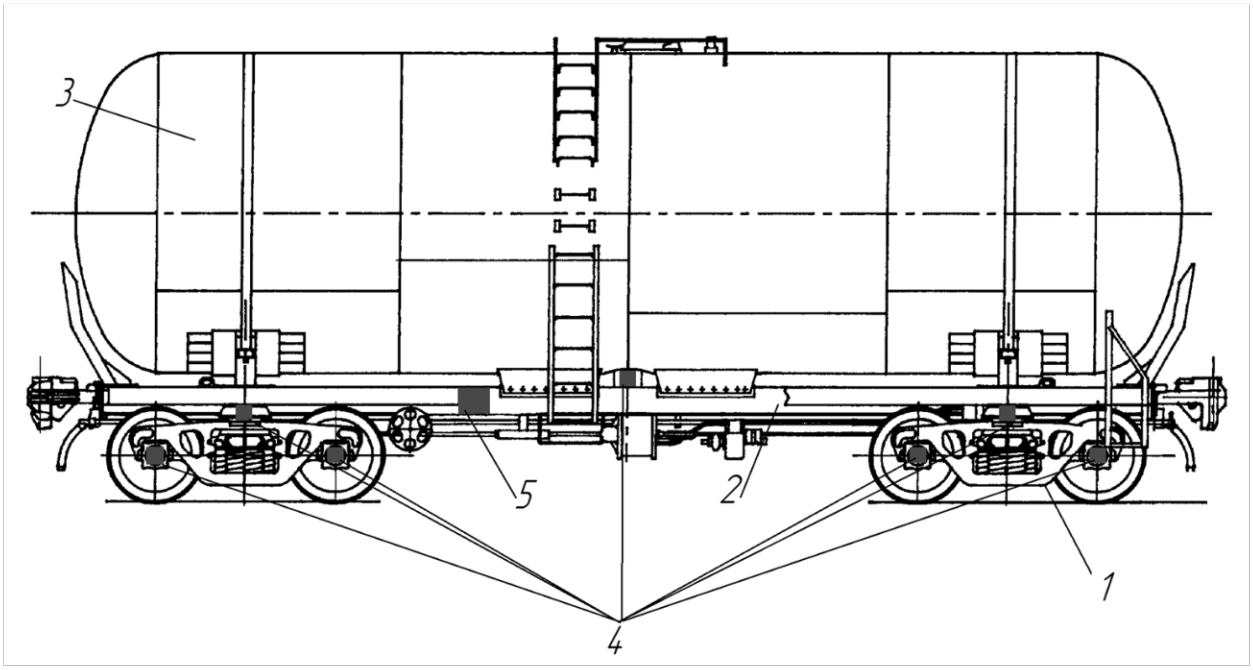

Fig. 1 – Railway tank wagon

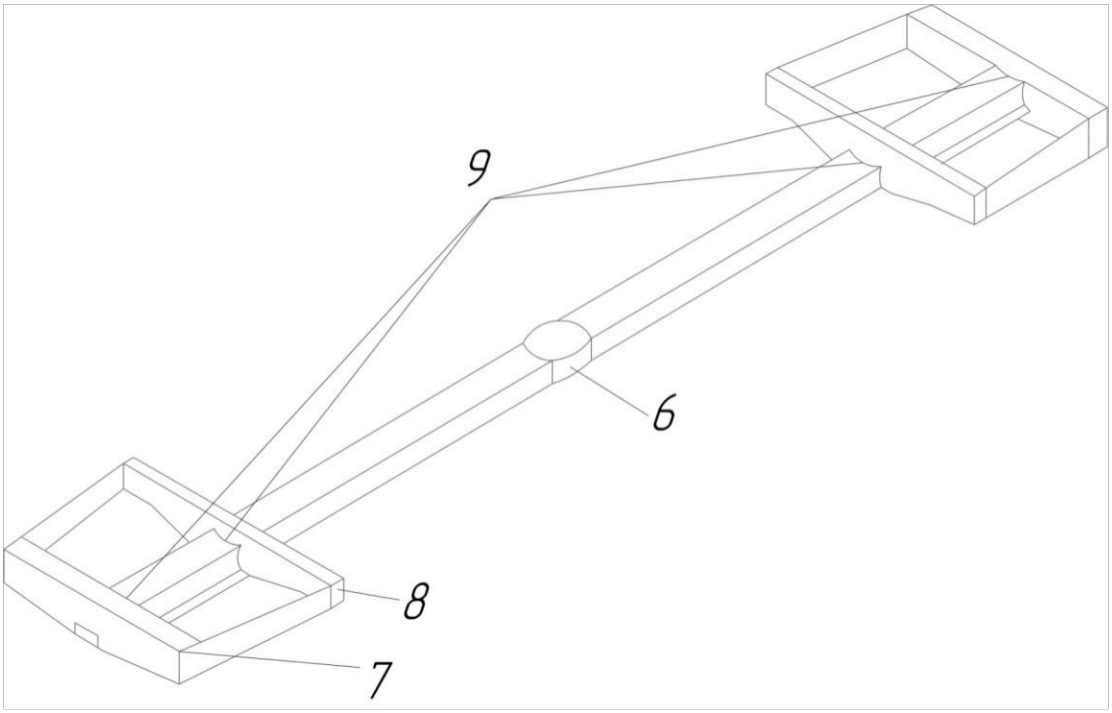

Fig. 2 – Railway tank

A.13. RAILWAY GOND POCKET WAGON

The utility model relates to railway transport, to the modernization, construction and operation of freight wagons and can be used for technical control and improving the safety of carriage movement.

A specialized gondola wagon with a solid body is known, the design of which contains bogies, automatic coupling devices, braking equipment, a body, a frame with center, end, pivot, and intermediate beams.

The disadvantages of this design are as follows: gondola wagons of this model are characterized by unreasonably reduced overhaul intervals, unsatisfactory motion dynamics and a reduced service life due to unsatisfactorily lower dynamic and strength load resistance indicators, which determines their operation on railway transportation networks operation and competitiveness of railway transport and imposes additional restrictions on the transportation of cargo volumes

The utility model is based on the task of improving a solid-bottomed gondola wagon by having an autonomous module for diagnosing the quality of movement of the wagon, introducing hinged elements into supporting structures instead of existing fixed elements (solid beams, welded joints), namely the presence of a hinged element in the middle part of the spinal beam; the presence of hinge elements at the junction of the center beam with: end, pivot and intermediate beams. The introduction of new features in interaction with known ones provides the opportunity to constantly diagnose traffic quality indicators that characterize the technical condition of the wagon and track; the appearance of additional degrees of freedom of the design and implements in it the principle of adaptive perception of operational loads in a loaded or unloaded state, which, as a consequence, improves the dynamics and strength of a solid-bottomed gondola wagon, ensures a reduction in material consumption and, accordingly, increases the load capacity and increases the service life of the wagon.

The objective is achieved by the fact that in a solid-bottomed gondola wagon containing bogies, automatic coupling devices, braking equipment, a body with side and end walls, a frame with backbone, end, pivot, intermediate beams according to the utility model, there is an autonomous module for diagnosing the quality indicators of the wagon's movement, consisting of recorder-transmitter, accelerometers (which are installed on the unsprung and sprung parts of the wagon), GPS transmitter and power module with a hinged piezoelectric element; existing hinge element in the middle part of the spinal beam; There are hinge elements at the junction of the center beam with: end, pivot and intermediate beams.

The advantages of the proposed technical solution are the constant diagnosis of the technical condition of the wagon, improvement of the dynamics and strength of a solid-bottom gondola wagon, an increase in the carrying capacity and service life of the wagon.

The essence of the utility model is explained by illustrative material, where in FIG. Figure 1 shows a solid-bottom gondola wagon containing bogies 1, a frame 2, a body with side and end walls 3, accelerometers 4, a recorder-transmitter 5, while the solid-bottom gondola wagon includes (Fig. 2) a frame with a spinal (with articulated piezo) 6), end 7 , intermediate 8, pivot beams 9, in which there are hinge joints 10.

The proposed solid-bottom gondola wagon works as follows.

When moving, vertical and horizontal forces from the body are transmitted to a spinal beam with a hinged piezoelectric element, which is pivotally connected to the pivot, end, and intermediate beams (Fig. 2), which partially absorb vibration energy and improve dynamics and strength in turn, the vibrations of the articulated piezoelectric element convert the vibration energy into electrical energy and accumulate in the power module of the autonomous diagnostic module (Fig. 1). When moving, accelerometers 4 and a recorder-transmitter 5 record indicators of the wagon's movement dynamics and provide constant monitoring of the technical condition of the wagon and track.

The use of the proposed technical solution will make it possible to constantly diagnose indicators of the quality of wagon movement that characterize the technical condition of the wagon and track, improve dynamics and strength indicators, increase the load capacity of a solid-bottomed gondola wagon and service life.

Utility model formula

A solid-bottom gondola wagon containing bogies, automatic coupling devices, braking equipment, a body, a frame with vertebral, end, pivot, intermediate beams, characterized in that the existing autonomous module for diagnosing indicators of the quality of movement of the wagon, consisting of a recorder-transmitter (accelerometer) is installed on unsprung and sprung parts of the wagon), GPS transmitter and power module with a hinged piezoelectric element; existing hinge element in the middle part of the spinal beam; There are hinge elements at the junction of the center beam with: end, pivot and intermediate beams.

Essay

Utility model object: railway solid-bottom gondola wagon.

Scope of application: railway transport, the utility model can be used in the design of a solid-bottom gondola wagon for the transportation of goods that do not require protection from atmospheric influences.

The essence of the utility model: a solid-bottom railway gondola wagon containing bogies, automatic coupling devices, braking equipment, a body including a frame with an articulated center beam, end, pivot, intermediate, beams that have hinged connections and an existing autonomous diagnostic module for the wagon indicator.

Technical result: constant diagnosis of traffic quality indicators characterizing the technical condition of the tank wagon and tracks, improvement of dynamics and strength indicators, increase in load capacity and service life.

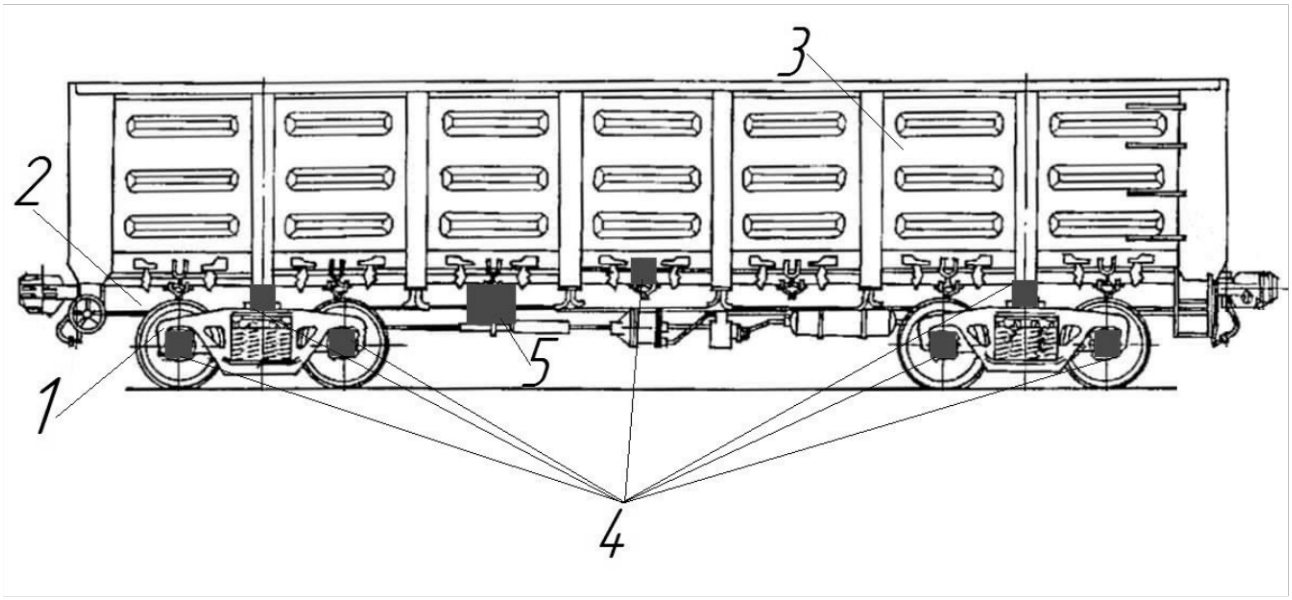

Fig. 1 – Railway gondola wagon with solid bottom

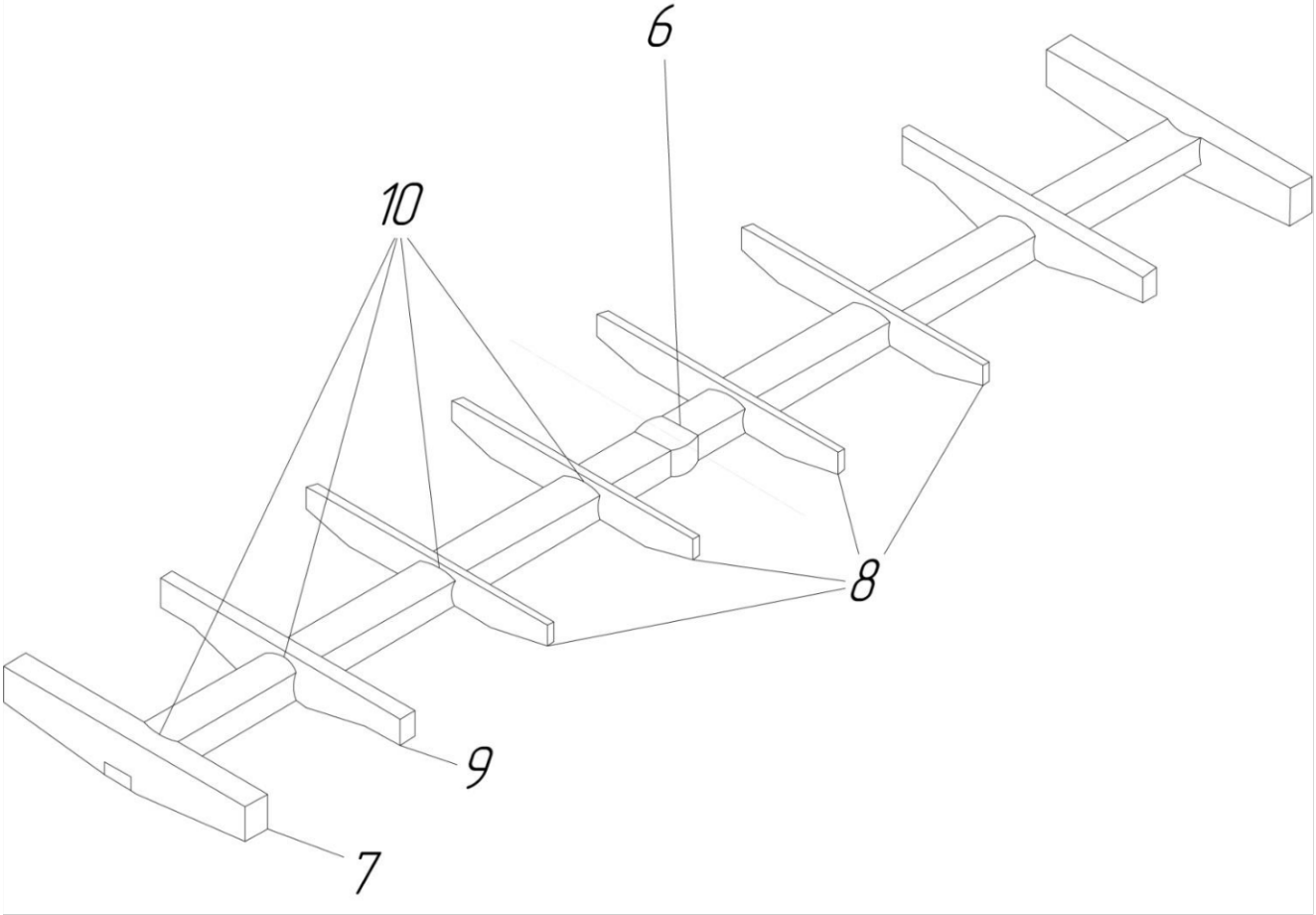

Fig. 2 – Railway gondola wagon with solid bottom

SCIENTIFIC EDITION

Oleksij FOMIN, Doctor of Engineering Science, Professor
Pavlo PROKOPENKO, Ph.D.

REDUCING THE ACCIDENTAL RATE OF WAGONS BY IMPROVING THE SYSTEM FOR ASSESSING THEIR TECHNICAL CONDITION

Monograph

The monograph will be valuable for researchers, designers, and engineers engaged in activities associated with reducing the accident rate of railway cars through the enhancement of systems assessing their technical condition. Specifically, it addresses issues related to the utilization of laboratory cars during full-scale tests for evaluating motion quality, acceptance, and commissioning of railway rolling stock. However, the current state of measurement equipment development enables the abandonment of such laboratory cars in favor of mobile hardware-software complexes during dynamic testing of rolling stock units in most cases.

The organization of freight train traffic in Ukraine is a critical factor in integrating the country's railway transport into the European system. Currently, a situation has arisen that demands a significant upgrade of the freight wagon fleet with modern wagons to meet the requirements of freight transportation. Another substantial drawback of Ukraine's railway transport is the speed limitation for trains with wagons having reduced tare weight, impacting the speed of rail freight transport. Therefore, there is an immediate need to improve the methodological and software support, along with testing tools, for evaluating the performance and safety indicators of such wagons. Due to their unsatisfactory dynamic behavior, a specific group of freight wagons, such as platform wagons, has a speed limit of 60 km/h, negatively affecting rail freight speed.

Crucial indicators of the railway rolling stock's motion quality include vertical and horizontal dynamics, the wheel flange stability coefficient against derailment, frame forces, and body accelerations. These aspects largely depend on the weight of the rolling stock's tare and the interaction indicators between the crew part and the track. The monograph's objective is to illuminate the results of conceptual solutions aimed at assessing the technical condition and motion quality indicators of wagons under the conditions of operation using modern mobile systems. The book also presents the outcomes of prior theoretical and practical works, including an analysis of railway traffic safety issues and existing systems for determining motion quality indicators. A proposed mobile system for determining the motion quality indicators of wagons in operation and a complex of hardware, software, and mathematical solutions for determining the motion quality indicators of wagons are included. Concepts of freight wagons with improved motion quality characteristics are also discussed.

The book can serve as a textbook for the training of bachelor's, master's, and doctoral students in various specialties related to transport mechanics, including railway transport, transport technologies, mechanical engineering, materials science, and others.

Published (PDF): 23.02.2024.
Conventionally printed sheets 21,04.

Publisher [ISBN]**:** Primedia E-launch LLC.
TX 75001, United States, Texas, Dallas.
E-mail: info@primediaelaunch.com | URL: www.primediaelaunch.com